

PARAMETRIC SENSITIVITY IN LARGE DEFORMATION ANALYSIS BY SMOOTHED PARTICLE HYDRODYNAMICS (SPH)

Nafisa Tabassum^{*1,2}, Md. Aftabur Rahman² and Mohammed Russedul Islam³

¹*Graduate Student (M.Sc Engg. Candidate), Chittagong University of Engineering & Technology, Chattogram-4349, Bangladesh, email: nafisa_t@cuet.ac.bd*

²*Faculty, Department of Civil Engineering, Chittagong University of Engineering & Technology, Chattogram-4349, Bangladesh, email: maftabur@cuet.ac.bd*

³*Faculty, Department of Civil Engineering, Military Institute of Science & Technology, Mirpur Cantonment, Dhaka-1216, Bangladesh, email: ce_russel@yahoo.com*

***Corresponding Author**

ABSTRACT

Handling of large deformation with traditional grid-based method suffers mesh distortion and in the extreme case, blow up of the problem domain can occur. To address this, Particle-based approach is the rational way to simulate the behavior of large deformation. Among several Particle-based methods, Smoothed Particle Hydrodynamics (SPH) is proven to be an effective mesh-free method owing to its true particle nature. The application of SPH in the diverse field of engineering, to be specific large deformation analysis of geomaterials is justified by many researchers. However, the sensitivity of parameters often lead to unphysical outcomes and provide an ambiguous response to the problem statement. Notably, the effect of particle spacing, smoothing lengths, kernel functions, constitutive laws are critically important. Moreover, some additional treatments are also necessary to stabilize the numerical simulation. Therefore, highlighting this problem, an attempt is made to quantitatively evaluate the effect of different sensitive parameters on the response of large deformation simulation. A benchmark case of ideal dam break simulation with different configurations and material properties are simulated and their responses are critically discussed.

Keywords: *Large deformation, Mesh-free method, Smoothed particle hydrodynamics, Sensitivity, Parameters.*

1. INTRODUCTION

The limitation of handling large deformation in traditional Finite Element Method (FEM) takes Particle Methods under the spotlight as particle methods are capable of considering large deformation without numerical divergence. From a list of particle methods developed in last few decades, the Smoothed Particle Hydrodynamics (SPH) is proven to be an effective numerical tool. The true nature of particle method and adaptive nature turn this method very effective capturing large deformation despite the limitation of boundary condition. Likewise, some particle methods, no background mesh is required in SPH. This method was firstly developed for solving astrophysical problems in three dimensional open space (Gingold & Monaghan, 1977; Lucy, 1977). Later, it was used in many sectors, such as in both computational solid and fluid mechanics. The earliest applications were on fluid dynamics related fields such as elastic flow (Swegle, 1992), free surface fluid flows and multi-phase flows (Monaghan, 1994, 1997; Monaghan & Kocharyan, 1995; Joseph P. Morris, 2000), turbulence flows (Monaghan, 2002), low-Reynolds number viscous fluid flows (J.P. Morris, Fox, & Zhu, 1997; Takeda, Miyama, & Sekiya, 1994), incompressible fluid flows (Cummins & Rudman, 1999; Shao & Lo, 2003), flow through porous media (J. P. Morris, Zhu, & Fox, 1999; Zhu, Fox, & Morris, 1999). The preceding reviews express the vast application of SPH not limited to hydrodynamics but also free surface and multi-phase flows. The accuracy of those simulations attracted researcher in the field of geotechnical hazard analysis to apply the SPH to see the insight of the related problems. To be specific, the mostly common geotechnical and geological hazard, landslides and debris flows have been simulated in SPH environment by many researchers around the world. Starting from the simplified and idealized viscous model to complicated mixture theory have been formulated and replicate the real scenario in many instances. However, the SPH formulation needs several parameters for numerical stability and assumed based on case studies. The sensitivity of those parameters may influence the outcome and the necessity of critical evaluation of some parameters are due. Specially, for large deformation landslides or debris flows, the sensitivity of numerical parameters are necessary to evaluate the accuracy of the model. No straight forward research works on sensitivity of parameters used in landslides/debris flows have been reported. Considering the fact, an attempt is made to simulate different conditions in SPH environment and sensitivity of different parameters on the response of the model is extracted. The following sections describe in detail the sensitivity analysis of different parameters for modelling large deformation geotechnical hazards.

2. SPH FORMULATIONS

In the SPH method, a set of finite discretized particles represents the entire computational domain. These particles possess certain volume and mass of the material, having physical properties such as velocity, acceleration, density, stress, etc. and move according to the governing conservation equations. The integral representation of a function in the SPH method can be expressed as follows:

$$f(x) = \int_{\Omega} f(x') \delta(x - x') dx' \quad (1)$$

Where, $f(x)$ represents a function of the three-dimensional position vector x , Ω is the volume of the integral which holds x and $\delta(x - x')$ is the Dirac Delta function. This Dirac Delta function is given by,

$$\delta(x - x') = \begin{cases} 1 & x = x' \\ 0 & x \neq x' \end{cases} \quad (2)$$

If a smoothing function $W(x - x', h)$ is used in place of Dirac Delta function $\delta(x - x')$, the integral representation of $f(x)$ using kernel approximation operator $\langle \rangle$ is given by,

$$\langle f(x) \rangle = \int_{\Omega} f(x') W(x - x', h) dx' \quad (3)$$

where, W is the kernel or smoothing function which must satisfy the normalized condition and dirac delta function, h is the smoothing length.

The dimension of the compact support is defined by the smoothing length h and a scaling factor k , where, k =constant, kh specifies the non-zero area (effective) of the smoothing function at point x i.e. radius of the influence domain. This effective area is called the support domain for the smoothing function of point x . Using this compact condition, integration over the entire problem domain is localized as integration over the support domain of the smoothing function.

After some trivial mathematical formulations, for a given particle i , the particle approximation for a function and its spatial derivative at particle i can be expressed as:

$$\langle f(x_i) \rangle = \sum_{j=1}^N \frac{m_j}{\rho_j} f(x_j) \cdot W_{ij} \quad (4)$$

where,

$$W_{ij} = W(x_i - x_j, h) = W(|x_i - x_j|, h) \quad (5)$$

and,

$$\langle \nabla \cdot f(x_i) \rangle = \sum_{j=1}^N \frac{m_j}{\rho_j} f(x_j) \cdot \nabla_i W_{ij} \quad (6)$$

where,

$$\nabla_i W_{ij} = \frac{x_i - x_j}{r_{ij}} \frac{\partial W_{ij}}{\partial r_{ij}} = \frac{x_{ij}}{r_{ij}} \frac{\partial W_{ij}}{\partial r_{ij}} \quad (7)$$

where, ∇W is the gradient of the smoothing function W ; r_{ij} indicates the distance between particle i and j .

Different types of smoothing functions are available for implementation in the SPH literature. Each kernel function has its special feature to use in particular problems. The most widely used one is cubic spline function, proposed by (Monaghan & Lattanzio, 1985), having the following form:

$$W_{ij} = \alpha_d \begin{cases} \frac{2}{3} - q^2 + \frac{1}{2}q^3 & 0 \leq q < 1 \\ \frac{1}{6}(2 - q)^3 & 1 \leq q < 2 \\ 0 & q \geq 2 \end{cases} \quad (8)$$

where α_d = normalization factor, which is $\frac{1}{h}$, $\frac{15}{7\pi h^2}$ and $\frac{3}{2\pi h^3}$ in 1D, 2D and 3D space, $q = \frac{r_{ij}}{h} = \frac{x_i - x_j}{h}$ = the relative distance between particles i and j . $k = 2$ is taken for cubic spline function. The kernel function drops to zero for $|r_{ij}| \geq 2h$, implying that the influence domain in Eq. (8) has a radius of $2h$.

3. GOVERNING EQUATIONS

The governing equations is composed of continuity and motion equations as follows:

$$\frac{D\rho}{Dt} = -\rho \frac{\partial v^\beta}{\partial x^\beta} \quad (9)$$

$$\frac{Dv^\alpha}{Dt} = \frac{1}{\rho} \frac{\partial \sigma^{\alpha\beta}}{\partial x^\beta} + f^\alpha \quad (10)$$

The total stress tensor $\sigma^{\alpha\beta}$ consists of an isotropic hydrostatic pressure p and a deviatoric shear stress s .

$$\sigma^{\alpha\beta} = -p\delta^{\alpha\beta} + s^{\alpha\beta} \quad (11)$$

Where $\delta^{\alpha\beta}$ is Kronecker's delta.

The fluid hydrostatic pressure p in traditional SPH is calculated based on the fluid density change by an equation of state, assuming a weakly compressible fluid (Monaghan, 1994; J.P. Morris, Fox, & Zhu, 1997). The deviatoric shear stress is considered as purely viscous and depends on the fluid models.

4. POST FAILURE BEHAVIOR OF GEO-MATERIAL

Post failure behavior of soil mass can be considered as fluid flow. Fluids can be classified as Newtonian or non-Newtonian fluid based on their viscosity characteristics. However, the fast moving nature of the detached mass and to consider the accumulation at the depositional end, simplified Newtonian Model is effective and have many applications in real analysis. Keeping this issue, simplified Newtonian model is chosen in the current simulation.

According to the Newtonian fluids, flow behavior of fluids follows a linear relationship between shear stress and strain rate with a zero intercept. The slope of the flow curve is constant and is called the viscosity of the fluid. This relationship is known as Newton's Law of Viscosity.

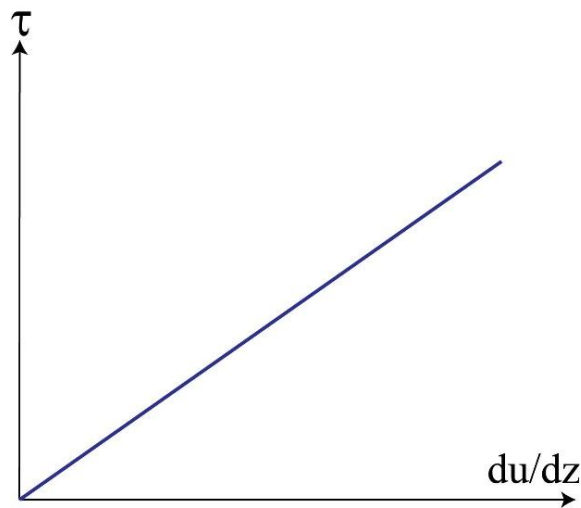


Figure 1: Stress-strain rate relationship of Newtonian model

In 3D analysis , this model is expressed as below:

$$\tau^{\alpha\beta} = \mu \varepsilon^{\alpha\beta} \quad (12)$$

$$\varepsilon^{\alpha\beta} = \frac{\partial v^\beta}{\partial x^\alpha} + \frac{\partial v^\alpha}{\partial x^\beta} \quad (13)$$

where, μ is the dynamic viscosity of a fluid, $\tau^{\alpha\beta}$ is the shear stress tensor, $\varepsilon^{\alpha\beta}$ is the strain rate tensor, α and β are Einstein summation index.

5. EVOLUTION OF PRESSURE

Calculation of pressure in SPH method is generally conducted by solving Equation of State (EOS) or Pressure Poisson Equation (PPE). For incompressible SPH (ISPH), the actual EOS will lead to extremely small-time steps, making the entire solution unstable. In this case, pressure is obtained by solving PPE and provide a smoothing pressure distribution especially near the boundary (A. Khayyer, Gotoh, & Shao, 2008; Abbas Khayyer, Gotoh, & Shao, 2009; Ran, Tong, Shao, Fu, & Xu, 2015; Shao & Lo, 2003). However, a comparison was made between standard SPH & ISPH (Shadloo, Zainali, Yildiz, & Suleman, 2012) and compatible results are found for some benchmark tests. Hence, in the current research, pressure was approximated using the widely used EOS (Liu & Liu, 2003), which is given in the following form:

$$p = B \left[\left(\frac{\rho}{\rho_0} \right)^\gamma - 1 \right] \quad (14)$$

where, ρ_0 is the reference/initial density, ρ is the density at current time step, γ is a dimensionless parameter taken as 7.0 based on literatures, B is the problem dependent parameter and calculated using the following equation.

$$B = \frac{c^2 \rho_0}{\gamma} \quad (15)$$

where, c is the speed of sound.

6. USE OF XSPH VARIANT

XSPH technique was first proposed (Monaghan, 1992; Monaghan & Kocharyan, 1995) to correct the velocity term of each particle in SPH problem domain. According to this technique, the particle movement can be obtained as:

$$\frac{dx_i}{dt} = v_i - \varepsilon \sum_{j=1}^N \frac{m_j}{\rho_j} v_{ij} W_{ij} \quad (16)$$

where, m_j mass of particle j , ρ_j is density of particle j , $v_{ij}(= v_i - v_j)$ is the velocity difference between particle i and j , W_{ij} is the smoothing function and ε is a constant value ($0 \leq \varepsilon \leq 1.0$). This technique considers the contribution from its neighboring particles. As a result, the particle moves in a velocity closer to the average velocity of its neighboring particles. Most of the applications use $\varepsilon=0.3$ and particles are seen to move more orderly for incompressible flows with XSPH technique (Liu & Liu, 2003). Unphysical penetration between approaching particles can be reduced for compressible flows.

7. BOUNDARY CONDITION

The deficiency of particles near the boundary line often lead to penetration of particles beyond the domain or particle blow up can occur. To get rid of this problem, a suitable boundary condition is needed. There have been several methods developed to model this solid boundary condition. Ghost particles were developed to model the free-slip boundary condition for SPH application to solids (Libersky, Petschek, Carney, Hipp, & Allahdadi, 1993). Virtual particles with repulsive forces were proposed for modelling free-slip boundary conditions of a fluid (Monaghan, 1994). For viscous fluid,

no-slip boundary condition was used (J.P. Morris, Fox, & Zhu, 1997; Takeda, Miyama, & Sekiya, 1994). For SPH application to computational geomechanics, no-slip boundary condition was extended to account for stress boundary conditions (Bui, Fukagawa, Sako, & Ohno, 2008).

8. NUMERICAL MODEL FOR SENSITIVITY ANALYSIS

A 3D model was considered to simulate the flow problems under different conditions. The size of the model is chosen in such way that it represents the real scenario (Rahman & Konagai, 2017). Post flow behavior of the detached mass was analyzed in current research. Therefore, the simulation was started in a dam break fashion by releasing the gate at front of the model instantaneously. Afterward, the failed mass started flowing and normalized run-out and height of the flow process was evaluated. The time history of flow path was considered to be a key criterion to check the influence of different parameters. For the current parametric analysis, the different aspect ratio, viscosity, smoothing length, and xSPH coefficient were critically considered.

9. RESULTS & DISCUSSIONS

An attempt is made in this research to quantitatively evaluate the effect of different sensitive parameters on the response of large deformation simulation. A benchmark case of ideal dam break simulation with different configurations and material properties were simulated and their responses were critically discussed.

At first, a simulation was carried out considering normalized run-out distance with time elapse with varying particle sizes ($dx=10\text{mm}$, 15mm , 20mm) for different aspect ratios (1.0, 0.8 & 0.6).

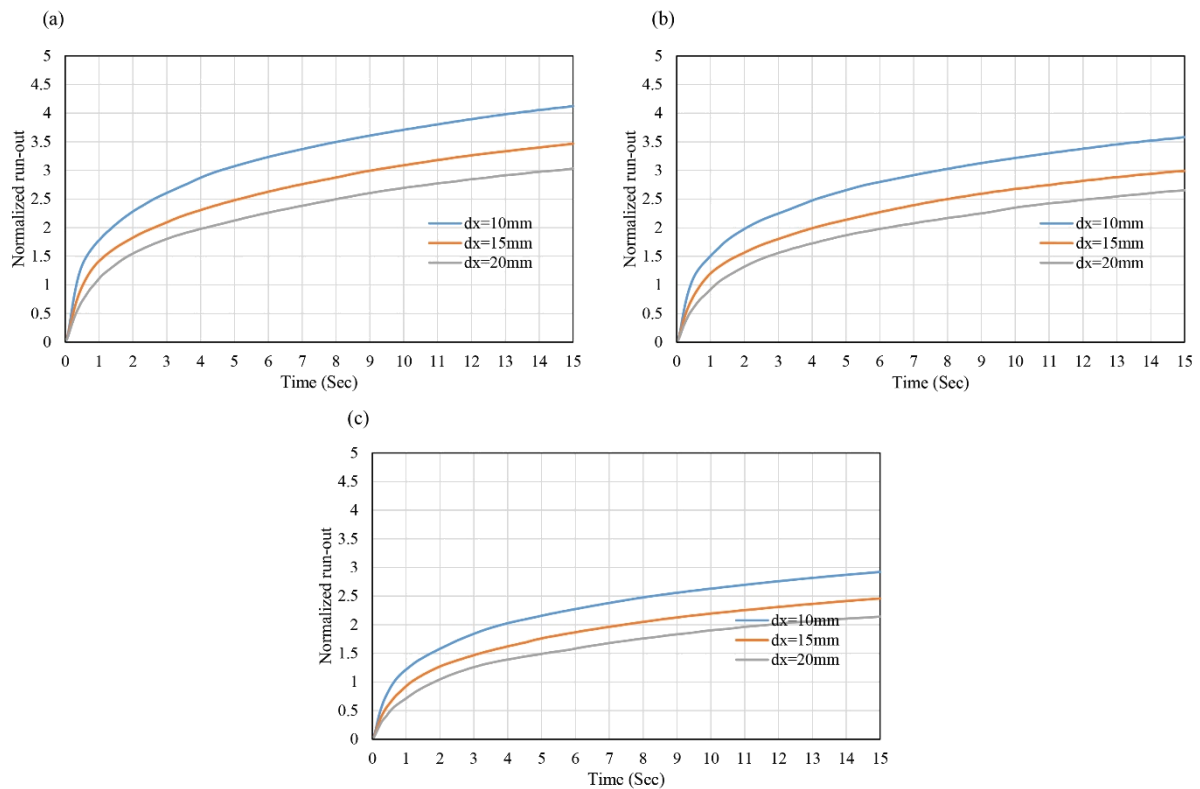


Fig.2: Time-history of normalized surge front; (a) aspect ratio = 1.0, (b) aspect ratio=0.8, (c) aspect ratio=0.6

The time history of normalized surge front for different aspect ratios and different particle sizes are shown in Fig.2. It is seen that normalized run-out distance is found to be increasing with the elapse of time for all cases. Particles with smaller sizes ($dx=10\text{mm}$) show greater runout values than smaller ones. Highest normalized run-out value is found 4.2 for aspect ratio=1.0, whereas this highest value is observed 2.9 for aspect ratio=0.6.

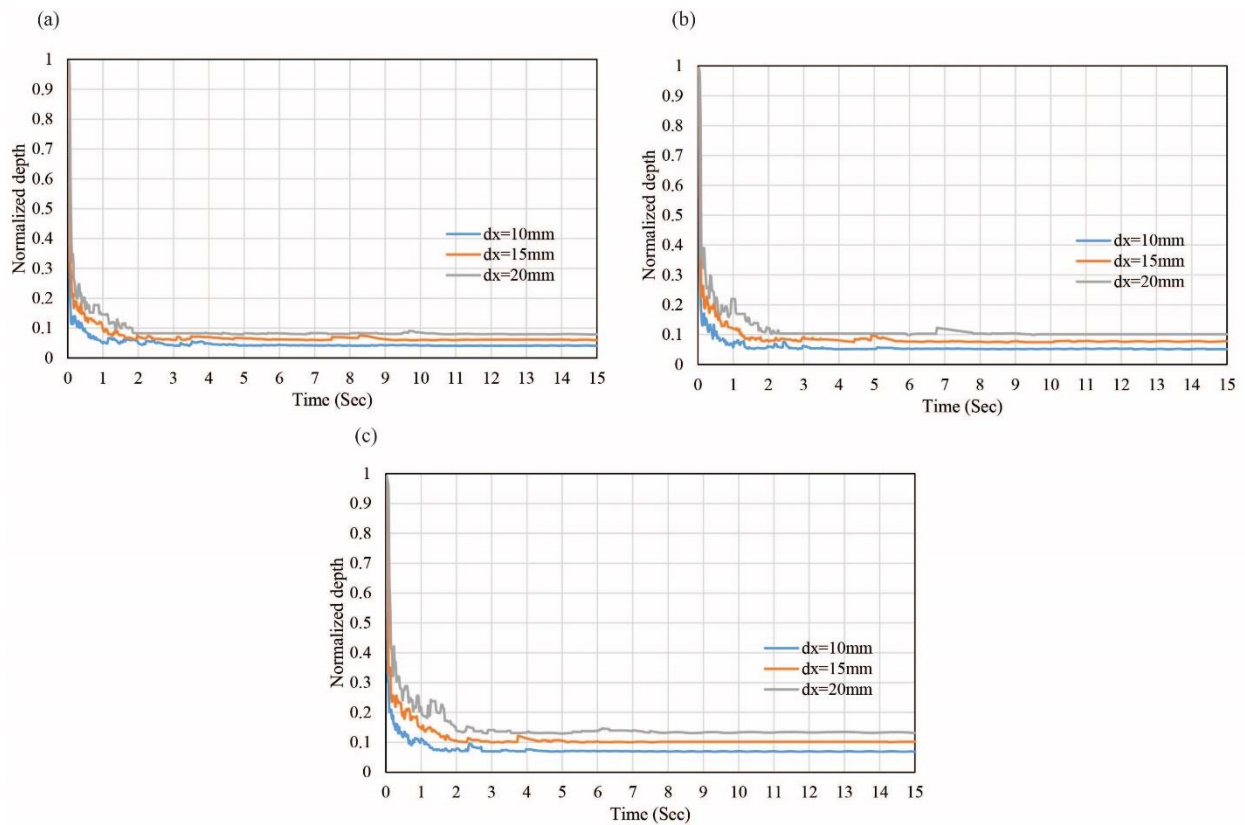


Fig.3: Time-history of normalized front depth; (a) aspect ratio = 1.0, (b) aspect ratio=0.8, (c) aspect ratio=0.6

From the normalized depth vs. time plot shown in Fig.3, it is seen that normalized depth is found decreasing with an increase in time for each aspect ratios. Again, a high fluctuation is observed in the initial 2-3 sec time duration. After that, a quite straight parallel lines are observed for different particle sizes. Again, normalized depth is found greater for larger particle sizes ($dx=20\text{mm}$) than smaller particles ones for three aspect ratio cases (1.0, 0.8 & 0.6).

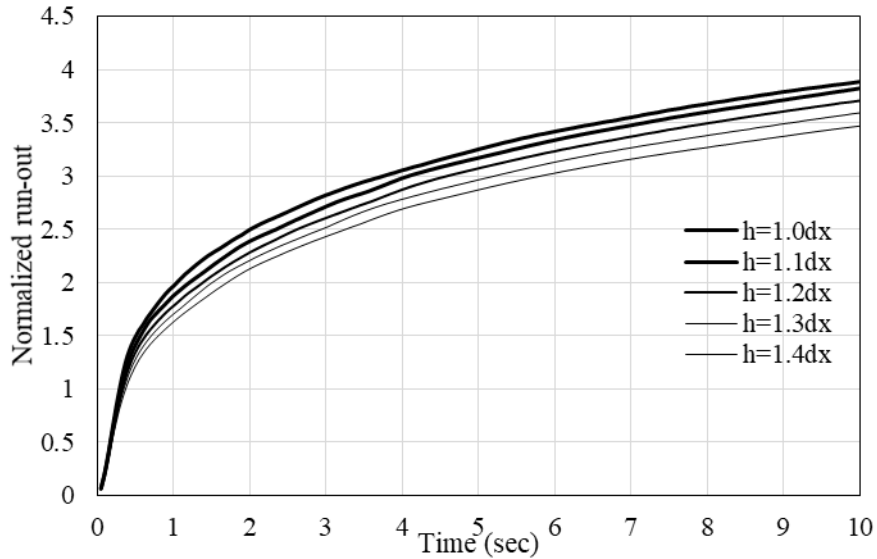


Fig.4: Effect of smoothing length on run-out length in SPH simulation

Later, different smoothing lengths ($h=1.0dx$, $1.1dx$, $1.2dx$, $1.3dx$, $1.4dx$) are taken into consideration and their influences on normalized run-out distance were also simulated and a graphical representation was plotted (Fig.4). From the plot, normalized run-out was found higher for smaller smoothing lengths ($h=1.0dx$), whereas it is found lesser for higher smoothing lengths ($h=1.4dx$).

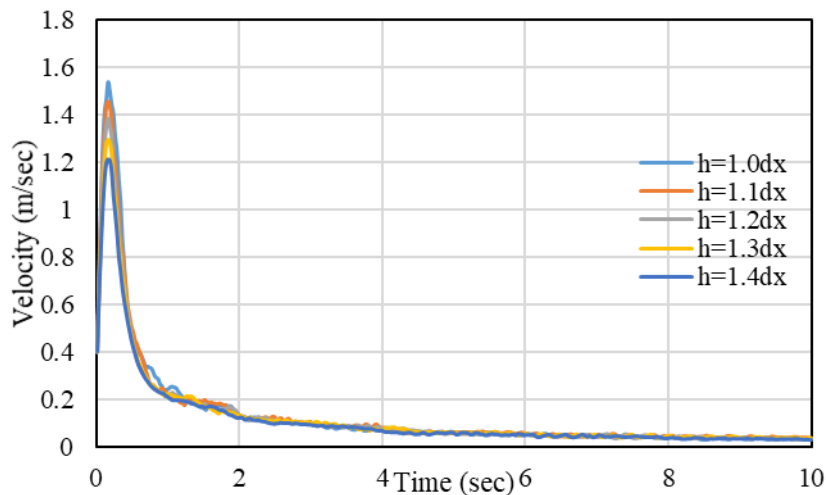


Fig.5: Effect of smoothing length on velocity response in SPH simulation

Next, a simulation was carried out to observe the effect of various smoothing lengths on velocity response of the material. From the graphical plot (Fig.5), it is seen that velocity is found suddenly increasing from a value of 0.4 m/s at time 0 sec to 1.5 m/s at time less than 1 sec ($h=1.0dx$), followed by a sharp fall to a value less than 0.2 m/s . After 2 sec, velocity profile shows a straight-line pattern with a value less than 0.1 m/s for all smoothing lengths ($h = 1.0dx$, $1.1dx$, $1.2dx$, $1.3dx$, $1.4dx$). But velocity profile depicts variation at the peak curves showing a maximum velocity of 1.5 m/s for smaller smoothing length ($h=1.0dx$) and a minimum value of 1.2 m/s for larger smoothing length ($h=1.4dx$).

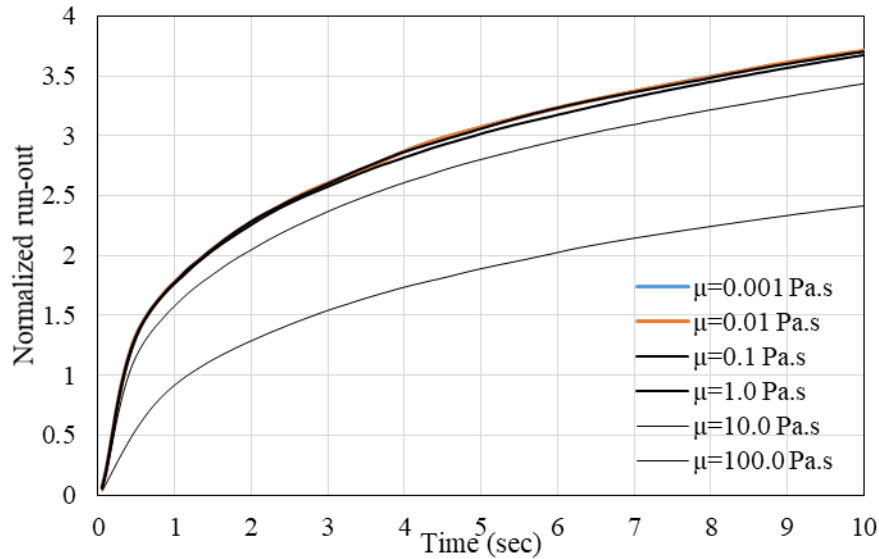


Fig.6: Effect of viscosity on run-out length in SPH simulation

Different viscosity values are taken into consideration to evaluate its effect on run-out distance in our current simulation. Normalized run-out is found decreasing (2.4) with higher viscosity values (100.0 Pa.s), whereas it shows higher value (3.7) for smaller viscosity values less than 1.0 Pa.s (Fig.6).

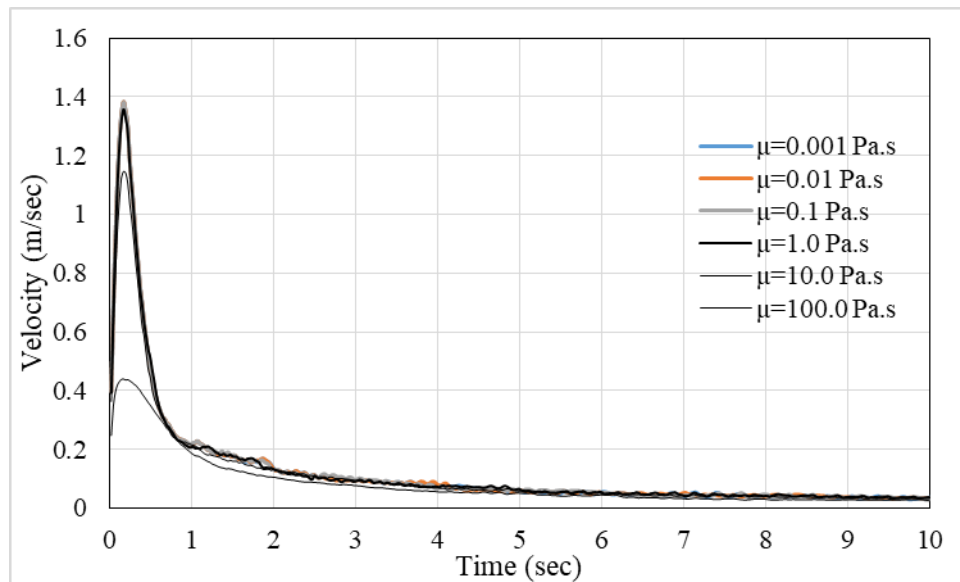


Fig.7: Effect of viscosity on velocity response in SPH simulation

Next, viscosity values on velocity response is simulated. From graphical representation (Fig.7), it is seen that velocity gets its peak almost 1.39 m/s at a time less than 1 sec from 0.25 m/s at time 0 sec. Then velocity profile follows a sudden fall, reaching velocity 0.2 m/s at around 1 sec. After 1 sec, velocity decreases gradually following a straight-line trend for all ranges of viscosity values. Again, less than 1 sec, velocity fluctuates greatly showing 0.43 m/s for higher viscosity (100.0 Pa.s). But peak velocity (1.39 m/s) is observed for smaller viscosity values less than 1.0 Pa.s.

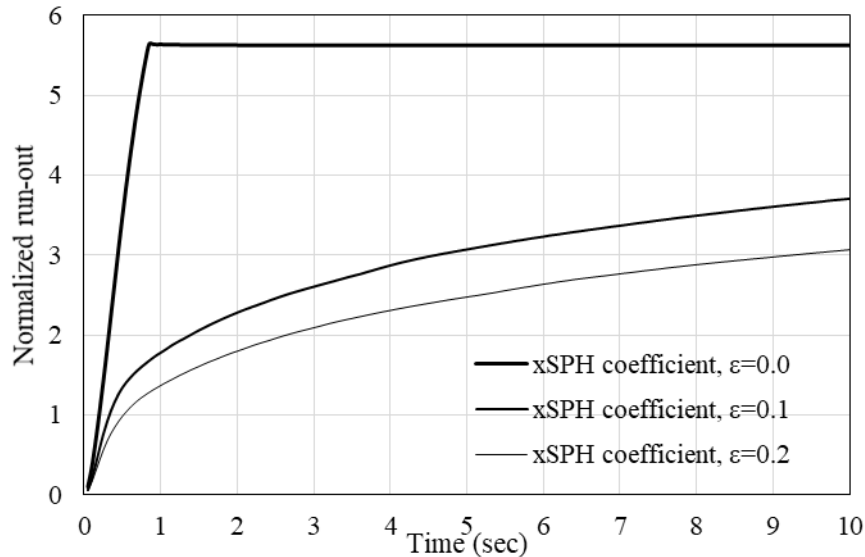


Fig.8: Effect of XSPH coefficient in SPH simulation

XSPH coefficient parameter ϵ has a great influence on normalized run-out values (Fig.8). For $\epsilon = 0.0$, run-out distance suddenly increases from 0 to 5.6 up to time 1 sec. After 1 sec, run-out distance follows a constant value 5.6. Again, run-out values are found to increase with a decrease in XSPH coefficient parameter.

10. CONCLUSIONS

The sensitivity of critical parameters was evaluated from series of numerical simulations. A 3D dam break type model, similar to real scale mass considering law of similarity was chosen for numerical analysis. For each cases, simulations were continued to sufficient time to capture the whole scenario. It was found that the particle sizes significantly affect the surge front in SPH environment, which needs to be quantitatively described in real landslide/debris flow simulation by SPH method. The effect of smoothing length and viscosities were not strongly significant and may have freedom in numerical application. In addition, the xSPH coefficient performed quite well in averaging the velocity of particles as the simulation without xSPH coefficient showed divergence for long time simulation. Overall, the sensitivity analysis conducted in this research may provide some useful guidelines for numerical landslide or debris flow modelling in SPH environment. However, the research extent is limited to viscous model, thought there are other methods need to be critically analysed. The future works may highlight the sensitivity of diverse constitutive modelling in SPH environment.

REFERENCES

- Bui, H. H., Fukagawa, R., Sako, K., & Ohno, S. (2008). Lagrangian meshfree particles method (SPH) for large deformation and failure flows of geomaterial using elastic-plastic soil constitutive model. *International Journal for Numerical and Analytical Methods in Geomechanics*, 32(12), 1537–1570. <https://doi.org/10.1002/nag>
- Cummins, S. J., & Rudman, M. (1999). An SPH Projection Method. *Journal of Computational Physics*, 152(2), 584–607.
- Gingold, R. A., & Monaghan, J. J. (1977). Smoothed particle hydrodynamics - Theory and application to non-spherical stars. *Monthly Notices of the Royal Astronomical Society*, 181, 375–389.
- Khayyer, A., Gotoh, H., & Shao, S. D. (2008). Corrected Incompressible SPH method for accurate water-surface tracking in breaking waves. *Coastal Engineering*, 55(3), 236–250.

- <https://doi.org/10.1016/j.coastaleng.2007.10.001>
- Khayyer, Abbas, Gotoh, H., & Shao, S. (2009). Enhanced predictions of wave impact pressure by improved incompressible SPH methods. *Applied Ocean Research*, 31(2), 111–131. <https://doi.org/10.1016/j.apor.2009.06.003>
- Libersky, L. D., Petschek, A. G., Carney, T. C., Hipp, J. R., & Allahdadi, F. A. (1993). High Strain Lagrangian Hydrodynamics: A Three-Dimensional SPH Code for Dynamic Material Response. *Journal of Computational Physics*, 109(1), 67–75.
- Liu, G. R., & Liu, M. B. (2003). Smoothed Particle Hydrodynamics: A Meshfree Particle Method. *World Scientific Publishing Co. Pte. Ltd.*
- Lucy, L. B. (1977). A numerical approach to the testing of the fission hypothesis. *The Astronomical Journal*, 82(12), 1013–1024. <https://doi.org/10.1007/s00769-003-0757-y>
- Monaghan, J. J. (1992). Smoothed Particle Hydrodynamics. *Annual Review of Astronomy and Astrophysics*, 30, 543–574. <https://doi.org/10.1109/fie.1994.580564>
- Monaghan, J. J. (1994). Simulating Free Surface Flows With SPH. *Journal of Computational Physics*, 110(2), 399–406.
- Monaghan, J. J. (1997). Implicit SPH Drag and Dusty Gas Dynamics. *Journal of Computational Physics*, 138(2), 801–820.
- Monaghan, J. J. (2002). SPH compressible turbulence. *Monthly Notices of the Royal Astronomical Society*, 335(3), 843–852. <https://doi.org/10.1046/j.1365-8711.2002.05678.x>
- Monaghan, J. J., & Kocharyan, A. (1995). SPH simulation of multi-phase flow. *Computer Physics Communications*, 87(1–2), 225–235. [https://doi.org/10.1016/0010-4655\(94\)00174-Z](https://doi.org/10.1016/0010-4655(94)00174-Z)
- Monaghan, J. J., & Lattanzio, J. C. (1985). A refined particle method for astrophysical problems. *Astronomy and Astrophysics*, 149(1), 135–143.
- Morris, J. P., Zhu, Y., & Fox, P. J. (1999). Parallel simulations of pore-scale flow through porous media. *Computers and Geotechnics*, 25(4), 227–246. [https://doi.org/10.1016/S0266-352X\(99\)00026-9](https://doi.org/10.1016/S0266-352X(99)00026-9)
- Morris, J.P., Fox, P. J., & Zhu, Y. (1997). Modeling Low Reynolds Number Incompressible Flows Using SPH. *Journal of Computational Physics*, 136(1), 214–226. <https://doi.org/10.1515/polyeng-2016-0102>
- Morris, Joseph P. (2000). Simulating surface tension with smoothed particle hydrodynamics. *International Journal for Numerical Methods in Fluids*, 33(3), 333–353. [https://doi.org/10.1002/1097-0363\(20000615\)33:3<333::AID-FLD11>3.0.CO;2-7](https://doi.org/10.1002/1097-0363(20000615)33:3<333::AID-FLD11>3.0.CO;2-7)
- Rahman, M. A., & Konagai, K. (2017). Substantiation of debris flow velocity from super-elevation: a numerical approach. *Landslides*, 14(2), 633–647. <https://doi.org/10.1007/s10346-016-0725-3>
- Ran, Q., Tong, J., Shao, S., Fu, X., & Xu, Y. (2015). Incompressible SPH scour model for movable bed dam break flows. *Advances in Water Resources*, 82, 39–50. <https://doi.org/10.1016/j.advwatres.2015.04.009>
- Shadloo, M. S., Zainali, A., Yildiz, M., & Suleman, A. (2012). A robust weakly compressible SPH method and its comparison with an incompressible SPH. *International Journal for Numerical Methods in Engineering*, 89(8), 939–956. <https://doi.org/10.1002/nme.3267>
- Shao, S., & Lo, E. Y. M. (2003). Incompressible SPH method for simulating Newtonian and non-Newtonian flows with a free surface. *Advances in Water Resources*, 26(7), 787–800. [https://doi.org/10.1016/S0309-1708\(03\)00030-7](https://doi.org/10.1016/S0309-1708(03)00030-7)
- Swegle, J. W. (1992). *Report at Sandia National laboratories.*
- Takeda, H., Miyama, S. M., & Sekiya, M. (1994). Numerical Simulation of Viscous Flow by Smoothed Particle Hydrodynamics. *Progress of Theoretical Physics*, 92(5), 939–960. <https://doi.org/10.1143/ptp/92.5.939>
- Zhu, Y. I., Fox, P. J., & Morris, J. P. (1999). A pore-scale numerical model for flow through porous media. *International Journal for Numerical and Analytical Methods in Geomechanics*, 23(9), 881–904. [https://doi.org/10.1002/\(SICI\)1096-9853\(19990810\)23:9<881::AID-NAG996>3.0.CO;2-K](https://doi.org/10.1002/(SICI)1096-9853(19990810)23:9<881::AID-NAG996>3.0.CO;2-K)

EVALUATION OF LOW VOLUME RURAL ROAD DAMAGE IN COASTAL AREAS OF BANGLADESH

Md. Jahangir Alam¹, Md. Shamsul Hoque², Muhammad Saiful Islam^{*3} and Mohammed Emdadul Karim⁴

¹*Professor, Department of Civil Engineering, Bangladesh University of Engineering and Technology, Bangladesh, e-mail: Jahangir.buet@gmail.com*

²*Professor, Department of Civil Engineering, Bangladesh University of Engineering and Technology, Bangladesh, e-mail: shoque@ce.buet.ac.bd*

³*Research Assistant, Department of Civil Engineering, Bangladesh University of Engineering and Technology, Bangladesh, e-mail: saifulislamce@gmail.com*

⁴*Research Assistant, School of Natural and Built Environments, University of South Australia, Australia e-mail: mohammad.karim@mymail.unisa.edu.au*

****Corresponding Author***

ABSTRACT

The developing country, like Bangladesh spends a lot of budget each year for elevating, widening or repairing the existing coastal rural roads. These rural roads are constructed for a design life of 10 years. But these low volume roads loose serviceability within two or three years due to improper construction and design. To find out the reasons of less sustainability, different rural road sites in coastal region were visited by the authors and sandy soil (used for Improved Subgrade) and clayey soil (borrow pit soil used for side slope and shoulder) were collected from 28 sites. And several tests were conducted to identify geotechnical properties. DCP tests were conducted in field and results were analyzed by AfCAP LVR-DCP software which show inadequate value of pavement and shoulder. Several reasons were identified which are responsible for less sustainability of rural roads. The reasons are use of unsuitable material, poor compaction, borrow pit location at toe, vehicle movement over soft shoulder, consolidation settlement due to soft soil under road embankment, inadequate design of palasiding and slope protection, erosion of side slope by wave action

Keywords: Rural road construction, DCP, Soft soil, Coastal road, Climate impact.

1. INTRODUCTION

The design life of the rural road pavement is 10 years (Road Design Standards of LGED, 2005). But most of the rural roads damaged within 2-3 years as per road users' opinion. Every year huge amount of money is used to maintain or repair the rural roads. In Figure 1, the total maintenance cost of last ten years is shown.

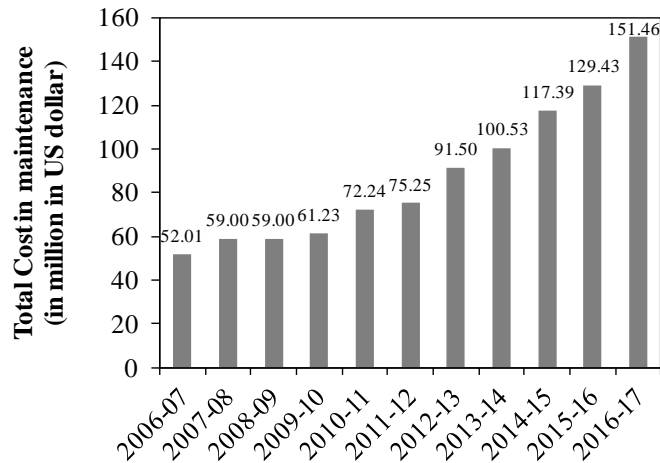


Figure 1. Yearly rural road maintenance cost (LGED, October 2017).

Field investigations have been carried out to identify causes of road damages in coastal regions. A lot of challenges were identified in rural road construction in coastal areas of Bangladesh. At the same time, a lot of bad practices also were identified. This paper describes the challenges and bad practices in rural road construction. In this case study, randomly selected roads in rural coastal areas were visited and the reasons of damage were identified based on visual observations and engineering judgement.

Among the many reasons of poor quality of road construction, unavailability of construction materials, lack of compaction or poor compaction and inappropriate design of palisading in challenging roads adjacent to pond or khal or river are three major causes which should be addressed immediately.

2. DAMAGE EVALUATION

Existing earthen roads are upgraded as shown in Figure 2. Earthen roads are widened using borrow pit soil from nearby land. Mud or wet clay from borrow pit are used in widened part without compaction. 300 mm thick Improved Subgrade (ISG) is prepared using available local sand filling into box cut on top of the existing road. 150 mm thick sub-base is prepared using available local sand and brick chips mixed in 1:1 ratio. Then 150 mm thick base is prepared using brick chips only. 25 mm thick bituminous carpeting is done on base.

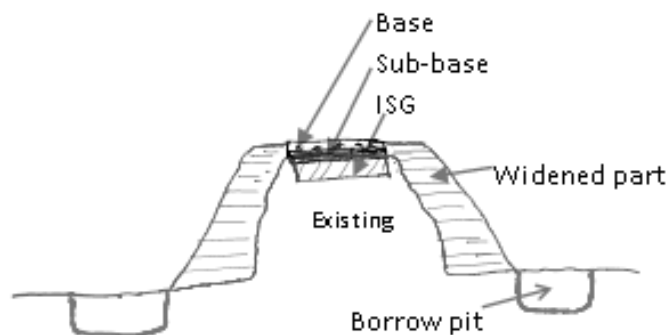


Figure 2. Typical rural road widening.

2.1 Soil sample

Borrow pit samples from randomly selected 28 spots in coastal districts are collected to classify the soil. Location of soil samples are mentioned in the legend of Figure 3 and Figure 4. Sand samples which are used in ISG and sub-base were also collected to see whether those meet the specification prepared by LGED. Grain size distributions of sandy soils are shown in Figure 3. Liquid Limit and Plasticity Index of borrow pit samples are shown in plasticity chart in Figure 4.

Among the 28 sand samples, 5 samples are poorly graded sand, 5 samples are sandy silt and other 18 samples were silty sand as per the Unified Soil Classification System (USCS) (Figure 4). The Fineness Modulus (FM) of 4 samples are more than 0.80, 2 samples between 0.50 and 0.80. Other samples have the FM ranged from 0.00 to 0.50. As per AASTHO, 14 samples are of group A-4, 7 samples of A-3 and of A-2-4 group 6 samples. Fines content of the sandy soil varied from 0 to 82%. Most of the sand samples did not meet the requirement of LGED specification. Due to unavailability of specified sand of FM greater than 0.80, contractors frequently use locally available very fine sand, silty sand and sandy silt in ISG and sub-base with poor compaction control. This is one of the reasons of unsustainable rural roads in Bangladesh.

Among 28 borrow pit samples, 6 samples were silt, 6 samples were fat clay and 18 samples were lean clay (as per USCS) (Figure 4). These soils are used in widened part and shoulder of embankment without compaction. Benching and layer by layer compaction is not done in widened part. So, this is not integrated with existing embankment. As a result, shoulder and widened part of embankment is soft where vehicle runs frequently during passing over.

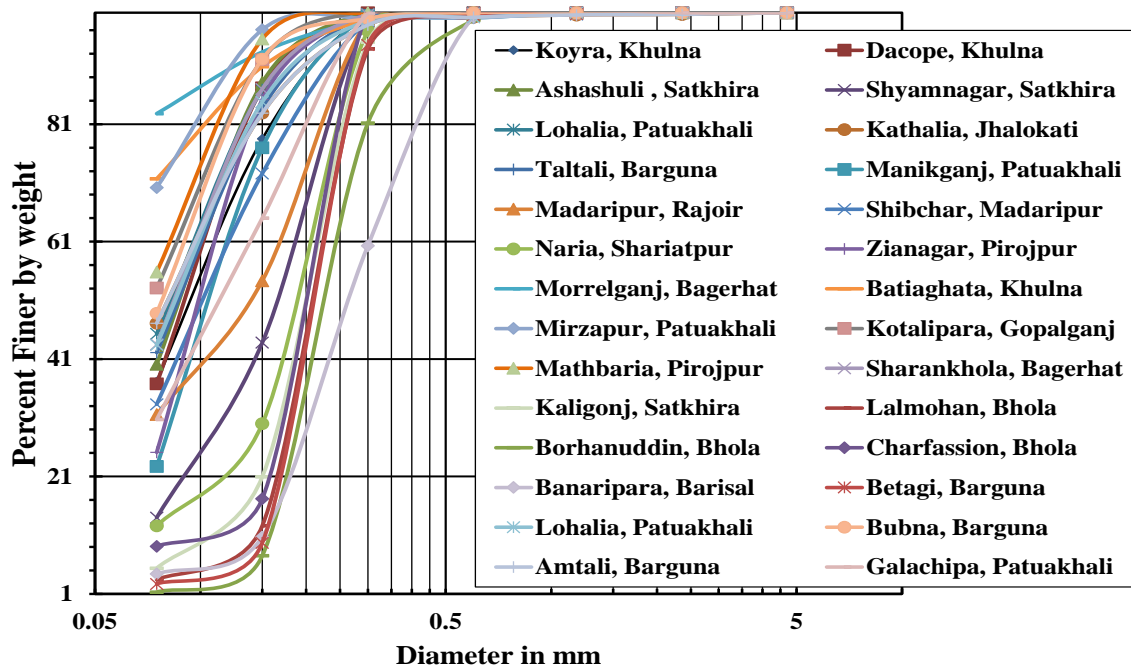


Figure 3. Grain size distribution of sands used for ISG and subbase in coastal districts of Bangladesh.

2.2 Sub-base and Base

Recommended size of the clay burned brick chips for subbase and base is 38mm down well graded brick chips (Road Design Standards of LGED, 2005). In many cases, it was found that 70% (by weight) of the total brick chips are larger than 38mm (see Figure 5). As per LGED specification, the ratio of the brick chips and sand should be 1:1 in subbase. In such a mixture, the brick chips become isolated and suspended in the fine sand matrix where property of sand dominates in stress-strain behaviour of the mixture. This ratio need to be revised based on experimental study using different mix ratios. In the field, more than 65% fine sand was found in sand-brick chips mixture. In the base, used brick chips are made from 2nd class clay bricks which are not properly burned in many cases. This type of brick chips are easily break-down during vehicle movement resulting rutting at wheel position of the road. These sub-base and base are responsible for rural roads with rutting, a lot of pot holes and damage.

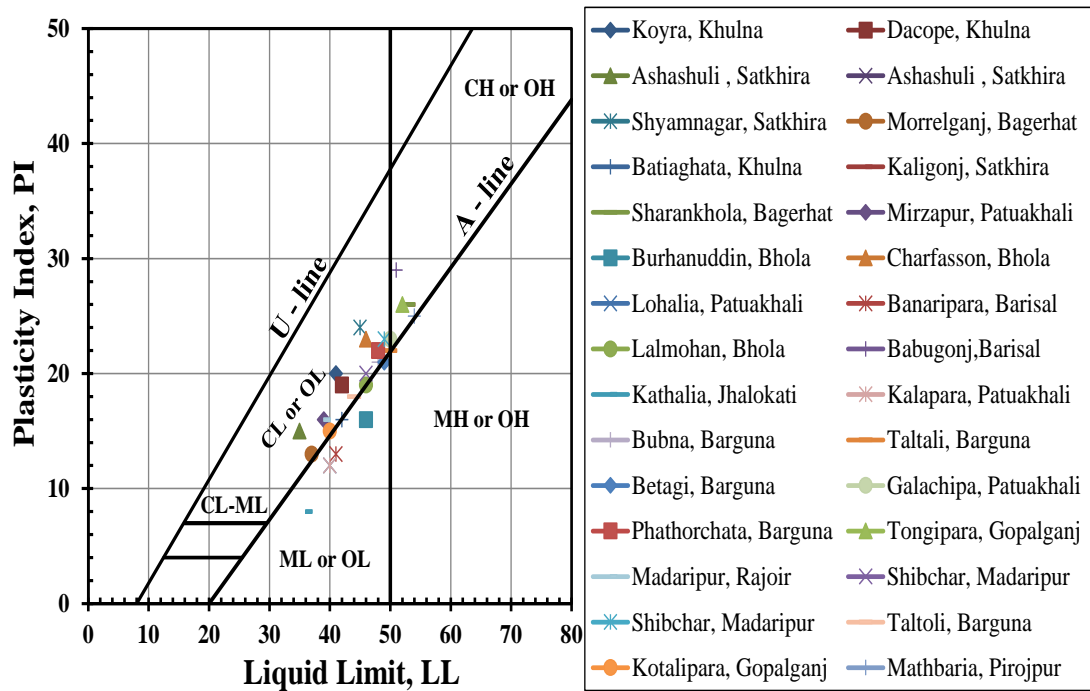


Figure 4: Position of borrow pit soil samples of coastal districts in the plasticity chart



Figure 5: Sub base and base sample collected from kaliganj, Satkhira

2.3 Moisture Content

During site visit, it is found that workers do not have any training or knowledge about optimum moisture content. It is possible to get better CBR value by maintaining the moisture content and proper compaction. So, better performance of road can be achieved by supplying the portable moisture meter and giving training to the workers, how to measure the moisture content and do better compaction.

2.4 Side Slope

Side slopes of roads were found steeper (1V:1H) than the design value (Rural Road Design Standards of LGED (2005) is 1V:1.5H for clayey soil, 1:2 clayey sand and 1:3 for sand or silty sand). Figure 6 shows a road at Bilaspur, Kaziarchar, Shariatpur. As the slope is steeper and the height of the road is more than 3.66 m, a surface crack was observed on the slope. Due to the steeper side slope and poor compaction, the crack also appeared on the shoulder of the road at Uttarpara, Uzirpara, Barisal (see Figure 7).

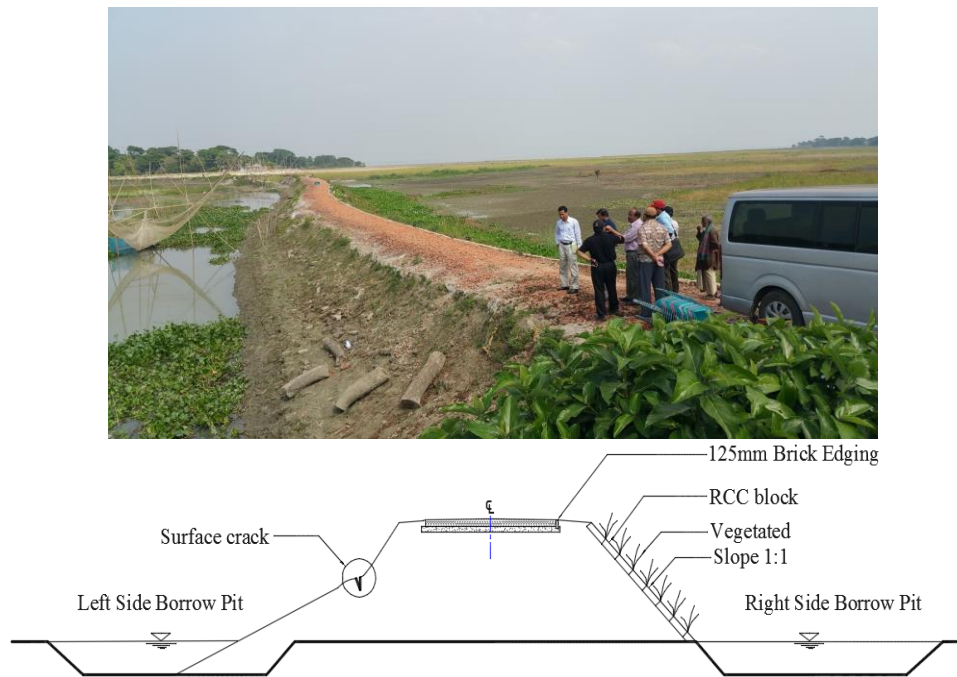


Figure 6: Failure line is observed in a road of Bilashpur, Kaziarchar, Shariatpur: Photograph, schematic diagram.



Figure 7: Steep side slope of rural roads in the study area (Location: Uttarpara, Uzirpar, Barishal).

2.5 Borrow pit location

Borrow pit locations were found at the toe of embankment. Borrow pit location should be at least 3 m or 1.5 times of road height (which one is greater) away from toe line (Road Design Standards of LGED, 2005). But in Figure 8, it is observed that the location of the borrow pit is at the toe of embankment. This is a reason of unsustainable rural road.



Figure 8: Borrow pit was at the toe of the road. (Location: Babubazar, Barishal).

2.6 Road along Bank or River/Khal

Some rural roads run along the bank of river or khal (Figure 9). This kind of road needs slope protection works for sustainable road construction. Sometimes, slope protection work is done using CC block revetment as shown in Figure 10. This is a typical design which is followed everywhere without any slope stability analysis. That is why sometimes slope failures are observed as shown in Figure 11. Limited fund of rural road construction is a reason of not doing any proper slope protection design.



Figure 9: Road along khal/river

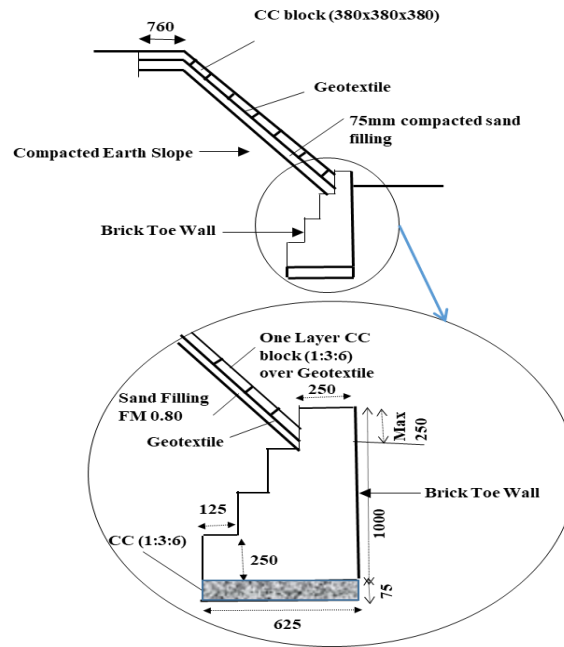


Figure 10: Schematic diagram of designed slope protection.

Palisading is done to stabilize the slope. In most of the cases palisading does not work properly. Figure 12 shows the design of palisading followed by LGED. Firstly, the precast piles of 3 m length are driven into the existing soft soil at a c/c distance of 0.90 m. Thereafter the RCC precast plates are hooked using nuts and bolts. After one or two years of construction the nuts and bolts become corroded and slipped from hooked piles (see Figure 13). Besides, in between two vertical RCC plates small gap exist through which the soil washed away day by day and erode the slope (Figure 13). Later this design is modified by LGED. They used cast in place plates instead of precast plates. However, this system is not stable in many soil conditions of coastal districts. The posts are inserted within the soft soil layer. Existing typical design and construction methodology of palisading need to be revised. Palisading design need to be modified with proper stability analysis.



Figure 11. Embankment slope failed.

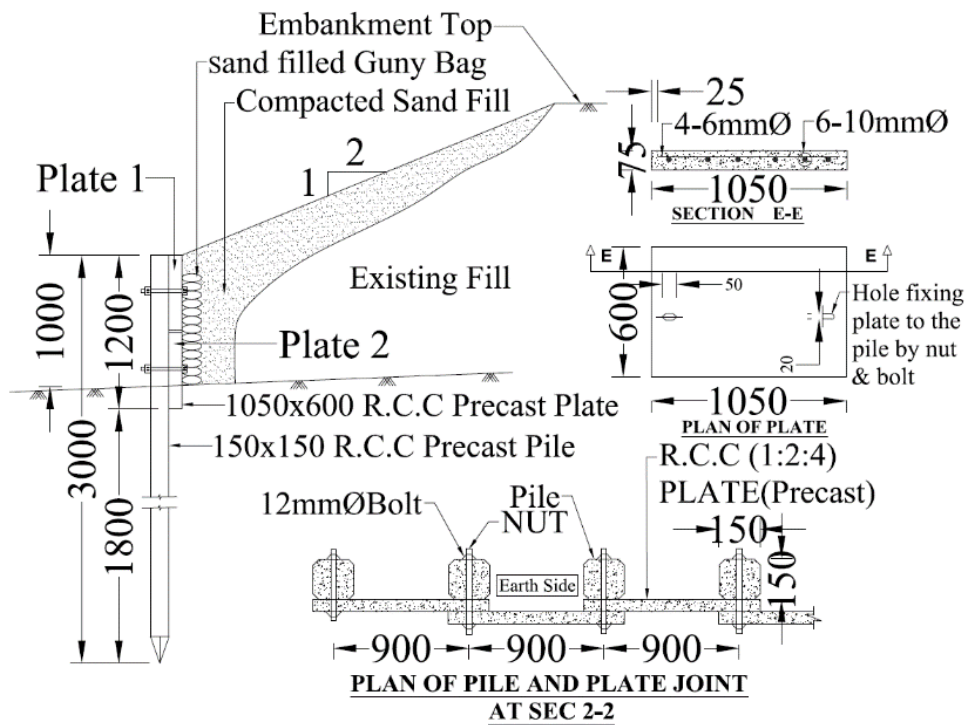


Figure 12: A typical design of palisading implemented by LGED.



Figure 13: Nut corroded, and Soil washed out in between the plates.

2.7 Fish Farming along Road

Crab, lobster and other fish farming in the coastal area are very common in Bangladesh. So, in the both side of the road the water exists throughout the year. Due to shallow water, wind generated waves erode side slopes (see Figure 14). In such location, soil is not available for widening and elevating road. To overcome this problem, dewatering of fish farm is done for road construction and

the muds of the fish farms are used for road widening. Figure 15 shows damaged slope repairing using mud of dewatered fish farm. The soil is too wet to compact.



Figure 14: Side slope of rural road washed away by wave action.



Figure 15: Mud dumping at side slope from dewatered fish farm (Location: Dumuria, Khulna)

2.8 Approach road

Approach road must be designed and constructed in proper way to avoid differential settlement between abutment and approach road. In Figure 16, photograph are added to show the settlement of approach road. Geotextile and CC blocks were used for slope protection at approach embankment. Consolidation settlement of underlying soft soil, lack of compaction of approach embankment and inadequate wing wall are the major reasons of approach road damages.

2.9 Rain Cut Erosion and Slip Circle Failure

Vegetation don't naturally grow immediately after construction. Bare soil is vulnerable to rain cut erosion during rainy season immediately after completion of construction. Figure 17 shows such a situation.



Figure 16: Damages of an approach road of a bridge.



Figure 17: Rain cut erosion in shoulder without vegetation

Vegetation is eco-friendly and has a very beneficial effect on the side slope protection. But, due to lack of maintenance and inadequate sunlight, it does not grow properly to protect the slope (Figure 18). Sometimes, deep seated slope circle failure occur which cannot be protected by vegetation only.

2.10 Overloading

When a road network is developed in rural area, economic activity increases. Some people build multi-storied buildings beside road. So, loaded trucks enter into rural roads for which the road is not designed. During passing other vehicle, wheels of truck go on soft shoulder causing initiation of

damage at pavement edge and shoulder (Figure 19). Because of frequent movement of loaded truck the small damage becomes greater.



Figure 18: Slope failed in a vegetated slope



Figure 19: Truck position at the edge of pavement and shoulder

2.11 Road Settlement

Nearly 85 percent of Bangladesh is underlain by deltaic and alluvial deposits of Ganges, Brahmaputra, and Meghna river systems (Alam et al, 1990). In the previous studies of the coastal region of Bangladesh, it was found that the sub-surface soil is soft (Kabir et al, 2000; Nath et al, 2017). At least 4-8 m soft clay exists at top layer of subsoil in coastal districts. Figure 20 shows a bore log of plot for Civil Surgeon office, Gopalganj. In another research report on “Ground Improvement on Khulna Soft Soil” revealed that more than 15 m soft clay layer exist at top of subsoil in Khulna region (AsCAP final report, 2017). The soft soils consist of silt or clay. Besides, in that region, in some places, an organic clay layer of 3-5m thickness was found. This organic layer was formed from the decomposition of mangrove vegetation of the largest mangrove forest of Bangladesh (Kabir et al, 2000). As the soils of the coastal area are soft and sometimes those are organic, settlement of the newly constructed road or widened or elevated road continues more than 10 years. This settlement is not uniform along longitudinal direction of road.

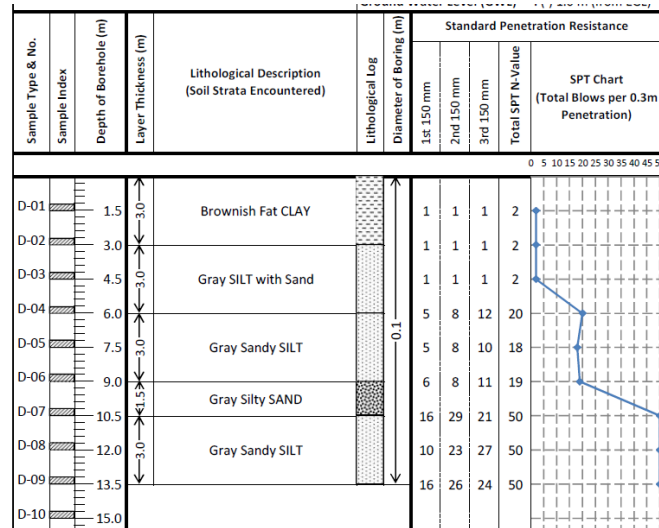


Figure 20: A subsoil bore log at Civil Surgeon Office, Gopalganj, Dhaka

When roads are constructed on this subsoil, consolidation and squeeze out of soft clay cause subsidence, cracking and rutting of constructed road. Subsoil investigation should be mandatory for road project in coastal areas. Special attention should be given in the planning and design phase of road projects. Figure 21 shows the settlement of road on soft soil. In the both sides of the road fish farm is full of water.

2.12 Rutting and Water Logging

When roads are constructed, crown and 3% lateral slope is maintained (Road Design Standards of LGED, 2005). After one year of construction, rutting and subsidence of pavement create water logging on the road pavement. This water logging damages the bituminous carpeting and subsequently base layer. Two photographs of Khulna region are exhibited in Figure 22 shows the field scenario.



Figure 21: A Portion of road settled



Figure 22: Water logging on the settled pavement and wide spread pot holes

3. DCP TEST ON PAVEMENT AND SHOULDER

The recommended CBR value versus DCP penetration per blow for rural road construction was collected from LGED as shown in Figure 23. To compare the LGED recommended DCP values with field DCP values, total 34 DCP (Dynamic Cone Penetration) tests were conducted in rainy season on some village roads in Khulna district, Bangladesh. Test locations are listed in Table 1. Results of DCP tests done on road pavement are shown in Figure 24 whereas results of DCP tests done on shoulders are shown in Figure 25. In Figure 24 and Figure 25, the black lines are the LGED recommended maximum DCP penetration per blow (denoted as DN in mm/blow) for various layers of pavement. Where DN exceeded black line indicates not meeting the requirement set by LGED.

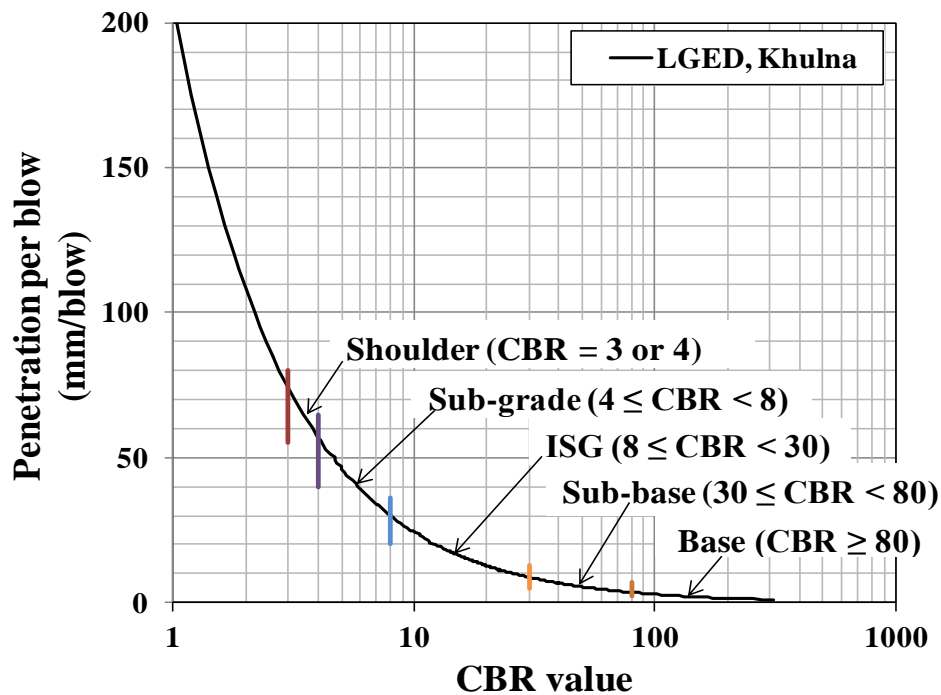


Figure 23. CBR versus DCP penetration rate (mm/blow) recommended by LGED for rural road.

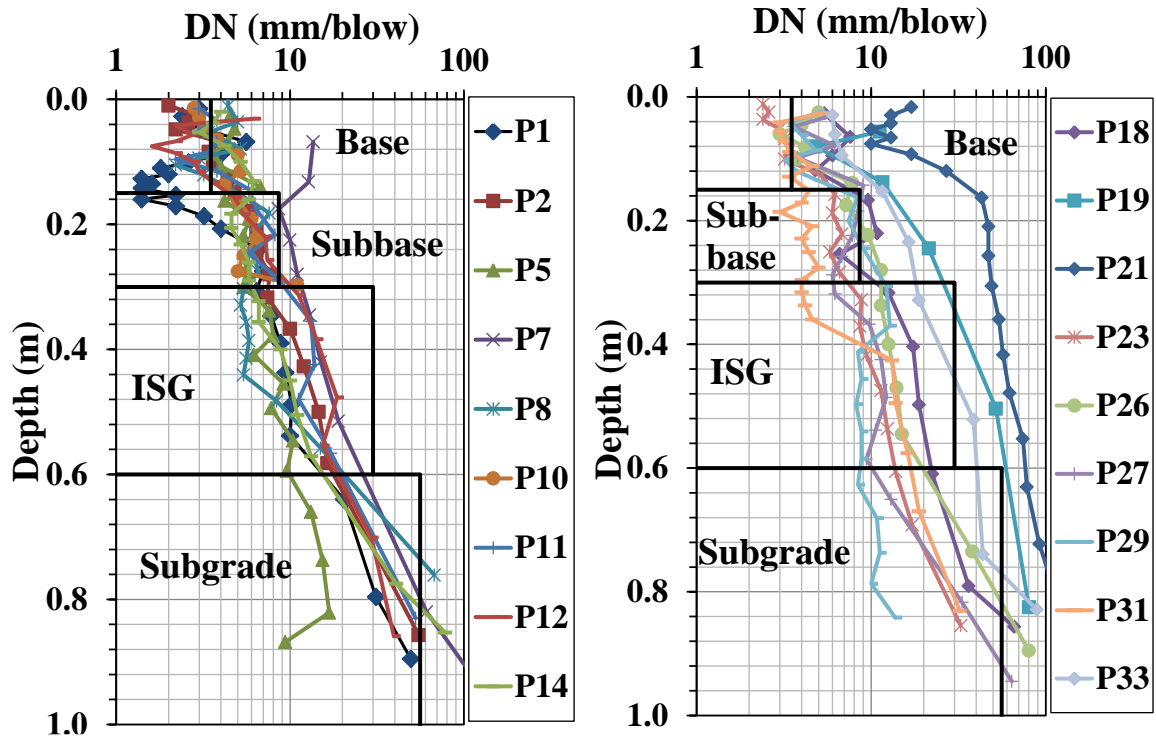


Figure 24. DCP test results conducted on the village road

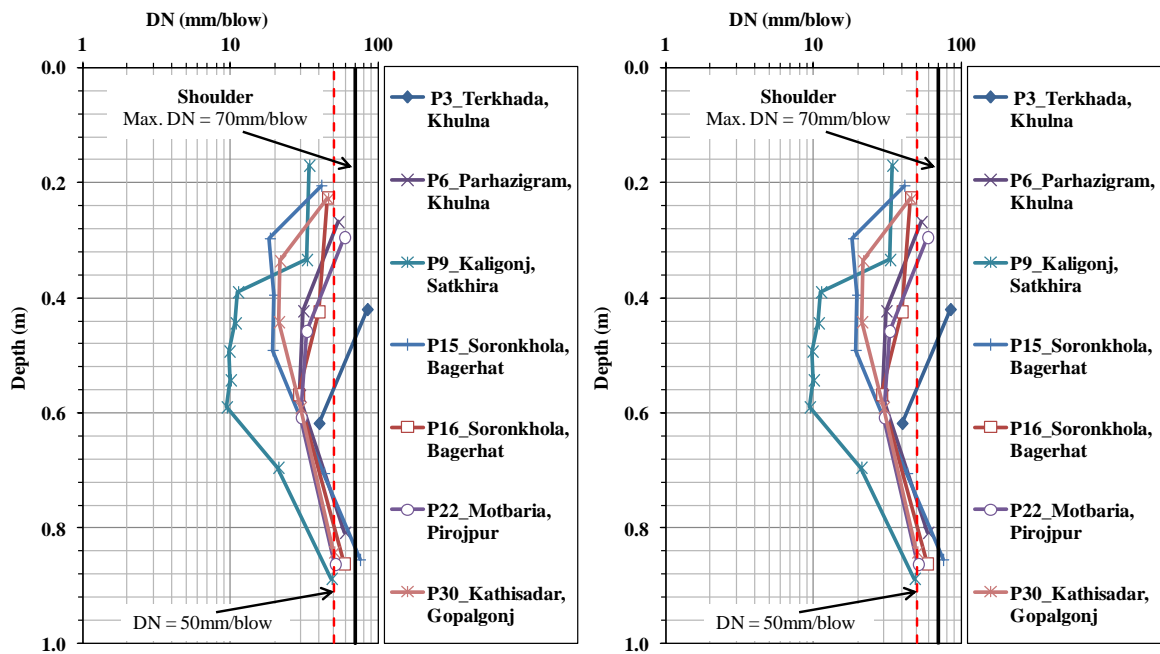


Figure 25. DCP tests conducted on the shoulder of the rural road

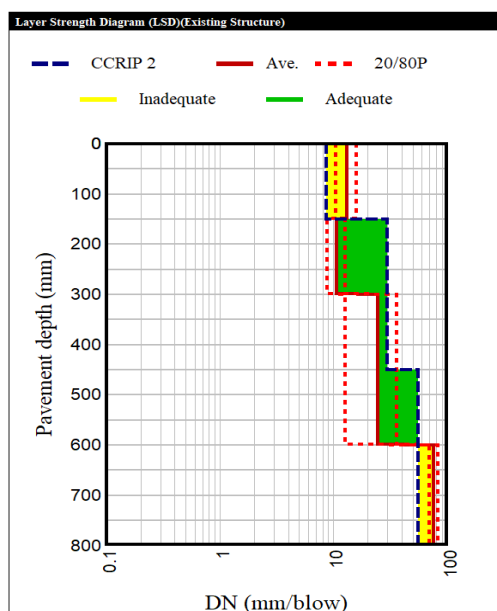


Figure 26. Analysed DCP test result (P7_Modhupur, Khulna): Layer strength diagram

Table 1. Condition) of Road and Shoulder by using AfCAP-DCP software.

No.	Point_Point_Location	Road Pavement*				Shoulder*
		Base	Sub-base	ISG	Sub-grade	
1	P1_P3_Terkhada, Khulna	A	A	A	A	I
2	P2_P4_Terkhada, Khulna	I	A	A	A	I
5	P5_P6_Parhazigram, Khulna	I	A	A	A	A
7	P7_Modhupur, Khulna	I	A	A	A	--
8	P8_P9_Kaligonj, Satkhira	I	A	A	A	A
10	P10_Kaligonj, Satkhira	I	A	A	A	--
11	P11_Kaligonj, Satkhira	I	A	A	A	--
12	P12_P13_Soronkhola, Bagerhat	I	A	A	A	I
14	P14_P15_Soronkhola, Bagerhat	I	A	A	A	A
16	P16_Soronkhola, Bagerhat			--		A
18	P18_P17_Soronkhola, Bagerhat	I	I	A	A	I
19	P19_P20_Motbaria, Pirojpur	I	I	I	I	I
21	P21_P22_Motbaria, Pirojpur	I	I	A	A	A
23	P23_P24_Motbaria, Pirojpur	I	A	A	A	I
26	P26_P25_Mathbaria, Pirojpur	I	I	A	I	I
27	P27_P28_Kathisadar, Gopalganj	I	A	A	A	I

No.	Point_Point_Location	Road Pavement*				Shoulder*
		Base	Sub-base	ISG	Sub-grade	
29	P29_P30_Kathisadar, Gopalganj	I	I	A	A	A
31	P31_P32_Kathisadar, Gopalganj	I	A	A	A	I
33	P33_P34_Kathisadar, Gopalganj	I	I	I	A	I

*A=Adequate I=Inadequate

A digital moisture meter was used to measure moisture content of the subbase and ISG after making a small hole on road pavement. Later it was filled with concrete. Moisture contents of roads were between 14 and 18 percent for subbase and ISG. In the shoulder the moisture content was more than 50 percent. The DCP test data were analysed by using the AfCAP LVR-DCP software (A software developed by Africa Community Access Program). In Figure 26, adequacy of each layer is checked by comparing with maximum recommended DN (mm/blow) values shown in Figure 23. Adequate layers are represented by green colour and inadequate layers by yellow colour. Thus, all DCP tests data were analysed and adequacy of layers is listed in Table 1. In most of the cases, bases were found inadequate. 10 points out of 16 points on shoulder were inadequate. Some sub-bases were found inadequate and few ISG (Improved Subgrade) were found inadequate.

Rutting on road pavement may be attributed to inadequate base layer. Initiation of damage at the edge of pavement may be attributed to inadequate shoulder. Shoulder and widened part of road acts as confinement to existing road. Soft shoulder is not capable of giving confinement to pavement layers. That is why authors think that shoulder should be hard type with herring bone brick under which there should be a sub-base layer. Dumping of mud at shoulder and side slope must be avoided to make sustainable rural road.

4. CONCLUSION

Based on the test results and field observations, following reasons of road damage were identified.

- i. Use of unsuitable soil for ISG, subbase, base and slope.
- ii. Lack of training and concern about relation of moisture content and compaction.
- iii. The side slope is steeper than the designed slope.
- iv. Borrow pit location is along the toe.
- v. No extra protection or proper protection for the road embankment along the river or khal.
- vi. Erosion of side slopes due to wave action from the shallow fish pond (Gher).
- vii. Settlement of the approach road due to underlying soft soil, uncompacted approach embankment and inadequate wing wall.
- viii. Rain cut erosion of soft lean clay or silt on the shoulder and slope.
- ix. Overloaded vehicle movement on the pavement and on the shoulder.
- xi. Soft subsoil under road embankment.
- xii. Rutting and water logging on the road.
- xiv. Lack of vegetation on side slopes.

ACKNOWLEDGEMENTS

Writers wish to express their gratitude to “Introduction of Quality Test Protocols for Road and Market Rehabilitation” under Coastal Climate Resilient Infrastructure Project (CCRIP) (Package No: CCRIP-S-05(C), LGED, GOB) for their financial support. Thanks to Dr. T. M. Al-Hussaini (Director of BUET-Japan Institute of Disaster Prevention and Urban Safety) for allowing us to conduct the tests in his laboratory.

REFERENCES

- Alam, M. K., Hasan, A. S., Khan, M. R., & Whitney, J. W. (1990). Geological Map of Bangladesh. Geological Survey of Bangladesh, Ministry of Energy and Mineral Resources, Government of the People's Republic of Bangladesh.
- Government of the People's Republic of Bangladesh. (2005). Road Design Standards (Rural Road). Bangladesh: Local Government Engineering Department (LGED) and Japan International Cooperation Agency (JICA).
- Huq, S., & Rabbani, G. (2011). Adaptation Technologies in Agriculture; The Economics of rice farming technology in climate - vulnerable areas of Bangladesh.
- Islam, M. T., Alam, J. M., Taufique, F. M., & Hasan, S. M. (2015). Effect of Sand Content on Plasticity, Compaction and CBR of Sand-Clay Mixture. International Conference on Recent Innovation in Civil Engineering for Sustainable Development (IICSD-2015). Gazipur, Bangladesh: Department of Civil Engineering, DUET.
- Kabir, M. H., Alam, J. M., Hamid, A. M., & Akhtaruzzaman, A. K. (2000). Foundations on Soft Soils for Khulna Medical College Buildings in Bangladesh. ISRM International Symposium, 19-24 November, Melbourne, Australia. International Society for Rock Mechanics and Rock Engineering.
- Nath, B. D., Molla, M. K., & Sarkar, G. (2017). Study on Strength Behavior of Organic Soil Stabilized. International Scholarly Research Notices, 2017.

BURIED PIPELINE UNDER SEISMIC EXCITATIONS: A REVIEW

Sanjoy Das¹, Md Aftabur Rahman*² and Sultan Mohammad Farooq³

¹*Assistant Professor, Department of Civil Engineering, CUET, Chattogram-4349, Bangladesh, e-mail: sanjoy0701098@gmail.com*

²*Assistant Professor, Department of Civil Engineering, CUET, Chattogram-4349, Bangladesh, e-mail: maftabur@cuet.ac.bd*

³*Associate Professor, Department of Civil Engineering, CUET, Chattogram-4349, Bangladesh, e-mail: farooq_sm@cuet.ac.bd*

***Corresponding Author**

ABSTRACT

Buried Lifelines are the systems & facilities that provide essential services to the function of an industrialized, modern country & important to emergency response & recovery after disastrous events. From previous post seismic failures, it was evident that the majority of the pipelines are buried in relatively shallow depths and are critically susceptible to damage during seismic excitations in earthquake prone areas. Damage or interruption of these underground lifelines could cause major, even catastrophic, disruption of essential services. If such disruption is caused by an earthquake, the effect of the loss of vital service would be greatly amplified by impeding fire-fighting, preventing essential energy transmission, communications, transportation, and causing widespread disease. To evaluate the seismic response of buried pipelines, a lot of researches was performed experimentally, numerically & analytically. Hence it is quite necessary to investigate proper soil-buried pipe interaction, proper modelling techniques & seismic behavior of buried pipelines. In this perspective, the present study explains a state-of-the-art review of the response of Buried lifelines under seismic excitations. The review includes existing modelling techniques of soil-pipe system, different failure modes of buried continuous pipelines subjected to seismic excitations, methods of response analysis of buried pipelines, seismic behavior of buried pipelines under different parametric variations, seismic stresses at the bends & intersections of network of pipelines, pipe damage in earthquakes & seismic risk analysis of buried pipelines. Based on the review, research gaps have been evaluated & future scopes for further research are identified, which may be helpful for researchers & designers.

Keywords: *Buried lifelines, Soil-buried pipe interaction, Seismic analysis.*

1. INTRODUCTION

Pipelines are often referred to as "Lifelines" because of their role in the delivery of life-dependent resources. Some examples of lifelines are natural gas or oil pipes, sewage and water supply pipelines, storage facilities, tunnels, power lines and communications lines. Although its importance is underestimated or even unknown to the common society or public, its failure can result in drastic effects to the public. It is therefore important in all circumstances to preserve the integrity of these lifelines.

A large proportion of lifelines are placed underground. Interruption of these underground lifeline systems may result in major disruption to essential services, even catastrophic ones. The damage to the buried lifelines during an earthquake is evident and reported in many technical writings. For instance, the San Francisco earthquake in 1905 destroyed many buried lifelines. The rupture of water supplies in Yokohama caused fire and flooding. Moreover, in Kanto 1923, Long Beach 1933, Fukui 1948, Alaska 1964, San Fernando 1971, Managua 1972 earthquakes, there have been extensive damage to the underground pipelines. The 1952 Kern County earthquake caused serious damages to four railroad tunnels ("Response of underground lifeline systems to earthquakes," 1975). literature study revealed that pipelines are subjected to high stresses during earthquake and ultimately lead to failure of the pipelines. Depending on the material transmitted via the pipeline, pipeline failure may trigger the sources of pollution, water crises, fire, explosion, etc. The mitigation of such hazards has been realized by the researcher and they emphasized on estimating the responses of buried structures during extreme event. The research in buried pipeline was first reported when Newmark developed the procedure to analyse the buried pipeline under fault rupture. Later, other researcher developed some sophisticated models to account for fault effect on buried pipeline. The high computation facilities encouraged the researchers to numerically simulate the response of buried pipeline under fault rupture. To date, a significant number of analytical and numerical model has been developed to understand the behaviour of buried pipeline during fault movement. However, the direct response of buried pipeline under seismic loading is seldom found in technical writings. In addition to analytical and numerical modelling, some experimental observations are also available. over the last few years, researchers have paid more attention to the complex behaviour of buried pipelines in order to properly understand the phenomenon of soil-pipe interaction. The dynamic behaviour of the buried pipelines depends on several factors, such as the type and frequency of incoming waves, the properties of the surrounding soil, the material and dimensions of the pipe the flexibility of the joint, the internal pressure, etc. In addition to the remaining straight portion of the pipe, it was found that more pressure would produce at the pipeline intersection. A thorough understanding of the pipe-soil interaction is needed for dynamic analyses of the buried pipeline, because it has an important role to play during seismic excitement.

Identifying the need for seismic response analysis of buried pipeline, a compilation of so far developed procedure is necessary. Therefore, this research aims to sum up the available soil pipe modeling techniques and analysis methodologies from previous research projects. The study proposes certain research lacunes that need to be further explored based on the merits and demerits of existing methods.

2. DYNAMIC BEHAVIOUR OF BURIED PIPELINES

Interactions and features of ground motion play a key role in the study of structures below the ground. Field observations and various studies indicate that damage to underground structures, mainly buried pipelines during the earthquake, is due to excessive axial and bending stresses and strains developed at various points along pipe lengths due to various reasons such as wave propagation characteristics, large displacements due to fault movements, uplifting or landslides caused by soil liquefaction. (Youssef M. A. Hashash, Jeffrey, J. Hook, 2014) published a summary report on the current state of seismic analysis and layout of underground structures, which explains the methods used by engineers

to measure the seismic effect on the underground structure. The study also briefly addresses the design of appropriate ground motion parameters, including peak accelerations and velocities, target response spectra and ground motion time histories.

2.1 Soil Pipe Interaction

The soil and pipe interactions have a profound effect on the behavior of the buried pipe that is subjected to earthquake excitations. (F. Behnamfar, n.d.), 2015 studied the effect of soil pipe interaction on bending of buried pipeline and concluded that the axial strain at bends is larger in stiffer soil due to smaller slippage and that the bend strain is direct, whereas the relative displacement of the soil pipe is inversely proportional to the diameter to thickness ratio. Analytically, (J. P. Dwivedi, 2010) & (Pitilakis, 1996) have shown that axial analysis is the critical analysis and the pipeline's dynamic soil-pipe interaction (SSI) effects for axial response are significant while those are negligible for lateral response. (Liu, n.d.) found that the soil around the pipeline plays a very important role in the seismic activity of the pipeline. He showed that soil pipe contact induces both axial and bending stresses in continuous pipelines, which may ultimately lead to the buckling and crushing of pipelines. (V. Corrado, B. D'Acunto, N. Fontana, 2009) demonstrated that interaction between the soil structure and the end constraint can significantly affect the dynamic response of a buried, seismically excited finite pipe. They also showed that the end points of the pipe are the weakest areas, where high stresses can cause breaks or fractures.

2.2 Permanent Ground Deformation

The permanent ground deformation (PGD) is nothing but a large-scale deformation of the ground caused by soil liquefaction, landslide or fault movement. Effect of permanent ground deformation (PGD) on dynamic behaviour has been studied by various researchers. (Arya, A. K., Shingan, B., and Prasad, 2015) presented guidelines for calculating seismic resistance and outlined various measures to be taken to prevent oil and gas continuous buried steel pipeline failure under various seismic events such as fault, landslide, etc. causing permanent deformation of the ground. (LI Hongjing, 2008) found that permanent ground deformation (PGD) due to faults in buried pipelines, peak stress increases rapidly as the ratio diameter to thickness ratio increases. The researchers have demonstrated that the buried pipeline's seismic response increases with soil displacement and crossing angle increases and decreases with buried depth increases. The greater the angle of crossing, the greater the pipe's response under normal movement. The greater buried depth, the pipe's poorer performance.

2.3 Wave Propagation

There are primarily two types of seismic waves, body waves and surface waves. Body waves are slower waves of high propagation velocity. There is much less ground strain caused by the propagation of body waves. On the other hand, the frequency of surface wave propagation is much lower and the resultant ground stress is higher. Therefore, surface waves are more dangerous than body waves for submerged pipelines. Effect of wave propagation on dynamic behaviour of buried pipeline has been studied. (Othman A. Shaalan, Tarek N. Salem, Eman A. El shamy & Mansour, 2014) found that stiffer soils tend to intensify and encourage earthquake waves to move faster, whereas softer soils tend to dampen movement values slightly and hamper the movement and propagation of earthquake waves. (Hosseini, 2015) indicated that stress levels or rotations along the pipelines are negligible in joint pipe networks under the influence of transient ground waves and that effective damage is likely only at the intersection points or where the direction of the lines has shifted, i.e. at the bends.

2.4 Other governing factors

Pipe diameter, burial depth and other soil and excitation characteristics play a major role in underground pipeline seismic behaviour. (Hassan Sharafi, 2015) found that soil friction angle, pipe diameter and pipe burial depth played an important role in the uplifting actions of shallow buried pipelines caused under cyclic loading by soil liquefaction. (Prashant Mukherjee, N U Khan, 2013) found that slippage depends mainly on pipe diameter and installation depth in the pipe line network. As the diameter of the pipeline increases, its axial strain also increases as it is a direct function of the

diameter of the pipeline that ultimately increases the pipeline slippage. While the likelihood of slippage decreases with an increase in burying depth as the depth increases the confining stress. (Seyyed Omid Hosseiny & Vaghefi, 2014) investigated the effect on pipe stability during earthquake excitation of various fluid properties such as fluid density and velocity, pipe slope, soil depth and soil behaviour.

3. DOMINANT FAILURE MODES OF BURIED CONTINUOUS PIPELINES

The various buried steel pipeline failure modes reported by (Psyrras & Sextos, 2018), (Singh & Kareem, n.d.) are subjected to seismic excitation.

3.1 Shell mode buckling

The result of this kind of buckling is compressive load or pure bending. This is the most common type of buckling and this type of buckling is usually observed in large pipes buried in deep trenches. fig. 1(a).

3.2 Beam mode buckling

In this type of buckling, compressed pipe will bend upward and soil will attempt to resist it. Such type of failure occurs in pipes with a comparatively smaller diameter that are shallowly buried. It was clear from the past earthquake that the probability of failure in this category is low compared to buckling in shell mode. fig. 1(b).

3.3 Tensile failure

Such failure occurs when there is tension in the pipelines. Pipelines with more ductile actions are less likely to fail. In the pipeline, seismic hazards such as fault, landslide liquefaction and relative ground motion are causing tensile strain. fig. 1(c).

3.4 Cross section Ovalization

Under bending stress, this type of failure occurs. The initial pipe diameter will change in this case and its shape will also change from circular to oval. fig. 1(d).

3.5 Local buckling

Local pipe wall instability causes local pipeline buckling and wrinkling. Both wave propagation and geometric distortion caused by ground deformation due to local shell wrinkling initiation tends to concentrate on these wrinkles. Therefore, circumferential cracking of the pipe wall and leakage occurs in the pipe wall due to the expansion of the local curvature.

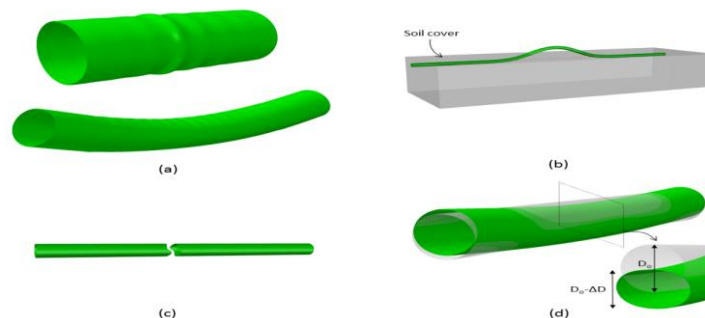


Fig. 2. Common failure mechanisms in buried, continuous steel pipelines: (a) shell-mode buckling due to uniform axial compression (top) and pure bending (bottom); (b) beam-mode buckling; (c) tensile fracture and (d) cross-section ovalization.

4. DOMINANT FAILURE MODES OF BURIED SEGMENTED PIPELINES

4.1 Axial pull-out

The common failure mechanism of a segmented pipeline in the areas of tensile ground strain is axial pull-out at joints as the shear strength of the joint caulking material is significantly less than that of the pipe.

4.2 Crushing of Bell & Spigot joints

Crushing of bell-and-spigot joints is a very common failure mechanism in compressive strain areas.

4.3 Flanged joint failure

Due to the breaking of the flange connection the flanged joint pipeline can fail at the joint in the tensile ground strain areas.

4.4 Circumferential flexural failure & joint rotation

When a segmented pipeline is bent due to lateral permanent ground movement or seismic shaking, any combination of joint rotation and flexure in the pipe segments accommodates the ground curvature. Over a wide geographical area, pipelines are usually buried. Continuous pipeline failures are a tensile rupture local or beam buckling, and unnecessary joint bending in individual pipelines are the main modes of segmented pipeline failure.

5. AVAILABLE MODELING TECHNIQUES OF SOIL-BURIED PIPE SYSTEM

Different types of modeling of the underground pipelines are available, starting from extremely simple to complex three-dimensional modeling of the soil–structure system. (Datta, 1999) stated that one of the following four ways of simulating soil-pipe interaction systems can be modelled as a soil-pipe system. As shown below, each strategy has some advantages and disadvantages.

5.1 Beam model on elastic springs

Figure 2(a) shows the beam model in elastic foundation modelling where the pipe is defined as a long beam and the surrounding soil is represented as a spring. Spring stiffness and dashpot coefficient can provide soil-pipe interaction. This technique is not capable of capturing dynamically loaded pipeline buckling and fracturing phenomenon. This model is used to represent long buried pipelines in which bending and axial deformations are of main concern.

5.2 Shell model

Instead of single-dimensional beam objects as shown in figure 2(b) the pipe can also be represented by three-dimensional cylinder shells. In contrast to beam component, the shell integrates pipeline buckling and fracturing phenomenon. The shell model is assumed to be resting within a viscoelastic medium.

5.3 Plane strain model

Buried pipelines can be viewed as a plane strain problem, as the dimension is much larger than the other two cross directions in an axial direction for pipelines. The plane strain model is shown in Figure 2(c). This method of modelling can be used to evaluate hoop stress and radial deformation.

5.4 Hybrid model

In the hybrid model shown in Fig. 2(d), the interior region (R1) is modeled by the finite element method (FEM), while the outer region (R2) is modeled by the half space continuum. A plane strain model is adopted for both regions. Continuity of displacement and strain is maintained at the interface boundaries between the two regions.

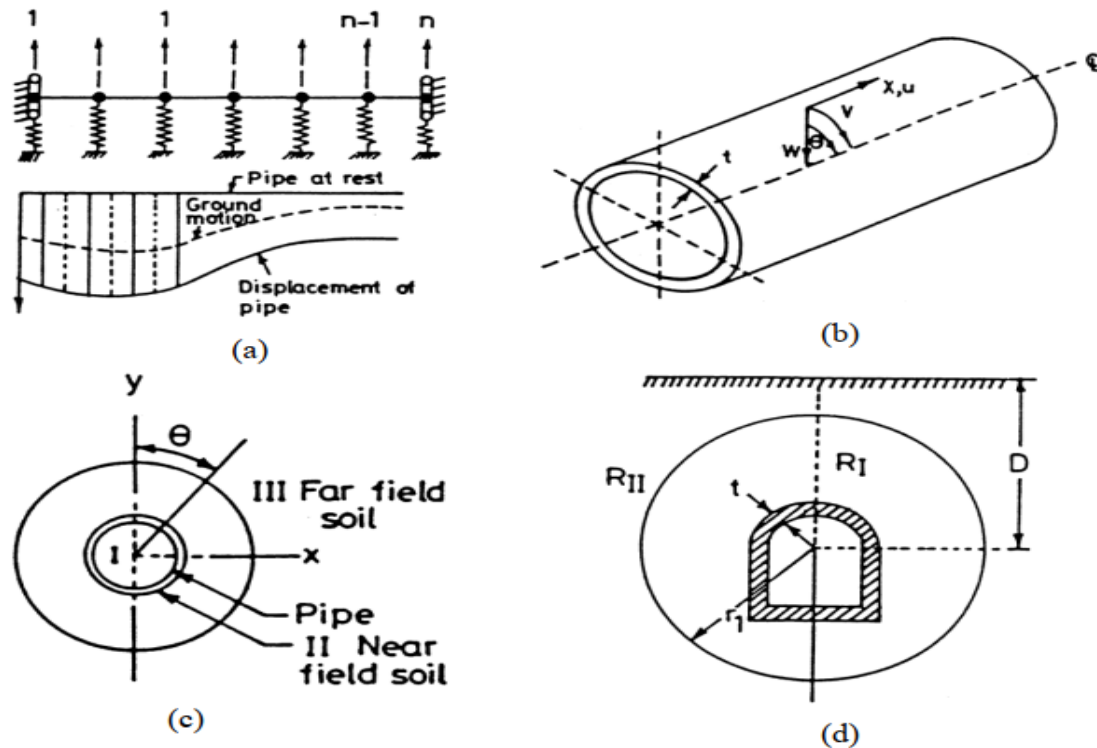


Figure 2. (a) Beam on elastic foundation (b) Shell model (c) Plane-strain model and (d) Hybrid model (Datta, 1999)

6. ANALYSIS METHODOLOGIES

At the beginning of the study, the soil-pipe relationship has not been addressed. Later, other experiments were also conducted with a view to complex pipe-to-soil interactions. The following parts are categorically defined by the current soil-pipe system response methodologies under seismic excitation.

6.1 Analysis avoiding soil-structure interaction

In this situation, it was believed that the pipe was moving with the ground, i.e. no relative motion between the pipe and the soil. Few studies have been carried out in the buried pipeline area without recognizing the interaction of soil-structure (Newmark, N.M. & Rosenbluth, 1971) (Hindy, A. & Novak, 1979)(Shah, H. & Chu, 1974). The researchers primarily proposed several simplistic methods to obtain responses in seismic loads by neglecting soil-structuring interactions. This phenomenon is acceptable for certain conditions, for example if the stiffness of soil that surrounds the pipe are very high compared to the pipes itself, the interaction of the soil pipes may be ignored.

6.2 Quasi static analysis with soil–structure interaction

In this analysis, the soil deformations are matched by a combination of pipe deformations and relative deformations of joints. In order to obtain the response from a buried structure with flexible joints during earthquake agitation, (Singhal, A.C, Zuroff, 1990), with the concept of beams on elastic foundations suggested a quasi static analysis.

6.3 Analysis Considering soil–structure Interaction Phenomenon

In this case, the pipe should consider the phenomenon of soil-pipe interaction if the pipe passes through a soil that is relatively soft and soil stiffness is not much greater than the pipe stiffness. Initially, dynamic analysis was carried out on the basis of Beam on Elastic Foundation Theory

(Hindy, A. & Novak, 1979), (Datta, T.K. & Mashaly, 1986) which integrates the effect of soil-structure interactions. Nevertheless, these methods did not integrate the phenomenon of buckling and fracturing of the pipeline under seismic loading. The pipe was later modelled as a cylindrical shell, instead of a beam to resolve these demerits (Datta, S.K., Shah, A.H., & El-Akily, 1982), (Muleski, G.E. & Ariman, 1985). In addition, the existence of pipeline motion during an earthquake has indicated that a beam or a cylindrical shell did not consider modifying free field motion (Wong et al., 1986). The plain strain model or finite-element analysis, which represents a practical conduct for the complete interaction of soil-structures ((Datta, S.K., Shah, A.H., & Wong, 1984), (Patil, M., Choudhury, D., Ranjith, P.G., & Zhao, 2018)). Considerable work was carried out in the context of simple beam theory, i.e. the theory of beam on the elastic foundation or the perception of pipes as cylindrical shells. But there is very little work on seismic analysis of the pipeline with respect to the method of three-dimensional finite elements. Such numerical analyses are conducted using Finite Element Method or Finite Differences Method-based computers like ABAQUS, FLAC, PLAXIS2D etc. ((Saeedzadeh, R. & Hataf, 2011), (Boron, P. & Dulinska, 2017), (Ghiasi, V. & Mozafari, 2018)).

6.4 Time history analysis

This is a dynamic analysis that is nonlinear. A selective earthquake ground motion is applied directly to the structure base in this analysis process. Instantaneous stresses throughout the structure were measured at small intervals during the entire duration of the earthquake. The time history method is not generally used in an analysis system due to its long running machine, but this method provides more accurate results compared to a pushover test as it inculcates real earthquake information as an input file.

7. RESPONSE OF BURIED PIPELINE UNDER SEISMIC EXCITATION

Responses to seismic excitement of buried pipelines include changes in pipe dimensions, pipe stiffness, soil conditions surround, burial depths, and so forth. (Lee, D.H., Kim, B.H., Lee, H., & Kong, 2009) conducted a comparative study of the seismic activity of the buried gas pipeline. Three different conditions of soil media have been considered, such as soft clay, loose and dense sand. The authors adopted different types of end support of the pipe and it was observed that under seismic excitation, at the end of the pipe, maximum strain is more dangerous among all types of end restrain fixed-fixed end condition. Furthermore, the maximum strain along the length of the pipeline is considerably higher in the case of soft clay than compared with dense or loose sand and this effect can be kept to a minimum by increasing pipeline burial depth. Hindy and Novak (1979) found that considering dynamic soil-pipe interaction decreases axial and bending stress responses relative to the case of no-interaction. In addition, the method of nonlinear finite elements provides more accurate results than the simplified methods stated by (Chen, 1995). The emphasis should be on the position of the pipe bend and pipe intersection (T or L intersection) in order to obtain dynamic responses as more stress is produced at these locations as seen from previous research (Soliman, H.O. & Datta, 1996). (Karamanos, S.A., Sarvanis, G.C., Keil, B.D., & Card, 2017) emphasized that by increasing the wall thickness of the pipe or by putting soft backfill around the pipe dynamic stresses on the pipe can be minimized. Nevertheless, care should be taken to put soft backfill as pipe buckling can be increased in such situations.

8. CONCLUSIONS

In order to study the dynamic behaviour of underground structures, the following points should be considered:

- A detailed seismic assessment should be carried out to study the effects of the earthquake, taking into account the type of soil and site conditions.
- Underground structures should be designed instead of inertial forces for imposed seismic ground deformations.

- Seismic excitation simulation can be achieved by considering parallel, perpendicular or skewed propagation of the P, S or Rayleigh wave to the longitudinal axis of the pipeline.
- Longitudinal seismic analysis should be conducted in combination with transversal analysis, and dynamic analysis should also be performed at critical points to determine stresses and strains.
- The dynamic time-history analysis using 3D finite element models should be conducted to model the soil-structure interaction effects.
- Experimentation is considered necessary by considering different variables combinations.

This review study presented a state of the art in buried pipeline's seismic behaviour. This study includes various modes of failure, modelling techniques, analysis methods, and buried pipeline responses considering the phenomenon of dynamic soil-pipe interaction with and without it. It was found that very little analytical research was conducted considering pipe as a shell model capable of simulating the phenomenon of buckling and fracture. However, less attention was paid to three-dimensional numerical analysis using methods of finite elements involving nonlinear interaction between soil and pipe. Due to the complex dynamic soil-pipe relationship, the activity of the buried pipeline under seismic loading is still not properly understood. The variance of the field conditions and the nonlinearity of the soil should also be included in the analyses. These could lead us to avail ourselves of the future scope of work.

REFERENCES

- American Society of Civil Engineers. (1974). Earthquake damage evaluation and design considerations for underground structures a Public Service paper, var.pag.
- Arya, A. K., Shingan, B., and Prasad, C. V. (2015). Seismic Design of Continuous Buried Pipeline. *International Journal of Engineering and Science*, 1(1), 6–17.
- Boron, P. & Dulinska, J. (2017). The dynamic analysis of a steel pipeline under a seismic shock. *Procedia Engineering*, 199, 104–109.
- Chen, Y. (1995). Simplified and refined earthquake analyses for buried pipes. *Mathematical and Computer Modelling*, 21(11), 47–60.
- Datta, S.K., Shah, A.H., & El-Akily, N. (1982). Dynamic behavior of a buried pipe in a seismic environment. *Journal of Applied Mechanics*, 49(1), 141–148.
- Datta, S.K., Shah, A.H., & Wong, K. C. (1984). Dynamic stresses and displacements in buried pipe. *Journal of Engineering Mechanics*, 110(10).
- Datta, T.K. & Mashaly, E. A. (1986). Pipeline response to random ground motion by discrete model. *Earthquake Engineering & Structural Dynamics*, 14(4), 559–572.
- Datta, T. K. (1999). Seismic response of buried pipelines : a state-of-the-art review, 192, 271–284.
- F. Behnamfar, M. V. and M. S. (n.d.). A Continuum Shell-beam Finite Element Modelling of Buried Pipes with 90-degree Elbow Subjected to Earthquake Excitations. *International Journal of Engineering*, 28(issue 3), pp 338-349.
- Ghiasi, V. & Mozafari, V. (2018). Seismic response of buried pipes to microtunnelling method under earthquake loads. *Soil Dynamics and Earthquake Engineering*, 113, 193–201.
- Hassan Sharafi, S. J. and P. P. (2015). Uplifting Behavior of Shallow Buried Pipelines Within Liquefiable Soils Under Cyclic Loading. *Electronic Journal of Geotechnical Engineering*, 20(16), 9675–9968.
- Hindy, A. & Novak, M. (1979). Earthquake response of underground pipelines. *Earthquake Engineering and Structural Dynamics*, 7(5), 451–476.
- Hosseini, A. B. and M. (2015). Sensitivity Analysis of Buried Jointed Pipelines Subjected to Earthquake Waves. *Open Journal of Earthquake Research*, 4, 74–84.
- J. P. Dwivedi, V. P. S. and R. K. L. (2010). Dynamic Analysis of Buried Pipelines under Linear Viscoelastic Soil Condition. *Advances in Theoretical and Applied Mechanics*, 3(12), 551–558.
- Karamanos, S.A., Sarvanis, G.C., Keil, B.D., & Card, R. J. (2017). Analysis and Design of Buried Steel Water Pipelines in Seismic Areas. *Journal of Pipeline Systems Engineering and Practice*, 8(4), p.04017018.

- Lee, D.H., Kim, B.H., Lee, H., & Kong, J. S. (2009). Seismic behavior of a buried gas pipeline under earthquake excitations. *Engineering Structures*, 31(5), 1011–1023.
- LI Hongjing, J. L. and Y. B. (2008). Response Analysis of Buried Pipelines Due to Large Ground Movements. In *14th World Conferences on Earthquake Engineering (WCEE), Beijing China, Oct 12-17*.
- Liu, R. F.-B. and X. L. (n.d.). Seismic vulnerability of buried pipelines. *Geofisica Internacional*, 42(2), 237–246.
- Muleski, G.E. & Ariman, T. (1985). A shell model for buried pipes in earthquakes. *International Journal of Soil Dynamics and Earthquake Engineering*, 4(1), 43–51.
- Newmark, N.M. & Rosenblueth, E. (1971). *Fundamentals of Earthquake Engineering*. Prentice-Hall, Englewood Cliffs.
- Othman A. Shaalan, Tarek N. Salem, Eman A. El shamy, and R. M., & Mansour. (2014). Dynamic analysis of two adjacent tunnels. *International Journal of Engineering and Innovative Techniques*, 4(4), 145–152.
- Patil, M., Choudhury, D., Ranjith, P.G., & Zhao, J. (2018). Behavior of shallow tunnel in soft soil under seismic conditions. *Tunnelling and Underground Space Technology*, 82, 30–38.
- Pitilakis, G. A. M. and K. D. (1996). Axial and Transverse Seismic analysis of buried Pipelines. In *11th World Conferences on Earthquake Engineering (WCEE), Acapulco Mexico, June 23-28* (p. paper no.1605).
- Prashant Mukherjee, N U Khan, B. B. P. and R. R. N. (2013). A Comparative Study of Lateral Pipe Bending Moment with Fixed Supporting Condition for Different Soil Types in India. *Electronic Journal of Geotechnical Engineering*, 18(G), 1279–1291.
- Psyras, N. K., & Sextos, A. G. (2018). Safety of buried steel natural gas pipelines under earthquake-induced ground shaking: A review. *Soil Dynamics and Earthquake Engineering*, 106(February 2017), 254–277. <https://doi.org/10.1016/j.soildyn.2017.12.020>
- Response of underground lifeline systems to earthquakes'. (1975). *Unsolicited Research Proposal Submitted to the National Science- Foundation by Weidlinger Associates, New York*.
- Saeedzadeh, R. & Hataf, N. (2011). Uplift response of buried pipelines in saturated sand deposit under earthquake loading. *Soil Dynamics and Earthquake Engineering*, 31(10), 1378–1384.
- Seyyed Omid Hosseiny, M. M. J. and M., & Vaghefi. (2014). Soil Structure Interaction Effects on the Seismic Behavior of Buried Pipeline. *International Journal of Current Life Sciences*, 4(8), 4535–4543.
- Shah, H. & Chu, S. (1974). Seismic analysis of underground structural elements. *Journal of the Power Division*, 100, Proc. Paper 10648.
- Singh, V. K., & Kareem, A. (n.d.). SEISMIC ANALYSIS OF BURIED PIPELINE : A STATE OF ART REVIEW.
- Singhal, A.C, Zuroff, M. S. (1990). Analysis of underground and underwater space frame with stiff joints. *J. Comput. Struct*, 35(1), 227–237.
- Soliman, H.O. & Datta, T. K. (1996). Response of over ground pipelines to random ground motion. *Engineering Structures*, 18(7), 537–545.
- V. Corrado, B. D'Acunto, N. Fontana, M. G. (2009). Estimation of dynamic strains in finite end-constrained pipes in seismic areas. *Mathematical and Computer Modelling*, 49, 789–797.
- Youssef M. A. Hashash, Jeffrey, J. Hook, B. S. and J. Ic. Y. (2014). Seismic design and analysis of underground structures, Pipelines 2014: From Underground to Forefront of innovation and sustainability. *ASCE*, 1005–1019.

EFFECT OF ORDINARY PORTLAND CEMENT AND WHITE CEMENT ON UNCONFINED COMPRESSIVE STRENGTH OF CLAY

A S M Fahad Hossain*¹, Ubaidullah Al Mahfuz², Israt Jahan Tazin³ and Sheikh Shad Muhammad⁴

¹*Assistant Professor, Department of Civil Engineering, Ahsanullah University of Science and Technology (AUST), Dhaka, Bangladesh, e-mail: fahadrubel@gmail.com*

²*Graduate Student, Department of Civil Engineering, Ahsanullah University of Science and Technology (AUST), Dhaka, Bangladesh, e-mail: u.a.mahfuz@gmail.com*

³*Graduate Student, Department of Civil Engineering, Ahsanullah University of Science and Technology (AUST), Dhaka, Bangladesh, e-mail: tazinisrat21@gmail.com*

⁴*Graduate Student, Department of Civil Engineering, Ahsanullah University of Science and Technology (AUST), Dhaka, Bangladesh, e-mail: sheikhshd97@gmail.com*

***Corresponding Author**

ABSTRACT

Clay is a poor soil for support any construction on it if it is soft or water saturated without consolidation, so construction of any structure on clay soil needs strong foundation which is costly, but for better structural stability the clay soil must stabilized with admixture to increase its strength to take larger loads. In this research, clay soil was stabilized with ordinary Portland cement and white cement. Ordinary Portland cement and white cement were collected and mixed with clay soil with different proportion like 3%, 6%, 9%, 12% and 15%. Then Unconfined Compressive Strength Tests was performed. The test result revealed that mixing of 15% cement produced the growth of shear strength on the clay soil for both ordinary Portland cement and white cement.

Keywords: *Clay soil, Ordinary portland cement, White cement, Soil stabilization, Unconfined compressive strength test.*

1. INTRODUCTION

Clay cannot be very easily defined in exact expressions. In general, the term "clay" denotes a natural, earthy, fine-grained material which when mixed with a limited amount of water develops plastic properties. Plasticity, as related to Soil Mechanics, is that property which allows a material to undergo rapid deformation without break, volume change, or elastic rebound. Clays exhibit plasticity when mixed with water in certain proportions. However, when dry, clay becomes steady and when fired in an oven, permanent physical and chemical changes occur. Clays are distinguished from other fine-grained soils by differences in size and mineralogy. Cement is one of the most important building materials, is a binding agent that sets and hardens to adhere to building units such as stones, bricks, tiles, etc. White cement is the same as that of grey Portland cement but the only difference is in the color and fineness. This color of this cement is determined by its raw materials and the process of manufacture. The objective of this research was to get the improvement of clay soil by adding both ordinary Portland cement and white cement and also to observe the difference between the improvements of the clay by the two different cements.

2. METHODOLOGY

Firstly, clay soil sample was collected as a Shelby tube undisturbed sample from Sreepur upazila, Gazipur, Bangladesh. Ordinary Portland cement and White cement was purchased from nearest shop of laboratory. After confirming it as a clay soil by grain size analysis test (sieve analysis and hydrometer), the soil sample were mixed with ordinary Portland cement and white cement in 3%, 6%, 9%, 12% & 15% ratio with presence of a little portion of water in five plastic molds sized by 4 inch height and 1.5 inch depth. Then it was kept in sun for drying for 5 days. After 5 days the plastic mold was removed and Unconfined Confined Compressive Strength Test was performed for the mother soil and all the cement mixed soil. Figure 1 illustrates the plastic mold and the prepared sample.

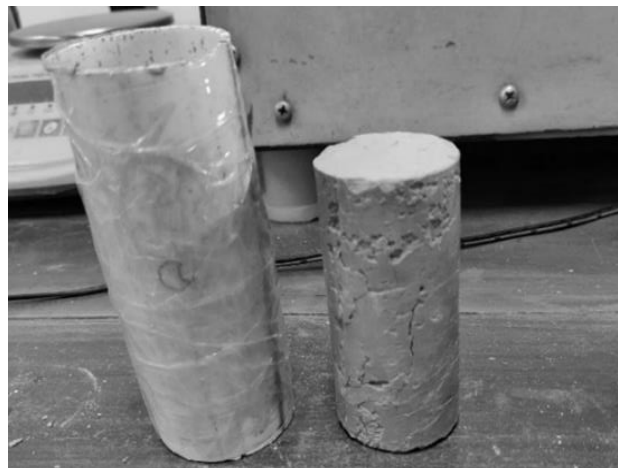


Figure 1: Clay soil mold with cement admixture

3. LABORATORY TEST RESULTS AND DISCUSSIONS

From the Unconfined Compressive Strength Test it was found that the unconfined compressive strength increased a little with the increase of % of ordinary cement & white cement. But it was found that in case of ordinary cement, 3% & 6% of cement mixing with the sample showed a poor value because of lack of bonding between cement & soil. But for 9%, 12%, 15% admixture content, the compressive strength of soil improved respectively is 3.1%, 7.7% and 13.7%. Similarly for white cement mixing the value of compressive stress for 9% & 12% mixing was poor than the mother soil, it was just cracked because of not proper bonding. But for 15% content, the compressive strength of soil improved 6.6%. So from these test results it can clearly noticeable that for 15% of mixture both

ordinary cement and white cement give the ultimate strength against compression load. The unconfined compressive strengths for different soil sample mixed with two types of soil are illustrated in figure 2 and figure 3.

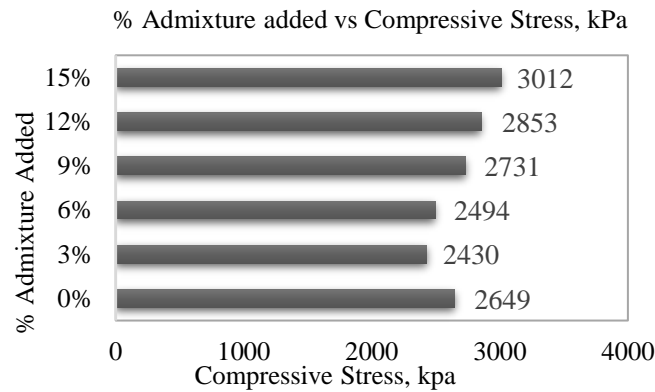


Figure 2: Unconfined Compressive Strength of soil mixed with Ordinary Portland Cement

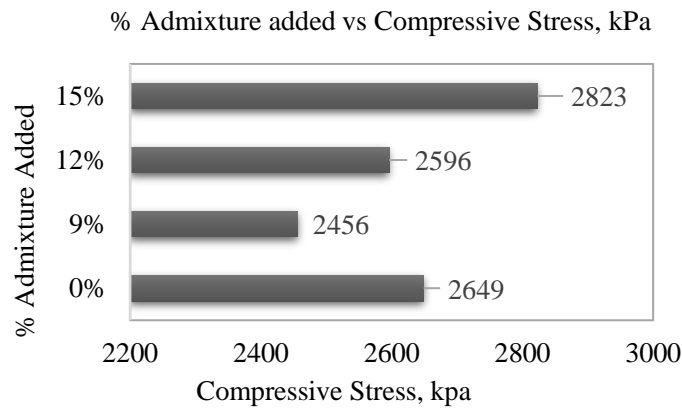


Figure 3: Unconfined Compressive Strength of soil mixed with White cement

The unconfined compressive strength gains for different samples for both ordinary cement and white cement is shown comparatively in figure 4. Figure 5 illustrates the percentage of improvement of the clay soil sample for the both type of cement.

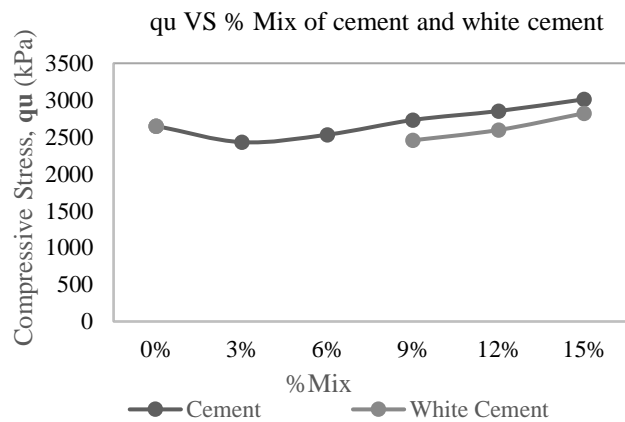


Figure 4: Unconfined Compressive Stress gained by different percentages of Ordinary Portland Cement and White Cement admixture

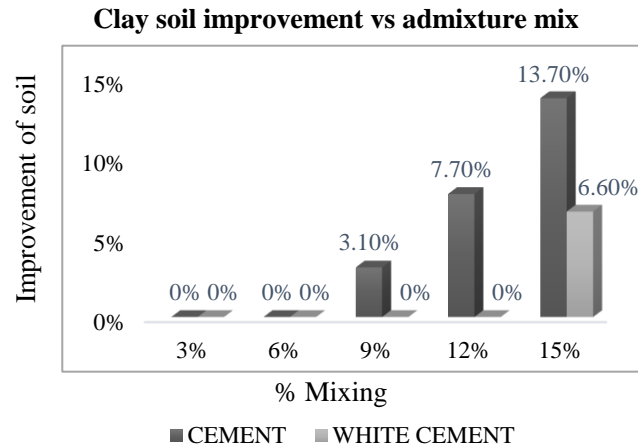


Figure 5: Ordinary Portland cement and White cement improvement by percentage

4. CONCLUSIONS AND RECOMMENDATIONS

The geotechnical properties of clay soils depend on particle size, texture, mineral composition. In particular these factors determine the structure of the soil with the void ratio and the water content increases when void ratio is increased. A Geotechnical engineer has to think and calculate a lot for foundation design and consideration if there is clay soil under the building foundation. The research report mainly focused on the shear strength effects of clay soil mixed with ordinary cement and white cement. Though the improvement was not considerably high but it was found that improvement pattern was most likely same for both type of cement. So that it is recommended that more analysis should be done for stabilizing clay soil by adding different types of cement and determining different index and engineering properties of the cement mixed soil.

REFERENCES

- ASTM D 2166 - Standard Test Method for Unconfined Compressive Strength of Cohesive Soil Engineering Properties of Soils Based on Laboratory Testing, Prof. Krishna Reddy, UIC.
- Punmia B.C. 2007, "Soil Mechanics & Foundations" Laxmi Publications Understanding the Basics of Soil Stabilization: An Overview of Materials and Techniques [online] <<http://www.cat.com> >
- Cement as building material written by: Thomas O. Mason, Frederick M. Lea www.britannica.com/technology/cement-building-material
- White Cement-"Thoughts from a Seasoned Decorative Concrete Contractor," *Concrete Contractor* magazine, October 13, 2014. www.cement.org/for-concrete-books-learning/materials-applications/architectural-and-decorative-concrete/white-cement
- Dynamic Clay Soils Behavior by Different Laboratory and In Situ Tests. A. Cavallaro, S. Grasso, M. Maugeri. Conference paper. link.springer.com/chapter/10.1007/978-1-4020-6146-2_39

DIFFERENT PROPERTIES OF COX'S BAZAR SEA SAND

A. S. M. Fahad Hossain^{*1}, Md. Nayem Hasan², Md. Tauhidul Islam Akanda Tonmoy³ and Moumita Khan Raka⁴

¹*Assistant Professor, Department of Civil Engineering, Ahsanullah University of Science and Technology (AUST), Bangladesh, e-mail: fahadrubel@gmail.com*

²*Graduate Student, Department of Civil Engineering, Ahsanullah University of Science and Technology (AUST), Bangladesh, e-mail: nayem16641664@gmail.com*

³*Graduate Student, Department of Civil Engineering, Ahsanullah University of Science and Technology (AUST), Bangladesh, e-mail: tonmoyaust744@gmail.com*

⁴*Graduate Student, Department of Civil Engineering, Ahsanullah University of Science and Technology (AUST), Bangladesh, e-mail: khanmoumitaraka@gmail.com*

****Corresponding Author***

ABSTRACT

The sea beach in Cox's Bazar is sandy and has a gentle slope with a unbroken length of 120 km (75 mi), it is the longest natural sea beach in the world. There is a huge chance of using these vast sources of sand if the property is properly analyzed. If Cox's Bazar sea beach is used as a source of sand, Bangladesh will be benefited. In this research work, Cox's Bazar sea sand was collected from two spots and some laboratory tests were conducted in Geotechnical Engineering Laboratory of Ahsanullah University of Science and Technology. Direct Shear Test, Proctor Compaction Test, Grain Size Analysis, Moisture Content, Specific Gravity Test and Compressive Strength of mortar were conducted for all the collected sea sand samples. To ascertain the strength properties of the sea sand, mortar made from sea sand were tested. It was found in the research that: the angle of friction of sea sand varied from 2.2° to 8.46°. Sample was uniformly graded with moisture content 11.32% to 11.90% and optimum moisture content varied from 23% to 28%, where, the dry density varies from 1.59 to 1.66 g/cm³. Specific gravity varied from 2.638 to 2.661 and the compressive strength of mortar varied from 1.1 MPa to 13.70 MPa.

Keywords: *Sea sand, Physical properties of sea sand, Mechanical properties of sea sand, Soil improvement.*

1. INTRODUCTION

Sand has a large business, meeting many demands for growing cities, from residential, commercial, and municipal construction, paving roads and driveways. It has various uses, including being used for mixing cement materials, such as concrete, mortar, and plaster. Construction projects couldn't be completed without the use of sand and our homes and cities wouldn't be what they are today. At present, river dredging is the main source of sand used for construction purpose. This has an adverse effect on environment. If Cox's Bazar sea sand can be used as a source of sand, this could minimize the adverse effect on environment. The objectives of this research were to collect sea sand from the Largest Cox Bazar Sea Beach and explore different properties of it.

2. METHODOLOGY

Sample Collection

The first step of this research work is sample collection. A team of two members was formed in order to collect the sample from Cox's Bazar sea beach. A small shovel was used for taking large samples from soil surface. Sample was taken from two spots. From spot 01 samples were collected from 6 and 24 inches respectively. Moreover, from spot 02 samples were collected from 6 and 18 inches respectively. All the samples were preserved in airtight plastic jars. 5kg from each depth were collected for the test purpose. The jars were airtight so that the sample could represent the actual moisture content and other properties of field condition. The locations of sample 01 and 02 are 21°20'23.0"N, 92°01'47.0"E and 21°21'21.5"N 92°01'24.9"E respectively.

Laboratory Tests

Direct shear, particle size analysis, proctor compaction test, moisture content determination, specific gravity determination and compressive strength of mortar determination tests were performed according to ASTM D3080, ASTM D422, ASTM D698, ASTM D2216, ASTM D854 and ASTM C109 respectively.

3. LABORATORY TEST RESULTS & DISCUSSION

Figures and Graphs

3.1.1 Direct Shear

From the tests, it is found that the angle of friction of sea sand of spot 1 and 2 varies from 2.2° to 8.46° which is very low. The result is provided from figure 1 to figure 9.

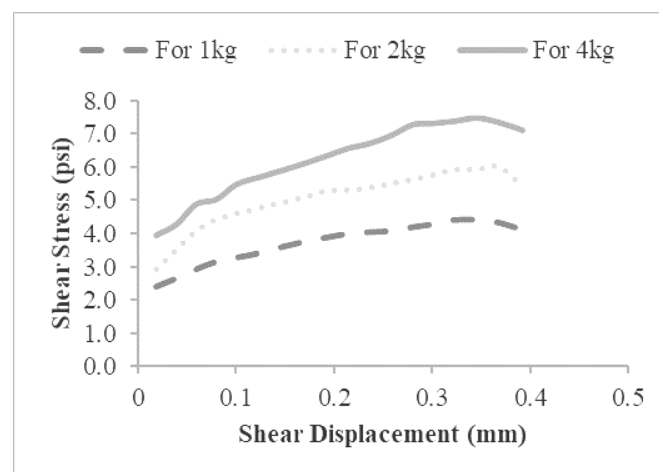


Figure 1: Shear Stress vs Shear Displacement (Spot 01 Depth 6 inch)

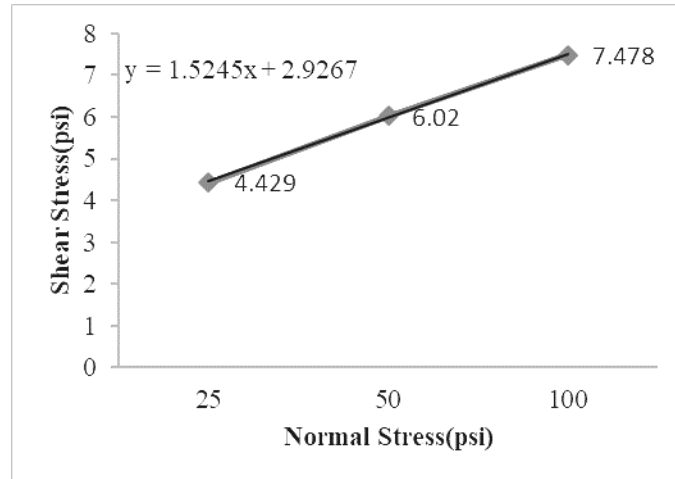


Figure 2: Shear Stress vs Normal Stress (Spot 01 Depth 6 inch)

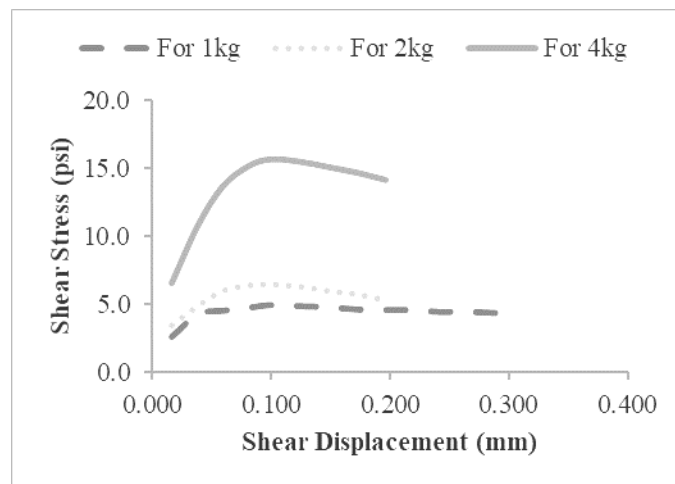


Figure 3: Shear Stress vs Shear Displacement (Spot 01 Depth 24 inch)

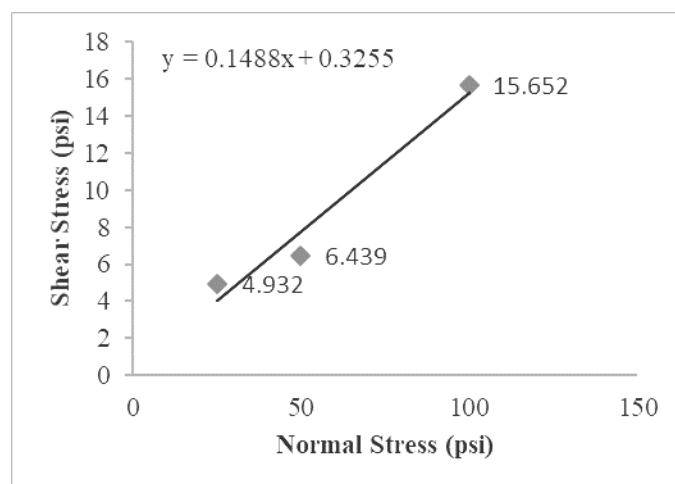


Figure 4: Shear Stress vs Normal Stress (Spot 01 Depth 24 inch)

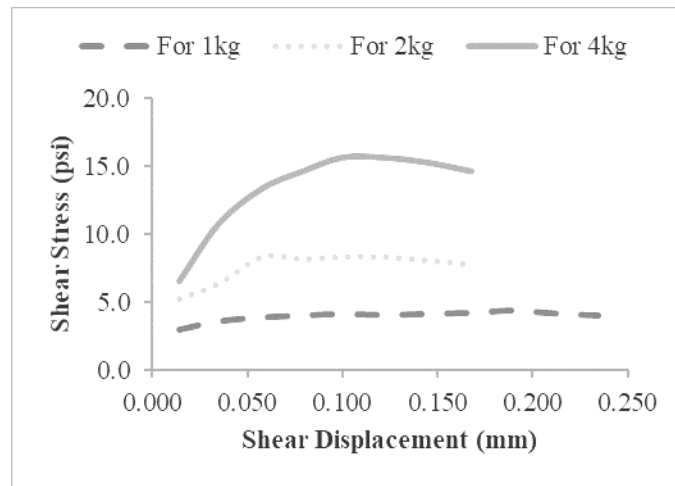


Figure 5: Shear Stress vs Shear Displacement (Spot 02 Depth 6 inch)

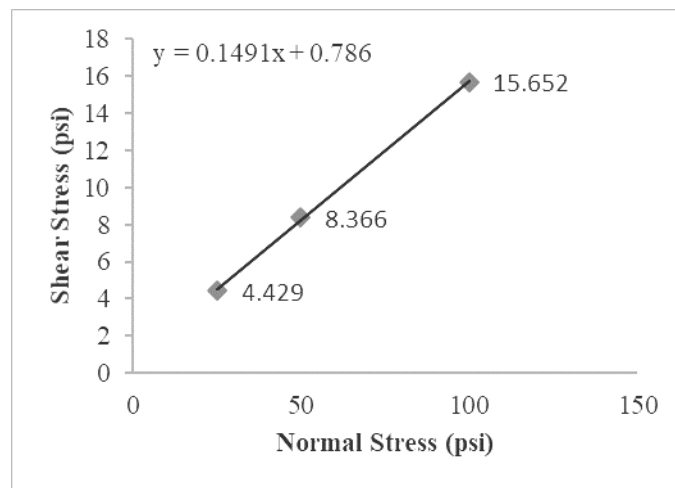


Figure 6: Shear Stress vs Normal Stress (Spot 02 Depth 6 inch)

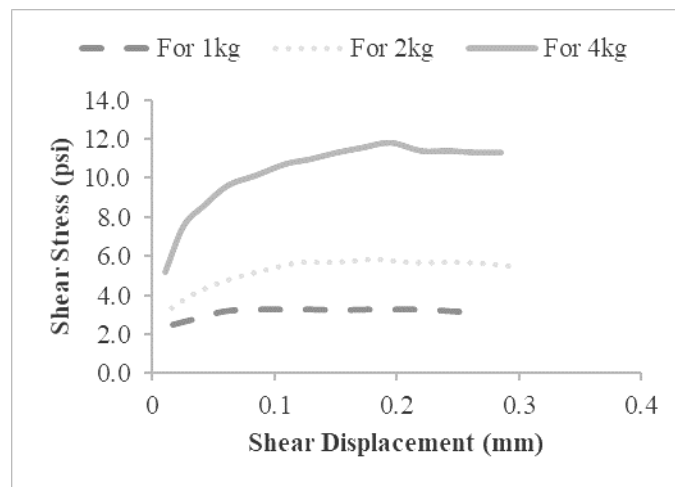


Figure 7: Shear Stress vs Shear Displacement (Spot 02 Depth 18 inch)

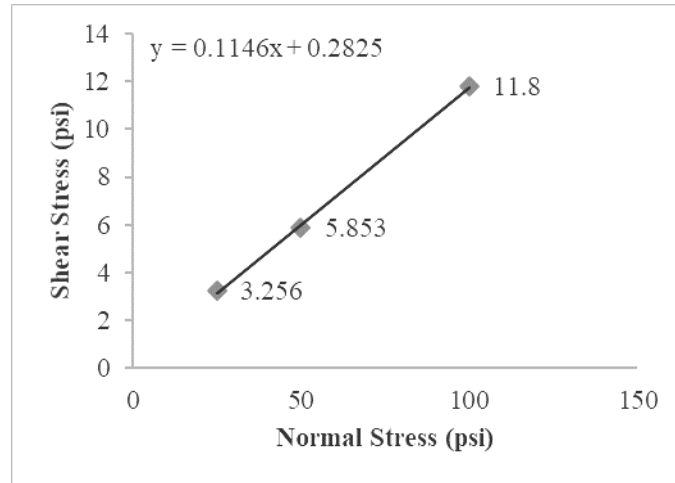


Figure 8: Shear Stress vs Normal Stress (Spot 02 Depth 18 inch)

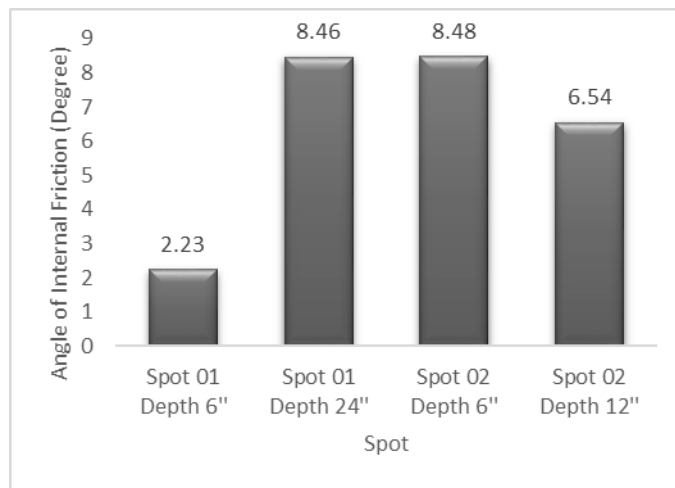


Figure 9: Angle of Internal Frictions of Different Spots

3.1.2 Particle Size Analysis

From gradation curve of all samples it is quite clear that sand samples are uniformly graded. 75-80% is between 0.11 to 0.12mm. The results are given in figures 10 to figure 13.

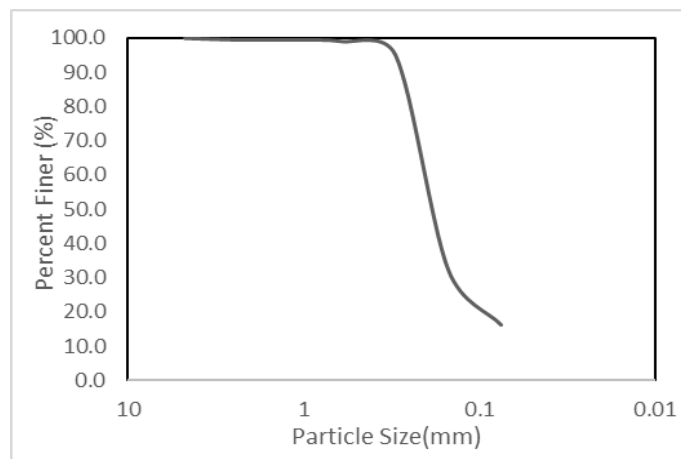


Figure 10: Grain Size Distribution Curve (Spot-01 Depth- 6 inch)

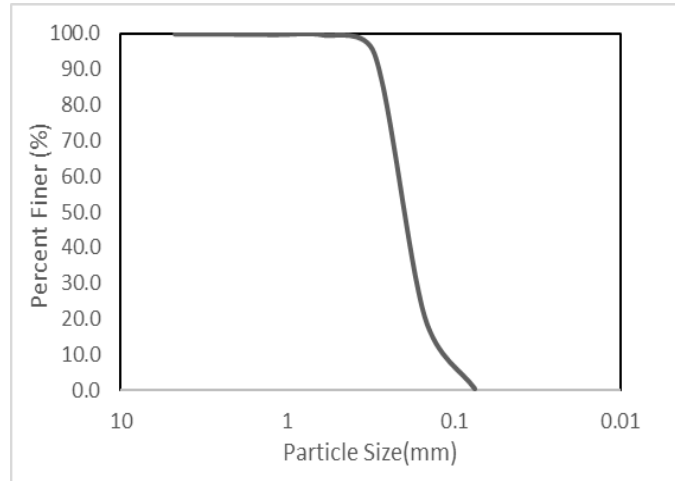


Figure 11: Grain Size Distribution Curve (Spot-01 Depth- 24 inch)

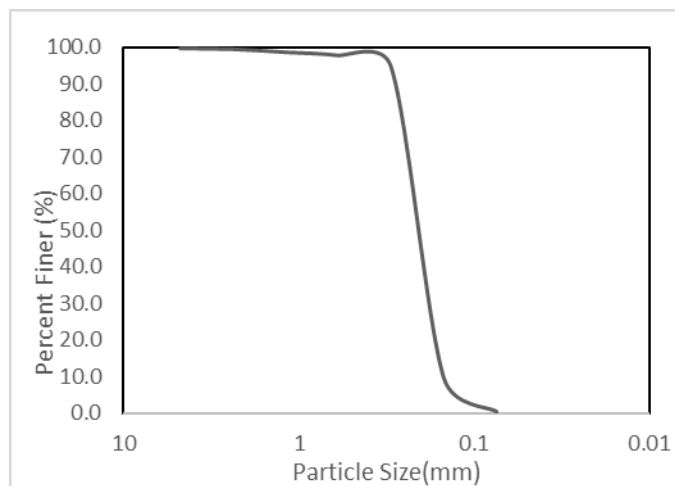


Figure 12: Grain Size Distribution Curve (Spot-02 Depth- 6 inch)

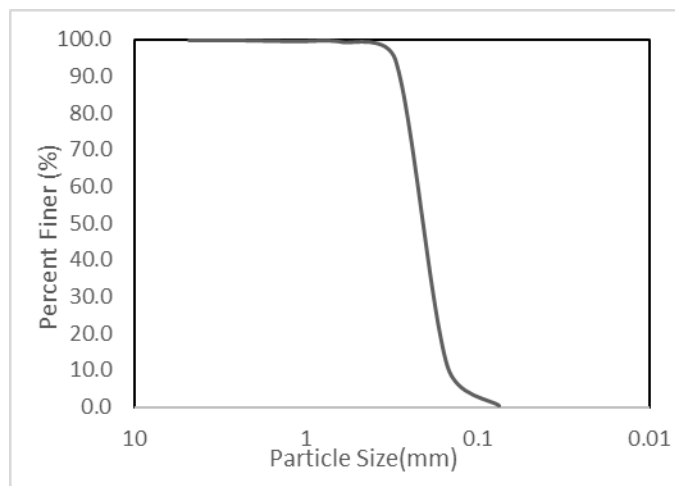


Figure 13: Grain Size Distribution Curve (Spot-02 Depth- 18 inch)

3.1.3 Proctor Compression Test

From the tests, it is found that the optimum moisture content of sea sand of spot 1 and 2 varies from 23% to 28%. Moreover, the dry density varies from 1.59 to 1.66 g/cm³. The results are shown in figure 3.14.

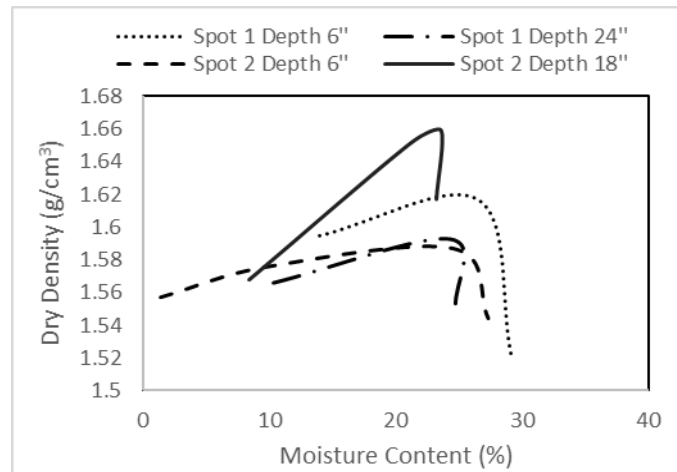


Figure 14: Optimum Moisture Content and Maximum Dry Density Determination of Different Locations

3.1.4 Moisture Content Determination

Moisture content of sea sand of spot 1 and 2 varies from 11.32% to 11.90%. The result is shown in the figure 15.

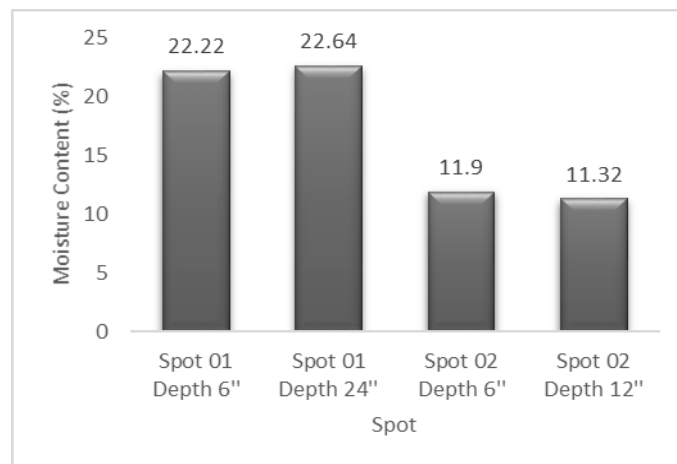


Figure 15: Moisture Content of Different Spots

3.1.5 Specific Gravity

Specific gravity of sea sand of spot 1 and 2 varies from 2.638 to 2.661. The result is illustrated in figure 16.

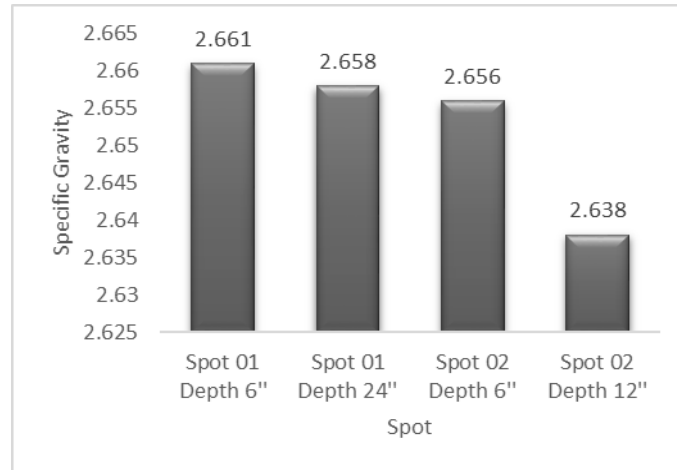


Figure 16: Specific Gravity of Different Spots

3.1.6 Compressive Strength of Mortar

The mortar using this sand has very low strength that varies from 1.1 MPa to 13.70 MPa. The result is shown from figure 17 to figure 20.

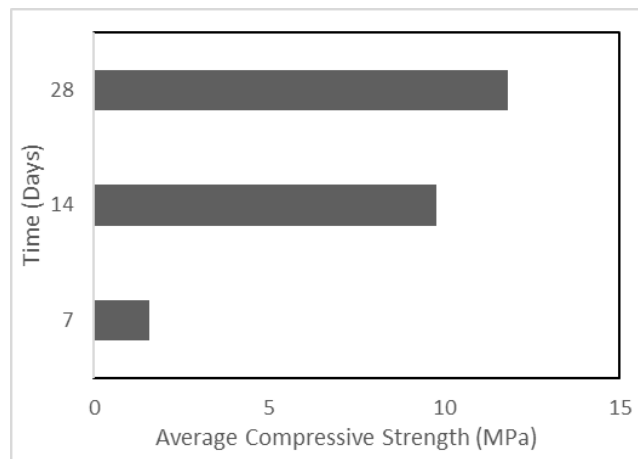


Figure 17: Variation of Compressive Strength (Spot-01 Depth- 6 inch)

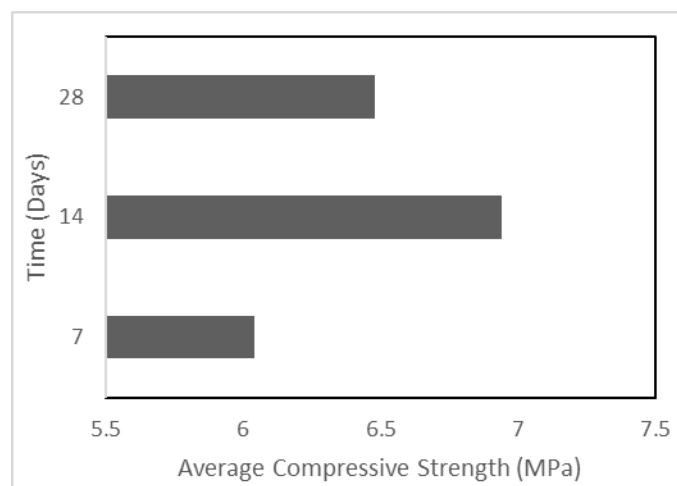


Figure 18: Variation of Compressive Strength (Spot-01 Depth- 24 inch)

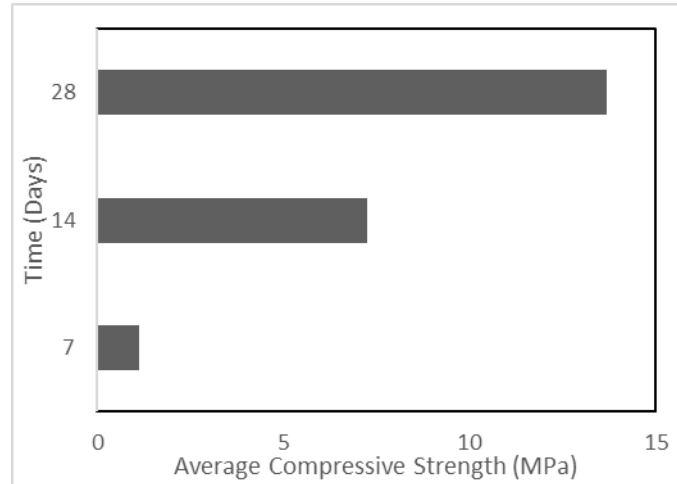


Figure 19: Variation of Compressive Strength (Spot-02 Depth- 6 inch)

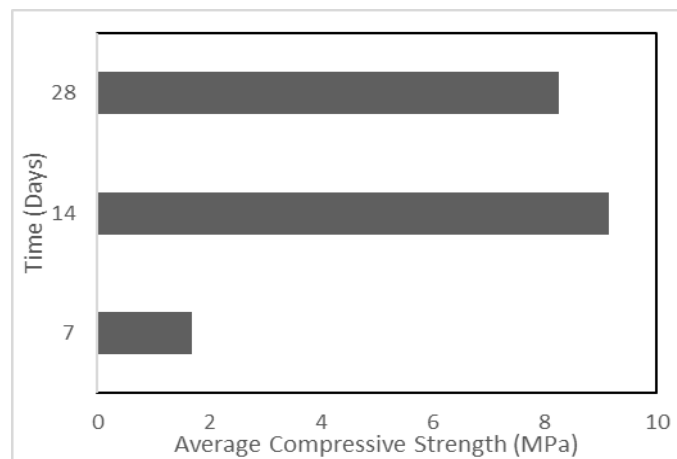


Figure 20: Variation of Compressive Strength (Spot-02 Depth- 18 inch)

5. CONCLUSIONS AND RECOMMENDATIONS

Though sand is a universal material and it has a lot of uses, different analysis of this material is required regarding its availability in nature. In this research paper sea sand was collected from two spots only and some laboratory tests were conducted only for determining some engineering and index properties. But further analysis with more samples should be performed for determining other index and engineering properties and also its salt concentration and extraction should be performed in future research work.

ACKNOWLEDGEMENTS

Thanks to the Civil Engineering Department of Ahsanullah University of Science and Technology for the laboratory support. Also thank to Amin Design and Consultancy (ADC) for the assistance at the fieldwork.

REFERENCES

- Yong R.N. and Japp R.D. (1966). soil water relationships and their engineering applications.
- Das, B. M. 'Principles of Geotechnical Engineering' (Seventh Edition).
- "Maximum Dry Density of Soil and Optimum Moisture Content Test." *The Constructor*, 6 Sept. 2018, theconstructor.org/geotechnical/soil-maximum-dry-density-optimum-moisture-content/18426/.
- Xiao, Jianzhuang, et al. "Use of Sea-Sand and Seawater in Concrete Construction: Current Status and Future Opportunities." *University of Miami's Research Profiles*, Elsevier Limited, 30 Nov. 2017, miami.pure.elsevier.com/en/publications/use-of-sea-sand-and-seawater-in-concrete-construction-current-sta.
- Sun, Wu, et al. "Study on the Influence of Chloride Ions Content on the Sea Sand Concrete Performance." *American Journal of Civil Engineering*, Science Publishing Group, 23 Mar. 2016, article.sciencepublishinggroup.com/html/10.11648.j.ajce.20160402.12.html.
- "The Importance Sand and Gravel in Our Lives." *A.L. Blair*, 30 Nov. 2018, alblairconstruction.com/importance-of-sand-and-gravel/.
- Britannica, The Editors of Encyclopaedia. "Sand." *Encyclopædia Britannica*, Encyclopædia Britannica, Inc., www.britannica.com/science/sand.
- Fang, Hsai-Yang. *Foundation Engineering Handbook*. CBS Publishers & Distributors, 2004
- ASTM D698 - 12e2." ASTM International - Standards Worldwide, www.astm.org/Standards/D698.htm.
- "ASTM C150/C150M-19a." ASTM International - Standards Worldwide, www.astm.org/Standards/C150.htm

LOCAL SOIL IMPROVEMENT WITH BENTONITE TO MAKE CRICKET PITCH SPEEDY AND BOUNCY

Md. Rezaul Islam¹, Pranta Roy², Md. Ashik Ahmed *³ and Rafiuzzamam Sadi⁴

¹*Post -Graduate Student, MIST, Bangladesh, e-mail: rezaul_islam29@outlook.com*

²*Lecturer, European University of Bangladesh, Bangladesh, e-mail: prantaku2k13@gmail.com*

³*Lecturer, European University of Bangladesh, Bangladesh, e-mail: ashik1788@gmail.com*

⁴*Lecturer, European University of Bangladesh, Bangladesh, e-mail: rafi.sadi.144@gmail.com*

***Corresponding Author**

ABSTRACT

Soil in Indian subcontinent is generally silt and clay type and its plasticity index is low. This study will present a way to change soil's various properties to make it more suitable for using while preparing speedy and bouncy cricket pitches with local soil. Soil sample was collected from different locations of Bangladesh. Hydrometer test and Atterberg limit tests were performed to determine silt, clay content, and plasticity index of soil samples. Comparing this with Australian pitches soil sample which is used to prepare their cricket pitches which is more speedy and bouncy than Bangladeshi cricket pitches. For this, local soil sample which is used to prepare cricket pitches is needed to increase clay content as well as improve its plasticity index is required to make speedy and bouncy like Australian pitches. From laboratory analysis, it's been shown that after using bentonite admixture in local soil increase clay content from 6% to 27% (sample 1) and 13% to 37% (sample 2), lowering silt content from 44% to 24% (sample 1) and 47% to 29% (sample 2), and organic matter are lowering near 5% for both samples. Liquid limit and Plastic limits for both samples are decreased after improvement with bentonite and plasticity index are increased from 4.39% to 4.53% (sample 1) and 1.22% to 3.82% (sample 2). Coefficient of restitution is increasing with decreasing moisture content. Four models have been developed two are with bentonite and another two are without bentonite and compare the speed and bouncy property of these four samples. Finally, it was found that improved soil model behaving more similarly with Australian cricket pitches. Therefore, with this improved soil sample speedy and bouncy cricket pitch in Bangladesh can be prepared as like as Australian cricket pitches.

Keywords: *Local soil, Bentonite, Silt and clay content, Plasticity index, Speed and bouncy test.*

1. INTRODUCTION

Cricket is one of the most popular sports in Bangladesh. People are delighted to watch this game as it is representing our country at the international level as well as the Bangladesh National Cricket team is doing well in this game. In Cricket, various factors are important to be concerned. Among them, weather, playing surface, ground conditions vary from country to country. The playing surface is known as Cricket Pitch. The cricket pitch consists of the central strip of the cricket field between the wickets. It is 22 yards (20.12 m) long and 10 feet (3.05 m) wide (Eudoxie & Nagassar, 2012). The surface is flat and normally covered with extremely short grass though this grass is soon removed by wear at the ends of the pitch. Cricket pitches are categorized according to their behavior. Fast and slow are the common categories of pitches. "Fast" pitches quite commonly are "Bouncy" pitches as well while "Slow" pitches tend to be "Low", dusty and conducive to "Spin"(Nawagamuwa, Senanayake, Silva & Sanjeewa, 2009). Most of the subcontinent pitches are slow and low even though it has been attempted, the creation of fast and bouncy pitches in the subcontinent has eluded. This study deals with the problem of creating fast and bouncy pitches by investigating how some of the physical property of a cricket pitch varies with soil used to make the pitch. Pace, bounce, spin, consistency, and deterioration are the significant behavior of cricket pitches (Baker, Cook & Adams, 1998). Pace describes how fast delivery will come at the batsmen after bouncing and it depends on the horizontal velocity component of the ball and the horizontal velocity retained after bouncing (Robinson & Robinson, 2016). Spin defines the cricket ball with rapid rotation so that when it bounces on the pitch it will deviate from its normal straight path, thus making it difficult for the batsman to hit the ball cleanly. The speed the ball travels is not critical and is significantly slower than that for fast bowling. A typical spin delivery has a speed in the range 70–90 km/h (45–55 mph) (Robinson & Robinson, 2016). Bounce describes the steepness of the path of delivery after bouncing and its governing factor is vertical velocity gained by the ball after impact with the pitch. Consistency means batsman's better predictability about the path of delivery as the highly inconsistent pace will make batting almost impossible while inconsistent bounce will be dangerous to the batsman. Deterioration describes the length of time a pitch is likely to maintain a certain level of pace and bounce (James, Carré & Haake, 2005). Cricket pitches are mainly categorized into 3 types: Dead pitch, Dusty pitch, Green pitch. Most of the dead pitches are mainly found in Indian subcontinents. ODI and T20 matches are mainly played in this type of pitches. As these wickets have nothing for bowlers the batsmen continue to put runs on the scoreboard leaving the bowlers in a state of trouble. But the game played in these wickets is very much interesting because of the huge maximums from the batsmen. Green pitches having green grass on it makes it less abrasive on the ball and helps the ball to swing easily (Ball & Hrysomallis, 2012). Along with swing, the bounce in these wickets is unpredictable. Even if these pitches seem to help the seam bowlers but serve absolutely nothing for a spinner. These types of pitches are found in western countries of the globe and mainly preferred for test cricket. The surface of the dusty pitch is soft and unrolled which creates a great help for the spin bowlers. These pitches are easier to bat as compared to the other two because in this wicket the bounce of the ball can be predicted by the batsmen. Dusty pitches are mostly found in subcontinents. These wickets are not that difficult to score as the deliveries normally stay low which can be easily faced by the batsmen (Gopinath, 2017). But spinners with great skills can pick up a bunch of wickets in these pitches. In the subcontinent, the dead pitch is prepared for ODI and T20 format whereas dusty pitches are prepared for longer version as this pitch have low pace and bouncy behaviour whereas Green pitches are prepared in Australia, England, and South Africa because of its high speedy and bouncy behaviour for all types of version. According to experts, Bangladeshi pitches differ from Australian, English and South African pitches in three of the above characteristics. They are namely pace, bounce and deterioration. Bangladesh's pitch has a slower pace and bounce and also deteriorates much faster.

The soil in Bangladesh is generally silt and clay type and its plasticity index is low (Payton et al., 2003). There are Seven Soil Tracts of Bangladesh and these are Madhupur Tract, Barind Tract, Tista Silt, Brahmaputra Alluvium, Gangetic Alluvium, Coastal Saline Tract, and Chittagong Hill Tract

(Payton et al., 2003). And considering the climate as the most active pedogenic factor, Bangladesh was divided into three zones: Humid, Semi-Humid, and Feebly Arid.

Cricket pitches of different locations in Bangladesh are usually made by local soil according to the location of the stadium. Cricket pitches are consisting of an aggregate mixture of coarse sand, fine sand, silt, and clay together by a strong binding agent. Silts are non-cohesive soil particles that reduce cohesiveness of soil, as a result, pitches become dusty (Gopinath, 2017). Higher organic content in soil reduces the binding strength of the soil and so reduces pace and bounce. Pitches of the subcontinent have higher silt and organic content that's why these pitches are slower and spiny. On the other hand, Pitches in Australia, England, and South-Africa have high clay content with a minimum percentage of silt and high plasticity index (Harwood, King & Yeadon, 2017). Because of these reasons, the behaviour of pitches in those countries is fast and bouncy. The objectives of this study are to improve soil properties by using bentonite admixture as it reduces organic content, silt content of soil and increases clay content, plasticity index which will help to create fast and bouncy cricket pitch. As Bangladesh is a tropical country, here most of the time temperatures are higher than English condition that's why heated bentonite was used to improve soil sample which increase plasticity index (Widjaja & Nirwanto, 2019). It was hypothesized that reducing the silt content, organic content and improving the plasticity by the introduction of Bentonite (a clay type with very high plasticity) into the soil would produce a faster and bouncier pitch of similar character to those in Australia, England, and South Africa (Nawagamuwa et al., 2009). Since bentonite is used to transform cohesion less soil into cohesive soil and this happens due to rearrangement of soil grains, decreasing the void between the grains and increasing the density of the soil.

2. METHODOLOGY

An experimental program was conducted to investigate the behavior of soil samples before and after improving with bentonite admixture (30% of soil sample weight). Two soil sample was collected from two different locations which were used to prepare four different model pitches. Among them, one was before improvement and the other one was after improvement. There are two types of bentonite is possible one is swelling type and other is non-swelling types. Here non-swelling type calcium bentonite was used at heated temperature of 120°C temperature.

2.1 Sample Location and Testing

Figures 1 and 2 show that Soil samples 1 were collected from Mymensingh and soil sample 2 were collected from Kishoreganj respectively. Both of them are in the semi-humid zone.



Figure 1: Soil Sample 1 from Mymensingh



Figure 2: Soil Sample 2 from Kishoreganj

Atterberg limit test, Hydrometer analysis, and organic matter content of two soil samples before and after improvement were performed to determine silt content, clay content, organic matter content, and plasticity index of the soil samples. Laboratory analysis of collected soil samples was done. Figures 3 and 4 representing the oven drying of soil samples and Atterberg limit test respectively.



Figure 3: Oven drying of soil sample



Figure 4: Atterberg Limit Test

2.2 Model Pitch Preparation and Testing

Four different model pitches were prepared by two soil samples before and after improvement having dimensions of 3 X 3 ft. and thickness of 6 inches. The sample pitch having thickness 6 inches where 3 inches of soil layer, 0.5 inches of metal plate and 2.5 inches of founding materials (stone chips). Each sample pitches were constructed into three layers with hammering and rolling. Figure 5 and figure 6 indicates the model pitch 1 with and without bentonite whereas figure 7 and figure 8 shows model pitch 2 with and without bentonite.

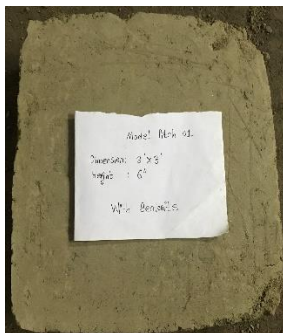


Figure 5: Model Pitch 1 with Bentonite

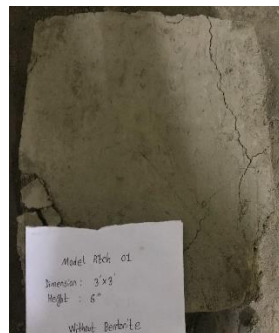


Figure 6: Model Pitch 1 without Bentonite

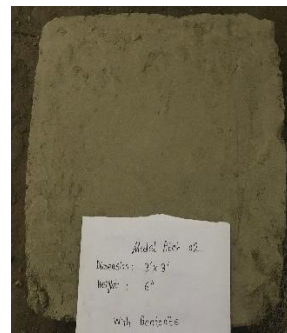


Figure 7: Model Pitch 2 with Bentonite

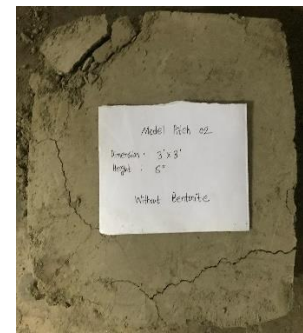


Figure 8: Model Pitch 2 without Bentonite

2.3 Speed Test

Figure 9 represents the experimental setup to determine the speed value of the model pitch by identifying the release point of the ball, impact point of the ball on pitch and bouncing point of the ball after impact on pitch with an android app called speed clock which helped to determine the speed value of each point above mentioned. Regular Cricket ball was used during this speed test.

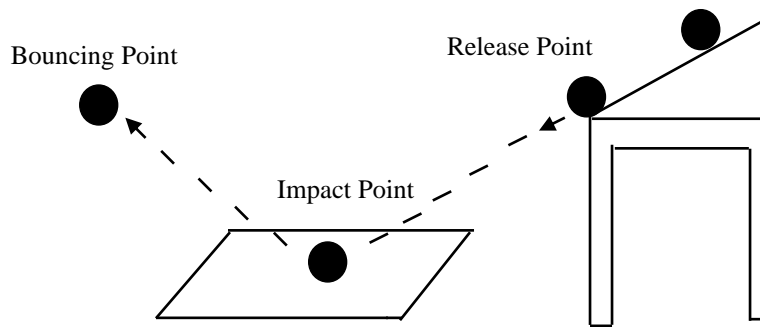


Figure 9: Experimental setup for Speed test

2.4 Bounce Test

Figure 10 shows that the experimental setup of bouncy test of the model pitches where the ball was released from a certain height 'H' with a definite velocity on the model pitch and after impacting rebound height 'h' was measured. Through this process and from the simple mechanic's coefficient of restitution of surface was determined. Bouncy property of cricket pitch will increase with increasing value of the coefficient of restitution.

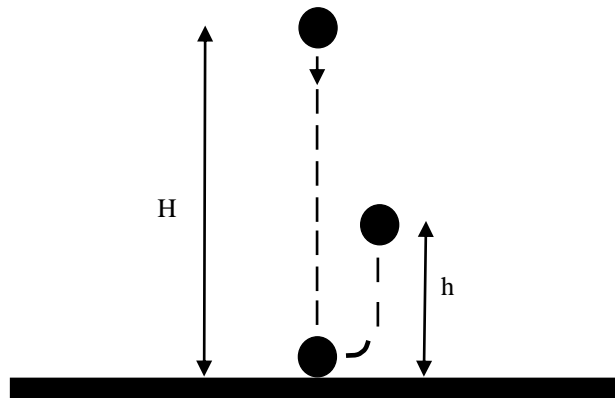


Figure 10: Experimental setup for Bounce test

3. RESULTS AND DISCUSSIONS

3.1 Soil Components and Atterberg Limit Test

Table 1 represents the comparison between soil properties of Australian pitches and local soil samples from Mymensingh and Kishorganj. Soil components of Australian Pitches represent that their clay contents are too high, silt content is low and organic content is near about 5%. Because these pitches are too fast and bouncy whereas local soil samples showing exactly opposite behavior. Improving soil samples with Bentonite admixture, it's been clearly indicating that the clay content was increased whereas silt content was decreased. Since non swelling types calcium bentonite after heating 120°C temperature was used, liquid and plastic limit of soil samples were decreasing but plasticity index was increased. And the most significant part is organic matter were decreased and its numerical value went down to almost 5%. This is a clear indicator that, the pitch with this improved soil will be faster and bouncier than before.

Table 1: Comparison between soil components of Australian pitches and local Soil Sample

Soil	Brisbane*	Perth*	Soil Sample 1		Soil Sample 2	
			Before Bentonite	After Bentonite	Before Bentonite	After Bentonite
Clay	68	82	6	27	13	37
Silt	6	6	44	24	47	29
Organic Matter	5.5	2.1	7	5.4	8	4.8

(*NZSTI Guide to Cricket Pitch Preparation)

It has been clearly shown from Table 2 that improving soil samples with Bentonite lowering the liquid and plastic limit value but increasing the plasticity index. This indicates that preparing a pitch with this improved soil will be more compacted and it will decrease the chance of crumbling.

Table 2: Atterberg limit of local Soil Sample

Soil	Soil Sample 1		Soil Sample 2	
	Before Bentonite	After Bentonite	Before Bentonite	After Bentonite
Liquid Limit	29.6	25.25	26	24.50
Plastic Limit	25.21	20.72	24.78	20.68
Plasticity Index	4.39	4.53	1.22	3.82

Figure 11 represents the comparison of soil components of different local soil samples with Australian pitches soil samples and figure 12 shows the Atterberg limits variation before and after improving soil with Bentonite.

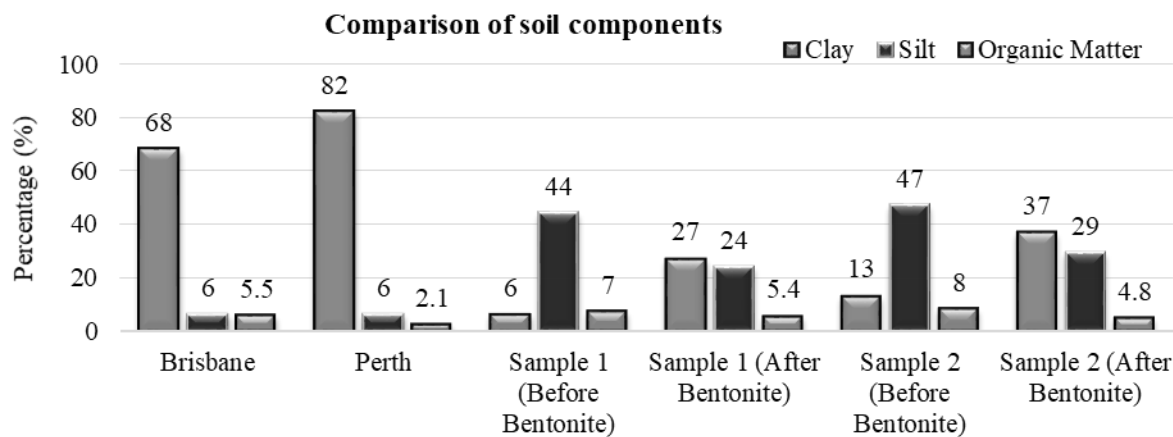


Figure 11: Comparison of soil components of different local soil samples with Australian pitches soil samples.

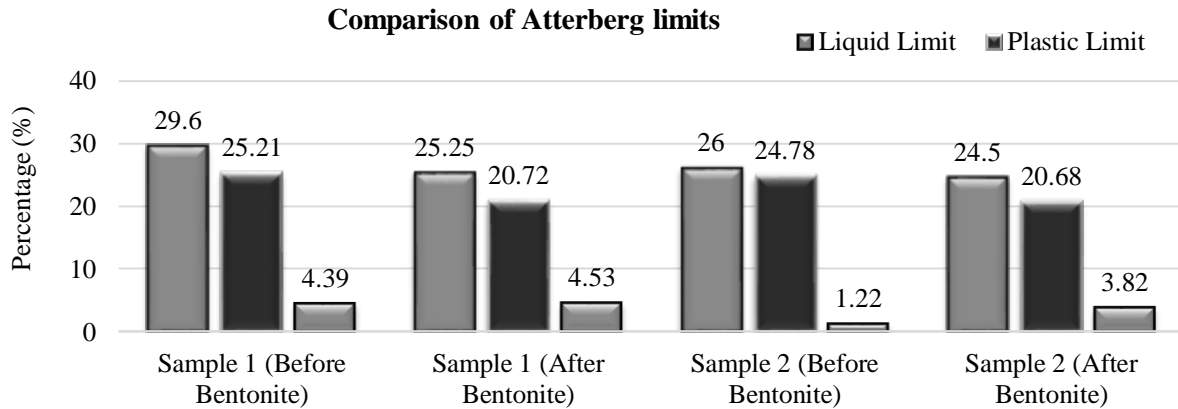


Figure 12: Comparison of Atterberg limits of different local soil samples before and after improvement.

Equations:

From simple mechanics, equations of coefficient of restitution can be determined and it shown below,

$$v_i = \sqrt{2gH} \quad (1)$$

$$v_o = \sqrt{2gh} \quad (2)$$

$$e = \frac{v_o}{v_i} = \sqrt{\frac{h}{H}} \quad (3)$$

Where, v_i = incoming velocity, v_o = outgoing velocity, e = coefficient of restitution

3.2 Speed Test

Cricket ball was thrown at a constant speed of 85 Kph on four different pitch models. In model Pitch 1 and 2 without Bentonite, speed was increased after the impact of ball on the pitch from 85 Kph to 94 Kph and 96 Kph respectively. Whereas Model Pitch 1 and 2 with bentonite, speed was increased from 85 Kph to 107 Kph and 111 Kph respectively. Table 3 represents the speed variation of cricket ball on different pitch models.

Table 3: Variation of Speed on different Pitch Models

	Model Pitch 1 (without Bentonite)	Model Pitch 1 (with Bentonite)	Model Pitch 2 (without Bentonite)	Model Pitch 2 (with Bentonite)
Releasing Point speed (Kph)	85	85	85	85
Bouncing Point speed (Kph)	94	107	96	111

3.3 Bouncy Test

Table 4 and 5 represents that cricket ball was released freely on Pitch models from 60 inches above in different moisture condition 5 %, 10%, 15% sequentially. As moisture content were increasing, rebounding heights were decreased. From equation (3) it calculated that the coefficient of restitution was decreasing with the increase of moisture content.

Table 4: Bounce Test Results for Model Pitch 1

	Moisture (%)	H (inch)	h (inch)	e
Model Pitch 1 (Before Bentonite)	5	60	20	0.577
	10	60	16	0.516
	15	60	11	0.428
Model Pitch 1 (After Bentonite)	5	60	22	0.606
	10	60	17	0.532
	15	60	13	0.465

Table 5: Bounce Test Results for Model Pitch 2

	Moisture (%)	H (inch)	h (inch)	e
Model Pitch 1 (Before Bentonite)	5	60	24	0.632
	10	60	21	0.592
	15	60	17	0.532
Model Pitch 1 (After Bentonite)	5	60	28	0.683
	10	60	22	0.606
	15	60	19	0.563

Comparison between moisture content (%) and the coefficient of restitution (e) of Model Pitch 1 and 2 are shown in Figures 13 and 14 respectively.

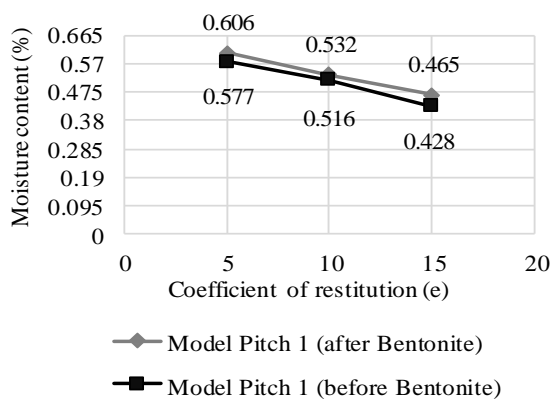


Figure 13: Moisture Content (%) vs. Coefficient of restitution(e) of Model Pitch 1

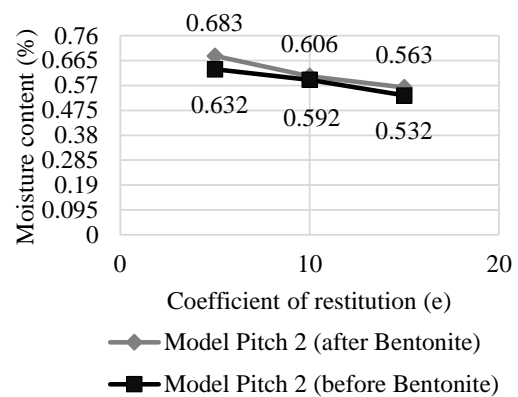


Figure 14: Moisture Content (%) vs. Coefficient of restitution (e) of Model Pitch 2

4. CONCLUSIONS

From this study, it observed that model pitch 1 and 2 without bentonite had comparatively low and slow characteristics than model pitch 1 and 2 with Bentonite. Compare with Australian pitches conditions with model pitch 1 and 2 with bentonite had achieved better results than the model pitch 1 and 2 without Bentonite. From the value of the coefficient of restitution, it analyzed that bounce of the ball in model pitches with improved soil has better bouncy behavior and in case of speed, it also showed from the table that model pitches with improved soil made speedy pitches than model pitches without improved soil. Though model pitches with improved soil cannot reach the level of Australian Cricket pitches, it gives a clear indication that if pitches with an improved soil sample of Bentonite admixture are prepared, it can be faster and bouncier than the regular cricket pitches of Bangladesh.

Also, here, the amount of Bentonite was 30% of the weight of soil sample if it increases up to 60-80% then more convenient results of prepare faster and bouncier pitches in Bangladesh are possible but there is a possibility of severe cracking. So, Model pitches with improved soil of Bentonite admixture have a greater possibility to construct much higher speedy and bouncy cricket pitches in Bangladesh.

REFERENCES

- Baker, S. W., Cook, A., & Adams, W. A. (1998). Soil characteristics of first-class cricket pitches and their influence on playing performance. *Journal of Turfgrass Science*.
- Ball, K., & Hrysomallis, C. (2012). Synthetic grass cricket pitches and ball bounce characteristics. *Journal of Science and Medicine in Sport*. <https://doi.org/10.1016/j.jsams.2011.10.010>
- Eudoxie, G., & Nagassar, D. (2012). Influence of cricket pitch preparation on resulting pitch surface hardness. *Tropical Agriculture*.
- Gopinath, R. . . . P. B. (2017). Utilization of Lateritic Soil to Make Fast and Bouncy Cricket Pitches. *International Journal of Science and Research (IJSR)*.
- Harwood, M. J., King, M. A., & Yeadon, M. R. (Fred). (2017). The influence of cricket pitch length on ball release by junior bowlers. *ISBS Proceedings Archive*.
- James, D. M., Carré, M. J., & Haake, S. J. (2005). Predicting the playing character of cricket pitches. *Sports Engineering*. <https://doi.org/10.1007/bf02844162>
- Nawagamuwa, U. P., Senanayake, A. I. M. J., Silva, S. A., & Sanjeewa, D. M. I. (2009). Improvement of Local Soils in Order to Make “Fast & Bouncy” Cricket Pitches. *Engineer: Journal of the Institution of Engineers, Sri Lanka*. <https://doi.org/10.4038/engineer.v42i4.7033>
- Payton, R. W., Barr, J. J. F., Martin, A., Sillitoe, P., Deckers, J. F., Gowing, J. W., ... Zuberi, M. I. (2003). Contrasting approaches to integrating indigenous knowledge about soils and scientific soil survey in East Africa and Bangladesh. *Geoderma*. [https://doi.org/10.1016/S0016-7061\(02\)00272-0](https://doi.org/10.1016/S0016-7061(02)00272-0)
- Robinson, G., & Robinson, I. (2016). Spin-bowling in cricket re-visited: Model trajectories for various spin-vector angles. *Physica Scripta*. <https://doi.org/10.1088/0031-8949/91/8/083009>
- Widjaja, B., & Nirwanto, A. F. (2019). Effect of various temperatures to liquid limit, plastic limit, and plasticity index of clays. In *IOP Conference Series: Materials Science and Engineering*. <https://doi.org/10.1088/1757-899X/508/1/012099>

EFFECT OF VARIATION OF WATER LEVEL AND GEOMETRY ON THE STABILITY OF THE PADMA RIVERBANK SLOPE FOR DIFFERENT SOIL PROPERTIES

Anika T Abha^{*1}, Azizul Islam², Eqramul Hoque³ and Ferdousul H Shikder⁴

¹*Graduate in Civil Engineering, Bangladesh University of Engineering and Technology, Bangladesh, e-mail: anikatabha@gmail.com*

²*Assistant Professor of Civil Engineering, Bangladesh University of Engineering and Technology, Bangladesh, e-mail: aziz.buet@gmail.com*

³*Professor of Civil Engineering, Bangladesh University of Engineering and Technology, Bangladesh, e-mail: ehq@ce.buet.ac.bd*

⁴*Graduate in Civil Engineering, Bangladesh University of Engineering and Technology, Bangladesh, e-mail: hsferdous95@icloud.com*

***Corresponding Author**

ABSTRACT

Natural riverside slopes are often hampered by the variation of water level. This study aims to investigate the stability of the riverbank of Padma due to the variation of water level as well as variation of geometry by using PLAXIS-2D software based on Finite Element Method (FEM). Undisturbed soil samples at different depths were collected from the selected two locations called Paschimchor and Moinotghat which are two riverbanks of the Padma river. Four undisturbed samples were collected from field using Shelby tube. Then the samples were subjected to direct shear test to determine the strength parameters which were later used as input parameters in the software. Grain size analysis and specific gravity test indicated that the sample collected from Paschimchor was MC or clayey-silt (4.5% sand, 7.5% clay and 88% silt) and the sample collected from top layer of Moinotghat was SM or silty sand (56.8% sand, 37.2% silt and 6% clay) and sample collected from bottom layer of Moinotghat contains 23% clay and 76.4% silt. Considering different slope geometry (slope angle 30°, 35°, 42°, 53°, 58°) slope stability analysis had been performed for different water level (high water table, dry condition and rapid draw down) for riverbank slope of Moinotghat and Paschimchor. From the analysis, it had been observed that maximum factor of safety was found for high water table condition and minimum factor of safety was found at rapid draw down condition considering the same geometry and soil property. On the other hand, soil properties specially the cohesion, angle of friction and coefficient of permeability also had a great impact on stability of the slope considering same geometry. Considering different water level, relation of factor of safety with the geometry of the slope (slope angle) has been represented here also. As the steepness of the slope increases, factor of safety decreases. Steepness of the slope has different effect on factor of safety considering rapid draw down, high water table and dry condition for sandy soil and silty soil.

Keywords: *Slope-stability, Water-level, Geometry, Cohesion, Plaxis-2D.*

1. INTRODUCTION

Slope failure has become an acute problem at Dohar, one of the banks of Padma River and it leads to a huge erosion of land every year. People living around the riverside areas become homeless for this reason. Waterfront slopes are affected by water-level fluctuations originating from as well natural sources (e.g. tides and wind waves), as non-natural sources; in this study, three different approaches used for hydro-mechanical coupling in FEM-modelling of slope stability, have been evaluated. A fictive slope consisting of a till-like soil material has been modelled to be exposed to a series of water-level fluctuation cycle (Johanson, J., 2014). Development of stability, vertical displacements, pore pressures, flow, and model-parameter influence, has been investigated in this study. Factor of safety changes with the change of water level, specially the factor of safety decreases at rapid draw down condition (Fatema & Ansary, 2014). In that research work, the soil sample was collected from Basuria in Sirajgonj near the bank of Jamuna river; the soil sample was SW-SM and numerical analysis in performed here using software STBN2010. Another research presented examines the effect of declining water levels on the stability of riverbank slopes. Where climatic factors, geometry of the slope, material properties of the soil and time taken to vary water level all influenced the stability of the slope (Schiller & Wynne 2010). To make reasonable estimates of slope performance, it is necessary to have knowledge of expected changes in pore water distributions within the earth mass (Allen, Deen & Hopkins, 1975). This research work aimed to establish a correlation between some function of resistivity and a corresponding measure of moisture content. Some research works briefly discussed the way of numerical analysis like Finite Element Method, using a software as calculation tool. In this study Mohr-Coulomb yield criterion and Drucker-Prager yield criterion were converted to equivalent area circle yield criterion, at the same time strength reduction technology combined with convergence criterion, catastrophe criterion and plastic zone penetrability criterion was used (Zhang, H., 2012). Some research works have distinguished the numerical analysis done by FEM and LEM (Mamun & Rahman, 2016). These research works show that analysis done by FEM method shows more conservative result to some extent.

2. METHODOLOGY

For this study four soil samples have been collected. Sample – 1 has been collected from riverbank of Paschimchor (Latitude 23°34'21" and Longitude 90°8'42"). The sample was collected from the depth of 2.5ft from the top surface of the riverbank. Sample – 2 has been collected from riverbank of Moinotghat (Latitude 23°43'5.11" and Longitude 90°4'5.89"); the sample was collected from the depth of 1ft from the top of the surface. The sample – 3 has been collected from bottom layer of the Moinotghat (Latitude 23°37'4.6" and Longitude 90°4'6.65") at the depth of 5.5ft from the top surface of the riverbank. Sample – 4 has been collected from Moinotghat (Latitude 23°37'15.1" and Longitude 90°3.54'4.48") at the 7ft from the top surface of the riverbank. All the samples were collected by using Shelby tube; these four samples were subjected to specific gravity test, grain size analysis test and direct shear test.

2.1 Specific Gravity Test

The specific gravity test was performed for soil of Paschimchor (sample – 1), Moinotghat top layer sample (sample – 2) and Moinotghat bottom layer sample (sample – 3 and sample – 4). Volumetric flask was weighed and 50g soil sample was placed in the pycnometer. Then water was poured into the pycnometer and was filled upto $\frac{3}{4}$ of total volume. Then the sample was allowed 10 minutes for soaking. Then the sample was boiled until the soil-water mixture started to boil. Vacuum was applied for 10 minutes during boiling of soil water mixture. Then the pycnometer containing the soil water mixture was removed and the sample was allowed for cooling. The following day the pycnometer was weighed. The sample was removed and then pycnometer was filled with water up to the mark. The specific gravity of the soil samples is listed in Table 1.

Table 1: Specific gravity of collected soil samples

Soil Sample	Specific Gravity
Soil of Paschimchor riverbank (sample - 1)	2.745
Soil of top layer of Moinotghat riverbank (sample - 2)	2.683
Soil of bottom layer of Moinotghat riverbank (sample - 3)	2.742
Soil of bottom layer of Moinotghat riverbank (sample - 4)	2.703

2.2 Grain Size Analysis Test

In unified classification system soil is basically classified into two groups: Coarse Grained and Fine Grained. Besides these, there are two additional classes: Organic Soil and Peat Soil. On the basis of Unified Classifications coarse grained soils are classified according to grain size and fine grained are to their plasticity characteristics.

If more than 50 percent of soil material of total mass retains on # 200 sieve which means if more than 50 percent of soil material is coarser than $0.75\mu\text{m}$, then the soil is known as coarse grained soil. If 50 percent or more than 50 percent of soil material passes through # 200 sieve, then the soil is known as fine grained soil. If coarse grained soil has less than 5% of materials passing through # 200 sieve, according to USCS classification system, the soil may either be GW, GP, SW, SP. If the coarse-grained soil has greater than 12% finer material than $0.75\mu\text{m}$ (# 200 sieve), then the soil is classified as GM (silty gravel) or SM (silty sand). Soils having between 5 percent to 12 percent passing through # 200 sieve classified by dual symbol. First part of dual symbol describes whether the coarse fraction of the soil is well graded or poorly graded. The second part describes the nature of fineness. A soil classified as GW-GC indicates it is well graded gravel with 5% to 12% clay materials.

The fine-grained soils are subdivided into two class: silt and clay depending on plasticity characteristics. They are further qualified by their degree of compressibility (plasticity). Here liquid limit and plastic limit is identified by the portion of soil passing through # 40 sieve. This is expressed in

Figure 1 (ASTM D2487-17, 2017).

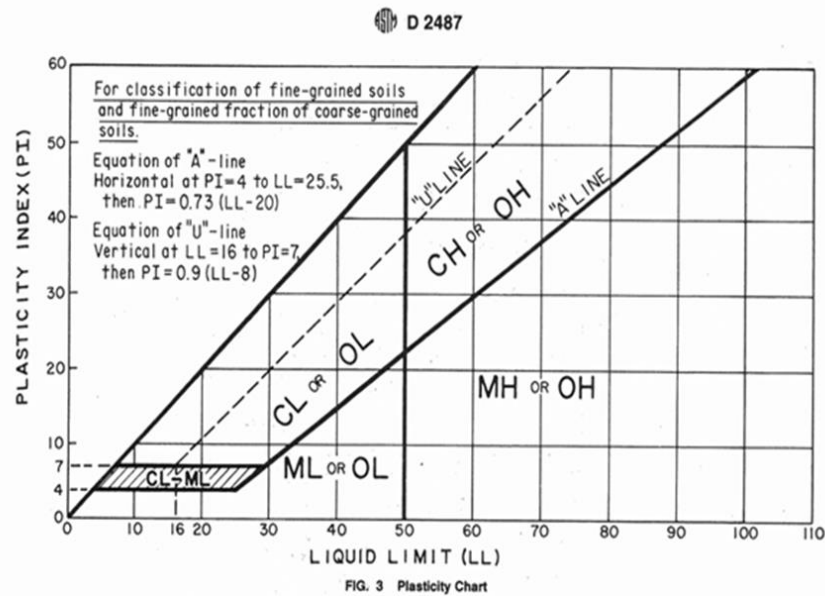


Figure 1: Plasticity Chart

2.2.1 Sieve Analysis and Hydrometer Test

The sample – 1 which was taken from the riverbank at Paschimchor is taken for sieve analysis. For this purpose, the soil is oven-dried and broken into as fine as possible. Then 100gm sample is taken and washed on # 200 sieve and the residue is kept oven-dry. Wash sieve method ensures that little dust will adhere to larger particles and reducible lumps will water softened and the clay and silt particles are washed through sieve. The following day the oven-dried sample is measured it weighs 4.5 gm. As 95.5 gm out of 100 gm soil passes through # 200 sieve which means more than 50% soil material passes through # 200 sieve, the soil is fine grained soil. In the same procedure sample 2,3,4 collected from Moinotghat is subjected to sieve analysis test. For sample-2, As 43.2gm out of 100 gm soil passes through # 200 sieve which means more than 50% soil material retains on # 200 sieve, the soil is coarse grained soil. For sample 3, As 95.9 gm out of 100 gm soil passes through # 200 sieve which means more than 50% soil material passes through # 200 sieve, the soil is fine grained soil. For sample 4, As 99.4gm out of 100 gm soil passes through # 200 sieve which means more than 50% soil material passes through # 200 sieve, the soil is fine grained soil.

Then Hydrometer test has been performed. Hydrometer analysis is widely used method of obtaining an estimate of distribution of soil particle size from no. 200 (0.075mm) sieve to around 0.001mm. Soils where more than 10 to 12 percent passes through # 200 sieve, hydrometer analysis is performed. Hydrometer analysis utilizes the relationship among velocity of fall of spheres in a fluid, the diameter of the spheres, specific weights of the spheres and that of fluid. The rate at which particles settle in a fluid media is an indicator of their size. The hydrometer analysis is based on Stock's law which states that particles in suspension settle out at a rate which varies with their size and settling of the particles is influenced by the viscosity of the fluid.

Here sample – 1, 2, 3 and 4, collected respectively from Paschimchor and Moinotghat, are subjected to hydrometer test as all samples do have more than 12% finer particle than # 200 sieve.

The soil of Paschimchor was basically fine-grained soil as 95.5% soil grains passed through # 200 sieve as shown in Figure 2. From grain size analysis it has been seen that there are 7% clay, 88% silt and 4.5% sand in the soil sample.

From grain size analysis, it can be seen that, soil collected from top layer of riverbank of Moinotghat was basically coarse-grained soil as 43.2% of soil grains which is less than 50%, passed through the # 200 sieve. From grain size analysis, it can also be seen that soil sample contains 56.8% sand, 37.2% silt and 6% clay. This can be visualised from

Figure 3.

Soil sample collected from bottom layer of Moinotghat was basically fine-grained soil and 95.9% soil grains passed through # 200 sieve as shown in

Figure 4. From grain size analysis it has been seen the soil sample contains 5% clay, 4.1% sand and 90.9% silt.

Soil sample collected from bottom layer of riverbank of Moinotghat was basically fine-grained soil and 99.4% soil grains passed through # 200 sieve, which is shown in

Figure 5. From grain size analysis it has been seen that the soil sample contains 23% clay and 76.4% silt and 0.6% sand.

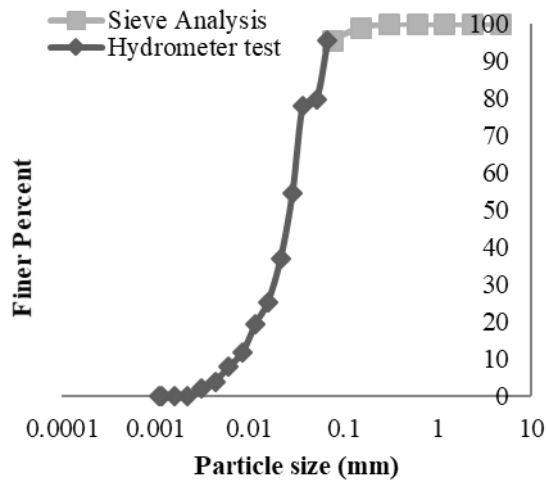


Figure 2: Grain size analysis for soil of Poschimchor riverbank (Sample - 1)

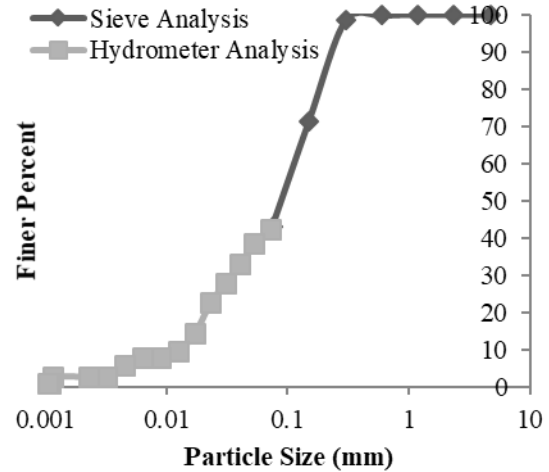


Figure 3: Grain size analysis for soil of top layer of Moinotghat (Sample - 2)

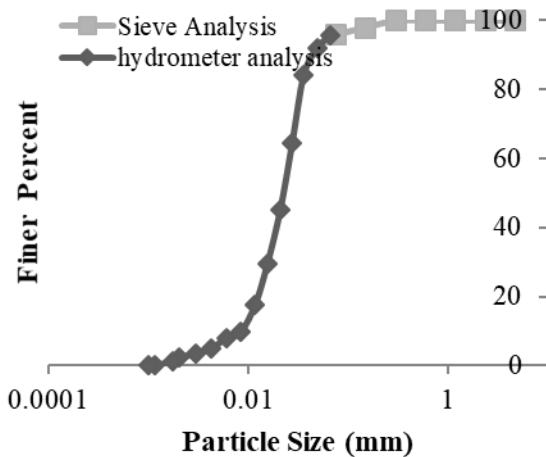


Figure 4: Grain size Analysis of Soil of Bottom Layer of Moinotghat (Sample - 3)

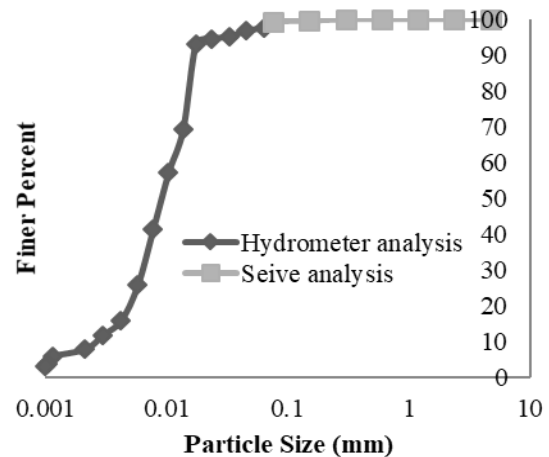


Figure 5: Grain size analysis of soil of bottom layer of Moinotghat (Sample - 4)

2.2.2 Atterberg Limit Test

From grain size analysis it has been seen that the soil of Paschimchor and that of bottom layer of riverbank at Moinotghat is fine grained soil. To differentiate between clay and silt, Atterberg limit test and plasticity test were performed for sample - 1 and sample - 4. But this test could not be done successfully as the soil could not be grooved.

2.2.3 Direct Shear Test

To determine the shear strength parameters of soil samples, direct shear test was conducted in the laboratory. Here, sample - 1 which was collected from Paschimchor, was subjected to direct shear test. The specific gravity of the sample was 2.72 and the sample was collected from 2.5 ft depth from the top surface. So, the soil sample was subjected to a normal pressure of 48.09 KPa. So, in laboratory, the soil was subjected to 8 kg, 16 kg and 32 kg normal load only. The test outcomes are shown in Figure 6 and Figure 7.

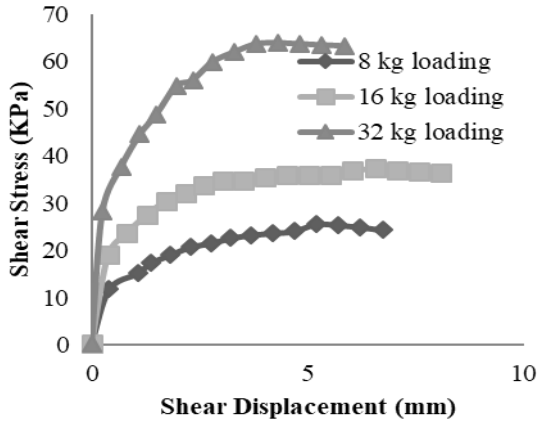


Figure 6: Shear Displacement Vs Shear Stress for Soil Sample of Paschimchor

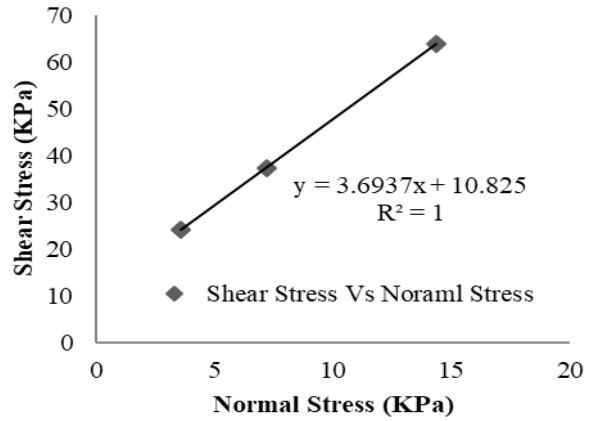


Figure 7: Failure envelop for soil sample of Paschimchor (Failure Envelope)

Soil sample – 2 was collected from the river bank at Moinotghat at 1ft depth from the top layer. As the soil sample was subjected to 24.77 KPa normal load at that place, the direct shear test was performed using 4kg, 8kg and 16 kg normal load in the laboratory. The test outcomes are shown in Figure 8 and Figure 9.

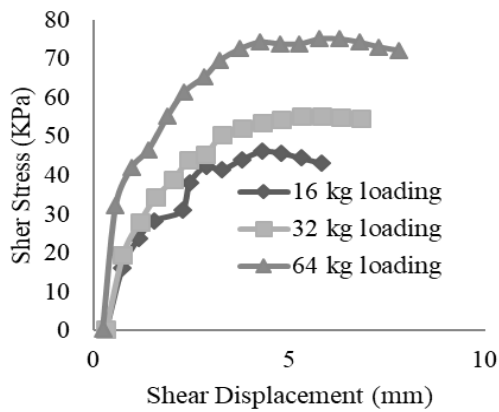


Figure 8: Shear Stress Vs Shear Displacement for Moinotghat Bottom Layer

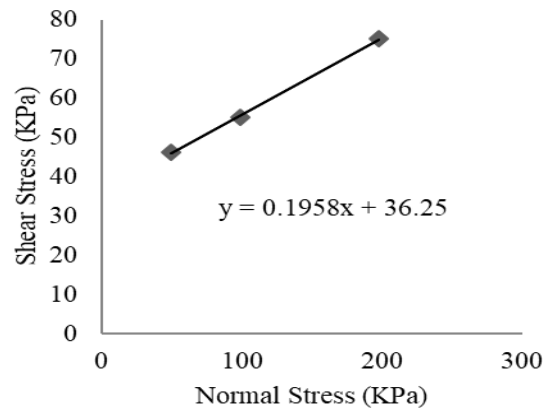


Figure 9: Shear Stress Vs Normal Stress for Moinotghat Bottom Layer (Failure Envelop)

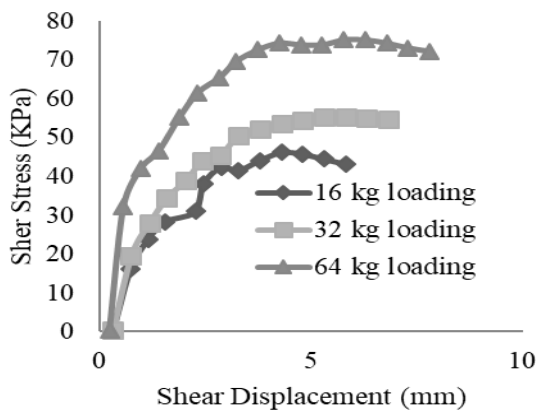


Figure 10: Shear Stress Vs Shear Displacement for Moinotghat Bottom Layer

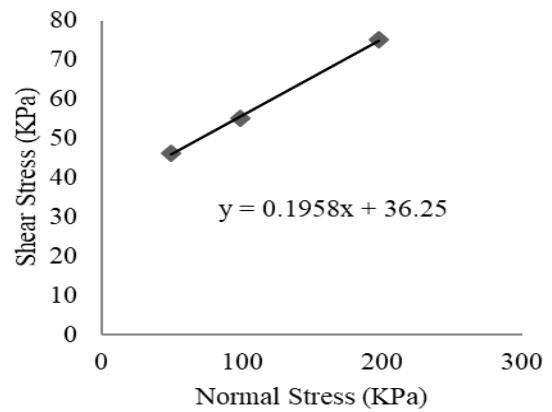


Figure 11: Shear Stress Vs Normal Stress for Moinotghat Bottom Layer (Failure Envelop)

Soil sample – 4 was collected from riverbank of Moinotghat at 7 ft depth from top surface of the riverbank. The soil sample was subjected 68.2 KPa normal load. So, in laboratory, the test was performed using 16 kg, 32 kg and 64 kg normal load. The test outcomes are shown in Figure 10 and Figure 11.

3. SOFTWARE ANALYSIS AND RESULTS

For analysis the problem of slope stability certain steps should be followed. If the geometry of the slope is known, and phreatic level of the slope is known any problem of slope stability can be analysed by Plaxis-2D.

3.1 Riverbank at Paschimchor

Soil of riverbank of Paschimchor was clayey-silt (7% clay, 88% silt and 4.5% sand). The model is done using Plaxis - 2D maintaining the slope angle of 30°, 35°, 42°, 53°, 58° for high water table, dry condition and rapid draw down condition.

The model is kept using plain strain 15 node element. The material was clayey silt and unsaturated unit weight was 13.69 KN/m³ and saturated unit weight was 17.69 KN/m³. Coefficient of permeability was kept 0.001cm/sec which is converted to m/day as 0.021 m/day along x direction and 0.001 m/day in vertical direction. The c was kept 14.15 KPa (gained from direct shear test) and ϕ value was kept 38° and V_s and V_p value was used as 46.97 m/s and 98.78 m/s. And E value was used as 12000 KPa and poisson's ratio was kept 0.33 and interface was kept manual and R_{inter} was kept 0.5 (Das, B, M., 2017). The factor of safety is calculated in strength reduction procedure which is shown in Table 2. From Figure 16, it can be seen that, the factor of safety decreases with increasing slope angle. It can also be seen that, the factor of safety follows a polynomial model with slope angle in these three conditions.

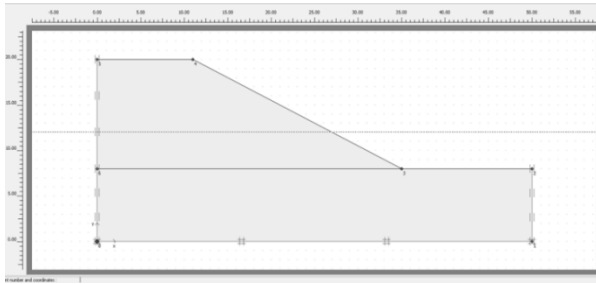


Figure 12: Slope geometry for slope of 30° for riverbank of Paschimchor

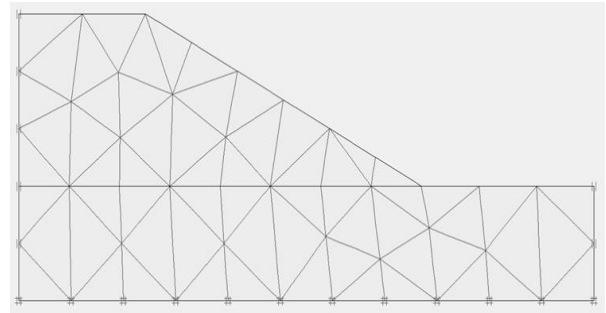


Figure 13: Meshing of the slope

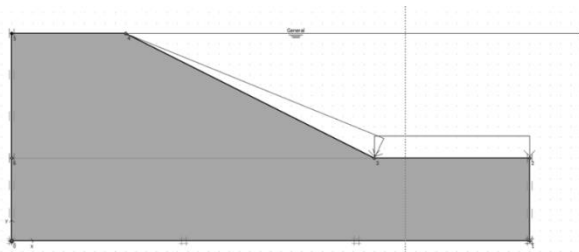


Figure 14: Defining phreatic level

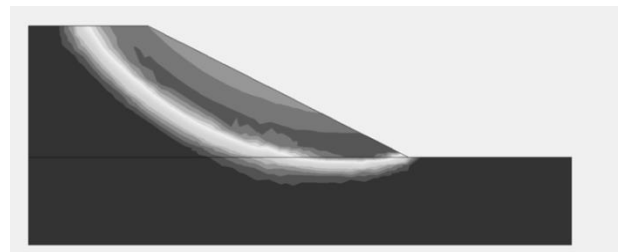


Figure 15: Total displacement (showing most applicable rupture surface of failure) at high water table

Table 2: Variation of Stability of Slope of Riverbank at Paschimchor with change of Geometry (slope Angle) and Water Level

	Change of Slope Geometry (Slope Angle)	Factor of Safety for High Water Table	Factor of Safety at Dry Condition	Factor of safety at Rapid Draw Down
	11	4.4	3.35	2.45
	35	4.02	3.02	2.25
	42	3.35	2.56	1.71
	53	2.75	2.15	1.38
	58	2.25	1.78	1.26

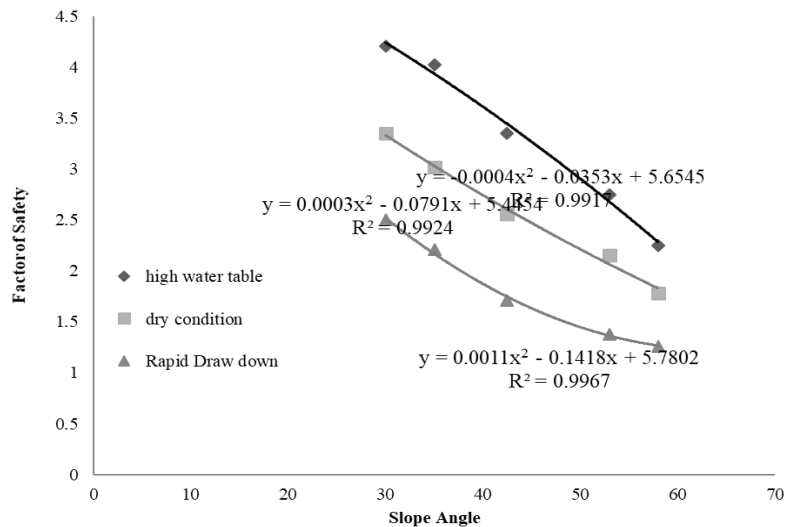



Figure 16: Factor of Safety Vs Slope Angle Considering Different Water Level for Riverbank at Paschimchor

3.2 Riverbank at Moinotghat

The riverbank of Moinotghat of two kind of layer of soil; upper layer is consisted of (silty-sand (contains 56.8% sand, 37.2% silt and 6% clay) and bottom layer is consisted of clayey-silt (5% clay, 4.1% sand and 90.9% silt). The model is kept using plain strain 15 node element. Unsaturated unit weight was kept 13.46 KN/m³ and saturated unit weight was 17.28 KN/m³. Coefficient of permeability was kept 0.01 cm/sec which is converted to m/day as 7.645 m/day along x direction and 0.001 m/day in vertical direction. The c was kept 5 KPa (gained from direct shear test) and φ value was kept 38° and V_s and V_p value was used as 51.93 m/s and 108.1 m/s respectively. And E value was used as 10,000 KPa and poisson’s ration was kept 0.35 and interface was kept manual and R_{inter} was kept 0.5 (Das, B. M. 2017). This is shown in Table 3.

Table 3: Variation of Stability of Slope of Riverbank at Moinotghat with change of Geometry (slope Angle) and Water Level

	Change of Slope Geometry (Slope Angle)	Factor of Safety for High Water Table	Factor of Safety at Dry Condition	Factor of safety at Rapid Draw Down
	30	2.56	2.2	1.35
	35	1.98	1.65	1.22
	42	1.45	1.25	0.99
	53	1.28	1.07	0.61

	Change of Slope Geometry (Slope) Angle	Factor of Safety for High Water Table	Factor of Safety at Dry Condition	Factor of safety at Rapid Draw Down
	58	1.2	0.95	0.5

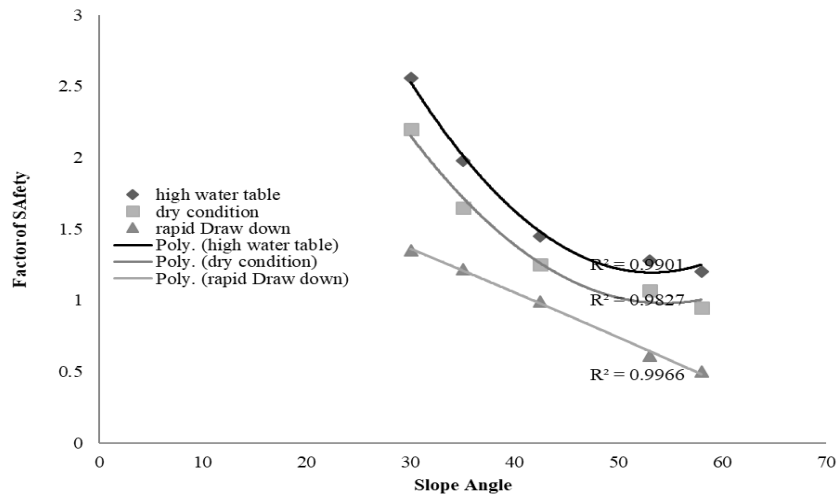


Figure 17: Factor of Safety Vs Slope Angle Considering Different Water Level for Riverbank at Moinotghat

4. CONCLUSIONS AND RECCOMENDATIONS

This study has been run focusing on the impact of water level and slope geometry on the stability of slope using software PLAXIS-2D based on finite element method for soil of different properties such as different shear strength parameter and coefficient of permeability. From above study it has been observed that for all type of geometry (considering varying slope angles) the highest factor of safety occurs at high flood level. This is because at high flood level there is water pressure on the both side of the slope and this balancing force increases the stability of the slope. The lowest factor of safety has been found at rapid draw down condition for all type of geometry (considering varying slope angles) due to the seepage force which acts as suction force on the slope and stability of the slope is reduced to a great extent by this phenomenon. As the steepness of the slope increases, the stability decreases. It has been also being seen that the type of the soil has a great impact on stability of the slope. The riverbank at Paschimchor has greater factor of safety than the riverbank of Moinotghat considering the same water table and geometry as the soil of Paschimchor was clayey silt and the soil of top layer of riverbank of Moinotghat was silty sand. As the clayey silt has greater cohesive force and less coefficient of permeability than silty sand, the slope of the riverbank of Paschimchor is much more stable than slope of riverbank of Moinotghat. So, slope protection measures should be taken for the riverbank at Moinotghat. It has been also observed that stability of the slope decreases linearly with the increase of steepness of the slope for clayey silt for high water table and dry condition where the stability of the slope decreases maintaining a power function with the steepness of the slope considering high water table and dry condition for silty sand.

In this research work, the relationship of deformation with time at rapid draw down condition is not shown here using software Plaxis-2D and it is the limitation of this research work. In this research

work, no necessary measures have been mentioned to stabilize the riverbank. The relation between factor of safety and slope geometry considering different water level is represented here graphically but it could be better research work if this relationship was expressed in linear or non-linear equation.

REFERENCES

- Allen D.L., Deen R.C., Hopkins T.C., (1975). "Effect of Water on Slope Stability", Kentucky Transportation Center Research.
- Alonso, E & Pinyol N., (2009). Slope Stability Under Rapid Draw Down Conditions. Universitat Politècnica De Catalunya, Barcelona.
- ASTM D2487-17, (2017). "Standard Practice for Classification of Soils for Engineering Purposes (Unified Soil Classification System)", ASTM International, West Conshohocken, PA.
- Das M., B. (2017). "Principles of Geotechnical Engineering", 9th Edition.
- Fatema, N., & Ansary, M., H., (2013). "Slope Stability Analysis of Jamuna River Embankment", Journal of Civil Engineering IEB, 42(1)2014 119-136
- Johanson, J., (2014). "Impact of Water Level Variations on Slope Stability", Licentlate Thesis, Issn 1402-1757
- Mamun, A.A., Rahman, I.F., Sazzad, M.M., (2016). "Effect of Water Level Variation on Stability of Slope by LEM and FEM"
Plaxis-2D Tutorial Manual 2016
Plaxis-2D Reference 2016
- Schiller, M., & Wynne. S., (2010). "The Effect of Declining Water Table on The Stability of The Slopes", School of Civil and Environmental Engineering, University of Adelaide.
- Ward, W.H., Stability of Natural Slopes. The Geographical Journal, Vol. 105, No. 5/6 (May-June 1945), Pp. 170-191
- Zhang, & He, B., (2012). "Stability Analysis of Slope Based on Finite Element Method", I, J Engineering and Manufacturing, 2012,3, 70-74.

A CASE STUDY ON FINITE ELEMENT SIMULATION OF THE STAGE CONSTRUCTION METHOD

Piash Saha*¹ and Md. Rokonuzzaman²

¹*Lecturer, Dhaka International University, Bangladesh, e-mail: piashbddotnet@gmail.com*

²*Professor, Khulna University of Engineering & Technology, Bangladesh, e-mail: rokon@ce.kuet.ac.bd*

***Corresponding Author**

ABSTRACT

This study is based on the field data of approach road on the Mawa-side of the Padma multipurpose bridge project which focuses on a group of points. Firstly, it validates the Finite Element Model (FEM) data by comparing it to field settlement data. Further, it estimates settlement with preloading and preloading with vertical drains with respect to time numerically. Lastly, its emphasis on selecting the preferable soil model. Preloading is one of the most cost-effective methods for soft soil stabilization. The results using PLAXIS 2D software showed that the excess pore water pressure for the case was significantly higher and gradually dissipated without vertical drains compared to the case with vertical drains. The explanation is that vertical drains reduce the excess pore pressure effectively and help accelerate its dissipation during the time of consolidation. In addition, the level of settlement with vertical drains during consolidation is higher than without vertical drains used in impermeable soil layers due to low hydraulic conductivity. These values are closer to the field measurements. Several different soil models of varying types were used when modeling the sample embankments; Mohr-Coulomb, Hardening soil, and Soft soil respectively. Because the study includes Mohr-Coulomb's first experience was the most desirable, and it provides fairly realistic results compared to field measurements. Based on the analysis, preloading without vertical drains can be said to be an economical method to avoid post-construction settlements in the Mawa-side project. If the time is highly constrained, a feasible method can be vertical drains with preloading.

Keywords: *Finite element method, Consolidation settlement, Soil model, With and without drains, Preloading.*

1. INTRODUCTION

Many Several techniques for improvement have been developed to match local soil conditions, often consolidation-based soft clay methods. Preloading with vertical drains is an effective ground improvement strategy, requiring ground surface loading to induce most of the underlying soft formation's ultimate settlement (B Indraratna, Rujikiatkamjorn, & Xueyu, 2012) Typically, an additional or surcharge load equal to or greater than the anticipated loading of the base is used to facilitate consolidation with the help of vertical drains (Iyathurai, 2005). Using vacuum pressure can reduce the amount of surcharge filling material required to obtain the same consolidation settlement because it produces suction, which increases the effective stress and accelerates consolidation (Buddhima Indraratna, Rujikiatkamjorn, Balasubramaniam, & Wijeyakulasuriya, 2015). Historically, designing foundation structures or keeping a high mass on soft soils (like clay) has created civil engineering problems. It may take many years simply to overload as a process of soil consolidation. Infrastructure projects are rapidly built on marginal soils worldwide due to rapid growth and urbanization (Abramson, Lee & Boyce, 2002).

One of the most successful and widely used methods is to increase the bearing capacity of these soils and reduce the excess pore water pressure in combination with preloading. After the Second World War, the use of sand drain or vertical drain has undergone enormous development, largely due to better installation methods and increased knowledge of the control factors (Parsa-pajouh, 2014). The key benefits of vertical drains are: (i) increasing the shear strength of the soil by decreasing the ratio of void and moisture content; (ii) decreasing the preloading time necessary to decrease the same rate of post-construction settlements; (iii) decreasing the differential settlement during primary consolidation; and (iv) curtailing the height of surcharge fill required to achieve desired pre-compression (Samson & Rochelle, 1972). It is difficult to quantify the immediate settlement as it is often dependent on the rate of construction of the embankment. For the development intent, the immediate settlement can be assumed to be in the range of 10–20 percent of the embankment's primary settlement. Consolidation settlement prediction can be based on a fully coupled numerical method as shown by Hsi and Small (Lim, 2003).

This approach measures the deformation of the soil and the dissipation concurrently of excess pore water pressure during the construction of the embankment (Fatahi, Minh Le, Quang Le, & Khabbaz, 2013). The reliability of the finite element system has been tested in several implementations on the surface, requiring integration by contrasting numerical results with field measurements (Connolly, Giannopoulos, & Forde, 2013).

1.1 Description of the study area

The Padma Bridge is a multipurpose road-rail bridge across the Bangladesh-based Padma River. It is our country's most daunting bridge project to date. This is a bridge with two tiers of steel truss. The bridge combines a 4-lane highway with another level rail bridge. The length of the bridge is about 6,15 km. On either side of the Padma River, there are two access paths. One is Janjira and the other is an access street known as Mawa. The path to janjira is bigger. The width is approximately 10.5 km. Mawa approach road is approximately 1.6 km long. The purpose of the study is a geotechnical analysis of the Mawa side approach route.

1.2 Description of the project

For the Mawa portion of the Padma Multipurpose Bridge Project, construction of an embankment with a side slope of 3:1 and a crest length of 9.5 m and a height of 6 to 3 m began in 2014. The embankment is situated in a valley with base sediments consisting of a 6.5-meter thick soft silty-clay layer for the investigated section of the road, finished within 600 days by phased construction. In the preliminary planning studies, Staged construction on the existing silty-clay layer was chosen for

economic reasons. In this study, for comparison with quantitative results, only the data from settlement plates are used (Tavenas, Chapeau, La Rochelle & Roy, 1974).

2. METHODOLOGY

2.1 Problem, geometry and material properties

The following table 1 gives a brief idea about the structure, status, and content of the parts replicated in the PLAXIS. It also displays the parameters of the material along with the material model used in the analysis. The model of the mohr-coulomb is used for simplicity.

Table 1: Material Model and Properties

Parameters	Relevant Test	Foundation Soil (Clay)			Fill
		MC	SS	HS	MC
Type		Undrained	Undrained	Undrained	Drained
Cohesion, c		1.00 kN/m ²	1.00 kN/m ²	1.00 kN/m ²	1 kN/m ²
The angle of friction, ϕ		35.00°	35.00°	35.00°	30.00°
γ_{sat} or, γ_{unsat} (kN/m ³)		14	14	14	19
$K_y=K_x$ (m/day)		0.01	0.01	0.01	-
Power, m		-	-	0.50	-
E_{50}^{ref}	CD TEST	-	-	5927.00 kN/m ²	-
$E_{ur}^{ref} = 3 * E_{50}^{ref}$		-	-	17724.00 kN/m ²	-
Unloading elasticity					
Poisson ratio, ν		0.330	-	-	-
Young modulus, E^{ref}		4000 kN/m ²	-	-	-
G^{ref}		1503.759 kN/m ²	-	-	-
E_{50}^{ref} or, E_{osd}^{ref}		2000 kN/m ²	-	-	20000 kN/m ²
Loading elasticity	1D				
Coefficient of compressibility, c_c	CONSOLIDATION TEST	-	0.21	-	-
Void ratio, e		-	0.9106	-	-
λ^* (lambda)		-	$\frac{c_c}{2.3(1+e)} = 0.048$	-	-
k^* (kappa)		-	$\frac{2+c_r}{2.3(1+e)} = 0.0183$	-	-

2.2 Construction Phases

Following the user manual of PLAXIS (Version 8.6) the calculation of the embankment stage were done. The process consists of the construction phase in which the embankment load is applied

incrementally over time and the dissipation phase in which a time interval is introduced to allow the excess pore water pressure to dissipate. The restructuring steps are shown in the figure 1 below.

Identification	Phase no.	Start from	Calculation	Loading input	Time	Water	First
Initial phase	0	0	N/A	N/A	0.00 ...	0	0
✓ Gravity	6	0	Plastic analysis	Total multipliers	0.00 ...	0	1
✓ Stage1	1	6	Consolidation analysis	Staged construction	13.0...	0	5
✓ Dissipation1	5	1	Consolidation analysis	Staged construction	135....	0	10
✓ Stage2	7	5	Consolidation analysis	Staged construction	16.0...	0	16
✓ Dissipation2	8	7	Consolidation analysis	Staged construction	72.0...	0	19
✓ Stage3	9	8	Consolidation analysis	Staged construction	20.0...	0	24
✓ Dissipation3	10	9	Consolidation analysis	Staged construction	1.00 ...	0	27
✓ Stage4	11	10	Consolidation analysis	Staged construction	27.0...	0	28
✓ Dissipation4	12	11	Consolidation analysis	Staged construction	243....	0	31
✓ ZeroEPWP	13	12	Consolidation analysis	Minimum pore pressure	205....	0	37
✓ HFL	2	13	Plastic analysis	Staged construction	0.00 ...	2	43
✓ Safetyafterconst...	3	12	Phi/c reduction	Incremental multipliers	0.00 ...	0	62
✓ SafetyLongTerm	14	13	Phi/c reduction	Incremental multipliers	0.00 ...	0	162
✓ SafetyHFL	4	2	Phi/c reduction	Incremental multipliers	0.00 ...	2	262

Figure 1: Calculation Steps for soil Section

3. ILLUSTRATIONS

3.1 Settlement result with and without drain

The figure 2 below illustrates the settlement-time curves of an embankment used on silty clay soil with and without vertical drains obtained through numerical analysis with PLAXIS 2D. Both curves are very close to each other and at the beginning show large displacements. It can be seen that most of the time both curves have nearly linear behavior. Using drain, it was shown in Figure 2 below that it takes around 538 days for the ultimate 288 mm settlement. Likewise, it requires about 581 days without using the drain for ultimate settlement. The ultimate settlement is established at an early stage with the aid of the sand drain. The purpose of using sand drain is thus fulfilled.

Nevertheless, as sand drains are, it depends on the user's economy. The immediate settlements, in the figure 3, come from the soil's elastic behavior. The second phase of settlement in the figure is primary consolidation settlements, which could result from volume shifts in the clay due to the gradual dissipation of excess pore water pressure by triggering the first part of the embankment. Finally, the last settlement could be attributable to the dissipation of excess pore water pressures and soil plastic modification by external load increases.

Table 2 below indicates the average vertical deformation in the middle of the embankment and the total excess pore water pressure after the time measurement.

Table 2: Results from the PLAXIS 2D analysis, with and without drains

Results	Deformation	Time	Excess pore pressure
Units	mm	Days	kN/m ²
With drain	288	538	0.1
Without drain	307	581	0.1

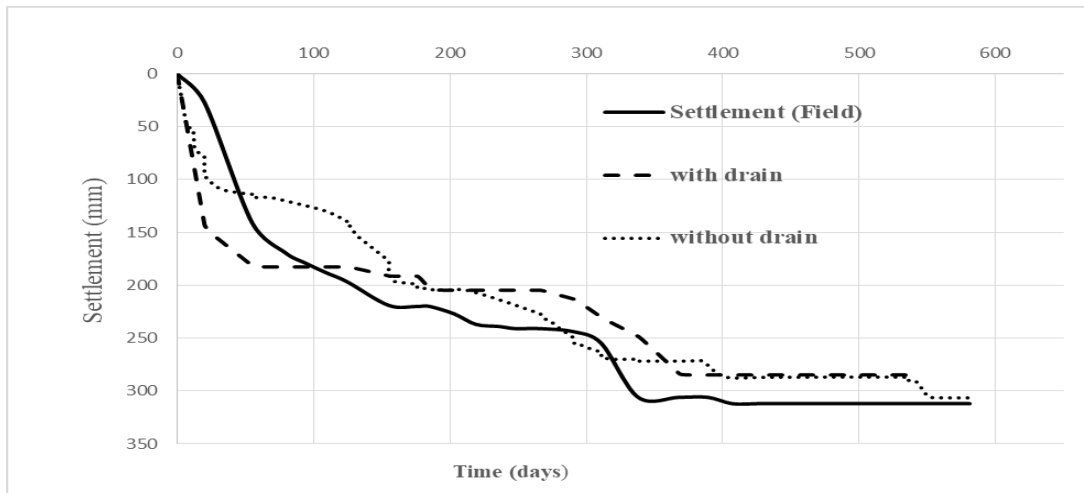


Figure 2: comparison of settlement vs. time curve of FEM data with field data

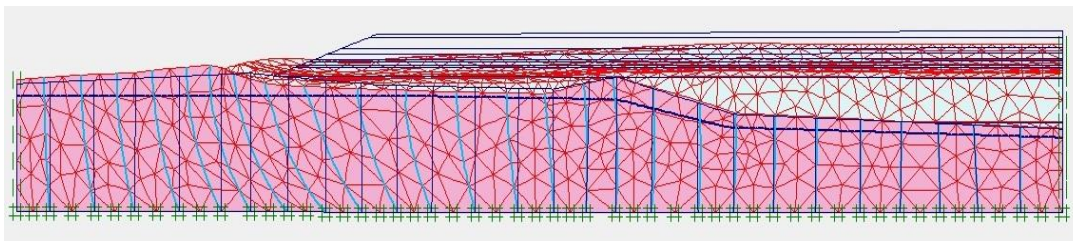


Figure 3: Deformed mesh generated using sand drain

3.2 Comparison of material model

This figure 4 indicates that the prototype from Mohr-Coulomb is superior to the other two. The Mohr-Coulomb model suits the field data much better than the soft soil in measurements at 0 m depth below the embankment. For deeper layers, the differences between these models are becoming less.

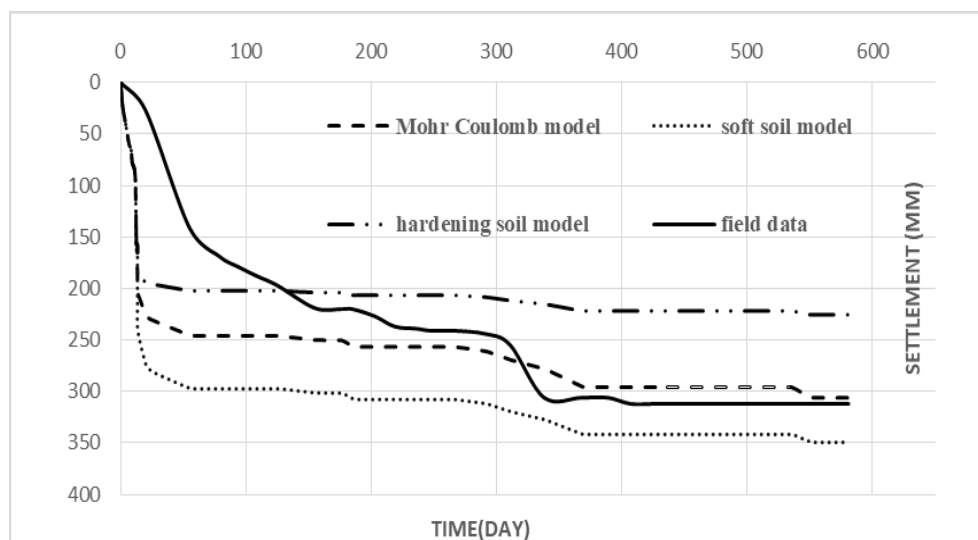


Figure 4: comparison of the time-settlement curve for different soil models with field data

3.3 Permeability Check

In the soil section, a detailed parametric analysis was carried out. The effect of variance has been worked out by comparing the horizontal and vertical permeability of each of the product models used in the system shown in figure 5. Settlement analysis shows that the Mohr-Coulomb soil model showed little settlement data result due to varying permeability in the undrained state of foundation soil. When permeability $k_x=k_y= 0.001$ m/day then it settled down to 306.19mm, for $k_x=k_y= 0.01$ m/day settlement was 306.04 mm and for $k_x=k_y= 1.0$ m/day was 306.18 mm.

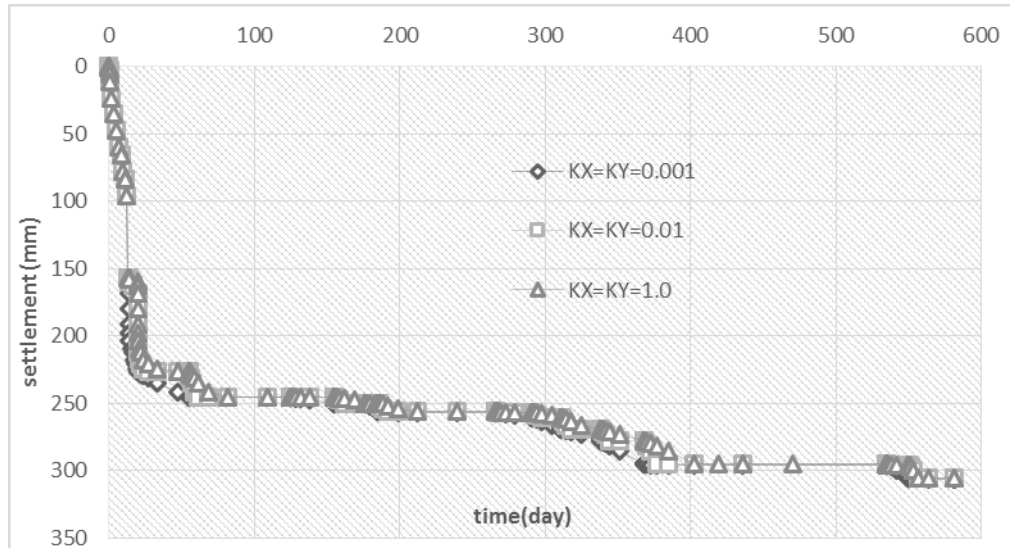


Figure 5: Time-settlement curve with isotropic permeability for the MC model

4. CONCLUSIONS

The main objective of this work was to show the validity of finite element program PLAXIS 2D compared with the field settlement data; with and without vertical drains and to find the best soil material model suitable for the foundation soil. The scope of this research was limited to analyze the model and predict the deformation by using the Mohr-Coulomb, hardening soil and the soft soil model in the numerical analysis.

- i. The results obtained from PLAXIS 2D are adequate in comparison to field observations. In both situations with and without vertical drains, the results were much similar for the total displacements but they differ for excess pore water pressures.
- ii. Out of the three material models, soft soil model data is most suitable for the project. As the Mohr-Coulomb model matches much better with the field data than the Soft soil and hardening soil model does.
- iii. We have also analyzed the change of permeability with three material models. It is seen that the change of permeability didn't show any significant change in the settlement with isotropic permeability.
- iv. But, in the case of anisotropic permeability, the settlement rate was found higher compared to isotropic one.
- v. We recommend the method of preloading the soil sample without vertical drains to stabilize the ground because it is an economical method and we don't need special equipment at the site.

ACKNOWLEDGMENTS

I convey my gratitude to Professor Dr. Md. Rokonzaman, my thesis supervisor who has encouraged me thoroughly during my thesis project with his precious explanations, patience on all occasions and providing relentless technical support. Without my supervisor, this project would not have been completed successfully.

REFERENCES

- Abramson, L. E. E. W., Lee, T. S., & Boyce, G. M. (2002). *Slope stability and Stabilisation Methods*.703.
- Connolly, D., Giannopoulos, A., & Forde, M. C. (2013). Numerical modelling of ground borne vibrations from high speed rail lines on embankments. *Soil Dynamics and Earthquake Engineering*, 46, 13–19. <https://doi.org/10.1016/j.soildyn.2012.12.003>
- Fatahi, B., Minh Le, T., Quang Le, M., & Khabbaz, H. (2013). Soil creep effects on ground lateral deformation and pore water pressure under embankments Soil creep effects on ground lateral deformation and pore water pressure under embankments. *Geomechanics and Geoengineering: An International Journal*, 8(2), 107–124. <https://doi.org/10.1080/17486025.2012.727037>
- Indraratna, B, Rujikiatkamjorn, C., & Xueyu, G. (2012). Performance and prediction of surcharge and vacuum consolidation via prefabricated vertical drains with special reference to highways , railways and ports. *ISSMGE - TC211 International Symposium on Ground Improvement*, II-145-II-168.
- Indraratna, Buddhima, Rujikiatkamjorn, C., Balasubramaniam, A. S., & Wijeyakulasuriya, V. (2015). Predictions and Observations of Soft Clay Foundations Stabilized with Geosynthetic Drains and Vacuum Surcharge. *Ground Improvement Case Histories: Embankments with Special Reference to Consolidation and Other Physical Methods*, 209–204. <https://doi.org/10.1016/B978-0-08-100192-9.00007-7>
- Iyathurai, S. (2005). Modelling of vertical drains with smear installed in soft clay. *PhD*, 305.
- Lim, G. (2003). *Stabilisation of an excavation by an embedded improved soil layer*. 219. Retrieved from <https://scholarbank.nus.edu/handle/10635/13635>
- Parsa-pajouh, A. (2014). *Analysing Ground Deformation Data to Predict Characteristics of Smear Zone Induced by Vertical Drain Installation for Soft Soil Improvement A thesis in fulfilment of the requirement for the award of the degree Doctor of Philosophy from Ali Parsa-Pajouh* , . (February).
- Samson, L., & Rochelle, P. La. (1972). Design and Performance of an Expressway Constructed Over Peat by Preloading. *Canadian Geotechnical Journal*, 9(4), 447–466. <https://doi.org/10.1139/t72-044>
- Tavenas, F. A., Chapeau, C., La Rochelle, P., & Roy, M. (1974). Immediate Settlements of Three Test Embankments on Champlain Clay. *Canadian Geotechnical Journal*, 11(1), 109–141. <https://doi.org/10.1139/t74-008>

INFLUENCE OF LIME STABILIZATION ON THE GEOTECHNICAL PROPERTIES OF AN EXPANSIVE SOIL

Maisha Masiyat^{*1}, Sadman Hossain² and Abu Siddique³

¹MSc Student, Bangladesh University of Engineering and Technology, e-mail: maisha.mashiat123@gmail.com

²MSc Student, Bangladesh University of Engineering and Technology, e-mail: sadman2362@gmail.com

³Professor, Bangladesh University of Engineering and Technology, e-mail: abusid@ce.buet.ac.bd

* Corresponding Author

ABSTRACT

In this research, geotechnical properties of a selected lime treated expansive soil have been investigated. For this purpose, initially, index and swelling properties of soil sample collected from Akhaura-Laksham were determined. The soil is classified as inorganic highly plastic clay as per USCS classification (Liquid Limit= 52%, Plastic Limit= 27%, Plasticity Index= 25%) and categorized as moderate to highly expansive soil according to recommended criteria given by various personals (Free Swell= 22%, Free Swell Index= 43%, Swelling Potential= 3.69%). The sample was treated with 3%, 6% and 9% lime content followed by index, swelling and engineering properties determination to examine the influence of lime stabilization on various geotechnical properties of this expansive soil. Compared with untreated soil samples, it has been seen that liquid limit of the treated samples initially decreased with the increasing lime content up to 6% but then increased with the increase in lime content Plastic limit of the treated sample increased considerably with increasing lime content. Compared with untreated sample, plasticity index and linear shrinkage of the treated samples decreased significantly with increasing lime content.

Swelling test results showed that free swell, free swell index and swelling potential decreased significantly with the increase in lime content. The experimental results on the influence of lime stabilization on swelling properties clearly demonstrate that lime can be considered as an effective and economical additive to reduce various swelling properties of expansive soil.

It has been found that with the increase in lime content, maximum dry density reduced while optimum moisture content increased.

Compared with untreated soil samples, the unconfined compressive strength of lime treated sample increased with the increase of lime content. It has been observed from the present investigation that long term curing has profound influence on the gain in strength. The effect of long term curing on the increase in unconfined compressive strength has been found to be more pronounced when samples were treated with higher lime contents.

It has also been observed that with the increase in lime content and curing age, the effective angle of friction and effective cohesion increased compared with untreated sample. It has also been seen that curing age plays a significant role in the increase of effective angle of friction and effective cohesion for a particular lime content.

Keywords: *Expansive soil, Free swell, Unconfined compressive strength.*

1. INTRODUCTION

1.1 General

Expansive soils are those which swell considerably on absorption of water and shrink on the removal of water. In many parts of the world, the possibility of damage to structures due to swelling of soils constitutes a severe problem in design and construction. Soils containing significant levels of silt or clay, have changing geotechnical characteristics: they swell and become plastic in the presence of water, shrink when dry, and expand when exposed to frost. Improvement of its properties may be essential to meet the required soil condition for construction.

Stabilization is one of the most economical and desirable method for improving the strength, durability and resistance to deformation of in situ soil. There are several methods of soil stabilization for improving the physical and engineering properties. Undoubtedly, the most widely applied methods involve the use of inorganic cementative bonds between the particles in the soil system. In general, fine-grained clay soils (with a minimum of 25 percent passing the #200 sieve (74mm) and a Plasticity Index greater than 10) are considered to be good candidates for stabilization.

Among several additives that are commonly used for the treatment of expansive clays, lime has, however, been most commonly used for the treatment of expansive clays and other clay soils as it improves the mechanical properties of expansive clays. Besides, it is economical and abundantly available in many parts of the world. Once treated with lime, soil can be used to create embankments or subgrade of structures, thus avoiding expensive excavation works and transport. The mineralogical properties of the soils will determine their degree of reactivity with lime and the ultimate strength that the stabilized layers will develop.

1.2 Statement of The Problem

One would expect an enormous amount of damage to lightly loaded buildings on shallow foundation founded on expansive soils as the water content changes. Heavy buildings, however, may not suffer much vertical movement. Unless special precautions are taken to eliminate the effect of expansive soil, light buildings are often badly damaged by differential uplift as the volume of the soil changes.

In the recent past, damage to buildings and other structures due to swelling of soils have been reported from different parts of Bangladesh. Several instances were reported by Hossain (1983) and Khan (1995). In the region between Rajshahi and Nawabganj and the area surrounding Sreepur, especially the small structures as offices and staff quarters are severely and strangely cracked (BRTC, 1997). It is obvious that the lightweight structures that are designed and built by conventional techniques will be damaged in case of heaving (Kehew, 1995). But although highway embankments and roadways are generally insensitive to vertical movements, high maintenance costs should be overcome if constructed on expansive soils (Mowafy et al. 1985). Especially soils containing the clay mineral montmorillonite generally exhibit these properties. To understand and overcome these problems, expansive soils should be examined carefully and unsaturated soil mechanics should be taken into consideration.

1.3 Background of Lime Stabilization

The modern era of soil stabilization began during the 1960s and 70s when general shortages of aggregates and fuel resources forced engineers to consider alternatives to the conventional techniques of replacing poor soils at building sites with shipped-in aggregates that possessed more favourable engineering characteristics. Lime provides an economical as well as powerful way of chemical improvement. The standard utilization of lime stabilization is in the treatment of clay subgrade to create improved road foundation without necessity for large amounts of imported granular aggregates. In United States and Europe, lime stabilization is popular regarding improving traffic ability, loading capacity of foundations of road and embankment and also for erosion control. Contrary to lime modification, lime creates long lasting improvements in soils characteristics offering structural benefits.

1.4 Objective of Present Research

The research program has been intended to evaluate the behaviour and engineering properties (moisture-density relations, compressive strength and stiffness, durability etc.) of lime treated and untreated expansive soil collected from the Akhaura-Laksham railway zone. Objectives to be carried out in this research are as follows:

- To investigate the effect of lime stabilization on the index properties (e.g. liquid limit, plastic limit, linear shrinkage) on the selected expansive soil treated with three different percentages of lime contents (3%, 6% and 9%).
- To investigate the effect of lime stabilization on the swelling properties (e.g. free swell, free swell index and swelling potential) of the selected soil treated with three different percentages of lime contents (3%, 6% and 9%).
- To observe the effect of lime stabilization on optimum moisture content and maximum dry density of soil sample treated with 3%, 6% and 9% lime content.
- To observe the effects of lime content and curing age on unconfined compressive strength (q_u) soil sample treated with 3%, 6% and 9% lime content and cured at 7, 14 and 28 days.
- To observe the effects of lime content and curing age on effective cohesion (c') and effective angle of friction (ϕ') from direct shear test for soil sample treated with 3%, 6% and 9% lime content and cured at 7, 14 and 28 days.

1.5 Geology of the Project Area

Bangladesh can be divided into three major physiographic units namely, (i) The tertiary hill formations, (ii) The Pleistocene terrace and (iii) The recent flood plains. According to the study of Morgan and McIntire (1959), there are two major areas of Pleistocene sediments, commonly known as the Modhupur tract and Barind tract and a small area in Akhaura. The Akhaura-Laksam residuum is composed of light-yellowish-grey, orange, light to brick-red and greyish-white, micaceous silty clay to sandy clay. The clay is plastic and abundantly mottled (patterned) in upper 8 m and contains small clusters of organic matter. Dominant clay minerals in this residuum are kaolinite and illite.

2. METHODOLOGY

Several equipment and instruments have been used for performing the tests required in this investigation. A detailed description of the laboratory investigations conducted on untreated and lime stabilized samples has been discussed here.

2.1 Laboratory Testing Program

The soil was collected from the Akhaura-Laksam railway zone. A comprehensive laboratory investigation program was taken to examine the physical, index, engineering and swelling properties of the soil. The sample collected from the field was disturbed sample.

2.1.1 Determination of Physical and Index Properties of Untreated Soils

The following tests were carried out to determine the index and physical properties of the sample:

- Specific gravity test (ASTM D 854)
- Grain size analysis (ASTM D 422)
- Atterberg limit test (ASTM D 4318)
- Linear shrinkage test (BS 1377)

2.1.2 Determination of Mechanical Properties of Untreated Soil Sample

The following tests were carried out on the soil samples to evaluate the mechanical properties.

- Standard Proctor compaction test (ASTM D 1577)
- Unconfined compressive strength test (ASTM D 2166)
- Consolidated drained Direct shear test (ASTM 3080)

2.1.3 Determination of Swelling Properties of Untreated Soil Sample

Swelling tests included determination of the following swelling properties:

- Free swell
- Free Swell index
- Swelling potential

2.1.4 Determination of Change in Index, Swelling and Mechanical Properties of Lime Treated Soil Sample

Based on the index and swelling properties, a suitable expansive soil to be treated with lime stabilization was selected. The following tests were carried out on the selected expansive sample:

- Index properties (e.g. Atterberg Limit, Linear Shrinkage) of the soil treated with three different lime contents (3%, 6% and 9%) were determined.
- Swelling properties (e.g. Free Swell, Free Swell Index, Swelling Potential) of the soil treated with three different lime contents (3%, 6% and 9%) were determined.

The following tests were also carried out on the selected expansive soil with three different lime contents (3%, 6% and 9%).

- Standard Proctor compaction test (ASTM D 1577)
- Unconfined compressive strength test (ASTM D 2166)
- Consolidated drained Direct shear test (ASTM 3080)

Compressive strength and direct shear test on the cured samples was carried out on curing at 7 days, 14 days and 28 days.

3. RESULTS AND DISCUSSIONS

The findings of the laboratory investigations on soil samples collected from Akhaura-Laksham are reported and discussed here. In the following sections, the physical and engineering characteristics comprising plasticity and shrinkage properties, swelling properties, moisture density relations, unconfined compression strength and direct shear strength of untreated and treated soil with 3%, 6% and 9% lime content are presented and discussed.

3.1 Index Properties of Soil

The flow curve of soil sample determined in the laboratory is shown in Figure 1. From the curve, liquid limit is found to be 52. Specific gravity and other index properties from the Atterberg limit test are shown in Table 1. For LL=52 and PI=25, it is found from Figure 2 that our soil is CH (highly plastic clay).

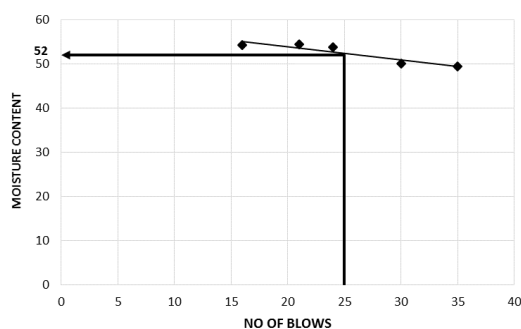


Figure 1: Flow Curve

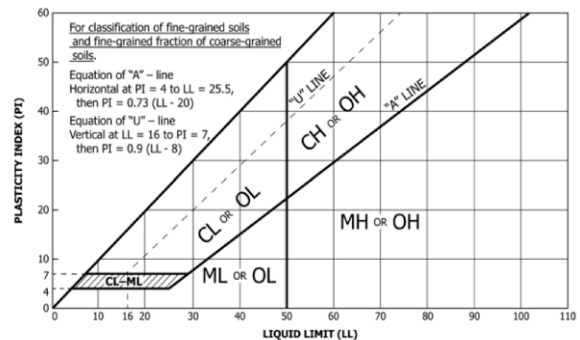


Figure 2: Cassagrande Plasticity Chart

From grain size analysis, it was found that soil sample contains Sand (larger than .06 mm) 1%, Silt (.002 to .06 mm) 45% and Clay (smaller than .002 mm) 54%. From Table 2, it can be seen that according to AASHTO classification soil sample is A-7-6 and USCS classification soil sample is CH.

Table 1: Identification of Index Properties

Specific Gravity	2.62
Liquid Limit	52%
Plastic Limit	27%
Plasticity Index	25%
Linear Shrinkage	11%

Table 2: Summary of Results Derived From Grain Size Analysis

Sand	Silt	Clay	Soil Classification	
1%	45%	54%	USCS	AASHTO
			CH	A-7-6

3.2 Swelling Properties of Soil

A summary of swelling properties is presented in Table 3. Assessment of degree of expansion based on different parameters proposed by various shown in Table 4.

Table 3: Identification of Swell Properties

Free Swell	Free Swell Index	Swell Potential
22%	43%	3.69%

Table 4: Assessment of Degree of Expansion

Plasticity Index and Shrinkage Limit (Holtz, 1956)	High
Liquid Limit and Plasticity Index (IS: 2911, 1980)	High
Liquid Limit and Plasticity Index (Snethen, 1959)	Marginal to High
Linear Shrinkage (Hossain, 1983)	Medium
Free Swell (IS: 1948, 1970)	Low
Free Swell Index (IS: 2911, Part III, 1980)	Medium
Swelling Potential (Seed et al., 1962)	Medium

3.3 Moisture Content- Dry Density Relationship

Standard Proctor was carried out to know the compaction energy of the soil sample. Maximum dry density and optimum moisture content were found for the compaction energy. Moisture- density curve is shown in Figure 3. From this Figure, it has been seen that the optimum moisture content was found to be 17% for Standard Proctor. The maximum dry density was found to be 16.65 kN/m³.

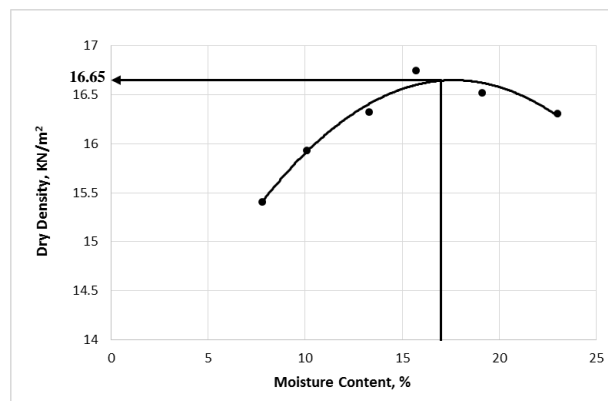


Figure 3: Moisture Content vs. Dry Density Relationship for Standard Proctor Compaction

3.4 Effect of Lime on Index Properties

The values of plasticity and shrinkage properties of untreated and lime stabilized samples of expansive soil are shown in Table 5.

- Compared with the untreated sample, the liquid limit of the lime stabilized samples initially decreased with the addition of lime content and then increased.
- Compared with the untreated sample, the plastic limit increased.
- Compared with the untreated sample, the plasticity index and linear shrinkage decreased.

Table 5: Comparison of Index Properties of Untreated and Lime Treated Expansive Soil

Index and Shrinkage Properties	Lime Content (%)			
	0	3	6	9
Liquid Limit (%)	52	49	45	46
Plastic Limit (%)	27	30	32	35
Plasticity Index (%)	25	19	13	10
Linear Shrinkage (%)	11	8	6	3

Figure 4 and 5 show the variation of liquid limit and plastic limit with the increase in lime content while Figure 6 shows the change in plasticity index with increasing lime content. From Figure 4, it is observed that the liquid limit initially decreases with the increase of lime content up to 6% and then slightly increases with increasing lime content. Figure 5, however, shows that the plastic limit increases remarkably with increasing lime content. Compared with the untreated samples, plastic limits of treated samples were found to increase by 11% to 30% because of stabilization of 3% to 9% lime content. Figure 6 shows that plasticity index decreases markedly by 24% to 60% with the increase of lime content from 3% to 9%. Figure 7 presents that linear shrinkage decreases significantly with the increase in lime content. Compared with the untreated samples, linear shrinkage of lime treated samples were found to be reduced by 27% to 72% due to stabilization with 3% to 9% lime content.

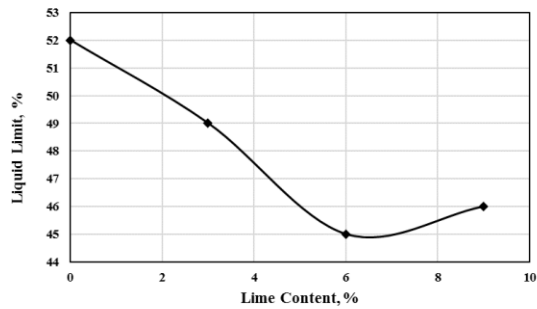


Figure 4: Effect of Lime on Liquid Limit

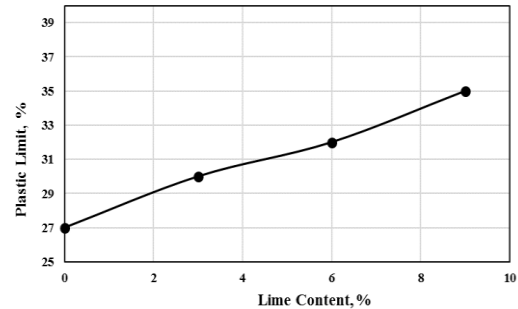


Figure 5: Effect of Lime on Plastic Limit

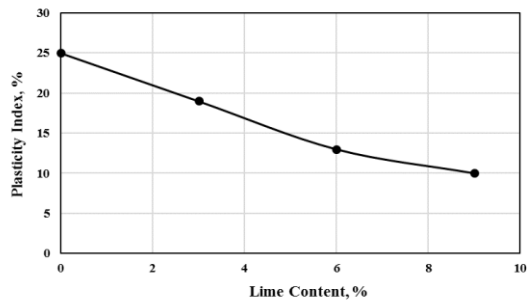


Figure 6: Effect of Lime on Plasticity Index

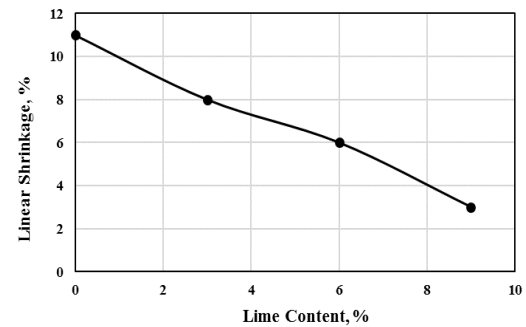


Figure 7: Effect of Lime on Linear Shrinkage

3.5 Effect of Lime on Swelling Properties of Expansive Soil

Attempts have been made to investigate the influence of lime on the swelling properties of expansive soil. Table 6 presents a comparison of the swelling properties of untreated and lime stabilized samples of the expansive soil. Table 6 shows, compared with the untreated samples, free swell, free swell index and swelling potential decreased with the increase in lime content.

The variations of free swell, free swell index and swelling potential of the treated sample with the increase of lime content are shown in Figure 8 to 10 respectively. Compared with the untreated samples, it has been seen that free swell, free swell index and swelling potential decreases by 18% to 64%, 51% to 83% and 38% to 77%, respectively, due to stabilization with 3% to 9% lime.

Table 6: Comparison of Swelling Properties of Untreated and Lime Treated Expansive Soil

Swelling Properties	Lime Content, %			
	0	3	6	9
Free Swell (%)	22	18	13	8
Free Swell Index (%)	43	21	12	7
Swelling Potential (%)	3.69	2.27	1.24	0.84

3.6 Effect of Lime on Optimum Moisture Content and Dry Density of Expansive Soil

Several experiments have been performed to investigate the effect of lime content on the optimum moisture content and dry density of soil. Moisture-density relations of lime treated samples of the expansive soil are shown in Figure 11. From the relations presented in Figure 11, the maximum dry density (γ_{dmax}) and optimum moisture content (w_{opt}) of samples of the expansive soil have been determined. It has been observed that with increasing lime concentration the optimum moisture content of the soil increased while dry density decreased. Table 7 illustrates the variation of optimum moisture content and dry density with increasing lime content.

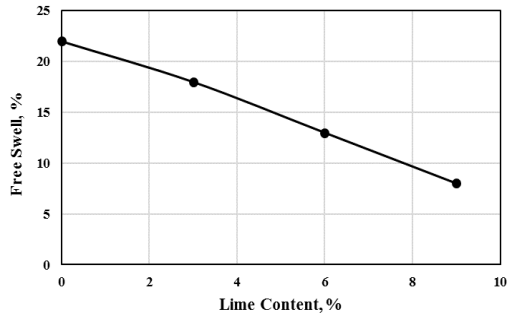


Figure 8: Effect of Lime on Free Swell

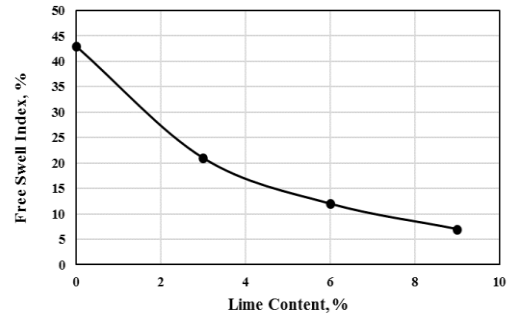


Figure 9: Effect of Lime on Free Swell Index

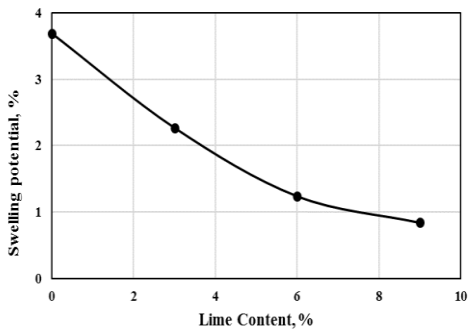


Figure 10: Effect of Lime on Swelling Potential

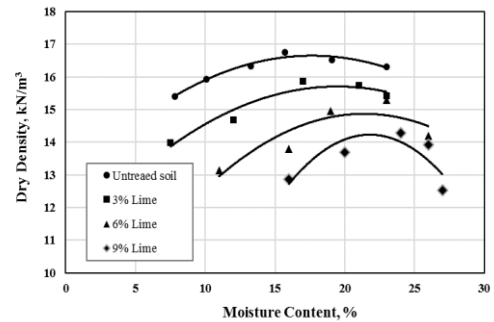


Figure 11: Moisture-Density Relationship of Soil Treated with Different Lime Content

Table 7: Comparison of optimum moisture content and dry density of untreated and lime treated soil

Compaction Properties	Lime Content (%)			
	0	3	6	9
Optimum Moisture Content (%)	17	19	22	23
Dry Density (KN/m ³)	16.65	15.78	14.89	14.23

The reduction in γ_{dmax} with the increase in lime content for the stabilized samples is shown in Figure 12 while Figure 13 shows the increase in optimum moisture content with the increase in lime content. It has been found that compared with the untreated sample, the values of γ_{dmax} decreased by 5% to 14% for an increase in lime content from 3% to 9%. The values of w_{opt} have been found to increase by 11% to 35% due to stabilization with 3% to 9% lime.

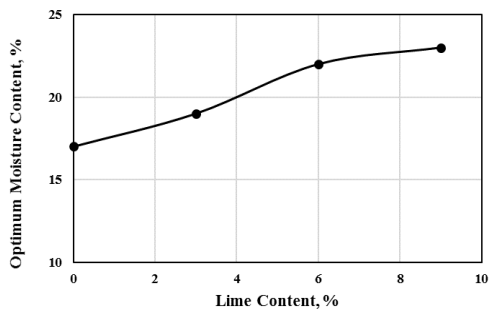


Figure 12: Effect of Lime on Optimum Moisture Content

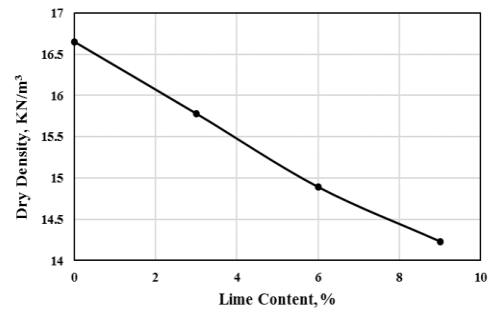


Figure 13: Effect of Lime on Maximum Dry Density

3.7 Effect of Lime Stabilization on Unconfined Compressive Strength of Expansive Soil

The values of unconfined compressive strength (q_u), drained shear strength (s_u), axial strain at failure (ϵ_f) for the untreated samples and samples treated with different lime contents of 3%, 6% and 9% and cured for 7 days, 14 days and 28 days are presented in Table 8.

Table 8: Summary of Unconfined Compressive Strength Test Results of Untreated and Lime Treated Expansive Soil

Lime Content (%)	Curing Age (days)	q_u (kN/m ²)	S_u (kN/m ²)	ϵ_f (%)
0	-	162	82	15
3	7	184	92	13
	14	268	134	9
	28	373	186.5	6
6	7	233	116.5	10
	14	312	156	5
	28	410	205	3
9	7	294	147	7
	14	389	194.5	4
	28	455	227.5	1.5

From the above table it has been seen that with the increase in lime concentration, the unconfined compressive strength increased markedly. The relationship between q_u and different lime contents and curing ages are shown in Figure 14 and 15, respectively. Figure 14 illustrates that the unconfined compressive strength of treated samples cured at any particular age increased with increasing lime content while Figure 15 shows that values of q_u of samples treated with particular lime content increased with the increase in curing age. From our experiment, we have seen that, compared with an untreated soil sample, the unconfined compressive strength of sample cured at 28 days increased by 130%, 153% and 181% with 3%, 6% and 9% lime content respectively. The effect of curing age on the increase in q_u thus is more pronounced when samples are stabilized with higher lime contents.

Table 8 also shows that compared with the untreated samples, the values of ϵ_f of the stabilized samples reduced. This finding indicates that the treated samples became more brittle due to lime stabilization. Figure 16 shows that with the increase in lime content for a particulate curing age axial strain decreases while Figure 17 shows that with the increase in curing age for a particulate lime content axial strain at failure decreases. However, the curing age played a significant role here.

3.8 Effect of Lime on Direct Shear Strength Parameters of Expansive Soil

Variation has been seen in cohesion and angle of friction while performing the drained direct shear tests on untreated and treated soil samples with various lime concentrations. Figure 18 shows the change in effective cohesion for different lime concentration. It has been observed that the cohesion of soil increases significantly with increasing lime content. For a certain curing age, the effective cohesion of soil increases up to 2.5 with increasing lime content. Figure 19, on the other hand, illustrates the effect of curing age on cohesion. For a fixed lime content, the effective cohesion is found to be increasing with long term curing.

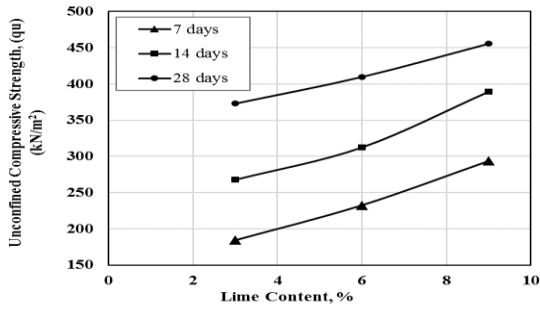


Figure 14: Effect of Lime Content on Unconfined Compression Strength

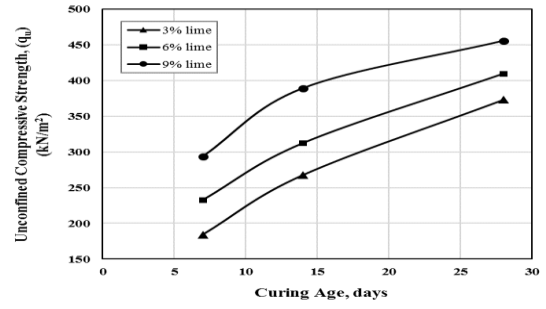


Figure 15: Effect of Curing Age on Unconfined Compression Strength

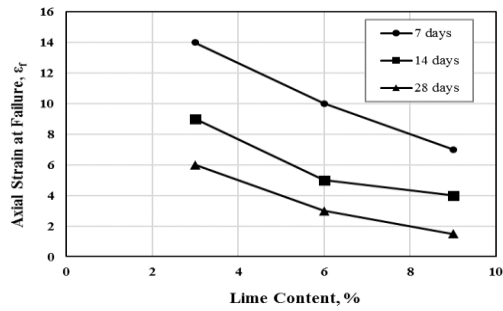


Figure 16: Effect of Lime Content on Axial Strain at Failure

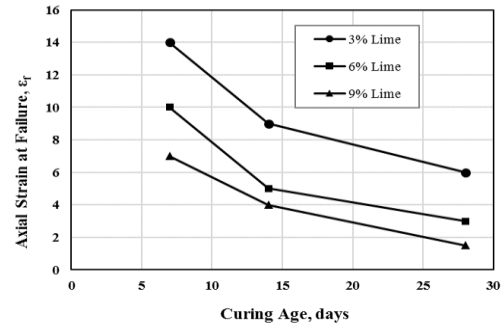


Figure 17: Effect of Curing Age on Axial Strain at Failure

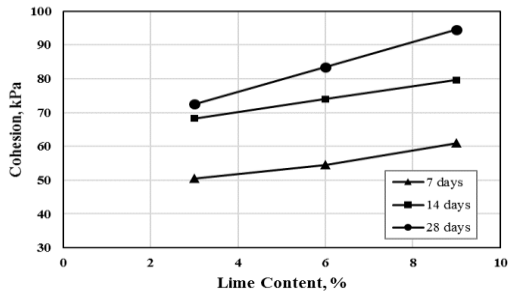


Figure 18: Effect of Lime Content on Effective Cohesion

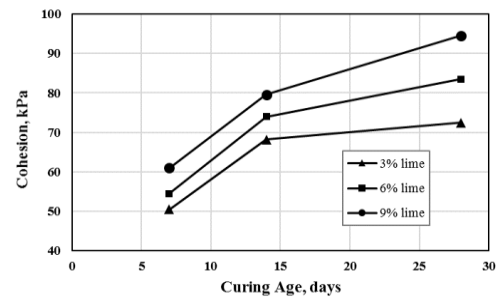


Figure 19: Effect of Curing Age on Effective Cohesion

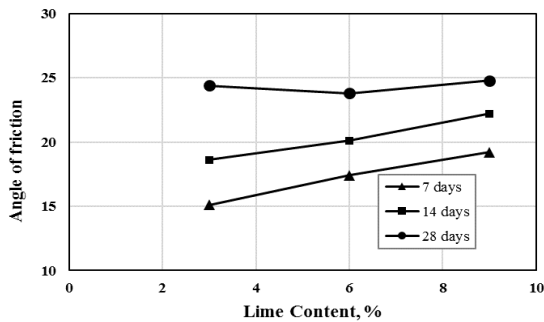


Figure 20: Effect of Lime Content on Effective Angle of Friction

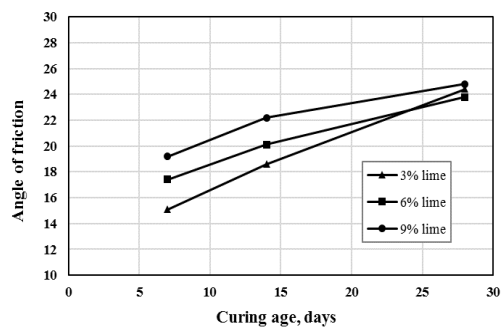


Figure 21: Effect of Curing Age on Effective Angle of Friction

Figure 20 shows the variation in effective angle of friction for different lime concentrations and curing age. It has been seen that the angle of friction of soil increases significantly with increasing lime content. For a certain curing age, the effective angle of friction of soil increases up to 95% with increasing lime content, compared with untreated soil. Figure 21, however, illustrates that the change of effective angle of friction with long term curing.

4. CONCLUSIONS

The major findings and conclusions drawn on various aspect of this study on the selected expansive soil may be summarized as follows:

- With the addition of lime, plasticity index and linear shrinkage decrease, thus reducing the shrinkage and plastic properties of soil.
- The swelling problem of expansive soil can be eliminated by introducing a small amount of lime into the soil.
- With the addition of lime, maximum dry density decreases while OMC increases. Thus, the required density can be easily achieved for a broad range of water content, thereby conserving time, effort and energy.
- With increasing lime content, the unconfined compressive strength increases though the soil becomes brittle.
- The addition of lime increases the effective cohesion and effective angle of internal friction of soil thus in turns increases the ultimate bearing capacity and skin friction of soil.

ACKNOWLEDGEMENTS

The authors would like to express their sincere gratitude and profound indebtedness to Dr. Abu Siddique, Professor of Civil Engineering, Bangladesh University of Engineering and Technology (BUET), Dhaka, Bangladesh. His Constant supervision, Continuous guidance, helpful criticism, suggestion and encouragement at every stage made this work possible. This dissertation would not have been possible without him. The authors are indebted to the Civil Engineering Department, BUET, Dhaka, Bangladesh for having provided them with all facilities and equipment, which enabled them to carry out the research work.

REFERENCES

- Holtz, W.G. and Gibbs, H.J. (1956), "Engineering Properties of Expansive Clays", ASCE Transactions, Vol. 121, Paper No. 2814, PP 641-663, Discussions, PP. 664-677.
- Hossain, M.M. (1983), "Swelling Properties of Selected Local Soils" M. Sc. Engineering Thesis.
- IS: 1948 (1972) "Classification and Identification of Soils for General Engineering Purposes", Indian Standard Institution, New Delhi.
- IS: 2911, Part III (1980), "Code for Practice for Design and Construction of Pile Foundations", Part III, under renamed Piles (First Revision), Indian Standards Institution, New Delhi.
- Kehew, E.A., (1995), "Geology for Engineers and Environmental Scientists", 2nd Ed., Prentice Hall Englewood Cliffs, New Jersey, PP.295-302.
- Khan, A.J. (1995), "Effect of Sand Layer on Swelling of Underlying Expansive Soil", M.Sc. Engineering Thesis, Department of Civil Engineering, Bangladesh University of Engineering and Technology, Dhaka.
- Morgan, J.P. and McIntire, W.G. (1959), "Quaternary Geology of the Bengal Basin, East Pakistan and India", Bulletin of Geotechnique Society, America, Vol. 70. PP. 319-336.
- Mowafy, Y.M., Bauer, G.E. and Sakeb, F.H. (1985), "Treatment of Expansive Soils: A Laboratory Study", Transportation Research Record 1032, PP.34-39.
- Seed, H.B., Woodward, R.J. And Lundgren, R. (1962), "Prediction of Swelling pressure for Compacted Clays", Journal of Soil Mechanics and Foundations Division, ASCE. Vol. 88.
- Snethen, D.R. (1990), "Technical Guidelines for Expansive Soils in Highway Subgrades".

CLIMATE RESILIENT RURAL ROAD CONSTRUCTION IN COASTAL DISTRICT OF BANGLADESH

Md. Jahangir Alam¹, Md. Shamsul Hoque² and Muhammad Saiful Islam^{*3}

¹*Professor, Department of Civil Engineering, Bangladesh University of Engineering and Technology, Bangladesh, e-mail: Jahangir.buet@gmail.com*

²*Professor, Department of Civil Engineering, Bangladesh University of Engineering and Technology, Bangladesh, e-mail: shoque@ce.buet.ac.bd*

³*Research Assistant, Department of Civil Engineering, Bangladesh University of Engineering and Technology, Bangladesh, e-mail: saifulislamce@gmail.com*

***Corresponding Author**

ABSTRACT

Rural roads in coastal districts are subjected to extreme climatic situations such as flooding due to storm surges, submergence due to flooding and sea level rise and erosion due to current and wave actions. Rural road construction in coastal districts of Bangladesh is a challenging job due to scarcity of suitable construction materials, compaction difficulty and lack of skilled manpower. The aim of this paper is to provide proper guideline in rural road construction so that climate resilient road can be constructed. Here, climate resilient road indicates that road which can sustain extreme climatic situations and minimize the life-cycle cost. This paper focuses especially for village and union roads of coastal districts of Bangladesh. Road construction guidelines are suggested for two cases including general situation (say Paddy land in both side) and challenging situation (say pond or khal at one side of road where pond or khal bottom slope is steep). In those situations, different side slope, ground treatment processes are recommended. Also considering soft soil layer thickness, different types of pile design are formulated.

Keywords: *Rural road, Soft soil, Pond side road, Khal side road, Palisading, Road manual.*

1. INTRODUCTION

The road which can sustain extreme climatic situations and minimize the life-cycle cost may be termed as climate resilient road. Construction of durable rural road in coastal districts is really challenging task. Lack of suitable materials, wrong methodology of construction and social and management problems made the situation extremely difficult. (Alam, Tanvir & Hoque, 2017).

This manual is primarily based on LGED works in Bangladesh. In most of the cases, LGED upgrade existing earthen road rather constructing new road. Upgrading an existing earthen road need elevating and widening in either side or one side. Different circumstances and situations are encountered during upgradation of rural road. Considering difficulties of quality control of embankment construction and flexible pavement construction, durability of flexible and rigid pavement, climate and subsoil condition of coastal districts and socio-economic condition of rural areas, guidelines of constructing climate resilient road is described in this paper.

2. CHALLENGES OF MAKING CLIMATE RESILIENT RURAL ROAD

Challenges of climate resilient road construction are summarized in this section.

2.1 Compaction

Layer by layer compaction by maintaining optimum moisture content and layer thickness 150 mm is considered as the most important parameter of quality control of road embankment construction. Compaction is most challenging part in rural road construction. It can be said that “no compaction, no road”. Following reasons can be summarized why the compaction is difficult to achieve in coastal districts.

- I. **Scarcity of compactor:** Compactor is not available or number of compactors is limited compared to constructions works going on in those areas. Usually small contractors are awarded these rural road works. They don't have compactors of any kind. They borrow roller compactors from LGED which are not enough for all the running construction works.
- II. **Lower estimation of cost:** Estimation of cost was found lower than required in many situations where contractors avoid compaction to minimize their loss or maximize their profit. In challenging situation, cost estimations should be done after proper design of slope protection.
- III. **Optimum moisture content:** Contractors are not aware of optimum moisture content during compaction. They collect mud from borrow pit and dump at side slopes without benching and compaction.
- IV. **Narrow shoulder and widened part:** Widened part of road and shoulder is so narrow that rollers cannot move there. Plate compactor is needed for these situations. Contractors don't have and never use plate compactor.
- V. **Water logged area:** In the water-logged area where two or one side of road is water body. Water body may be pond, khal, fish farm or beel. These are the situations where road widening is very difficult and expensive. Soils are dumped at side slopes without any benching and compaction.
- VI. **Rainy Season:** It is very difficult to maintain optimum moisture content during rainy season. Filling material is not available at that time. Compaction is also extremely difficult during rainy season.

2.2 Unsuitable Materials

Locally available soil and materials are not suitable for subgrade and pavement layers. Locally available borrow pit soils are mostly silty clay, clayey silt, sandy silt and silty fine sand. As per specification of tender documents and Road Design Standard of LGED (LGED and JICA, 2005), borrow pit soils don't meet the requirements for subgrade, Improved Subgrade (ISG) and sand required for subbase.

2.3 Slope Protection

Rural roads on the bank of khal and pond require retaining structure and side slope protection which are expensive. Sometimes, there are fish farms (locally called "Gher") or marshy land on two sides of rural road. These situations make the construction of road extremely difficult. As synthesis of observations in all the site visits, causes of sides slope erosion may be summarized as follows:

- i. Improper location of borrow pits
- ii. Lack of vegetation
- iii. Steep side slope
- iv. Vertical cliff created by farmers at toe of side slopes
- v. Current and wave action of water during rainy season
- vi. Lack of layer by layer compaction and moisture control
- vii. Dispersive nature of local soils which are used for embankment fill
- viii. Absence of clay cladding at sand filled side slopes
- ix. Road widening without following benching and compaction
- x. Lack of proper drainage and channelization of rainwater

3. EMBANKMENT WIDENING GUIDELINES AT DIFFERENT SITUATIONS

During upgradation of any rural road, widening is the most challenging part of construction. Different difficult situations arise during widening of rural road in the coastal districts. Based on investigation, road construction guidelines are suggested for two cases including general situation (say Paddy land in both side) and challenging situation (say pond or khal at one side of road where pond or khal bottom slope is steep).

3.1 Pavement Widening General Guideline

In general, following steps must be followed during widening and upgradation of road.

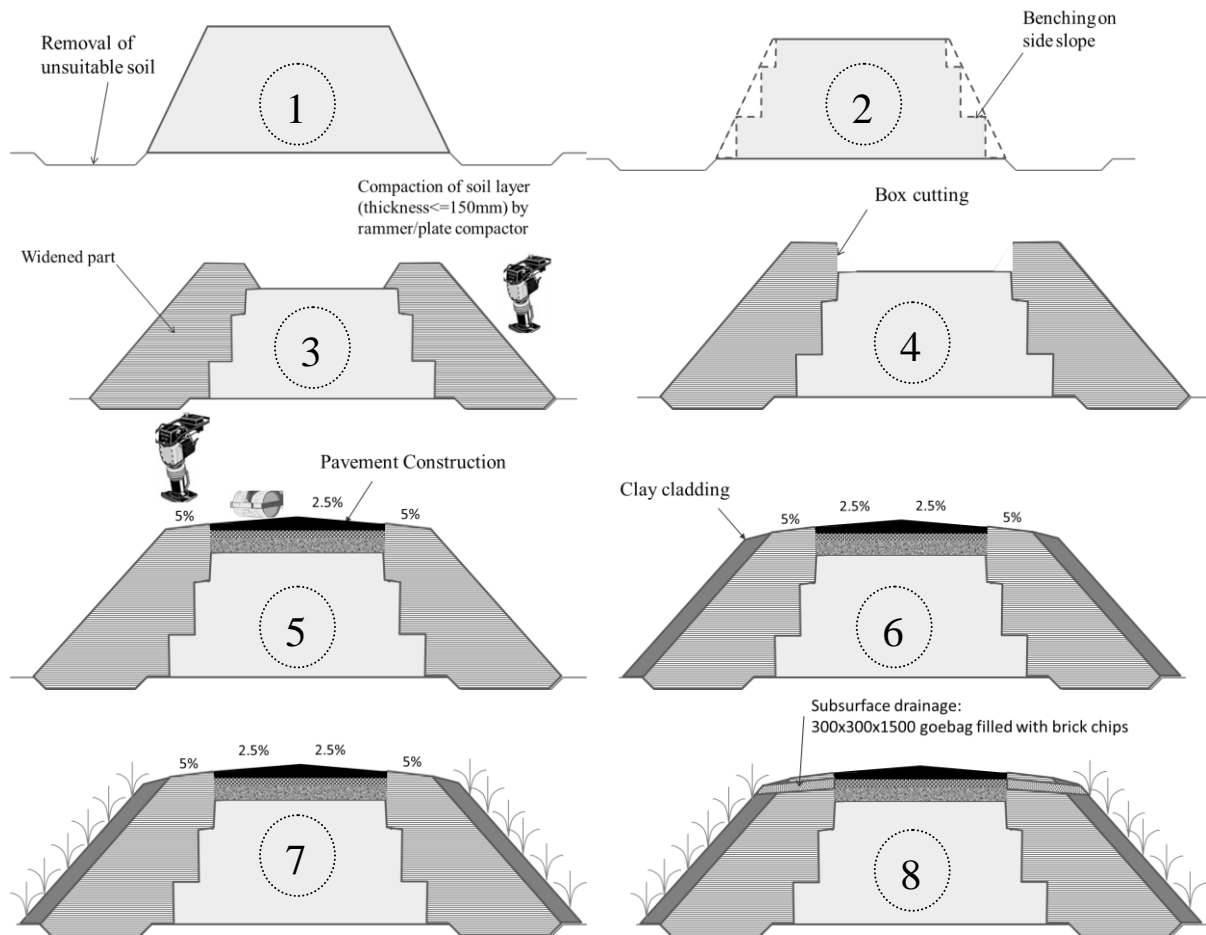


Figure 1: Step by step procedure for general road widening

- I. **Removal of unsuitable soil:** Grass and topsoil with humus must be removed from the ground on which widened part of embankment will be constructed. If mud or very soft clay exists under the top soil, that part should also be removed. This removed soil may be preserved somewhere, so that it may be used on side slopes after completion of widened part. Vegetation will grow faster on this type of soil.
- II. **Benching on existing side slopes:** All grasses and trees shall be removed from existing side slopes. Benching shall be done with convenient size of steps.
- III. **Construction of widening part:** Compaction and treatment of widening part shall be properly done. Widening part or embankment construction can be done using borrow pit soil or dredged sand. Digital moisture meter must be used to monitor moisture content of fill soil before compaction. If the borrow pit soil is lean clay, silty clay or clayey silt with moisture content more than 20%, the soil shall be cut and spread for drying. Moisture content shall be monitored during drying. If the moisture content comes within 12-18%, the soil shall be spread in 200 mm thick layer with lumps not larger than 50 mm. compacted layer thickness shall be less than 150 mm. Plate compactor or rammer shall be used for compaction. If the borrow pit soil contain less than 12% moisture content, water need to be sprinkled after spreading. If the borrow pit soil is sandy silt or silty sand or nonplastic silt, moisture content shall be maintained within 6-10% before compaction. Loose thickness of one layer shall be 200 mm. If dredged sand need to be used for filling widening part or top of embankment, dredged sand cannot be directly poured in the embankment from the outlet of dredging pipe. At first, dredged sand shall be dumped in a dumping site. Dredged sand shall be placed in 200 mm thick loose layers in embankment with controlled moisture content 6-10% and then compacted. In many instances, there is not enough space to maintain the suggested side slopes of rural roads. Treated soil should be used for filling widening part so that steep slope (1:1)

can be used. All types of soil can be treated using CEM-II cement or Ground Granulated Blast Furnace Slag (GGBFS). 5% cement or 5% GGBFS shall be mixed with the soil and compacted by rammer or plate compactor. Compaction method is same as mentioned above. Mixing of cement or GGBFS is not an easy task for rural road construction because mixing equipment is not available. Alternative option is to spread the soil in 100 mm layers on which cement or GGBFS shall be sprinkled. Sandy silt, silty sand and nonplastic silt is preferable for soil treatment.

Table 1: Recommended side slope for different soil types

Soil Type	Side Slope (Vertical : Horizontal)	Clay Cladding Requirement on Side Slopes
sandy silt, silty sand, nonplastic silt (untreated)	1 : 1.75	Yes
Lean clay, silty clay, clayey silt (untreated)	1 : 1.50	No
All types of soil (treated)	1 : 1.00	Yes

- IV. **Box cutting:** Box cutting is done for constructing pavement layers.
- V. **Pavement construction:** Pavement construction shall be done as per design. Before constructing pavement layers, compacted sand filling may be required if total thickness of pavement layers don't cover the required elevation of top surface of road. Considering durability, frequent flooding, socio-economic condition of Bangladesh, environment protection, and bad practices and examples of flexible pavement construction, rigid pavement should be constructed instead of flexible pavement. Rigid pavement increases the road construction cost 10-15%. During pavement construction most important point shall be maintaining proper camber and shoulder slope as per Figure 1. Transverse slope at pavement shall be 2.5% and at shoulder 5%. If these slopes are properly done, there shall be no requirement of surface drainage. Rain water will sheet flow on vegetated side slopes. Pavement construction includes ISG, subbase, base, bituminous carpeting and seal coat in case flexible pavement. In case of rigid pavement, base and RCC shall be the main two layers for low and medium traffic road. For heavy traffic road, subbase shall be needed. Layer thicknesses shall be as per design requirement.
- VI. **Clay cladding:** Rain cut erosion need to be prevented in side slopes where widened part is filled with sandy silt, silty sand or nonplastic silt. 200 mm thick clay shall be used cladding on side slopes.
- VII. **Vegetation on side slopes:** Vegetation is eco-friendly and has a very beneficial effect on the side slope protection. In many cases, it helps to make a sustainable slope. But, due to lack of maintenance and inadequate sunlight, it does not grow properly to protect the slope. At the side slopes, trees are planted to protect slopes. Side slopes must be protected immediately after completion of road construction. Biotechnology shall be the best and environment friendly option for this purpose. Vetiver or local grasses shall be planted on side slopes before commencement of monsoon. Watering shall be done to grow the vegetation in dry season. Large tree plantation shall be avoided on shoulders. Large trees may be planted 1 m below the shoulder level.
- VIII. **Installation of subsurface drainage:** Pumping need to be prevented by installing subsurface drainage which will be connected to base layer. Subsurface drainage is geobag of size 300x300x1500 filled with 20 mm down well graded brick chips. 3 mm thick geotextile shall be used to make geobag. 325 mm wide and 450 mm deep trench will be cut on shoulder @ 5m interval. Subsurface drainage shall be placed into the trench and top shall be covered with the compacted shoulder soil.

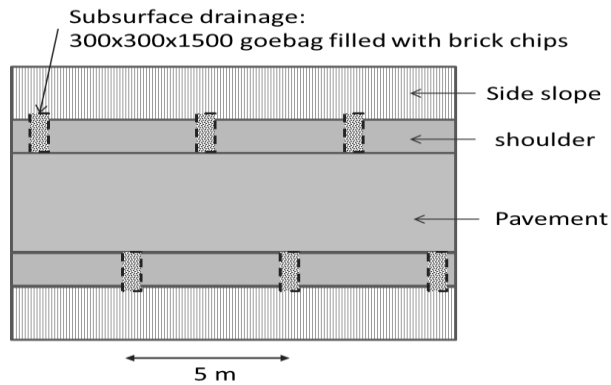


Figure 2: Typical layout of subsurface drainage of road

3.2 Challenging Situations of Rural Road Upgradation

Various situations are being encountered during up gradation of existing road in the coastal districts of Bangladesh. Such as pond or khal (canal) at one side of road as per figure below where one side of road. Side slope is very steep (1:0.5 or less). Other side of road is paddy land. There is no scope of maintaining slope by filling at the pond side or khal side of road. Below the embankment toe, there is steep slope (1:1.4 or less) (figure 3).

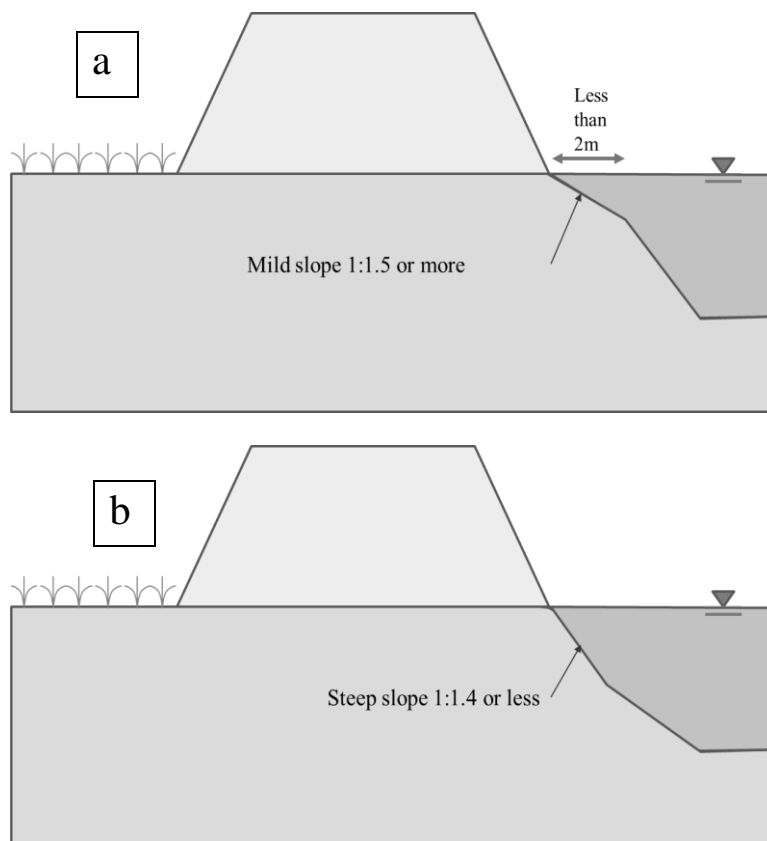


Figure 3: Challenging Condition; (a) situation with less than 2 m wide mild slope under toe of embankment (b) situation with steep slope under toe of embankment

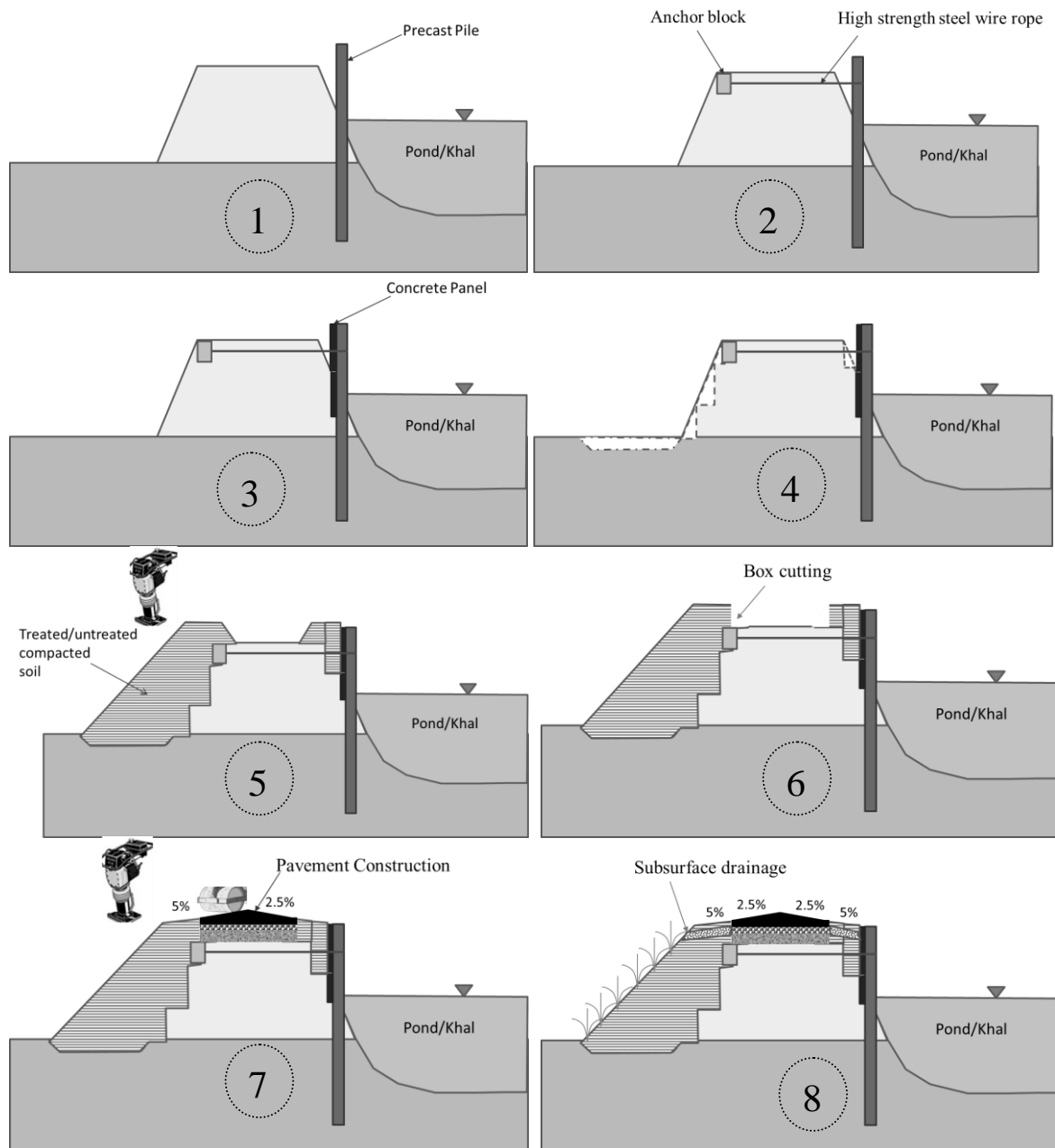


Figure 4: Step by step construction sequences for one side pond/khal situation

Step by step construction sequences for the Type are described below.

- I. **Pile Installation at canal (khal) side:** Geotechnical investigation is essential for designing pile size and reinforcement in anchored pile. Depending on the embankment height and soft soil thickness, pile length, section and rebar shall vary. Details of precast pile and panel are given in Figure 5. Embankment height shall be measured at 2 m distance from the edge of existing road top as shown in Figure 6. Concrete class will be as per climate resilient concrete manual (Alam & Hoque, 2019).

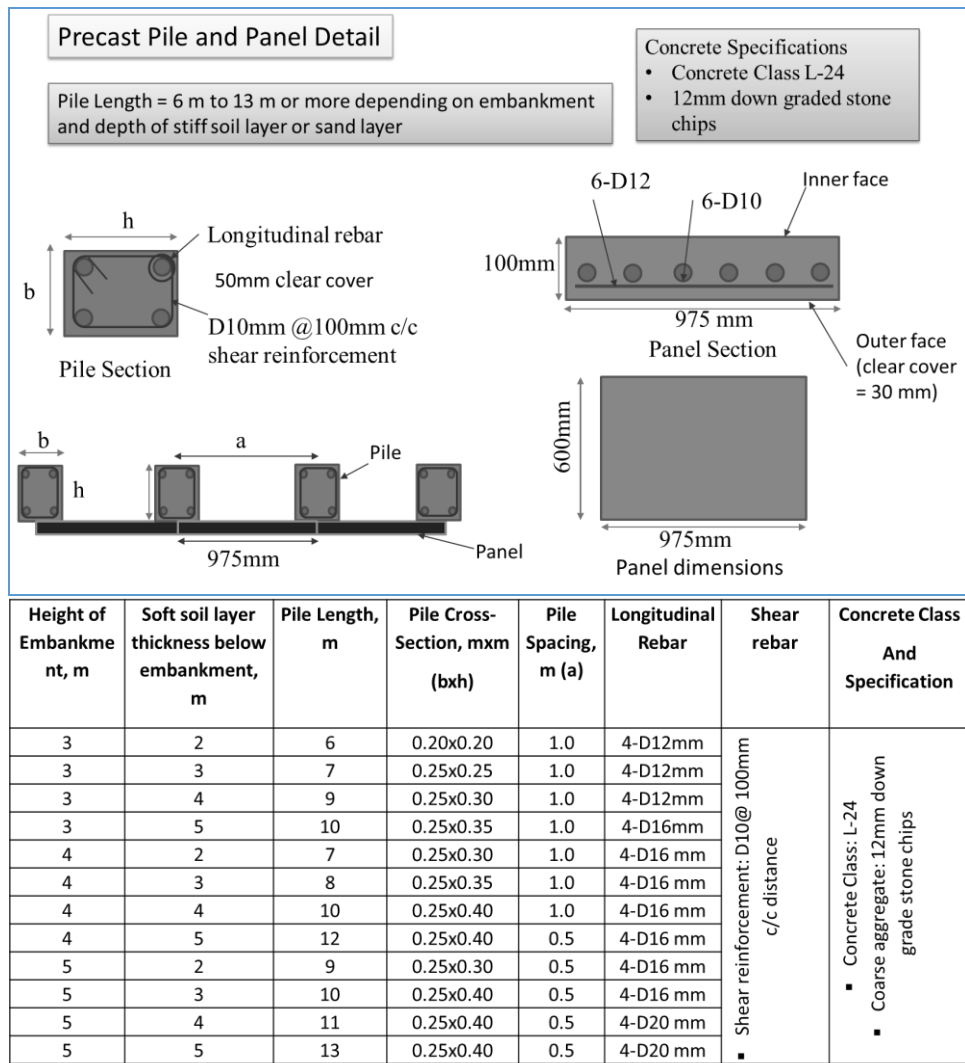


Figure 5: Details of precast pile and panel for one/both side pond or khal situation

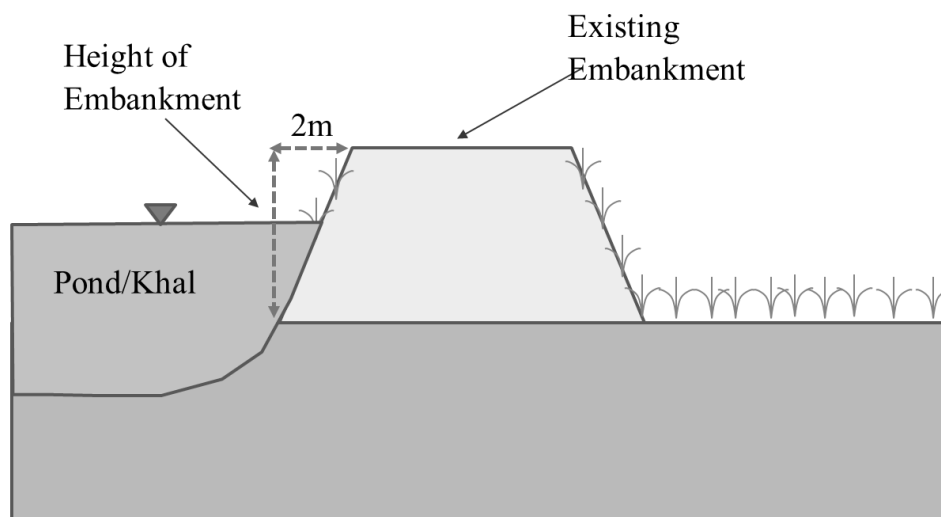


Figure 6: Selection of embankment height

- II. **Anchoring precast concrete pile:** Precast concrete pile is anchored by high strength steel wire rope. Details of anchor block and high strength steel wire rope is given in figure 7.

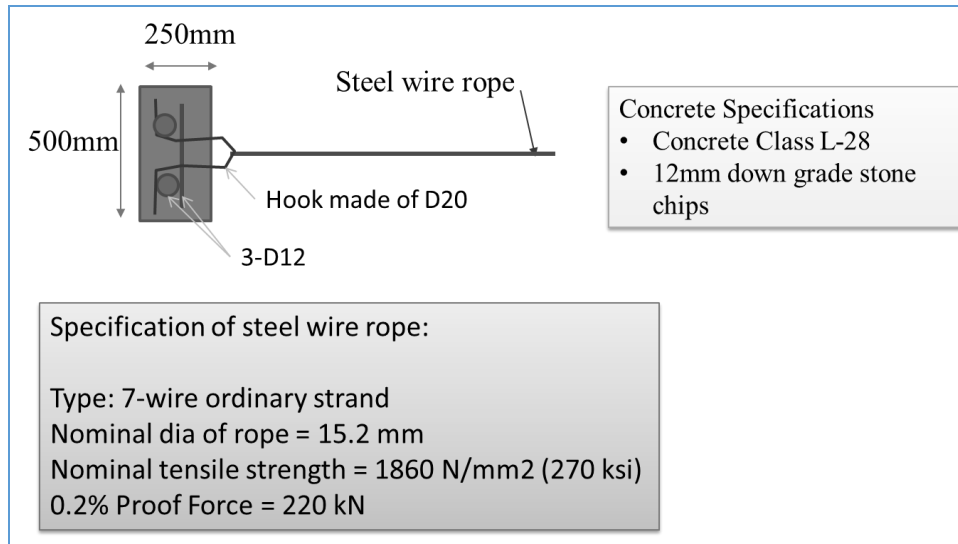


Figure 7: Details of anchor block and steel wire rope

- III. **Placement of concrete precast panel:** Details of concrete precast panel are given in figure 5.
 IV. Remaining part (other side) of this construction procedure will be as per section 3.1.

4. EFFECTIVENESS OF ANCHOR PLACEMENT AT TOP PORTION OF PILE

To investigate the effectiveness of anchor at top portion of pile a geo5 model is done. From the analysis it is found that for the same soil condition, the structure is unstable without anchoring whereas same structure is stable with anchoring as shown in figure 4. Considering displacement of anchor block and elongation of steel wire, spring constant of anchoring is assumed as 1130.0 kN/m.

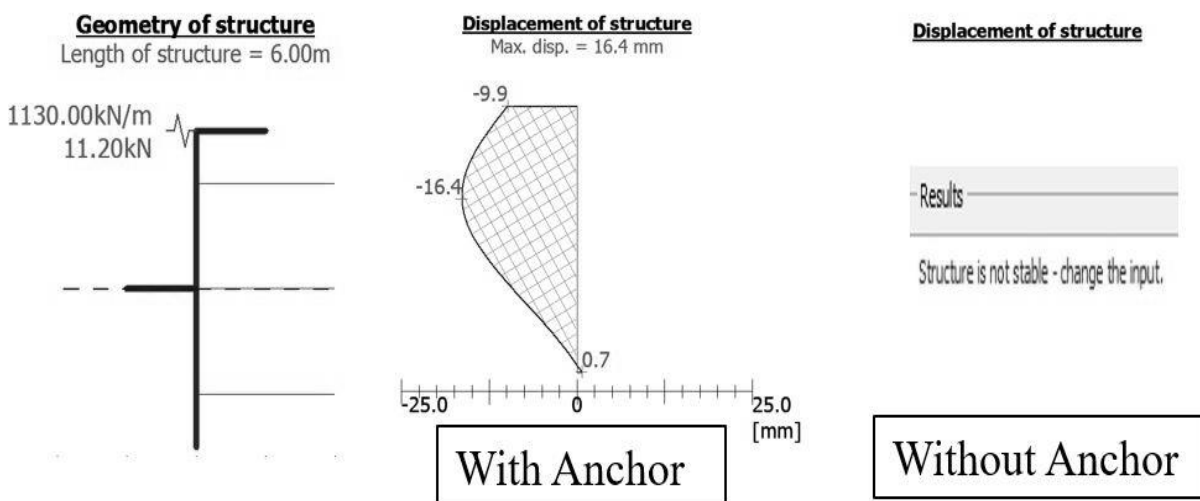


Figure 8: Displacement pattern of pile with anchor and without anchor option

5. CONCLUSIONS

Transportation contributes to the industrial, economic, social and cultural development of a nation. So it is very important to establish transportation system in such a standard way to get maximum output. Among the different types of adverse field condition, two types of situations are described in this paper. The construction guidelines described in this paper would be useful for engineers and contractors to ensure quality of rural road construction in coastal district of Bangladesh. Climate resilient road can be made if these guidelines are followed.

ACKNOWLEDGEMENTS

Authors wish to express their gratitude to “Introduction of Quality Test Protocols for Road and Market Rehabilitation” under Coastal Climate Resilient Infrastructure Project (CCRIP) (Package No: CCRIP-S-05(C), LGED, GOB) for their financial support.

REFERENCES

- Alam, M. K., Hasan, A. S., Khan, M. R., & Whitney, J. W. (1990). Geological Map of Bangladesh. Geological Survey of Bangladesh, Ministry of Energy and Mineral Resources, Government of the People's Republic of Bangladesh.
- Alam, Tanvir, & Hoque, (2017) Final Report of the Sub-Project “Introduction of Quality Test Protocols for Road and Market Rehabilitation
Government of the People's Republic of Bangladesh. (2005). Road Design Standards (Rural Road). Bangladesh: Local Government Engineering Department (LGED) and Japan International Cooperation Agency (JICA).
- Huq, S., & Rabbani, G. (2011). Adaptation Technologies in Agriculture; The Economics of rice farming technology in climate - vulnerable areas of Bangladesh.
- Islam, M. T., Alam, J. M., Taufique, F. M., & Hasan, S. M. (2015). Effect of Sand Content on Plasticity, Compaction and CBR of Sand-Clay Mixture. International Conference on Recent Innovation in Civil Engineering for Sustainable Development (IICSD-2015). Gazipur, Bangladesh: Department of Civil Engineering, DUET.
- Kabir, M. H., Alam, J. M., Hamid, A. M., & Akhtaruzzaman, A. K. (2000). Foundations on Soft Soils for Khulna Medical College Buildings in Bangladesh. ISRM International Symposium, 19-24 November, Melbourne, Australia. International Society for Rock Mechanics and Rock Engineering.
- Md. Jahangir Alam & Md Shamsul Hoque (2019), Climate Resilient Concrete Manual for Local Government Engineering Department (LGED)
- Nath, B. D., Molla, M. K., & Sarkar, G. (2017). Study on Strength Behavior of Organic Soil Stabilized. International Scholarly Research Notices, 2017.

EFFECT OF ORGANIC CONTENT ON STIFFNESS OF CRICKET PITCH SOIL

Md. Kausar Alam Anik^{*1}, Md. Fyaz Sadiq² and Md. Zoynul Abedin³

¹*Assistant Professor, Daffodil International University (DIU), Bangladesh,
e-mail: kausar.ce165@gmail.com*

²*Under Graduate Student, Military Institute of Science and Technology (MIST), Bangladesh,
e-mail: fyaz.sadiq.ce@gmail.com*

³*Senior Professor, Military Institute of Science and Technology (MIST), Bangladesh,
e-mail: zabedin@ce.mist.ac.bd*

***Corresponding Author**

ABSTRACT

The main objective of this study was to investigate the effect of organic content on the stiffness of cricket pitch soil. Limited research has been carried out focusing on the preparation of grass mixed pitch soil in the laboratory that could simulate in-situ conditions. Soil samples were collected from selected international cricket pitches of Bangladesh. Soil mixture was prepared by mixing pitch clay powder specimens thoroughly with fixed portions of wooden dust (as an organic content like grass) and water (near optimum moisture content). A number of test specimens with varying proportions of wooden dust were prepared. The prepared soil specimen placed in the compaction mold and compacted as per ASTM D1557-12. The prepared soil cakes were tested just after preparation and also after saturation in 24 hours beneath the water. Both soil cake used as unconfined compression test specimens. The investigation reveals that approximately 2% of organic content may be preferable considering stiffness and other factors like maximum dry density, optimum moisture content.

Keywords: *Cricket pitch, Maximum dry density, Organic content, Optimum moisture content, Unconfined strength.*

1. INTRODUCTION

The quality and behavior of the cricket pitch surface is the prime concern of the cricketers. As per ICC operating manual 29.1, guidance for very good pitch rating outfield is well grassed, even covering, no bare patches, no irregularity of bounce, fast/medium pace, etc. The favorable conditions for consistent pitches may vary considerably from country to country, venue to venue and even from match to match depending upon prevailing soil physical/chemical parameters (Baker et al., 2003). The relationships among pace and bounce depend on particle size distribution, dry bulk density and organic content (Baker et al., 2003). He studied the positive correlation between pace and the dry bulk density and sand content of a soil, but there was a negative correlation between pace and moisture content, silt content and organic matter. Factors like moisture content, temperature, humidity, compaction, soil texture and composition, organic matter, etc. affect the properties of a pitch (James et al, 2004). Grasses are also an important factor because it ensures the consistency of a good pitch (Taiton and Klug, 2002). However, the accumulation of grassroots in the pitch increases organic content in pitch. As a result, the bouncing capacity of the pitch becomes low (Taiton & Klug, 2002).

A well-developed root system could increase moisture content in the range of two to five percent with depth (Taiton & Klug, 2002). However, the shear strength of clay soil is known to be highly sensitive to moisture content (Henkel, 1959). Therefore, during preparing pitches, soil moisture content must be kept to a minimum. Hence, for a good bouncy pitch, the optimization of grasses is required to balance the organic and moisture content and maintain stiffness of the pitch soil.

The present study introduces a simplified sample preparation method, which can be used as a representative of grass mixed cricket pitch soil. Cricket pitch clay was first collected from a number of stadiums in Bangladesh. Those clay samples were naturally dried, grounded and passed through 75 μm sieve. To obtain a wide range of moisture content, various amounts of organic content (wooden dust of Shal tree) were added with the clay to prepare the reconstituted samples. Compaction tests were then completed on reconstituted samples. The shear strength characteristics of these samples were studied on both optimum moisture and saturated soil condition. The test results were also compared with the established relationships.

2. SAMPLE COLLECTION AND PREPARATION

In Bangladesh, there are seven international venues of the cricket stadium. For the present study, three samples were collected from different stadiums. The soil collecting sites were namely Bangladesh Cricket Board (BCB-Mirpur), Bangladesh University of Engineering and Technology (BUET) and Rangpur Stadium. The samples were clay soil. Clays collected from BCB had black color, samples collected from BUET and Rangpur had a brown color. The collected clay sample used in this study contained 93% to 98% fines passing through 75 μm sieve. The specific gravity (Gs) of the samples ranged from 2.62 to 2.67. The results obtained from the tests provided liquid limit (LL) ranging from 61% to 84% and plasticity limit varying from 17% to 25%. Table 1 shows a summary of the physical properties of the soil samples collected from several locations. It is noted that the clays of Bangladesh predominantly consisted of illitic or chloritic minerals (Islam et al., 2002).

There are different types of organic matter available. Wooden dust was used as organic material having a specific gravity of 1.57. Wooden dust is locally available and less expensive. The properties of the wood dust were determined and presented in Table 1.

Table 1: Physical properties of clay samples

Material	Specific Gravity, G _s	Liquid limit, LL (%)	Plastic limit, PL (%)	Shrinkage limit, SL (%)	Linear Shrinkage, LS (%)	Flow Index
BCB	2.67	84	25	31	14.9	46.5
BUET	2.62	64	17	13	7.9	39.9
Rangpur	2.65	61	18	8	7.8	17.1
Wooden Dust (shal tree)	1.57	-	-	-	-	-

Table 2: Test scheme used for assessment of stiffness of cricket pitch soil

Pitch Sample	Organic Content	Compaction Test(CT)	Unconfined Compressive Strength(UCS)	
			Saturated Condition	Optimum Moisture Condition
BCB	0%	CT-1	UCS-1	UCO-1
	2%	CT-2	UCS-2	UCO-2
	4%	CT-3	UCS-3	UCO-3
BUET	0%	CT-4	UCS-4	UCO-4
	2%	CT-5	UCS-5	UCO-5
	4%	CT-6	UCS-6	UCO-6
Rangpur	0%	CT-7	UCS-7	UCO-7
	2%	CT-8	UCS-8	UCO-8
	4%	CT-9	UCS-9	UCO-9

3. TEST METHODOLOGY

Reconstituted clays were prepared using collected clay samples with different proportions of organic content. The concept of a reconstituted (RC) soil sample was introduced in the past to simulate the behavior of a normally consolidated clay sample. RC samples were used to assess the influence of soil structure on the mechanical behavior of natural sedimentary clays (Nagaraj & Srinivasa Murthy, 1986; Burland, 1990; Hong & Tsuchida, 1999; Liu and Carter, 1999; Chandler, 2000; Cotecchia & Chandler, 2000). Existing methods for preparing reconstituted clay samples can roughly be divided into two categories, i.e., the compaction and consolidation methods respectively (Yin & Miao, 2015). The reconstituted clay samples were conducted under compacted conditions. Standard testing procedures followed by ASTM D1557-12 was carried out to obtain the maximum dry density and optimum water content. Soil samples were then mixed at optimum water content and cured for a certain period of time. Then the samples were compacted in the compaction mold to prepare test specimen.

Prepared soil cakes were compacted to assess the shear strength behavior of reconstituted modified clays. The soil cakes were submerged in water for 24 hours to observe the behavior in a saturated condition. After submerging, prepared soil cakes were trimmed to retrieve test specimens. To obtain optimum moisture conditions, the test specimen was prepared from reconstituted soil cake after trimming to the required dimension (diameter of 38 mm and height of 76 mm). The test specimen was preserved in an air controlled desiccator. The loading device was adjusted carefully so that the upper plate just made contact with the specimen. Each specimen was tested under strain-controlled conditions. During the progress of the test, load was applied continuously and without shock at a deformation rate of approximately 0.5 millimeters per minute. The total load and corresponding deformations were recorded at sufficient intervals. The test was continued until failure or 20% axial strain of the specimen. The test scheme is presented in Table 2 where CT, UCS, and UCO represent

the compaction test, unconfined compression in saturated and unconfined compression in optimum moisture condition.

4. TEST RESULTS

4.1 Compaction Test

A series of compaction test was conducted and results are presented in Figure 1. The ideal water content for maximum compaction is known as the optimum water content. Determining the optimum water content is time-consuming, but once known for a specific bulli, it can be used to assist in achieving a range of compaction options (Hillel, 1980). Optimum moisture content was determined by plotting a curve of dry density versus moisture content of the soil sample. The maximum compaction can be achieved by rolling with a roller at the optimum moisture content of pitch soil. From the test result, it is observed that optimum moisture content value is decreasing with the increasing of organic content

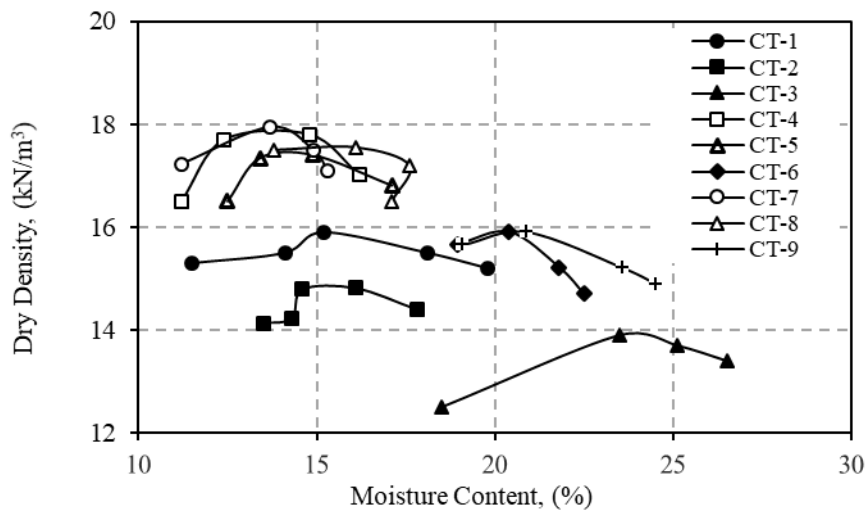


Figure 1: Dry density and optimum moisture content curve of different mixtures of clay

4.2 Effect of organic content on maximum dry density

Physical properties of soil like maximum dry density are affected by organic content. The dry density of soil decreases with an increase in the percent of organic content. This means organic content takes up the spaces that would have been occupied by soil particles and as a result, dry density is reduced. The results are shown below in Figure 2.

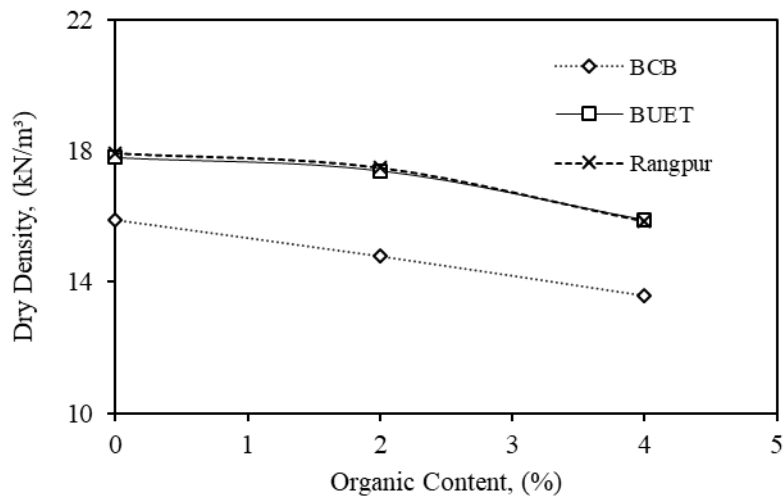


Figure 2: Variation of maximum dry density with percent organic content curve

4.3 Effect of organic content on optimum moisture content

Moisture content is one of the most important governing factors of pitch performance. Moisture content should maintain properly during pitch construction. Moisture content has a strong relationship with organic content. The test result revealed that by adding 4% of organic content with soil, the mixture could hold moisture in the range of 20% to 25%. The test result is shown in Figure 3.

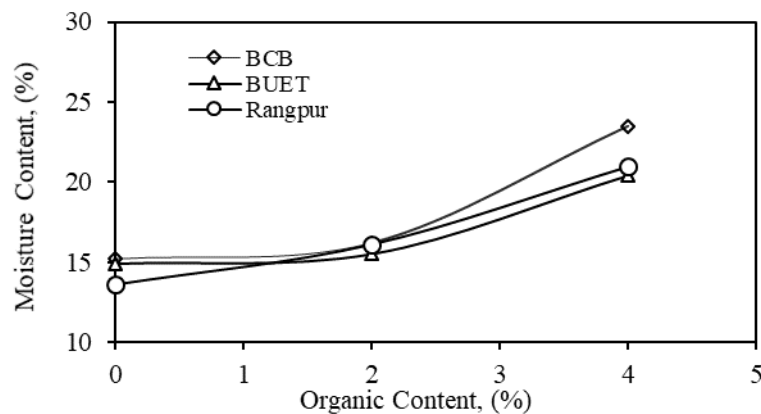


Figure 3: Variation of optimum moisture content and percent organic content curve

4.4 Unconfined compression test

Test specimen were prepared in two ways. Firstly, after submerging in water and other just after extracting from the mold. Both soil cake trimmed to retrieve test specimens. Figure 4 depicts the variation of deviator stress with axial strain at the saturated condition. The test result shown that deviator stress becomes half due to addition at 4% organic content.

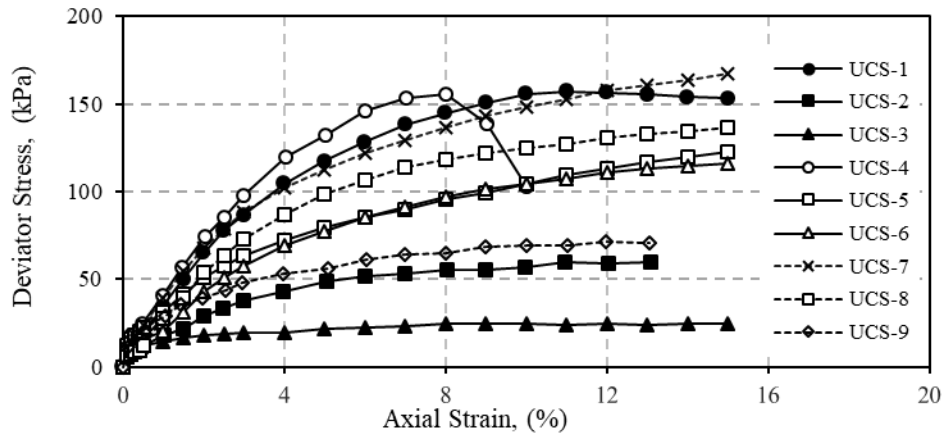


Figure 4: Variation of deviator stress with axial strain in clay at the saturated condition

The test specimen was also prepared by compacting the soil samples at optimum moisture content. The test result is shown in Figure 5. The results indicate that each type of reconstituted modified clays shows a similar trend under the same loading condition. The variation of deviator stress with the increase of organic content followed narrow-band than saturated condition.

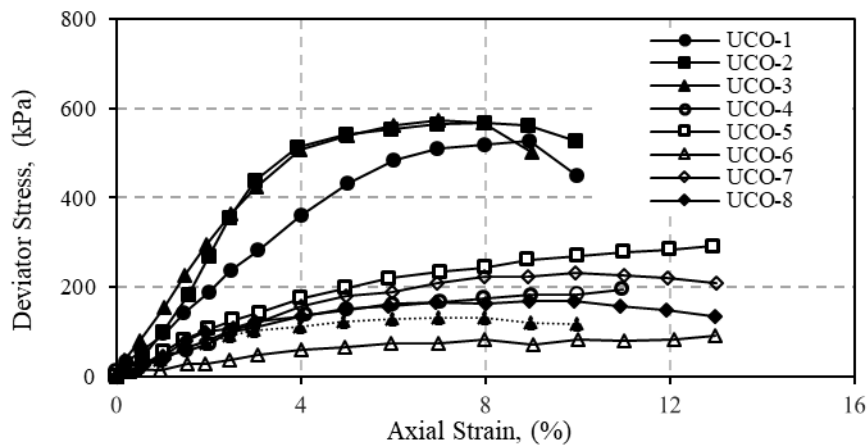


Figure 5. Variation of deviator stress with axial strain in clay at the saturated condition

For saturated cohesive soil, the deviator stress at failure, q_f and shear strength is $s_u = q_f/2$ in an unconfined compression test. The shear strength measured from the deviator stress at failure as shown in Figure 2. The undrained shear strength obtained from Figure 4 was plotted versus organic content in Figure 6. In general, the unconfined compressive strength (stiffness) at saturated water content found to decrease with increasing wooden dust because wooden dust can hold moisture that can reduce shear strength.

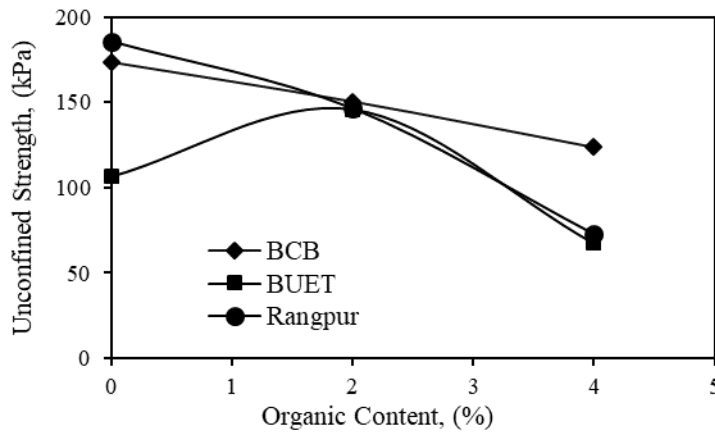


Figure 6: Effect of organic content on unconfined compressive strength (Saturated soil condition)

4.6 Effect of organic content on stiffness at optimum moisture content

When the percent of organic content was gradually increased, unconfined compressive strength (stiffness) also gradually increased. Beyond a certain organic content, any increase in the amount of organic content tends to reduce the strength. This phenomenon occurred because the organic content takes up the spaces that were occupied by soil particles, the organic content at which maximum strength is obtained is generally referred to as the optimum amount of organic content for this soil sample. Similarly, the shear strength measured from the deviator stress at failure as shown in Figure 5. The undrained shear strength obtained from Figure 5 was plotted versus organic content in Figure 5. The test result shown that with the increase of organic content, strength variation was small.

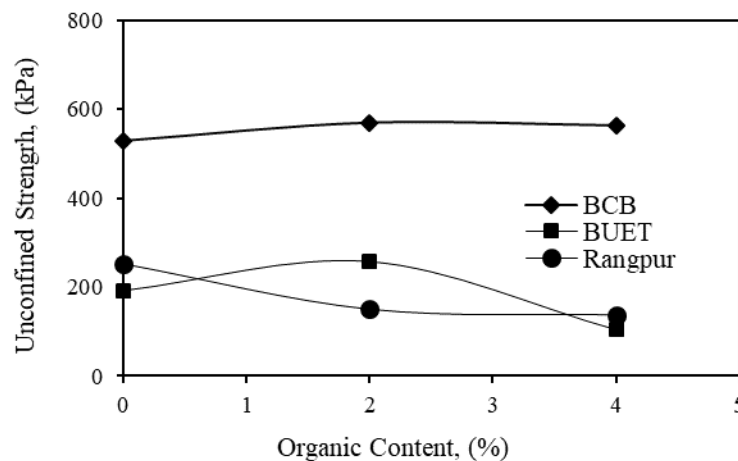


Figure 7: Effect of organic content on unconfined compressive strength (Optimum moisture condition)

5. CONCLUSIONS

The procedure proposed in this study is used to prepare the sample specimen. Moreover, the prepared soil samples successfully simulated the shear strength nature of the cricket pitch soils. The test results suggested that optimum moisture content value is decreasing with the increasing of organic content. Besides, the dry density of soil decreases with an increase in the percent of organic content. From the test result, it can be concluded that the optimum percent organic content found in an order of approximately 2% in this investigation. At this percentage, a variation of undrained strength was small in both saturated and optimum moisture content conditions and could hold moisture up to 30 percent. The percent presented are based on a limited number of data. It is noted that the findings

reported in this study are part of an ongoing extensive research program focusing on the Characterization of Reconstituted Clay.

ACKNOWLEDGMENTS

The authors are grateful to the Geotechnical laboratory of Military Institute of Science and Technology (MIST) and Bangladesh University of Engineering and Technology (BUET) for the experimental support.

REFERENCES

- Baker, S.W., Hammond, L.K.F., Owen, A.G. and Adams, W.A. (2003), Soil physical properties of first-class cricket pitches in England and Wales. 2. Influence of soil type and pitch preparation on playing quality, *Journal of the Sports Turf Research Institute*, 79, 13–21.
- Chandler, R. J. (2000), “Clay Sediments in Depositional Basin: the Geotechnical Cycle”, *Quarterly Journal of Engineering Geology and Hydrology*, Vol 33, No. 1, 7–39.
- Cotecchia, F. and Chandler, R. J. (2000), “A General Framework for the Mechanical Behaviour of Clays”, *Géotechnique*, 50, No. 4, 431–447.
- Hillel (1982), *Introduction to soil physics*. Academic Press, New York.
- Henkel, D.J. (1959), The relationship between the strength, pore-water pressure and volume-change characteristics of saturated clays. *Geotechnique*, 9, 119–135.
- Hong, Z. S. and Tsuchida, T. (1999), On Compression Characteristics of Ariake Clays, *Canadian Geotechnical Journal*, 36, No. 5, 807–814.
- Islam, M. R., Stuart, R., Risto, A. and Vesa, P. (2002), “Mineralogical Changes during Intense Chemical Weathering of Sedimentary Rocks in Bangladesh”, *Journal of Asian Earth Sciences*, 20, 889–901.
- James, D.M., Carré, M.J., Haake, S.J. (2004). The playing performance of county cricket pitches. *Sports Engineering*. 7(1): p. 1–14
- Liu, M. D., and Carter, J. P. (1999), Virgin Compression of Structured Soils, *Géotechnique*, 49, No. 1, 43–57.
- Nagaraj, T. S., and Murthy, B. R. S. (1986), A Critical Reappraisal of Compression Index Equation, *Géotechnique*, 36, No. 1, 27–32.
- Taiton, N. and Klug, J., (2002), “The cricket pitch and its outfield”, University of Natal, Pietermaritzburg.
- Yin, J. and Miao, Y. H. (2015), “An Oedometer-Based Method for Preparing Reconstituted Clay Samples”, *Applied Mechanics and Materials*, Vols. 719-720, 193-196.

QUANTIFICATION OF CRACKING BEHAVIOR OF COMPOSITE CLAY LINERS

Abdullah All Noman*¹ and Islam M. Rafizul²

¹*Department of Civil Engineering, Khulna University of Engineering & Technology (KUET), Khulna-9203, Bangladesh, email: allnoman1994@gmail.com*

²*Department of Civil Engineering, Khulna University of Engineering & Technology (KUET), Khulna-9203, Bangladesh, email: imrafizul@yahoo.com*

***Corresponding author**

ABSTRACT

Cracking is a complex phenomenon which is active in materials like soils. As crack is a natural process it involves chemical, biological and weathering changes. The study of cracking behavior of liners used in landfill is very essential and need to quantify. The development of crack depends on moisture content, soil thickness, rate of drying and wetting, surface configuration, total drying period etc. In this study, to prepare composite clay liners (CCLs), disturbed soil samples were collected at a depth of 5 ft from the existing ground surface from a selected waste disposal site at Rajbandh, Khulna, Bangladesh. In the laboratory, the physical and index properties of soil sample were measured through the standard test methods. The values of initial moisture content, optimum moisture content (OMC), maximum dry density (MDD), specific gravity, liquid limit (LL), plastic limit (PL), plasticity index, shrinkage limit (SL), sand, silt and clay were found 37.65%, 20%, 1.53gm/cc, 2.61, 54%, 31%, 23% and 35.11%, 4.6%, 64.7%, 30.7%, respectively. In this study, to prepare CCLs, 30 cm diameter of steel circular mold with varying thickness like 10, 20 and 30 mm were used. In the laboratory, the CCLs were prepared with fly ash (FA) at varying mixing proportions like 20, 30, 40, 50 and 60% and brick dust (BD) with mixing proportion 10, 20, 30 and 40% by weight. The cycles of wetting and drying were subjected on the prepared CCLs to simulate the field behavior of liners in landfills. The formation of cracks were constant after 7 days in dry cycle and became zero after 4 days in wet cycle. For this consequence the duration of the wet cycle was 7 days and that of the dry cycle was also 4 days. In the test with multiple wet-dry cycles, the amount of cracking parameters did not change significantly after second cycle. In the laboratory, the engineering properties of FA and BD were measured. The cracking parameters like crack area, crack intensity factor (CIF), and crack density factor (CDF) were analyzed using ImageJ technique through MATLAB. From results it is clear that maximum values of CIF, CDF and crack area were found in control soil. In addition, the minimum values of CIF, CDF and crack area were found at mixing FA content of 60% and brick dust of 40% in soils. All the studied geometrical parameters decrease with increase of liner thickness except CDF. The value of CDF increases with increase of specimen thickness. Maximum and minimum CDF were found in 30mm and 10mm specimen thickness, respectively. The maximum and minimum values CIF, CDF and crack area were found at moisture content equals to LL and OMC, respectively. In addition, the values of geometrical parameter increases in relation to the increasing of moisture content i.e. the liners with LL showed comparatively the higher values of cracking parameters than that of other counter parts. The cracks were found comparatively wider and longer in fly ash than that of liners with brick dust.

Keywords: *Composite clay liners, Desiccation, Cracking behavior, ImageJ, MATLAB.*

1. INTRODUCTION

Before and after dumping of Municipal Solid Waste (MSW) in landfill, cap and base liner is needed to safe the environmental components and the underlying soil layer. It is important to design of cap and base liners properly in landfill to protect surrounding environment including underlying soils, groundwater and surface water bodies by contaminated leachate that generated from decomposed MSW in landfill (Carey et al., 2000). For better performance of liners, landfill liners should be low permeable throughout its lifetime (Omidi et al., 1996). The character of clay soil used for liners can be highly compromised when desiccation cracks start to propagate through soil. If surficial tensile stress exists, soil tensile strength and volumetric shrinkage becomes constrained, desiccation cracks promote its geometrical characteristics (Corte and Higashi, 1960). Besides, moisture and density conditions, confining pressures, temperature, and cycles of wetting and drying are also responsible for crack formation (Morris et al., 1992). The formation of cracks at controlled weathering condition has a great impact on crack propagation rate and its geometric condition due to fluctuation of temperature. The design criteria of composite landfill liners such as hydraulic conductivity should be low i.e. $k < 10^{-9}$ m/s, $PI > 7$, at least 30% fines of which 15% clay and water content must be greater than plastic limit (Rafizul, 2014). The admixtures such as lime, cement, fly ash, bentonite, brick dust, sand, etc. have been commonly used to prepare composite liners with soil. Desiccation crack significantly affects the performance of clay liners. Cracks generate weak zone in a soil mass which reduce stability and overall strength of the liners. The formation crack also depends on moisture content, liners thickness, of drying and wetting, surface configuration, rate total drying period etc. Crack dimensions are generally measured using approximate method due to absence of established standard method. Now-a-days digital image analysis techniques are gaining more popularity in both crack quantification and characterization.

Yesiller et al. (2000) proposed that crack intensity factor (CIF) which is the ratio of the cracks area to the total area of surface of a drying soil specimen to quantify the extent of cracking of composite landfill liners. In their method, to calculate crack length, cracking images were skeletonized following Gonzalez and Woods (2002) method. A study conducted by Kleppe et al. (1985) and proposed a geometric parameter of crack density factor (CDF) which depends on the thickness of specimen. The CDF is the ratio of the summation of shrinkage area and crack area to initial specimen area. Therefore, Al Wahab and El-Kedrah (1995) stated that length and width of cracks can be determined using digital clipers. If directly measure the cracks parameters, larger error will fabricate in actual result due to irregular shape, length, width and depth of cracks as well as shrinkage (Tang et al., 2008). In this study, the commonly available admixtures such as fly ash and brick dust will be used to prepare composite landfill liners at varying mixing proportions. An image-based algorithm through MATLAB will be developed to quantify the desiccation cracks of composite landfill liners. Moreover, ImageJ will also be used to determine other relevant parameters so that geometrical characteristics of cracks can be easily described. The geometric parameters interms of CIF and CDF will be determined from binary image of MATLAB coding. In addition, the other features such as cracking area will be measured based on ImageJ software from binary image which is one of the output of MATLAB image analysis. In addition, the variation of CDF, CIF and crack areas with in relation to the changes of mixing water content in terms of OMC, PL and LL as well as specimen thickness will be investigated. In this study, a new window will may open for designers to construct cap and base liners in waste landfill easily and economically specially in least developed Asian countries like Bangladesh.

2. MATERIAL AND METHOD

To fulfill the desire objectives of this study, the soil samples were collected and then composite liners were prepared in the laboratory. In addition, the geometric parameters like CIF, CDF and crack area were computed and hence discussed in the following articles.

2.1 Collection of Soil Sample

In this study, disturbed soil samples were collected from a selected waste disposal site at Rajbandh, Khulna, Bangladesh which is approximately 20 km away from Khulna City. The soil samples were collected at a depth of approximate 5 feet below existing ground surface. In this study, the samples were

first air-dried and then powdered. The powdered samples were then sieved No. 4 and then the sieved samples were used to prepare composite liners. In the laboratory, the physical and index properties such as initial moisture content, OMC, MDD, specific gravity, LL PL, SL and constituents of soil particles in soil were measured through ASTM standard depicted in Table 1.

Table 1. Physical and index properties of soil used in this study

Properties	Unit	Values	Analytical method
Initial moisture content, w	%	37.65	ASTM D 2974
Optimum moisture content, OMC	%	20	ASTM D 558
Maximum dry density, MDD	gm/cc	1.53	
Specific gravity, G _s	--	2.61	ASTM D 854
Liquid Limit, LL	%	54	
Plastic Limit, PL	%	31	ASTM D 4318
Plasticity index, PI	%	23	
Shrinkage limit, SL	%	35.11	ASTM D 427
Sand: silt: clay	%	4.6: 64.7: 30.7	ASTM D222

2.2 Collection of Additives

To prepare composite landfill liners, different types of admixtures like fly ash (FA) and brick dust (BD) were collected from local market. In this study, the FA and BD passing through 4 no. sieve were used and the physical and index properties of FA and BD was also measured through ASTM standards methods.

2.3 Preparation of Composite Liners

In the laboratory, the saturated surface dry additives like FA and BD were mixed with soil at various percentages separately to make soil slurry. In this study, the mixing proportions of 10, 20, 30 and 40% of BD by weight with soil were used to prepare composite landfill liner. In addition, the mixing proportions of FA of 20, 30, 40, 50 and 60% by weight with soil was used to prepare composite landfill liner. Experimental work has been carried out at three different moisture content i.e. at OMC, PL and LL. A study conducted by Tiwari (2015) and prepared liners with bentonite and fly ash at varying mixing proportions with the mixing water content equal to OMC, PL and LL. In the present study, for preparing composite liners with water content, the statement postulated by Tiwari (2015) were followed. The mixing soil pastes were kept in air-tight polythene bags for 2 hours due to uniform water absorption in wooden chamber. In addition, the effect of the variation of different mixing amount of admixtures on OMC and MDD as well as CIF, CDF and crack area were formulated. In this study, the diameter of steel circular mold of 30cm was used. In addition, the thickness of mold of 10, 20 and 30mm were considered to prepare composite liners.

2.4 Drying and Image Taking Process

After the preparation of composite specimens, the desired amount of composite slurry was poured in mold at varying thickness of 10, 20 and 30mm in the wooden chamber, where six heat lamps of 100W light bulbs were connected. So that desiccation crack would be formed due to evaporation of moisture from liner specimens shown in Figure 1. In this stage, it was ensured that each specimen could get equal heat. In addition, a thermometer was connected to the chamber to measure the variation of temperature in a regular basis and the temperature was found approximately 44° C (Figure 1, a). During drying process, a digital camera (Nikon COOLPIX S2900) which was mounted at top of sample soil through steel made camera stand, used to take image of drying sample. A 1.5 feet of constant height was always maintained for taking image of one-day interval.

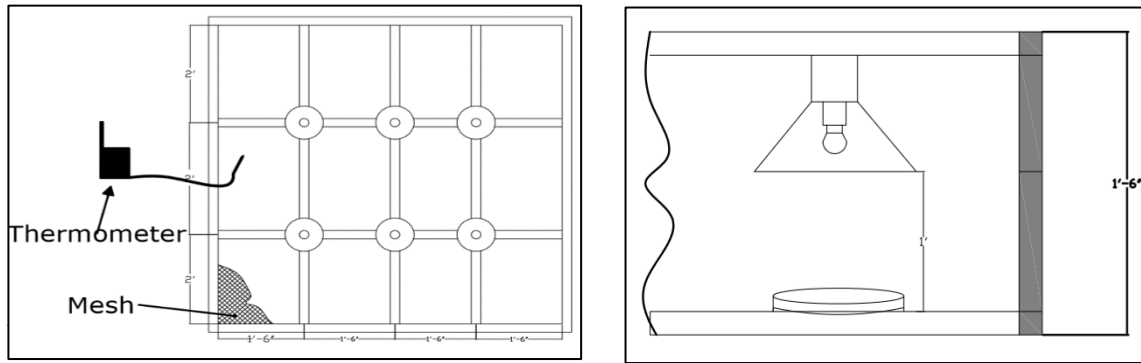


Figure 1: Chamber system for drying of soils (a) top view and (b) sectional view

Initially, all soils were subjected to two cycles: a dry cycle and a wet–dry cycle. The three cycles of wetting and drying were subjected on the prepared composite to simulate the field behavior of liners in landfills. In the wetting cycle, approximately 150ml/day of water for 4 days were used through spraying nozzle to simulate the percolation behavior of clay. At the beginning of drying and wetting cycle, the image of liners were taken at a short period of time <1hr, whereas, at the end of drying and wetting cycle, the image of liners were taken at a long period of time >24hrs.

2.6 Image Processing

Image analysis is a process where meaningful information are Extract from digital images clicked by digital camera. Image analysis is implemented in two basic steps.

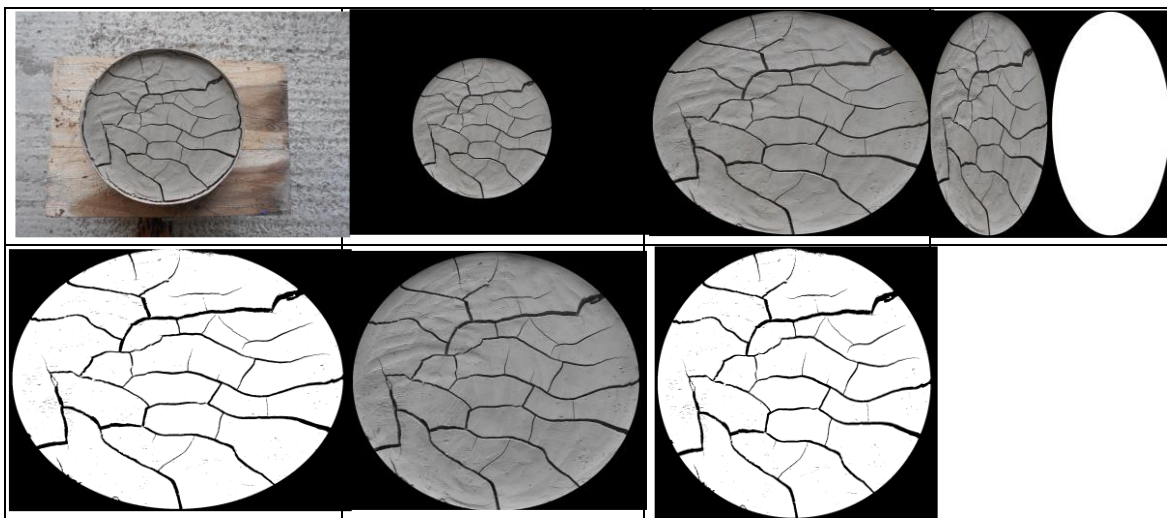


Figure 2. Image processing and analysis of a liners (20% fly ash with soil of 10mm thickness and at LL)

The first step implicates the image processing to prepare the image for analyses. This include cropping the unnecessary part of RGB image and then it convert to binary (black & white) image obtained by thresholding the RGB image shown in Figure 2. The second step comprises the investigation of image which is obtained and processed from step 1 to compute CIF, CDF and crack area.

2.7 Image Analysis

RGB Image obtained from camera were analyzed in MATLAB to calculate essential information. MATLAB program was set in such a way that it counts only the area of black pixels in the image. The black pixels were taken in MATLAB program as cracked area. In addition, summation of black pixels and white pixels were also calculated. Then set a program in MATLAB of the ratio of black pixels to the summation of black and white pixels which is known as CIF using Equation 1. For determine other

parameter used ImageJ software and Microsoft excel. In addition for the determination of diameter of reduced specimen, a known distance in the image like the diameter of mold is marked by straight line and scale is set in ImageJ by the option Analyse-Set Scale-give value 30 cm. Then length of the reduced specimen was calculated at the same image by measure command (Analyze-measure). Other parameters like total area of cracks was calculated through MS excel. In addition, the value of CDF was computed using Equation 2.

$$CIF (\%) = \frac{\text{Crack area} * 100}{\text{Reduced specimen area}} \quad (1)$$

$$CDF (\%) = \frac{(\text{Crack area} + \text{shrinkage area}) * 100}{\text{Reduced specimen area}} \quad (2)$$

3. RESULTS AND DISCUSSIONS

For the design of suitable liners in landfill with additives, the geometrical parameters like compaction characteristic, CIF, CDF are crack area are need to be analyzed. In this study, these parameters were analyzed and hence discussed in the following articles.

3.1 Compaction Characteristics

The variation of dry density to stabilized soil in relative to the changing of moisture content of stabilized soil with FA and BD content is revealed in Figure 3 and Figure 4, respectively. The following figures represents that the MDD decrease with the increase of of FA and BD content. The phenomenon behind this, the specific gravity of the FA and BD compared with soil and immediate formation of cemented products which is done by hydration which reduces the density of soil. As a results MDD decreases with the increase of admixture content in composite soils.

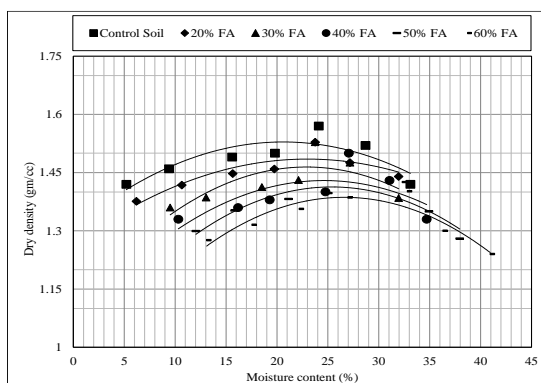


Figure 3: Variation of MDD with FA content

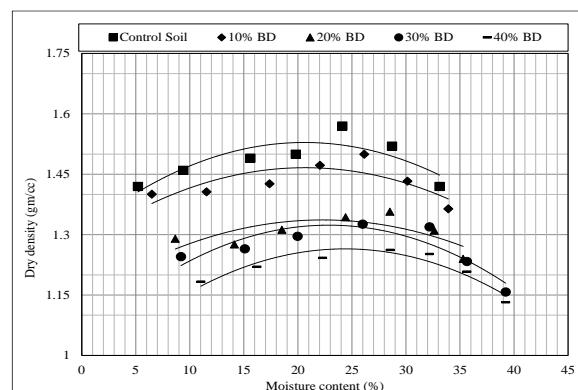


Figure 4: Variation of MDD with BD content

3.2 Crack Intensity Factor

The variation of crack intensity factor (CIF) with time, admixture content, moisture content and thickness of liners were analyzed and hence discussed in the following articles.

3.2.1. Variation of CIF with Time

The variation of CIF with time of liners having 10mm thickness at varying mixing proportions of FA and BD with mixing water content equals to OMC for different cycles is shown in Figure 5 and Figure 6, respectively. In the first dry cycle, CIF increases with time and become constant after four days (96hrs) for both liners. After end of first dry cycle with constant crack area at 168hrs for both liners, the amount of water was applied to start a wet cycle. In wet cycle, the developed cracks became zero and CIF was found to be zero for both liners. A study conducted by Yesiller et al. (2000) and stated that at the initial stage of dry cycle, the value of CIF increased upto certain level then became constant as well as at the wet cycle it goes to zero. The findings of the present study were well agreed with the postulation stated by Yesiller et al. (2000). Moreover, when the second dry cycle started, CIF increases rapidly in

first two days then increases slowly and constant after four days (96hrs.) for both liners with FA and BD.

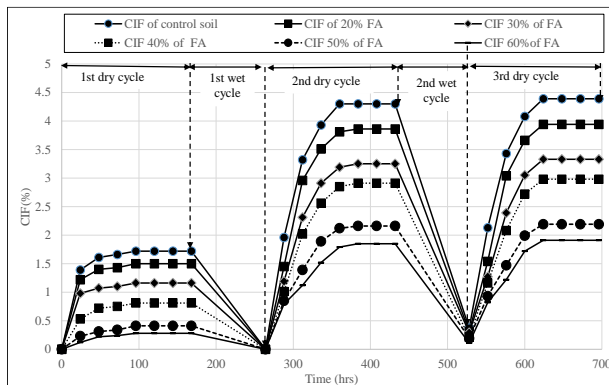


Figure 5: Variation of Cof with time of liners with FA having 10mm thickness for multiple cycles at OMC.

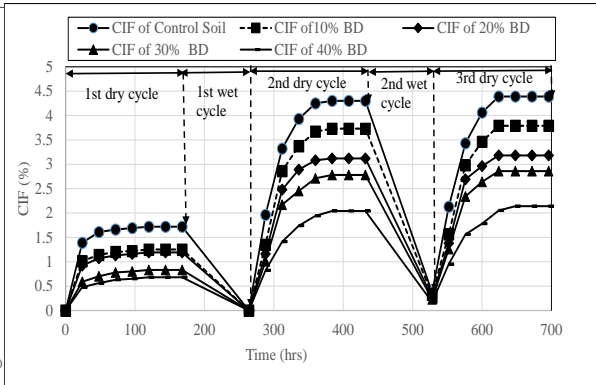


Figure 6: Variation of Cof with time of liners with BD having 10mm thickness for multiple cycles at OMC.

Figure 5 and Figure 6 reveal the values of Cof increased to 1.5 and 1.19 % in the first dry cycle for 20% of FA and BD respectively at 10mm thickness. On the other hand, it increases up to 3.84 and 3.12% in second wet-dry cycle for FA and BD respectively. In the test with multiple wet-dry cycles, the amount of Cof did not change significantly after second cycle. From figures it was observed that Cof was affected by fines content of the soils. In general high amount of Cof were observed in soil with high fine content (20% FA) and less Cof observed in soil with low fines content (20% BD) (Figures 5 and 6). The liners with BD for all mixing contents showed comparatively lower Cof for both first and second cycles than that of liners with FA. Figures depict lower Cof for both liners than that of control soil because the capacity of FA and BD are very low in terms of swell and shrink. For this reason it does not generate cracks. Crack area was reduced with the increase in FA content in the specimen and Cof was low. For this phenomena, liners with 60% FA and 40% BD shows comparatively lower Cof than that of other mixing content of FA and BD.

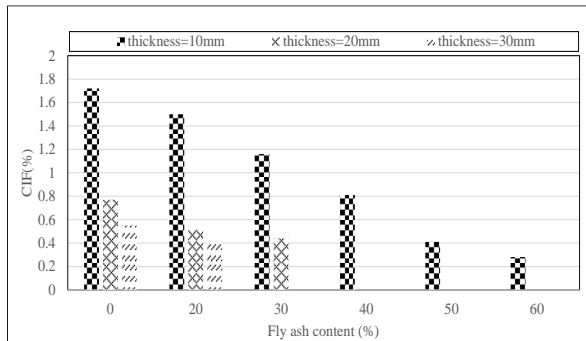


Figure 7: Variation of Cof with FA content at OMC for all the specimen thickness

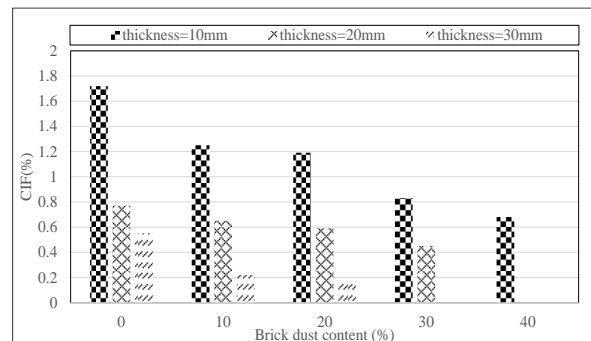


Figure 8: Variation of Cof with BD content at OMC for all the specimen thickness

3.2.2. Variation of Cof with Admixture Content

Figure 7 and Figure 8 illustrate the variation of Cof with the changing of FA and BD content at varying thickness with mixing water content equals to OMC for first dry cycle. Cof decreases with increase in FA and BD content. FA and BD have very low capacity to swell and shrink. For this consequence crack generally does not show. With the increase in FA in liners, crack area is reduced. As a result, low Cof was found. Figure 7 reveals Cof for control soil was 1.68% which decreases by increasing FA. Cof became zero for 30, 40, 50 and 60% of FA for 30mm thickness and 40, 50 and 60% of FA for 20mm thickness. On the other hand, Cof became zero with 30 and 40% for 30mm, while 40% for 20mm thickness of liner with BD.

3.2.3. Variation of CIF with Thickness

Figure 9 and Figure 10 clarifies the variation of CIF with moisture content and sample thickness at the end of dry cycle for FA and BD respectively. Intensity of cracks decrease with increase of specimen thickness. While for specimens of less thickness cracks were more. Figure 9 explains the values of CIF for 10, 20 and 30mm thickness at OMC are 1.5, .52 and 0.41 respectively. On the other hand, CIF increase with increase of moisture content. It were found 5.19, 4.69 and 4.13 for 10, 20 and 30mm thickness at LL respectively.

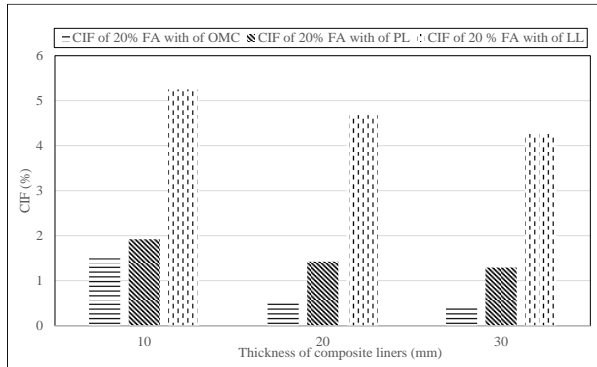


Figure 9: Variation of CIF with FA content at OMC, PL and LL for all the specimen thickness

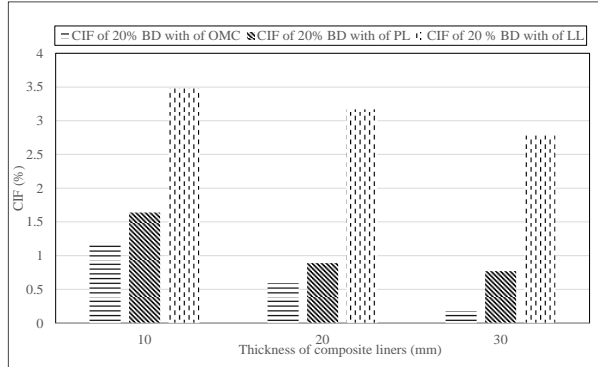


Figure 10: Variation of CIF with BD content at OMC, PL and LL for all the specimen thickness

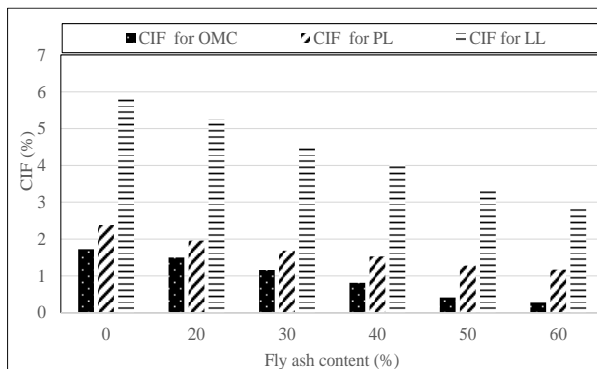


Figure 11: Variation of CIF with FA content at OMC, PL and LL for all fly ash content.

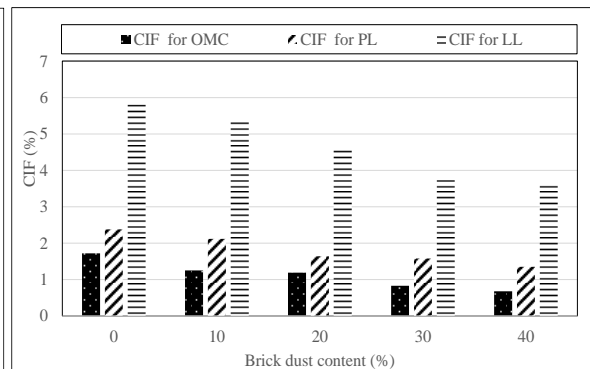


Figure 12: Variation of CIF with BD content at OMC, PL and LL for all fly ash content

3.2.4. Variation of CIF with Moisture Content

The variation of CIF with admixture content for FA and BD at varying moisture content equal to OMC, PL and LL shown in Figure 11 and Figure 12, respectively. Crack Intensity increases with increase of moisture content. For most of the specimens at OMC, cracks were almost zero with more reduced specimen area. While for specimens at PL and LL cracks were more with low reduced specimen area. As a result it accounts higher CIF for those specimen. CIF was .5, 1.96 and 5.25 for moisture content of OMC, PL and LL, respectively for (FA 20%). Figure 12 also proved that, CIF increases with increase of moisture content.

3.3. Crack Density Factor

The variation of crack density factor (CDF) with time, admixture content, moisture content and thickness of liners were analyzed and hence discussed in the following articles.

3.3.1. Variation of CDF with Time and Admixture Content

Figures 13 and 14 illuminate the variation of CIF of liners with FA and BD at OMC. The shrinkage potential of FA and BD are very low. Low shrinking materials means reduction in the percentage of high shrinking materials in the mix. For this reasons CDF values is reduced by means of more FA content. CDF generally increase with time and become constant after four days. After end of dry cycle wet cycle was started when CDF was Zero. When dry cycle started CDF increase rapidly in first three

days than increase slowly and constant after five days (120hrs). In the test with multiple wet-dry cycles, the amount of CDF did not change significantly after second cycle. From figures it was observed that CDF was affected by fines content of the soils. In general high amount of CDF were observed in soil with high fine content (20% FA) and less CDF observed in soil with low fines content (20% BD) (Figures 13 and 14).

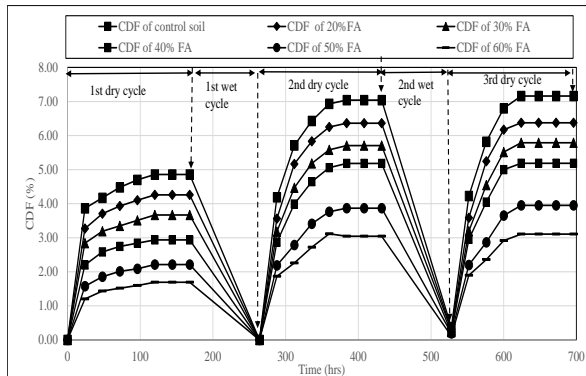


Figure 13: Variation of CDF of liners with FA having 10mm thickness with time for multiple cycles

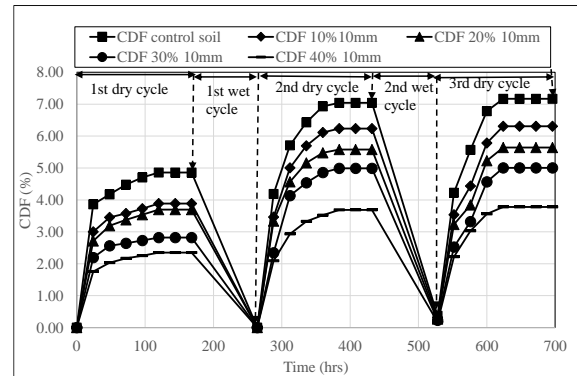


Figure 14: Variation of CDF of liners with BD having 10mm thickness with time for multiple cycles

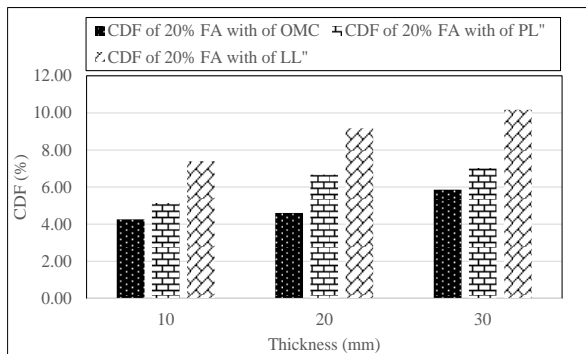


Figure 15: Variation of CDF with moisture content for all the specimen thickness for FA

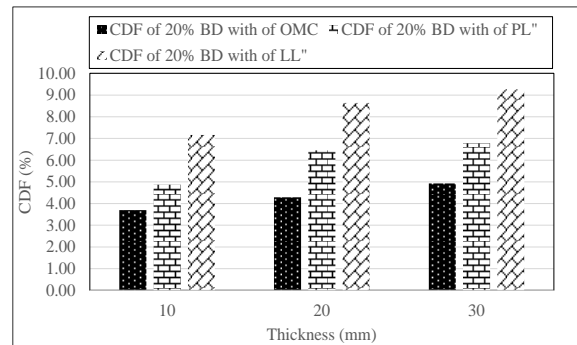


Figure 16: Variation of CDF with moisture content for all the specimen thickness for BD

3.3.2. Variation of CDF with Moisture Content and Specimen Thickness

In this study, composite liners with FA and BD at varying water content equals to OMC, PL and LL were prepared. The variation of CDF with moisture contents (OMC, PL and LL) as well as specimen thickness for 10mm thickness FA and BD is shown in Figure 15 and Figure 16, respectively. Soil can retain a large amount of water equals to LL and at constant FA or BD content. Greater values of moisture content in constant admixture content of liners specimen means low amount of solid soil particles. By the application of constant temperature, water will evaporate from the soil. As the small particles have very high cohesion they will move inwards. The movement of the particle will be more, if the amount of water is more or percentage of soil particles in the specimen is less. Increase in thickness leads to uneven drying of the layers of specimen, thus increases the surface cracks in a specimen which means increase of CDF. For this phenomenon, the values of CDF increase with the increase of Moisture content and thickness of the specimens. A study conducted by Tiwari (2015) and stated that CDF increase with increase of moisture content and specimen thickness which were agreed well with the findings with this present study.

3.4. Crack Area

The variation of crack area with time, admixture content, moisture content and thickness of liners were analyzed and hence discussed in the following articles.

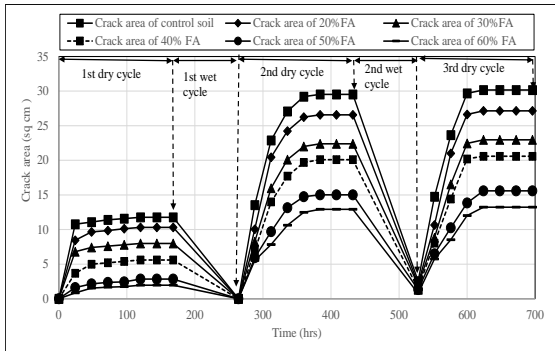


Figure 17: Variation of crack area of liners with FA having 10mm thickness with time for multiple cycles

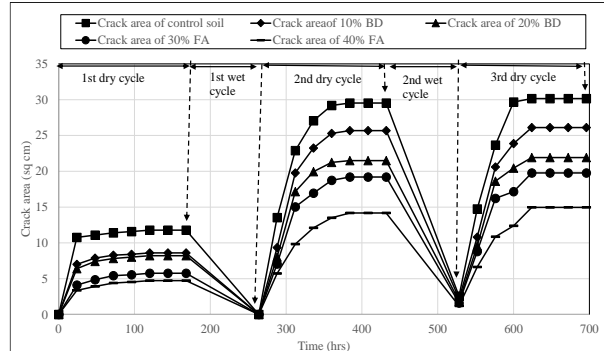


Figure 18: Variation of crack area of liners with BD having 10mm thickness with time for multiple cycles

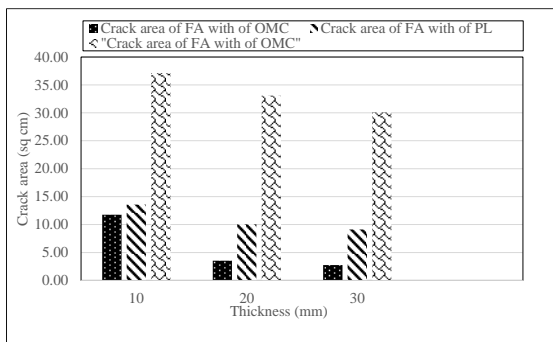


Figure 19: Variation of crack area with moisture content for thickness of liners with FA.

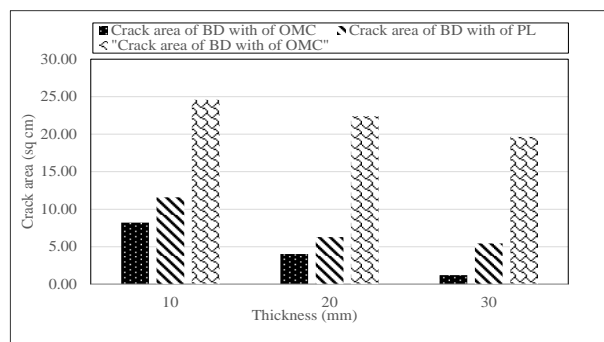


Figure 20: Variation of crack area with moisture content for thickness of liners with BD.

3.4.1 Variation of Crack area with Time and Admixture Content

Figure 17 and 18 clarify the variation of crack area of liners with FA and BD having 10mm thickness with time for dry and wet cycles respectively. After end of first dry cycle with constant crack area at 168hrs for both liners with FA and BD, the amount of water was applied to start a wet cycle. In this wet cycle, the developed cracks became zero and for both liners with FA and BD. Moreover, when the second dry cycle started, crack area increases rapidly in first three days then increases slowly and constant after four days (96hrs.) for both liners with FA and BD. Cracks area reduces with increase in admixture content for a fixed moisture content and specimen thickness. Result reveals that crack area decreases with the increasing of FA and BD content. In addition, control soil showed comparatively higher crack area than that of composite liners prepared with FA and BD at varying mixing proportions. The reason behind this phenomenon, crack area depends on the cohesion/adhesion behavior of soil, as liners prepared with admixture FA and BD, therefore liners showed lower crack area.

3.4.2. Variation of Cracks Area with Moisture Content and Specimen Thickness

Figure 19 and Figure 20 clarify the variation of cracks area with FA and BD at varying water content equals to OMC, PL and LL for all specimen thicknesses for 20% FA and BD respectively. Crack is form in liners which is increase with moisture content but decrease with thickness. FA and BD have very low capacity to swell and shrink. However, after adding FA or BD, cracks were decrease with increase of FA or BD content. The values of crack area increase with the increase of moisture content. Large amount of water can retain which means low soil particle at liners. As a result, it forms more crack with increasing of moisture content.

4. CONCLUSIONS

This study mainly focus on some relevant factors that affect the behavior of composite liners subjected to drying and wetting. From results it is clear that maximum values of CIF, CDF and crack area were found in control soil. In addition, the minimum values of CIF, CDF and crack area were found at mixing FA content of 60% and brick dust of 40% in soils. All the studied geometrical parameters decrease with increase of liner thickness except CDF. The value of CDF increases with increase of specimen thickness. Maximum and minimum CDF were found in 30mm and 10mm specimen thickness respectively. The maximum and minimum values CIF, CDF and crack area were found at moisture content equals to LL and OMC, respectively. In addition, the values of geometrical parameter increases in relation to the increasing of moisture content i.e. the liners with LL showed comparatively the higher values of cracking parameters than that of other counter parts. The cracks were found comparatively wider and longer in fly ash than that of liners with brick dust. In the test with multiple wet-dry cycles, the amount of cracking parameters did not change significantly after second cycle. Result reveals cracking was affected by fines content of the soils. High amount of cracking parameters were observed in soil with high fine content (20% FA) and less was observed in soil with low fines content (20% BD).

REFERENCES

- Al-Wahab, R.M. and El-Kedrah, M.H. 1995. Using fibers to reduce tension cracks and shrink/swell in compacted clay. *Geoenvironment 2000*. Geot. Special Publication No. 46, ASCE, 791-805.
- Protection Agency, 2000.
- Corte, A. and Higashi, A. 1960. Experimental research on desiccation cracks in soil. U.S. Army Snow Ice and Permafrost Research Establishment, Wilmetre, Ill. Research Report 66.
- Gonzalez, R.C. and Woods, R.E. 2002. *Digital Image Processing Second Edition*. Publishing House of Electronics Industry, Beijing.
- Kleppe, J.H. and Olson, R.E. 1985. Desiccation cracking of soil barriers. In: Johnson, A.I., Frobels, R.K., Cavalli, N.J., Petersson, C.B. (Eds.), *Hydraulic Barriers in Soil and Rock*, ASTM STP 874. ASTM, West Conshohocken, pp.263-275.
- Morris, P.H., Graham, J. and Williams, D.J. 1992. Cracking in drying soils. *Canadian Geotechnical Journal* 29 (2), 263–277. DOI:10.1139/t92-030.
- Omidi, G.H., Prasad, T.V., Thomas, J.C. and Brown, K.W. 1996. The influence of amendments on the volumetric shrinkage and integrity of compacted clay soils used in landfill liners. *Water, Air, Soil Pollution*, 86(1-4), 263-274.
- Rafizul, I.M 2014. Evaluation of contamination potential and treatment techniques of leachate generated from landfill lysimeter. PHD thesis, Department of Civil Engineering, Khulna University of Engineering & Technology, Khulna, Bangladesh.
- Tang, C., Shi, B., Liu, C., Zhao L. and Wang, B. 2008. Influencing factors of geometrical structure of surface shrinkage cracks in clayey soil. *Eng. Geology*, 101(3-4): 204-217.
- Tiwari, A. 2015. Quantification of crack and shrinkage using image analysis. M.Sc. Thesis, Department of Civil Engineering, National Institute of Technology, Rourkela, India.
- Yesiller, N., Miller, C.J., Inci, G. and Yaldo, K 2000. Dessication and cracking behavior of three compacted landfill liner soils. *Eng. Geology* 57(2000) 105-121.

SEISMIC STABILITY OF SLOPES IN LAYERED COHESIVE SOILS

A. Hossain¹, M. A. A. Sadman*² and M. M. Rashid³

¹*Assistant Professor, Rajshahi University of Engineering & Technology, Bangladesh, e-mail: ahmedhossain090001@gmail.com*

²*Student, Rajshahi University of Engineering & Technology, Bangladesh, e-mail: abdesakib12@gmail.com.com*

³*Student, Rajshahi University of Engineering & Technology, Bangladesh, e-mail: mdsaad96@gmail.com*

***Corresponding Author**

ABSTRACT

Earthquake is one of the major causes of slope failure throughout the world. It is pretty rare to find soil slope which has similar property throughout its whole formation. Significance attention ought to be given to layered slope dependability, in light of the fact that the real soil slope is regularly complex with an organization of multilayer soils because of natural arrangement or sometimes artificial filling. These slopes, when exposed to forces of an earthquake, leads to catastrophic events. Bangladesh is situated in the world's one of the most active earthquake zones and has often been exposed to the various magnitude of earthquakes over the years which sometimes led to catastrophes. Recent events have made it ever so important that a proper analysis must be done in order to avoid countless losses of lives, livestock, structures and other resources. However, cohesion (c) a shear strength parameter of soil can contribute to achieving a greater factor of safety.

The goal of this study is to analyze the relationship between cohesion of soil and the factor of security of a clay layered slope model under various combinations of horizontal and vertical seismic coefficients. This was done by assuming a standard slope model with two layers. Two cases were considered. In the first case, the cohesion value of the bottom layer was fixed and the value of cohesion of the other layer was varied. The second case was vice-versa. Then various combinations of earthquake force were applied on the slope model. All the other properties such as unit weight angle of friction etc. were kept constant for all cases. The effect of greater cohesion values on the top or bottom layer is also assessed. Suitability of greater cohesion value on either top or bottom layer was also assessed on the basis of the factor of safety for different combinations and conditions. From the study, two major decision was made for the particular layered slope model. It was observed that the factor of safety decreases with the increase in seismic coefficients and increases with the increase in cohesion value for all ratios of horizontal and vertical seismic coefficients. The second decision was that when the greater value of cohesion is placed at the top layer of the slope the factor of safety is substantially larger than the factor of safety which is achieved when the larger value of cohesion is placed at the bottom. This decision was made by observing the maximum and minimum factor of safety of the slope considering all ratios, all horizontal seismic coefficient values and all cohesion values.

It was observed that when greater cohesion placed and fixed at top layer maximum factor of safety that is achievable rose up to as high as 1.43 and a minimum factor of safety was 0.79 considering all of the bottom the layer the maximum factor of safety only got to rise as high 1.37 as and minimum factor of safety in was only 0.61. The LEM module of GEO5 software (2019 version) was used for this study.

Keywords: *Earthquake, Slope, Layer, LEM, GEO5.*

1. INTRODUCTION

Bangladesh is in a delta formed by three major rivers which are Brahmaputra, Ganges, and Meghna. The system drains a basin of some 1.76 million sq km and carries not only snowmelt water from the Himalayas but also runoff water from some of the highest rainfall areas of the world. During the last thousand years, the silt conveyed by the tremendous releases of these streams has assembled an expansive delta, framing the greater part of the huge zone of Bangladesh and the submerged delta-plain. These enormous residues are the significant wellsprings of the arrangement of 80% soils of the nation. (Brammer H., 1996) Soil slope related calamities cause loss of lives, livestock, buildings, structures overall contributing to massive tragedy in a country's economy. In Bangladesh, disasters such as landslide in the hilly areas of the country are mostly triggered by slope failure. So in a sense, the slope failure directly contributes to the massive loss of infrastructure, food insecurity, scarcity of safe drinking water, environmental challenges, poverty and livelihoods, environmental catastrophe etc. River embankment and bank failures also lead to the destruction of massive investments. Bangladesh is located in one of the most active seismic zones has always been a victim of slope related failure especially in CHT tracts. On 11 June 2007, heavy monsoon rain triggered a series of landslides and floods in Rangamati, Chittagong and Bandarban - three hilly districts of Bangladesh and killed at least 107 people. (Sarker & Rashid, 2013) On June 12, 2018, another 11 people died due to Landslide failure in Chattogram. Recent incidents of slope related failures such as landslides due to an earthquake in Sunamganj and Sylhet (2009), Chittagong (2017), Rangamati (2003) claimed numerous lives and added distresses to even more people. (Daily Star, n.d.). In this study, the factor of safety was evaluated for a fixed slope model having two layers. In the first stage, a fixed value of cohesion was kept in the bottom layer of slope and increasing the value of cohesion in the top layer of the slope. For each case, an earthquake is applied in the form of a seismic coefficient and the factor of safety is measured. Then the cohesion value of the top layer of the slope model is kept fixed and the same process is repeated. The pattern of factor safety was observed for a fixed bottom layer cohesion and fixed top layer cohesion under increasing seismic coefficient for various ratios of the horizontal seismic coefficient to the vertical seismic coefficient. The study was conducted by using the "Slope Stability" module of the GEO5 (2019) software.

2. METHODOLOGY

The basic of LEM is to assume a failure surface of a slope and then analyse that. This factor of safety is calculated by dividing the shear strength of the soil by the stresses working on that particular section.

2.1 Literature Review

Fellenius introduced this method with an ordinary slip circle(Fellenius, 1936). After that Bishop developed the method by considering the inter-slice normal force in the equation which then became non-linear(Bishop & Morgenstern, 1960). Janbu further developed the formula(Janbu, 1954) for all shapes of failure. Morgenstern-Price, Spencer, and others then took the method to another level by considering other factors and criteria of equilibrium condition.(Morgenstern & Price, 1965; Spencer, 1967). Fellenius introduced this method with an ordinary slip circle(Fellenius, 1936). After that Bishop developed the method by considering the inter-slice normal force in the equation which then became non-linear(Bishop & Morgenstern, 1960). Janbu further developed the formula(Janbu, 1954) for all shapes of failure. Morgenstern-Price, Spencer and others developed it considering other factors and criteria of equilibrium condition.(Morgenstern & Price, 1965; Spencer, 1967).

2.2 Horizontal and Vertical Seismic Coefficients

Horizontal and vertical earthquake force is defined by the following equations:

$$F_h = \frac{a_h * W}{g} = K_h * W \quad (1)$$

$$F_v = \frac{a_v * W}{g} = K_v * W \quad (2)$$

Here, a_h and a_v are, respectively, horizontal and vertical pseudo-static accelerations, g is the gravitational acceleration constant, and W is the slice weight. The acceleration ratio is given as a/g which is a dimensionless coefficient. The inertia effect is specified as K_h and K_v , the coefficients of acceleration in horizontal and vertical directions, respectively. The recommendations for choosing an earthquake coefficient value is given below. (Melo & Sharma, 2004)

Table 1. Recommended Horizontal Seismic Coefficients (Summarized by Cristiano Melo & Sunil Sharma)

Horizontal Seismic Coefficient, K_h	Description	
0.05 - 0.15	In the United States	
0.12 - 0.25	In Japan	
0.1	Severe earthquakes	Terzaghi
0.2	Violent destructive earthquakes	
0.5	Catastrophic earthquakes	
0.1	Major Earthquake, FOS > 1.0	Corps of Engineers
0.15	Great Earthquake, FOS > 1.0	

2.3 Geometry of Numerical Model

In all dimensions, the SI unit was adopted. The lateral width of the model slope was fixed by taking minimum X-axis distance as 0 and maximum X-axis distance as 30 meters. Also, the depth of the model below the deepest interface point was set to 5.0 meters. After fixing up the ranges, the slope was plotted textually by the following co-ordinates shown in the following table 2.

Table 2: Co-ordinates of Model Slope

	Step 1				Step 2		
x(meter)	0	6	18	30	x(meter)	6	0
z(meter)	0	0	12	12	z(meter)	30	0

The following figure 1 shows the geometrical model of the slope used.

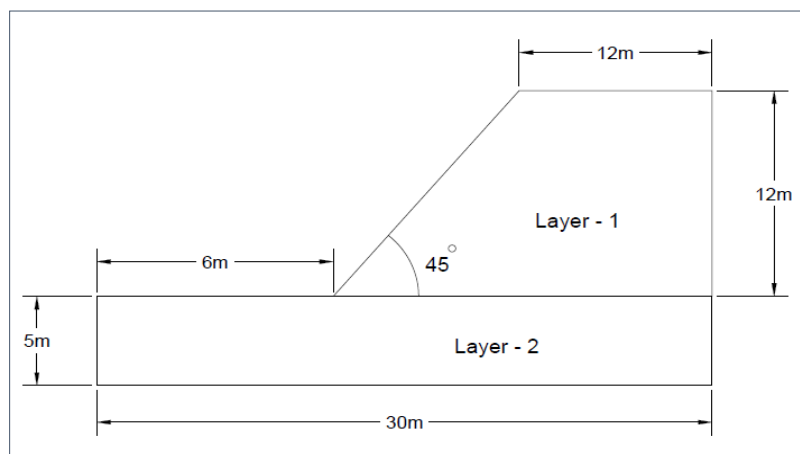


Figure 1: Geometry of Layered Slope Model

In the case of soil, by considering two layers of different soil cohesion, the work is done. The classification type of soil was set to Standard. CL, CI – Clay with medium or low plasticity was adopted for the study where the consistency of the soil was stiff consistency and degree of saturation, $S_r < 0.8$ (Easy to penetrate by a nail). Stress state was considered effective without the effect of soil foliation.

The mode of uplift pressure was considered standard. The properties of Soil used for this study are given in table 3.

Table 3: Properties of Soil used for this study

Properties	Values
Unit weight, γ (kN/m ³)	21.00
The angle of internal friction, ϕ_{ef} (°)	19.00
Saturated unit weight, γ_{sat} (kN/m ³)	21.00

The analysis was done by five methods. Bishop, Fellenius, Spencer, Janbu and Morgenstern by considering fixed cohesion value in one (top/bottom) layer and gradually increasing cohesion value in another layer. Earthquake force was applied as horizontal and vertical seismic coefficients and four ratios of K_v/K_h were considered (0.25, 0.5, 0.75 and 1.0). For horizontal seismic coefficient 4 values were considered (0.1, 0.2, 0.3 and 0.4).

At first bottom layer's cohesion is taken as fixed and the top layer's cohesion is changed randomly. After this, top layers cohesion is taken as fixed and the bottom layer's cohesion is changed randomly. Table 4 shows the cohesion values for the layered slope model.

Table 4: Cohesion values for the layered model

When cohesion for the bottom is fixed		When cohesion for the top is fixed	
Bottom Layer's Cohesion, kPa	Top Layer Cohesion, kPa	Top Layer's Cohesion, kPa	Bottom Layer's Cohesion, kPa
40	20	40	20
40	25	40	25
40	30	40	30
40	35	40	35

3. RESULTS & DISCUSSION

3.1 Relationship between Factor of Safety and Seismic Coefficients for all Cohesion Values

The analysis results for homogeneous layered clay slope model are shown in the following four tables i.e. table 6, table 7, table 8, and table 9. In the first part, the results are shown when the cohesion value of the bottom layer is fixed at 40 kPa. In the other part of the table, the results are shown when the cohesion value of the top layer is fixed at 40kPa. In both cases the cohesion value of other layer is varied. In the other layer at first, the cohesion value is put as 20 kPa. Then the cohesion value was gradually increased by 5 kPa. The value of K_h for all ratios of K_v/K_h is varied as 0.1 to 0.4. In all the tables C_1 represents bottom layer cohesion and C_2 represents top layer cohesion. The following tables show the variation of a factor of safety for layered clay slope model when the fixed value of cohesion is 40 kPa and the value of cohesion of other layers is varied from 20 KPa to 35 KPa.

Table 5: Factor of safety for all values of K_v/K_h for variable $C = 20\text{kPa}$

For $C_1=40\text{ kPa}$ and $C_2=20\text{ kPa}$						For $C_1=20\text{ kPa}$ and $C_2=40\text{ kPa}$					
K_v/K_h	K_h	0.1	0.2	0.3	0.4	K_v/K_h	K_h	0.1	0.2	0.3	0.4
0.25	Bishop	0.96	0.84	0.73	0.64	0.25	Bishop	1.30	1.13	0.98	0.85
	Fellenius	0.93	0.81	0.70	0.61		Fellenius	1.25	1.07	0.93	0.80
	Spencer	0.96	0.84	0.78	0.71		Spencer	1.32	1.14	1.03	0.91
	Janbu	0.96	0.84	0.79	0.71		Janbu	1.31	1.14	1.03	0.90
	Morgenstern	0.97	0.85	0.79	0.72		Morgenstern	1.33	1.15	1.00	0.90
0.5	Bishop	0.97	0.85	0.74	0.64	0.5	Bishop	1.31	1.14	0.98	0.85
	Fellenius	0.93	0.82	0.71	0.61		Fellenius	1.26	1.09	0.93	0.80
	Spencer	0.97	0.85	0.80	0.71		Spencer	1.33	1.16	1.08	0.92
	Janbu	0.97	0.85	0.85	0.77		Janbu	1.32	1.15	1.01	0.93
	Morgenstern	0.98	0.87	0.84	0.77		Morgenstern	1.34	1.16	1.01	0.93
0.75	Bishop	0.98	0.86	0.74	0.63	0.75	Bishop	1.32	1.15	0.99	0.84
	Fellenius	0.94	0.83	0.72	0.61		Fellenius	1.27	1.10	0.94	0.80
	Spencer	0.98	0.86	0.81	0.72		Spencer	1.34	1.17	1.01	0.91
	Janbu	0.98	0.87	0.84	0.79		Janbu	1.32	1.16	1.02	0.91
	Morgenstern	0.99	0.88	0.86	0.78		Morgenstern	1.35	1.18	1.02	0.95
1	Bishop	0.99	0.87	0.75	0.62	1	Bishop	1.34	1.17	0.99	0.84
	Fellenius	0.95	0.84	0.72	0.60		Fellenius	1.28	1.11	0.94	0.79
	Spencer	0.99	0.87	0.82	0.73		Spencer	1.36	1.18	1.04	0.92
	Janbu	0.99	0.88	0.87	0.79		Janbu	1.35	1.18	1.05	0.95
	Morgenstern	1.00	0.90	0.87	0.79		Morgenstern	1.37	1.19	1.05	0.95

Table 6: Factor of safety for all values of K_v/K_h for variable $C = 25\text{kPa}$

For $C_1=40\text{ kPa}$ and $C_2=25\text{ kPa}$						For $C_1=25\text{ kPa}$ and $C_2=40\text{ kPa}$					
K_v/K_h	K_h	0.1	0.2	0.3	0.4	K_v/K_h	K_h	0.1	0.2	0.3	0.4
0.25	Bishop	1.08	0.94	0.83	0.72	0.25	Bishop	1.36	1.18	1.03	0.90
	Fellenius	1.05	0.91	0.8	0.70		Fellenius	1.31	1.13	0.97	0.84
	Spencer	1.08	0.94	0.87	0.79		Spencer	1.37	1.19	1.05	0.95
	Janbu	1.08	0.95	0.89	0.84		Janbu	1.37	1.19	1.05	0.96
	Morgenstern	1.09	0.95	0.92	0.84		Morgenstern	1.39	1.2	1.07	0.94
0.5	Bishop	1.09	0.96	0.83	0.72	0.5	Bishop	1.37	1.2	1.04	0.90
	Fellenius	1.06	0.93	0.81	0.70		Fellenius	1.32	1.14	0.98	0.84
	Spencer	1.09	0.96	0.89	0.80		Spencer	1.38	1.21	1.07	0.98
	Janbu	1.09	0.98	0.89	0.86		Janbu	1.37	1.21	1.07	0.98
	Morgenstern	1.10	0.98	0.89	0.86		Morgenstern	1.40	1.22	1.07	0.98
0.75	Bishop	1.10	0.97	0.84	0.72	0.75	Bishop	1.39	1.21	1.04	0.90
	Fellenius	1.07	0.94	0.82	0.69		Fellenius	1.33	1.15	0.99	0.85
	Spencer	1.10	0.97	0.91	0.82		Spencer	1.40	1.23	1.12	0.98
	Janbu	1.10	0.99	0.97	0.87		Janbu	1.40	1.23	1.12	0.99
	Morgenstern	1.11	0.99	0.93	0.86		Morgenstern	1.42	1.23	1.08	0.99
1	Bishop	1.11	0.99	0.85	0.71	1	Bishop	1.40	1.23	1.05	0.90
	Fellenius	1.08	0.96	0.82	0.69		Fellenius	1.34	1.17	1.00	0.85
	Spencer	1.12	0.99	0.93	0.83		Spencer	1.41	1.24	1.21	1.01
	Janbu	1.11	1.01	0.99	0.90		Janbu	1.41	1.24	1.08	1.02
	Morgenstern	1.13	1.01	0.99	0.90		Morgenstern	1.43	1.25	1.08	1.02

Table 7: Factor of safety for all values of K_v/K_h for variable $C = 30$ kPa

For $C_1=40$ kPa and $C_2=30$ kPa						For $C_1=30$ kPa and $C_2=40$ kPa					
K_v/K_h	K_h	0.1	0.2	0.3	0.4	K_v/K_h	K_h	0.1	0.2	0.3	0.4
0.25	Bishop	1.20	1.05	0.91	0.80	0.25	Bishop	1.39	1.21	1.06	0.92
	Fellenius	1.16	1.02	0.89	0.77		Fellenius	1.35	1.18	1.02	0.88
	Spencer	1.20	1.05	0.96	0.88		Spencer	1.40	1.22	1.08	0.99
	Janbu	1.20	1.05	0.96	0.93		Janbu	1.40	1.22	1.09	1.01
	Morgenstern	1.21	1.06	0.97	0.93		Morgenstern	1.39	1.20	1.07	0.94
0.50	Bishop	1.21	1.06	0.93	0.80	0.5	Bishop	1.40	1.23	1.07	0.93
	Fellenius	1.18	1.03	0.90	0.78		Fellenius	1.36	1.19	1.03	0.89
	Spencer	1.21	1.06	0.99	0.89		Spencer	1.41	1.24	1.10	1.01
	Janbu	1.21	1.08	1.04	0.95		Janbu	1.41	1.24	1.10	1.03
	Morgenstern	1.22	1.08	0.99	0.95		Morgenstern	1.42	1.26	1.12	1.00
0.75	Bishop	1.22	1.08	0.94	0.80	0.75	Bishop	1.41	1.25	1.08	0.93
	Fellenius	1.19	1.05	0.91	0.78		Fellenius	1.38	1.21	1.04	0.89
	Spencer	1.22	1.08	1.02	0.91		Spencer	1.42	1.26	1.12	1.06
	Janbu	1.22	1.10	1.07	0.95		Janbu	1.42	1.27	1.12	1.01
	Morgenstern	1.23	1.10	1.07	0.97		Morgenstern	1.44	1.28	1.13	1.01
1	Bishop	1.24	1.10	0.95	0.80	1	Bishop	1.43	1.27	1.09	0.93
	Fellenius	1.20	1.07	0.92	0.78		Fellenius	1.40	1.23	1.05	0.90
	Spencer	1.24	1.10	1.04	0.95		Spencer	1.44	1.29	1.16	1.05
	Janbu	1.24	1.13	1.07	1.00		Janbu	1.44	1.29	1.25	1.06
	Morgenstern	1.25	1.12	1.06	1.00		Morgenstern	1.46	1.30	1.15	1.06

Table 8: Factor of safety for all values of K_v/K_h for variable $C = 35$ kPa

For $C_1=40$ kPa and $C_2=35$ kPa						For $C_1=35$ kPa and $C_2=40$ kPa					
K_v/K_h	K_h	0.1	0.2	0.3	0.4	K_v/K_h	K_h	0.1	0.2	0.3	0.4
0.25	Bishop	1.31	1.15	1.00	0.87	0.25	Bishop	1.41	1.23	1.08	0.94
	Fellenius	1.28	1.12	0.97	0.85		Fellenius	1.37	1.20	1.04	0.91
	Spencer	1.32	1.15	1.05	0.96		Spencer	1.42	1.24	1.11	1.00
	Janbu	1.31	1.15	1.06	0.98		Janbu	1.42	1.23	1.12	1.02
	Morgenstern	1.33	1.16	1.06	1.00		Morgenstern	1.43	1.25	1.13	1.05
0.5	Bishop	1.32	1.17	1.01	0.88	0.5	Bishop	1.43	1.25	1.09	0.95
	Fellenius	1.29	1.14	0.99	0.86		Fellenius	1.39	1.22	1.06	0.92
	Spencer	1.33	1.17	1.08	0.99		Spencer	1.43	1.26	1.14	1.02
	Janbu	1.33	1.19	1.09	1.01		Janbu	1.43	1.26	1.14	1.05
	Morgenstern	1.34	1.18	1.10	1.02		Morgenstern	1.44	1.27	1.16	1.04
0.75	Bishop	1.34	1.19	1.03	0.89	0.75	Bishop	1.44	1.28	1.10	0.95
	Fellenius	1.31	1.16	1.01	0.86		Fellenius	1.40	1.24	1.08	0.93
	Spencer	1.34	1.19	1.12	1.00		Spencer	1.45	1.28	1.16	1.07
	Janbu	1.34	1.21	1.15	1.02		Janbu	1.44	1.29	1.16	1.06
	Morgenstern	1.34	1.21	1.16	1.05		Morgenstern	1.46	1.31	1.19	1.06
1	Bishop	1.36	1.21	1.04	0.89	1	Bishop	1.46	1.3	1.12	0.96
	Fellenius	1.33	1.18	1.02	0.87		Fellenius	1.42	1.27	1.09	0.94
	Spencer	1.36	1.22	1.14	1.03		Spencer	1.47	1.31	1.18	1.12
	Janbu	1.36	1.24	1.17	1.13		Janbu	1.47	1.31	1.20	1.12
	Morgenstern	1.37	1.23	1.18	1.06		Morgenstern	1.48	1.33	1.21	1.12

From tables, it is visible that,

- The factor of safety decreases with the increase in the horizontal seismic coefficient for both cases for all ratios.
- The factor of safety increases when the cohesion value of the other layer is gradually increased for both cases for all ratios.

3.2 Relationship between Cohesion and Factor of Safety for All Ratios of Seismic Coefficients

The relation between cohesion and factor of safety is shown in figure 2 to figure 9. Worst cases were considered for each ratio i.e. considered the value of horizontal seismic coefficient as 0.4 for all the cohesion values of the variable layer. Following figure 2, figure 3, figure 4, and figure 5 show the relationship between the factor of safety and cohesion for all ratios of K_v/K_h when cohesion 40 kPa is fixed at the bottom layer.

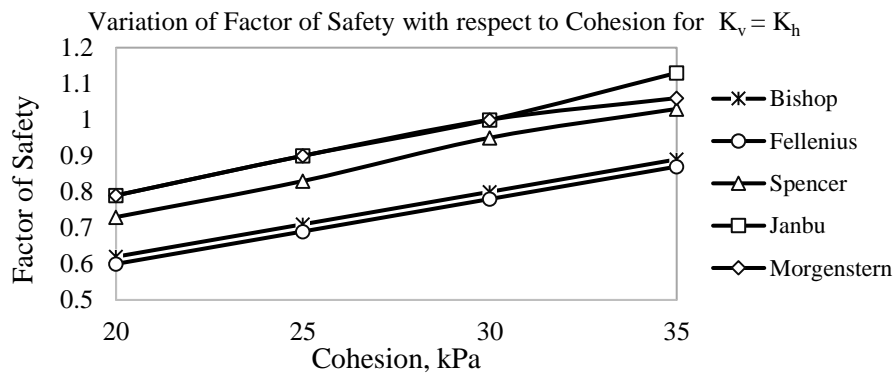


Figure 2: Variation of Factor of Safety with respect to Cohesion for $K_v = K_h$

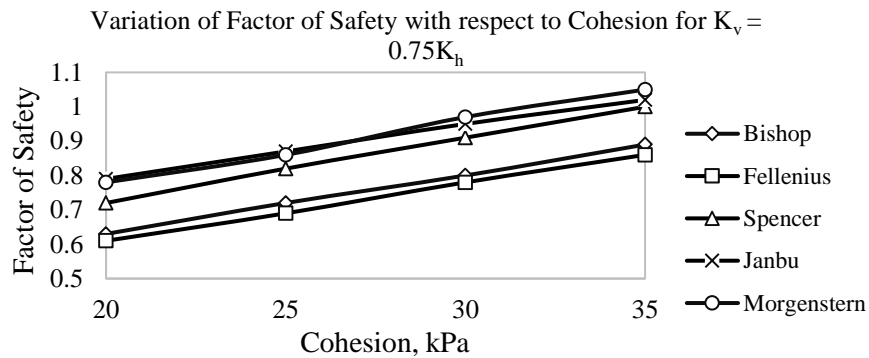


Figure 3: Variation of Factor of Safety with respect to Cohesion for $K_v = 0.75K_h$

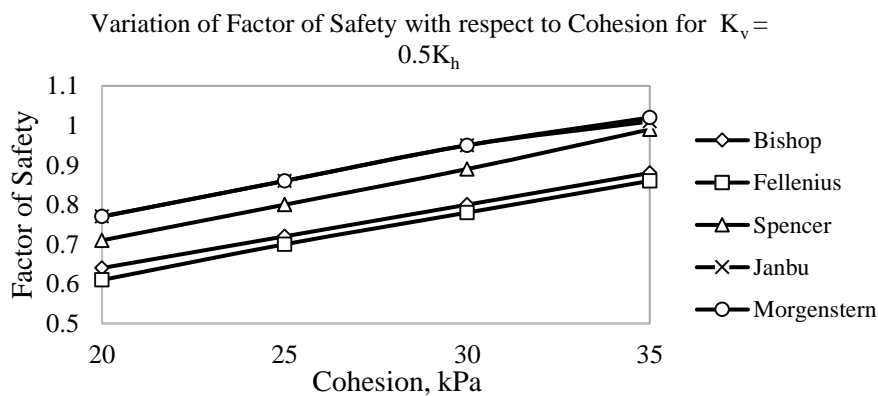


Figure 4: Variation of Factor of Safety with respect to Cohesion for $K_v = 0.5K_h$

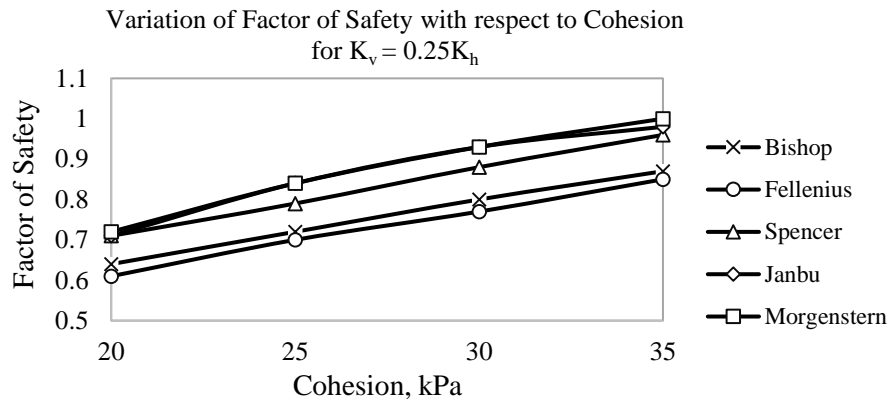


Figure 5: Variation of Factor of Safety with respect to Cohesion for $K_v = 0.25K_h$

Following figure 5, figure 6, figure 7, and figure 8 shows the relation between the factor of safety and cohesion for all ratios of K_v/K_h when cohesion 40 kPa is fixed at the top layer and bottom layer cohesion is varied from 20 kPa to 35 kPa.

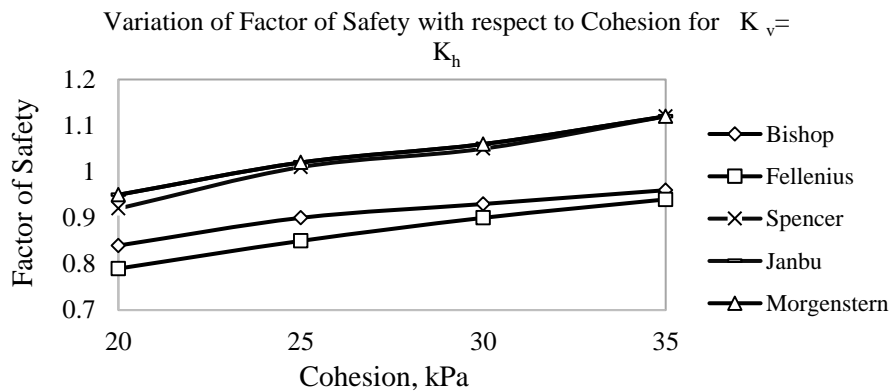


Figure 6: Variation of Factor of Safety with respect to Cohesion for $K_v = K_h$

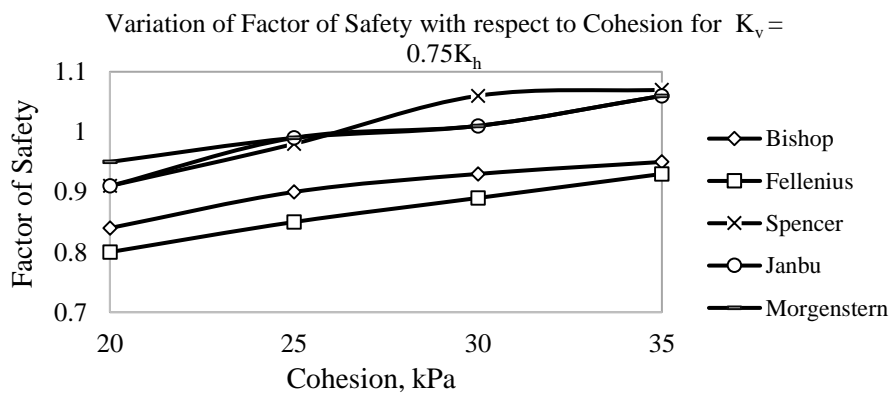


Figure 7: Variation of Factor of Safety with respect to Cohesion for $K_v = 0.75 K_h$

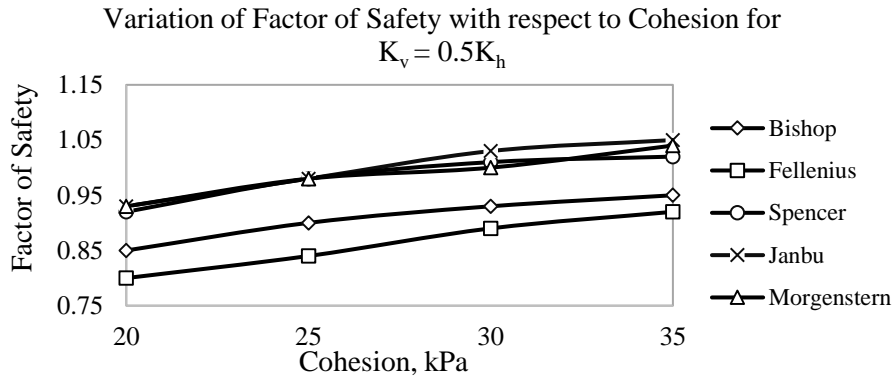


Figure 8: Variation of Factor of Safety with respect to Cohesion for $K_v = 0.5K_h$

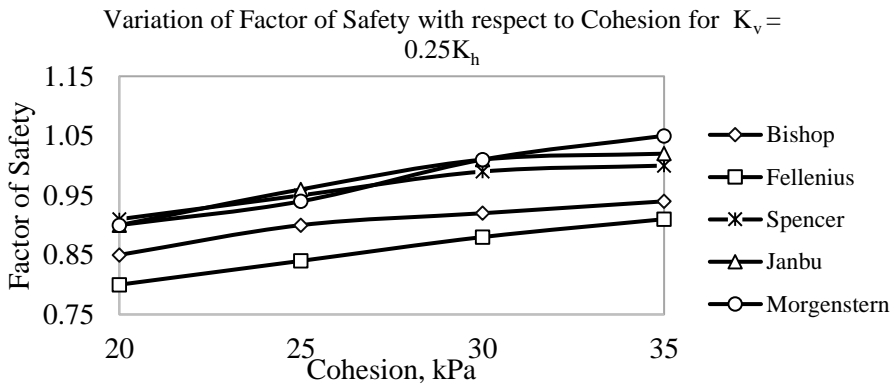


Figure 9: Variation of Factor of Safety with respect to Cohesion for $K_v = 0.25 K_h$

3.3 Comparison between Two Cases

Following table 10 shows the maximum and minimum factor of safety for the layered slope model. Note that, $C_{x,y}$ is used where x denotes top layer cohesion and y denotes bottom layer cohesion.

Table 10: Comparison between two cases of the layered slope model

Combination, $C_{x,y}$	Minimum FS when bottom layer cohesion is fixed at 40 kPa	Maximum FS when bottom layer cohesion is fixed at 40 kPa	Combination, $C_{x,y}$	Minimum FS when top layer cohesion is fixed at 40 kPa	Maximum FS when top layer cohesion is fixed at 40 kPa
$C_{20,40}$	0.61	1.00	$C_{40,20}$	0.79	1.37
$C_{25,40}$	0.69	1.13	$C_{40,25}$	0.84	1.43
$C_{30,40}$	0.77	1.25	$C_{40,30}$	0.88	1.46
$C_{35,40}$	0.85	1.37	$C_{40,35}$	1.00	1.48

It can be observed from table 10 that when 40 kPa is fixed at the top layer of the model, a greater factor of safety is achieved. This becomes even more evident from the following figure 10.

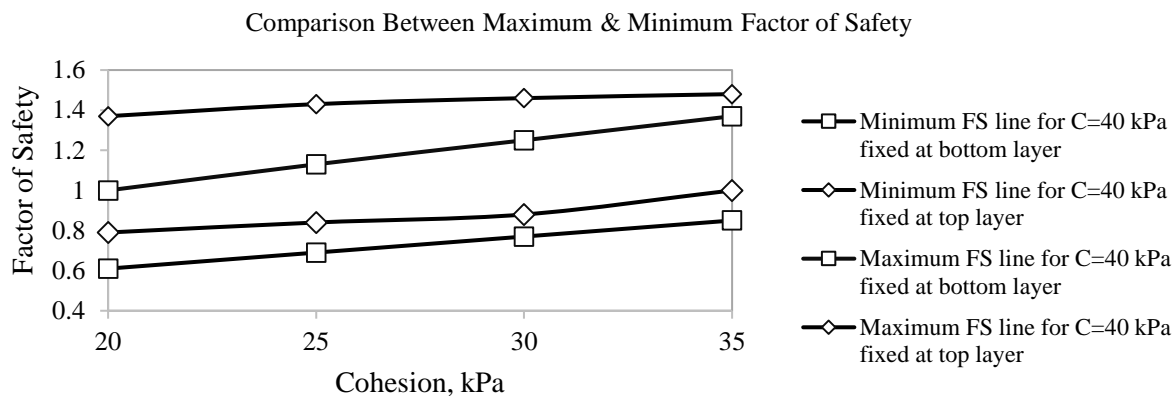


Figure 10: Comparison Between Two Cases for Minimum & Maximum FS

4. CONCLUSIONS

From the analysis in Results and Discussion, those following decisions can be made,

- For both cases, the factor of safety decreases with the increase in the horizontal seismic coefficient.
- For both cases, the factor of safety increases with the increase in cohesion value.
- The factor of safety is greater when the top layer cohesion value is fixed at 40 kPa and the bottom layer is varied than when the bottom layer cohesion value fixed at 40 kPa and top layer cohesion value is varied.

ACKNOWLEDGEMENTS

The authors would like to take the opportunity to recognize and thank the respected teachers of the Department of Civil Engineering of Rajshahi University of Engineering & Technology. The authors would also like to thank their respective parents and well-wishers for their support.

REFERENCES

- Bishop, A. W., & Morgenstern, N. (1960). Stability coefficients for earth slopes. *Geotechnique*. <https://doi.org/10.1680/geot.1960.10.4.129>
- Brammer H. (1996). *The Geography of the Soils of Bangladesh*.
- Bangladesh Landslide.(n.d.). Retrieved from <https://www.thedailystar.net/tags/bangladesh-landslide>
- Fellenius, W. (1936). Calculation of the stability of earth dams. *Proc. of the 2nd Congress on Large Dams, Washington, D.C., 4, U.S. Government Printing Office, 4*.
- Janbu, N. (1954). Application of composite slip surface for stability analysis. *Proceedings of European Conference on Stability of Earth Slopes, Stockholm*.
- Melo, C., & Sharma, S. (2004). Seismic Coefficients for Pseudostatic Slope Analysis. *13th World Conference on Earthquake Engineering*.
- Morgenstern, N. R., & Price, V. E. (1965). The analysis of the stability of general slip surfaces. *Geotechnique*. <https://doi.org/10.1680/geot.1965.15.1.79>
- Sarker, A. A., & Rashid, A. K. M. M. (2013). *Landslide and Flashflood in Bangladesh*. https://doi.org/10.1007/978-4-431-54252-0_8
- Spencer, E. (1967). A method of analysis of the stability of embankments assuming parallel inter-slice forces. *Geotechnique*. <https://doi.org/10.1680/geot.1967.17.1.11>

EFFECT OF SALINITY ON STRENGTH AND DEFORMATION PROPERTIES OF CEMENTED SAND AT DIFFERENT EXPOSURE CONDITIONS

Dipankar Chandra Barman*¹ and Md. Kamrul Ahsan²

¹*Undergraduate Student, Department of Civil Engineering, Khulna University of Engineering & Technology, Khulna-9203, Bangladesh, e-mail: dipankarce.15@gmail.com*

²*Assistant Professor, Department of Civil Engineering, Khulna University of Engineering & Technology, Khulna-9203, Bangladesh, e-mail: kamrulahsan@ce.kuet.ac.bd*

***Corresponding Author**

ABSTRACT

Cemented sand and gravel (CGS) is widely used in many constructions such as dam, levee, retaining wall etc. Moreover, it has wide application in ground improvement to increase engineering properties of soil such as bearing capacity, shear strength, stability etc. In general, low cement ratio is commonly adopted in weakly cemented sand. But, the mechanical properties can largely be affected by the repetitive wetting and drying condition due to water table fluctuation for seasonal weather condition, flood or heavy rain due to its high permeability. The situation may get exacerbated in saline or coastal zone as salinity has the potential to affect the strength of cemented sand. In this study, unconfined compressive strength of weakly cemented sand at different exposure cycle (i.e., 7 days drying and 7 days wetting condition) with two different concentration of salinity (i.e., 0.1 M and 1M) was evaluated. Cemented sand specimen were compacted at optimum water content and initially cured for 28 days (i.e., 3 days air curing and 25 days under water curing with tap water). After 28 days curing of the specimen, the unconfined compressive strength was evaluated to establish the reference condition. Then the samples were tested at different exposure interval at two different saline concentration and compared with the initial condition. Although, the unconfined compressive strength showed fluctuations at early stages but continued to decrease at higher cycles followed by an increase in moisture content which represent the negative impact of salinity intrusion on the peak strength properties of weakly cemented sand.

Keywords: *Cemented sand, Curing, Unconfined compressive strength, Salinity, Exposure condition.*

1. INTRODUCTION

Increase of soil strength by ground improvement has become important in civil engineering constructions due to non-availability of favorable sub-soil conditions. Nowadays, cemented sand is widely accepted as a ground improve technique for works relating to slope stability, embankment, dam and etc. Cemented sand and gravel (CSG) dam was originated in the 1970s, is a new style of dam and used for hydroelectric development of china (Xin et al., 2012). CSG reduced the dam section and works as a softening material which is an important property of engineering and has low energy consumption (De Gao et al., 2011). In Japan, CSG is extensively used for cofferdam, large dam, levees and its use is gradually increasing due to economic construction (Kim et al., 2005). However, cemented sand can be influenced by the curing condition, moisture condition as well as salinity (park, 2010). When cemented sand was mixed and cured with distilled water, the value of unconfined compressive strength is higher compared to the case when cured with sea water (Park and Lee, 2012). Particularly, when cement ratio in cemented sand is less than 10 percent, the strength of cemented sand drops 30% at immediate wetting condition after air dry curing (Park et al., 2009). In addition, during the heavy rain or flood, the strength of cemented sand may get affected.

The groundwater table may rise and subside due to the seasonal effect and other reasons. When groundwater table escalates and comes in contact with cemented sand, the cemented sand gets soaked. Again, when the groundwater table drops, the cemented sand experiences dry condition. The process of repetitive drying and wetting condition has the potential to affect the properties of cemented sand and the effect may get exacerbated if salinity is present in ground water. In 1973, 2000, 2009 soil salinity affected areas were 120040, 145250, 147960 ha respectively in Khulna region (Ahsan, 2010). The maximum value of Na^+ in groundwater is 1212.61mg/l at 54 m depth and minimum value is 13.18 mg/l at 21 m depth and average value is 647.20 mg/l which is 77% of the total cation. Again, Maximum, minimum and average value of Cl^- are 6270 mg/l at 54 m depth, 32.07 mg/l at 21 m depth and 1776.74 mg/l respectively which is 77.6% of total anion in Khulna region (Mohammad et.al, 2017). Salinity in groundwater is increasing day by day. If cemented sand is used in coastal areas, it will be affected by salinity. Hence, the main purpose of this research is to investigate the variation in unconfined compressive strength of cemented sand specimen at two different saline concentration and analysed its effect for different exposure conditions (i.e., 7 days drying and 7 days soaking condition). The saline concentration of water for soaking of the cemented sand specimen were selected as 0.1M and 1M (with NaCl).

2. MATERIAL PROPERTY

In the present study, laboratory produced cemented sand samples were considered for the investigation. Local sand having a fineness modulus of 0.78 was used to represent the widespread soil condition in the south-west zone of Bangladesh. The gradation curve is shown in Figure 1 and the grain size range falls is between 1.18 to 0.075mm. Furthermore, optimum moisture content of the sand was obtained 14.5% using standard proctor test, which was used to maintain the mixing water content. Figure 2 represent the compaction curve of the sand.

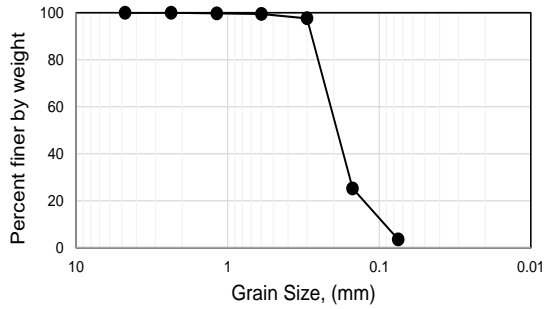


Figure 1: Grain size distribution of local sand

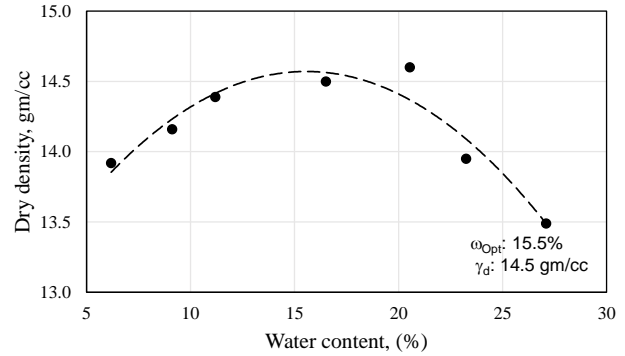


Figure 2: Compaction curve of local sand

Portland cement was used in the present study. In order to maintain the integrity of mechanical and chemical properties of the cement, the bag was kept in air tight condition after opening. Commercially available NaCl salt was used with tap water to produce the saline water of different concentration.

Table 1: Mix proportion of cement mixed sand (in weight)

Cement	15.45 gm
Local Sand	309 gm

3. SAMPLE PREPARATION

In this study, slenderness ratio of the cemented sand specimen was taken as two and locally available PVC pipe having a diameter of 50 mm and height of 100 mm has been used as the mold for sample preparation. The slenderness ratio is an important parameter for strength of sample. Decrease in slender ratio increases the strength of samples but reduction of slenderness ratio reduces to 0.75 show the nonlinear increase in strength (Abdullah and Kiouis, 1997). In this study, the cement ratio was used as 5% of the dry sand and initially sand and cement were thoroughly mixed. Then, tap water (following optimum moisture content of 14.5% for local sand) was added uniformly to prepare a homogeneous mixture of sand-cement-water for one mold sample. Hand mixing tools were used for sample mixing purposes. The cemented sand was divided into three layers and compacted in the mold layer by layer. After compacting one layer the top surface was scratched before another layer is added to confirm better adhesion. Grease was used as a lubricant at inner surface of mold for reducing friction between sample and mold. After preparation, the sample was kept in the air for initial curing.

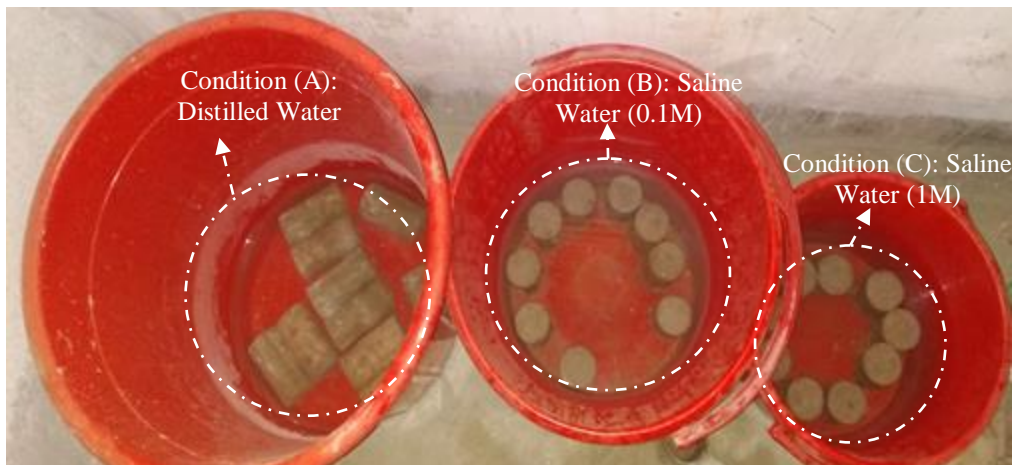


Figure 3: Soaking conditions after 28 days curing

4. CURING CONDITION

The strength of concrete depends on curing temperature, curing time and curing method. Insufficient water supply affects the hydration process and bond strength of cemented sand (Park et al., 2009). In addition, temperature affects the strength during curing of sample. High temperature increases the initial strength but decreases the final strength (Price, 1951). Simultaneous changes in mixing and curing temperature affect the concrete strength and continuous low humidity affect the strength (Cebeci, 1987). The cemented sand strength has shown dependency on the wetting-drying condition of curing period (Park, 2010). In this study, sample was air cured for 3 days for gaining initial strength and bond with cement materials. Later, sample was cured under tap water in a container for 25 days.

4.1 Soaking and drying condition

After 28 days curing, the samples were removed from the container and dried in room temperature for seven days. Then, the samples were divided and soaked in two different saline water concentrations (0.1M, 1M) for another seven days. For reference one set of samples were soaked in distilled water with a view to illustrate the variation of strength under non-saline condition. This process was repeated simultaneously and unconfined compressive strength tests were conducted as per test schedule. Figure 3 depicts the soaking condition of samples under distilled and saline environments.

4.1.1 Sample curing with blue vitriol

Although permeability of cement treated sand is low due to the discontinuous inter granular channel and continuous bonding developed during hydration process but not perfectly impervious due to low percentage of cement content. In addition, permeability characteristics of samples may vary due to sample preparation technique. As intrusion of saline solution in the sample is essential in the present study, to better understand the permeable nature of the sample, one sample was kept in blue vitriol solution after initial curing. Hypothetically, intrusion of solution should propagate inward from periphery characterized by the formation of two different color zones, i.e., bluish shade (penetrated zone) and ordinary sample color (zone not yet penetrated). Figure 4 represents a sample top submerged under blue vitriol solution for 30 days. From the figure it is clear that the solution has penetrated the sample partially and it is expected that it will continue to permeate inwards over time provided that other parameters remain same.



Figure 4: Sample cured in blue vitriol solution



Figure 5: Efflorescence formation on samples

5. RESULTS AND DISCUSSION

In order to study the effect of salinity concentration on strength and deformation properties under different exposure condition, a series of unconfined compression test under monotonic loading was conducted on samples at regular intervals.

Figure 6 and 7 represents the variation of peak strength-strain properties over time (here referred as cycles) for cement mixed sand under different conditions. First of all, unconfined compressive strength of samples continued to rise for the first two cycles irrespective of the curing environment representing the continued strength gain over the time period. However, at higher cycles peak strength continued to decrease almost in similar manner (for case-B and case-C) depicting the negative effect of drying and wetting cycles on the strength properties. Hence, it can be concluded that in the beginning positive strength achieved from cement hydration dominated the behavior of cement mixed sand but in the later stages salinity intrusion initiated micro-crack formation due to formation of crystals (volume expansion) which resulted in the reduction of strength. Reduction of moisture content followed by an increase in the later stages as shown in figure (8) also supports the aforementioned proposition. Formation of efflorescence can be clearly observed on the broken specimens in Figure 5. The moisture content varied from 28.46% to 34.17%. Although failure strain continued to increase but a sharp drop was observed in the later stages illustrating lower strain accumulation at higher cycles. The peak axial strain varied from 0.40% to 0.76%.

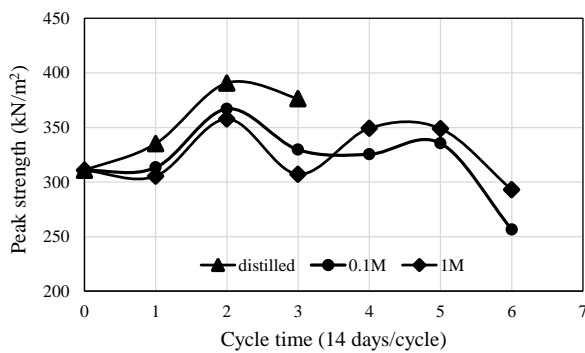


Figure 6: variation of peak strength with time

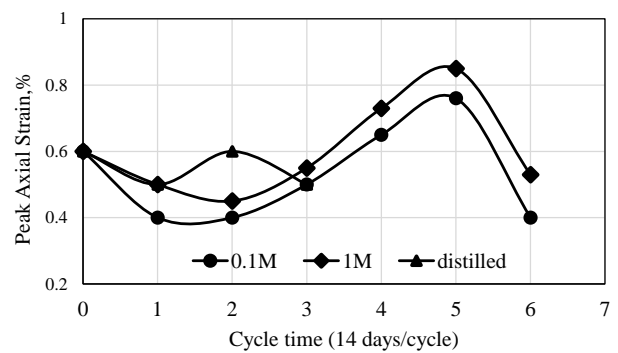


Figure 7: variation of peak Axial strain with time

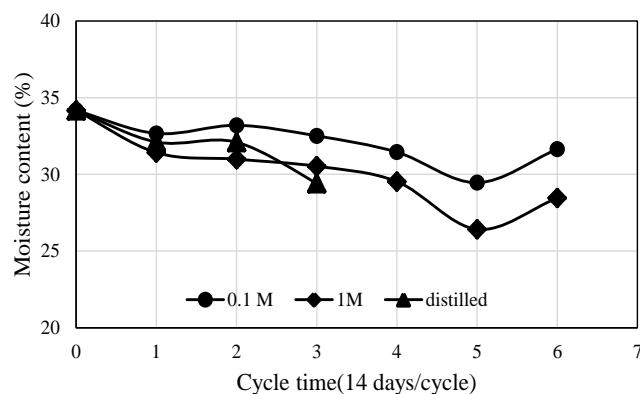


Figure 8: variation of moisture content with time

In addition, moisture content, failure pattern and failure strain data were recorded for each test to investigate the variation of the sample characteristics. All the data has been presented in Table 2 to 4. In general, the failure pattern of the samples was shear failure (brittle failure) but peak strength-strain varied. Figure-9 refers to the typical failure patterns of two random samples.

Table 2. Unconfined compressive strength or Peak strength of samples at different conditions

Wetting-Drying Cycle	Case A: Distilled water	Case B: 0.1M saline water	Case C: 1M saline water
0 (after 28 days)	310.6	310.7	310.7
1	335.2	313.4	305.4
2	390.7	367.0	357.8
3	376.2	329.6	307.1
4	-	325.4	349.3
5	-	335.5	348.9
6	-	256.7	292.9

Table 3. Moisture content (%) of samples after test

Wetting-Drying Cycle	Case A: Distilled water	Case B: 0.1M saline water	Case C: 1M saline water
0 (after 28 days)	34.17	34.17	34.17
1	32.11	32.67	31.42
2	32.10	33.20	30.99
3	29.42	32.51	30.53
4	-	31.45	29.53
5	-	29.46	26.42
6	-	31.65	28.46

Table 4. Peak strain (%) of samples at different conditions

Wetting-Drying Cycle	Case A: Distilled water	Case B: 0.1M saline water	Case C: 1M saline water
0 (after 28 days)	0.6	0.6	0.6
1	0.5	0.4	0.5
2	0.6	0.4	0.45
3	0.5	0.5	0.55
4	-	0.65	0.73
5	-	0.76	0.85
6	-	0.4	0.53



Figure 9: Typical failure pattern of the samples

6. CONCLUSIONS

Salt soaking is an important parameter for affecting the strength of cemented sand. The strength of the weak cemented sample varied with repetitive drying and wetting condition and the strength was reducing after 98 days and the slope indicates the further decrease of strength. The salt of soaking water may have attacked the sample aggregates and cements and deteriorated the structure of cement-sand bond, creating more pore space within the sample and finally affected the strength of sample. Although the present study primarily focuses on understanding the effect of salinity on the mechanical properties (strength-strain) of cement treated sand but long term negative effect on strength can be clearly understood. Further research needs to be conducted emphasizing chemical analysis to investigate the internal effects causing such strength discrepancies. Finally, when cemented sand is used for construction in coastal areas, this strength reduction characteristics of cemented sand should be of prime concern.

REFERENCES

- CEBECI, O. Z. (1987). Strength of concrete in warm and dry environment. *Materials and Structures/Matériaux et Constructions*, 20(4), 270-272.
- De Gao Zou, D. Q. (2011). Experimental Study on Mechanical Characteristics of CSG Materials. *Advance materials research*, 243-249, 2059-2064. doi:<https://doi.org/10.4028/www.scientific.net/AMR.243-249.2059>
- Kim Ki-young, P. H.-g.-s. (2005). Strength Characteristics of Cemented Sand and Gravel. *Journal of the Korean Geotechnical Society*, 21(10), 61-71.
- KIOUSIS, A. A. (1997). Behavior of cemented sands—I. Testing. *International Journal for numerical and analytical methods in Geomechanics*, 21, 533-547.
- Park sung sik, L. j. (2012). Effect of sea water on curing and strength of cemented sand. *journal of korean Geotechnical society*, 28(6), 71-79.
- Park Sung-Sik, k. K.-Y.-S.-W. (2009). Effect of Different Curing Methods on the Unconfined Compressive Strength of Cemented Sand. *journal of korean society of civil engineers*, 29(5C), 207-215.
- Park, s.-s. (2010). Effect of Wetting on Unconfined Compressive Strength of Cemented Sands. *Journal of Geotechnical and Geoenvironmental Engineering*, 136(12). doi:[https://doi.org/10.1061/\(ASCE\)GT.1943-5606.0000399](https://doi.org/10.1061/(ASCE)GT.1943-5606.0000399)
- Price, W. H. (1951). Factors Influencing Concrete Strength. *ACI Journal Proceedings*, 47(2), 417-432.
- Xin CAI, Y. W. (2012). Research review of the cement sand and gravel (CSG) dam. *Front. Struct. Civ. Eng.*, 6(1), 19–24. doi: DOI 10.1007/s11709-012-0145-y
- Ahsan, M. (2010). *Saline Soils of Bangladesh*. Soil Resource Development Institute, SRMAF Project, Ministry of Agriculture, Government of the People's Republic of Bangladesh.
- Mohammad, S. M. D. I., Hossain, A., & Tanjena, B. (2017). Hydrogeochemical investigation of groundwater in shallow coastal aquifer of Khulna District, Bangladesh. *Applied Water Science*, 7(8), 4219–4236. <https://doi.org/10.1007/s13201-017-0533-5>

CHP VALUE FROM PIEZOCONE DISSIPATION TESTS

Md. Julfikar Hossain*¹, Md. Amar Bin Ibne Noman² and Md. Razib Sarder³

¹Superintendent Engineer, Khulna University of Engineering & Technology, Khulna- 9203, Bangladesh, e-mail: kuetjewel@yahoo.com

²Department of Disaster Management, Khulna University of Engineering & Technology, Khulna- 9203, Bangladesh, e-mail: abinoman00@gmail.com

³Assistant Engineer, Khulna University of Engineering & Technology, Khulna- 9203, Bangladesh, e-mail: razibsarder08@gmail.com

* Corresponding author

ABSTRACT

A comprehensive understanding of soil properties requires time consuming and costly laboratory tests. There has been a lot of research for directly obtaining soil parameters from soil field investigation report to save both time and money. A similar approach has been taken in this study to correlate soil parameters with most commonly used soil investigation tools CPT (Cone Penetration Test). Piezocone test (uCPT) is now widely used as an economic and efficient site investigation method in geotechnical engineering. From the results of piezocone penetration and dissipation tests, soil profile and some of engineering properties of sub-soil, such as undrained shear strength (s_u) of clayey deposits, in situ hydraulic conductivity in horizontal direction (k_h) and coefficient of consolidation in the horizontal direction (c_{hp}) can be estimated. The symbol c_{hp} is used to emphasized the value is from piezocone test result. For a standard piezocone with filter for pore water pressure measurement at the shoulder of the cone (u_2 type), there are two types of dissipation curves. Standard and Non-standard curves are observed from the field piezocone dissipation tests. Two existing methods for estimating in-situ coefficient of consolidation in the horizontal direction (c_{hp}) from “non-standard” piezocone dissipation curves (initial u increased for a short period and then dissipated) are applied to the test results in 6 sites in Japan, Bangladesh, USA, UK, Italy and Canada. One method is correcting t_{50} , the time period of measured pore water pressure (u_2) dissipated from its maximum value to 50% of the maximum value (t_{50c} method), and another is extrapolating \sqrt{t} (t is elapsed time) $\sim u_2$ curve (\sqrt{t} method). The analysis results show that for most cases t_{50c} method results in higher c_{hp} value than that of \sqrt{t} method, and it is reasoned that c_{hp} value from t_{50c} method is closer to the field “true” value. Comparing c_{hp} values from t_{50c} method with the corresponding laboratory measured coefficient of consolidation in the vertical direction (c_v) indicates that for most data c_{hp}/c_v ratios are varied from about 3 to about 10.

Keywords: Piezocone test, Dissipation test, Coefficient of consolidation, Pore water pressure, Soil profile.

1. INTRODUCTION

Piezocoone test (uCPT) is now widely used as an economic and efficient site investigation method in geotechnical engineering (e.g., Campanella & Robertson 1988; Lunne et al. 1997). From the results of piezocone penetration and dissipation tests, soil profile and some of engineering properties of sub-soil, such as undrained shear strength (s_u) of clayey deposits (e.g., Campanella & Robertson et al. 1988), in situ hydraulic conductivity in horizontal direction (k_h) (Chai et al. 2011; Robertson 2010) and coefficient of consolidation in the horizontal direction (c_{hp}) (e.g., Teh and Houlsby 1991; Chai et al. 2012a) can be estimated. The symbol c_{hp} is used to emphasized the value is from piezocone test result.

For a standard piezocone with filter for pore water pressure measurement at the shoulder of the cone (u_2 type), there are two types of dissipation curves observed from the field piezocone dissipation tests. One type shows monotonic decreasing of measured pore water pressure (u_2) with elapsed time and it is designated as “standard” curve (Baligh & Levadoux 1986; Teh and Houlsby 1991). Generally this type of curves occurs in normal or lightly over-consolidated clay deposits. Another type is that when dissipation test started, u_2 first increasing from an initial value to a maximum, and then decreasing to a hydrostatic value, which is referred as “non-standard” curve (Burns and Mayne 1998; Sully et al. 1999; Chai et al. 2012a), which often occurs in heavily over-consolidated clay deposit or dense sand deposit. Several methods have been proposed to estimate c_{hp} values from the standard dissipation curve, and perhaps Teh and Houlsby (1991)’s method is the widely used one. As for the non-standard curve, only few methods are available, such as Sully et al. (1999)’s methods of shifting time origin and extrapolation root-time (\sqrt{t}) verses pore water pressure curve and Chai et al. (2012a)’s method which corrects the time corresponding to 50% dissipation of the measured maximum u_2 value. However, Sully et al.’s shifting time origin method ignored the effect of redistribution of u values around the cone during the process of u_2 reaches the maximum value, and the method of extrapolation of \sqrt{t} curve (\sqrt{t} method) does not has a fundamental basis.

For the two methods proposed by Sully et al., \sqrt{t} method can result in a slightly higher c_{hp} value than the shifting time origin method (Chai et al. 2012a). In this study, \sqrt{t} method and t_{50c} method have been used to interpret field c_{hp} values from available field measured non-standard piezocone dissipation curves in the literature. It is demonstrated that generally, t_{50c} method results in a higher c_{hp} value. Comparing the estimated c_{hp} values with available laboratory measured corresponding coefficient of consolidation in the vertical direction (c_v), possible ratios of c_{hp}/c_v are investigated.

2. METHODS FOR ESTIMATING c_{hp} VALUE FROM NON-STANDARD DISSIPATION CURVES

2.1 Sully et al.’s \sqrt{t} Method

Fig. 1 illustrates a non-standard dissipation curve of u_2 verses \sqrt{t} (t is elapsed time) plot. \sqrt{t} method issues that the initial part of measured dissipation curve is wrong, and can be corrected by extrapolating the close to linear part of the curve after the maximum value of u_2 . Taking the value of u_2 at the intersecting location of extrapolation line and vertical axis as initial value of u_2 (u_{20}), the t_{50} is the time for u_2 dissipated to $0.5 u_{20}$.

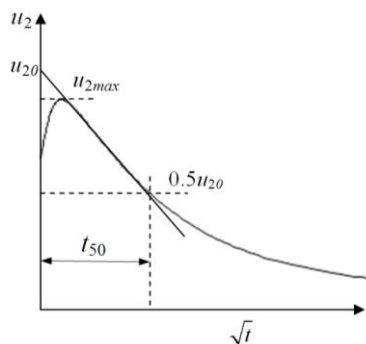


Figure 1: u verses \sqrt{t} plot

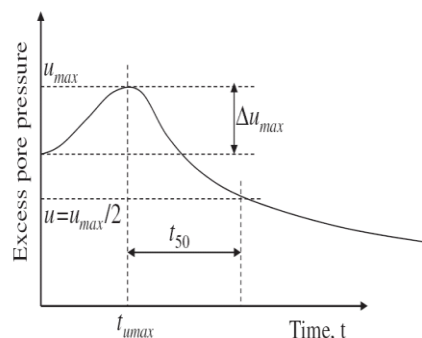


Figure 2: “Non-standard” curve
(Chai et al. 2012a)

Then the value of c_{hp} is calculated as (Teh and Houlsby 1991):

$$c_{hp} = \frac{c_p \cdot r_0^2 \cdot \sqrt{I_r}}{t_{50}} \quad (1)$$

where: r_0 is the radius of the cone, and I_r is the rigidity index of soil. c_p is a factor corresponding to 50% degree of consolidation, which is related to the location of the filter element. For a cone with a shoulder filter element, $c_p = 0.245$ (Teh and Houlsby 1991).

2.2 Chai et al.’s t_{50c} Method

The reasons considered for causing the non-standard dissipation curves are: (1) cone penetration induced dilatancy of dense sand or over-consolidated clayey soil adjacent to the face of the cone and (2) partial unloading effect when a soil element moves from the face to the shoulder of the cone in case of a standard piezocone (Chai et al. 2012a). The dilatancy and partial unloading effects will result in an initial excess pore water pressure (u_2) at the shoulder of the cone lower than that in the zone adjacent and slightly away from the shoulder. Then the non-standard dissipation curve is the result of the “non-standard” initial excess pore water pressure distribution around the cone. By conducting uncoupled dissipation analysis with different initial u distribution using finite difference method, Chai et al. (2012a) proposed an empirical equation for correcting t_{50} , the time period for u_2 dissipated from its maximum value to 50% of the maximum value of the non-standard dissipation curve. Then with the corrected t_{50c} , c_{hp} value can be estimated using Eq (1). Fig. 2 illustrates a non-standard dissipation curve with some variables illustrated. The correction equation by Chai et al. (2012a) is as follows:

$$t_{50c} = \frac{t_{50}}{1 + 18.5 \left(\frac{t_{u\max}}{t_{50}} \right)^{0.67} \left(\frac{I_r}{200} \right)^{0.3}} \quad (2)$$

where $t_{u\max}$ is time for measured excess pore pressure to reach its maximum value. Then substitute t_{50c} into Eq. (1) in the place of t_{50} to calculate value of c_{hp} .

3. c_{hp} VALUES FROM “NON-STANDARD” DISSIPATION CURVES

Non-standard dissipation curves at 6 sites in Japan, Bangladesh, UK, USA, Italy and Canada are collected and analyzed.

3.1 A Site in Saga, Japan

In Saga plain, around the Ariake Sea in Japan, exists a clayey soil (Ariake clay) deposit with a thickness of about 10 to 30 m. Piezocone penetration tests as well as dissipation tests at several depths were conducted at the site with its location shown in Fig. 3.

The test site is at the toe of a river embankment (Chai et al. 2004). At this site, the thickness of soft clay soil is about 12-14 m. The top crust is about 2.0 m thick and in an apparent over-consolidated state. Below it, the soil is normally to slightly over-consolidated. There is a borehole (BH) adjacent to piezocone test points (Fig. 4). Figure 5 shows some physical and mechanical properties of the soils retrieved from the BH. As shown in Fig. 4, piezocone penetration tests at six locations were arranged in three pairs, and each pair involved a continuous penetration test (Test point TA 1-1, 2-1 and 3-1) and a separate test that paused at about 1.0 m intervals to measure the dissipation of excess pore water pressure generated during the preceding penetration (Test point TA 1-2, 2-2 and 3-2). For the dissipation tests conducted at TA 3-2, there are some abnormal phenomena, and we judged that they are less reliable and excluded here. The ground-water level was about 0.8 m below the ground surface at BH location. Figure 6 shows some of the normalized field non-standard u_2 dissipation curves at TA 1-2 and TA 2-2 respectively. The normalization is made using the following equation:

$$U = \frac{u(t) - u_0}{u_{\max} - u_0} \quad (3)$$

where $u(t)$ is total pore water pressure at time t , u_{\max} is maximum measured total pore water pressure, and u_0 is the equilibrium in situ pore water pressure at the depth of interest.



Figure 3: Location of the piezocone test site in Saga, Japan

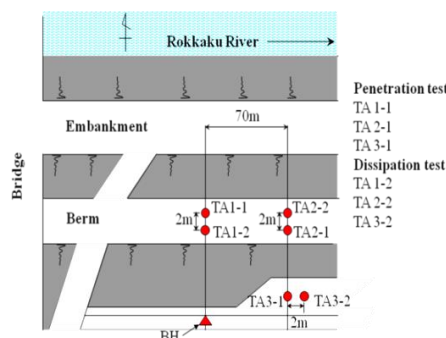


Figure 4: Plan layout of field tests (after Chai et al. 2004)

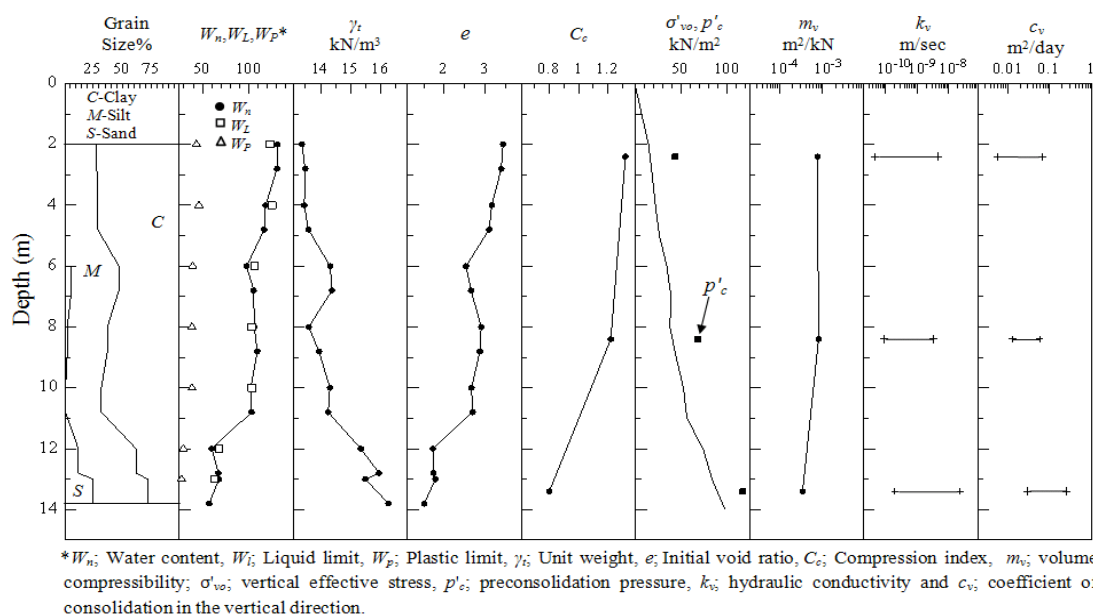


Figure 5: Some physical and mechanical properties of soil at Saga site

Most reported non-standard dissipation curves have been for heavily over-consolidated clayey deposits (Burns and Mayne 1998, Sully et al. 1999). The test results at Saga site indicate that the

phenomena can also occur in some lightly over-consolidated soils. Using Eqs (1) and (2) to calculate c_{hp} value, I_r value of the deposit is needed. It has been reported that the Ariake clay deposits in Saga area has a ratio of E_{50}/s_u (E_{50} is the secant modulus at 50% of peak deviator stress from unconfined compression tests, s_u is undrained shear strength) between 100 and 200 (Chai et al. 2005). Assuming a poisson's ratio of 0.5 (undrained) and E_{50}/s_u ratio of 150, an I_r value of 50 can be obtained and it has been used in calculations.

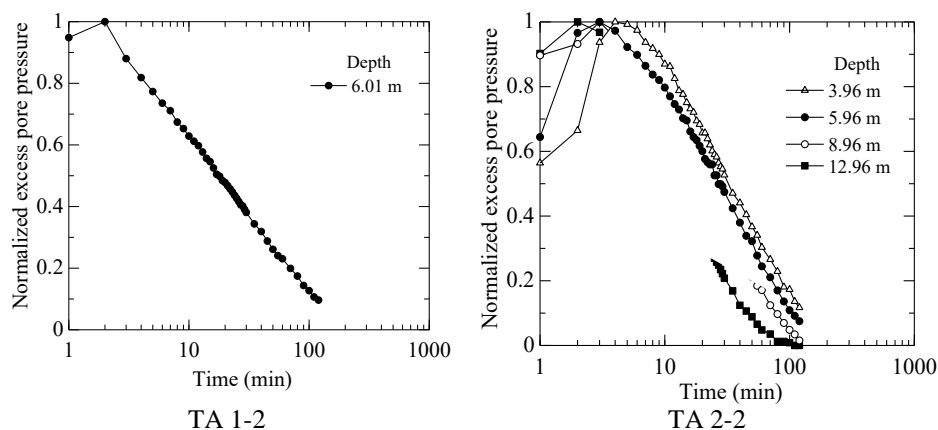


Figure 6: Non-standard dissipation curves at TA site, Saga, Japan

c_{hp} values have been calculated by using \sqrt{t} method and t_{50c} method from non-standard dissipation curves. The calculated c_{hp} values and some available values of coefficient of consolidation in the vertical direction (c_v) from laboratory consolidation tests are listed in Table 1.

Table 1: Summary of the field dissipation and laboratory consolidation test results at Saga site

Test point No.	Depth (m)		t_{umax} (min)	u_{max} (kPa)	t_{50} (min)	t_{50m} (min)	c_{hp} (cm ² /min)		c_v (cm ² /min) Oedometer
	CPTu	Oedometer					\sqrt{t} method	t_{50c} method	
TA 1-2	6.01	2.40*	2	252.12	16.00	3.97	0.831	1.400	0.375
TA 2-2	3.96		4	175.73	29.50	7.02	0.699	0.790	
	4.96		3	197.31	28.00	7.50	0.160	0.740	
	5.96		3	209.66	25.00	6.33	0.224	0.877	
	6.96		3	218.88	19.00	4.18	0.338	1.330	
TA 2-2	8.96	8.40	3	277.04	16.70	3.43	0.343	1.620	0.305
	9.96		2	301.35	21.00	5.95	0.275	0.932	
	10.96		2	324.01	21.00	5.95	0.276	0.932	
	11.96		2	349.90	22.50	6.59	0.308	0.842	
TA 2-2	12.96		2	391.87	11.50	2.40	0.537	2.310	
	13.46	13.40	2	359.61	5.40	0.74	1.090	7.480	0.711

*The value is the average depth of about 0.8 m long sample obtained by a thin-wall tube.

3.2 A Site in Munshiganj, Bangladesh

The data obtained through geotechnical investigation of proposed 'Shah Cement Vertical Roller Mill (VRM) Project was Situated in Mukhtarapur, Munsiganj, Bangladesh. Figure 7 shows The VRM project location map. SPT and Cone penetration and dissipation test was conducted at this site. Figure 8 shows the SPT and CPT Test locations in VRM project Site (DCL, 2016). There are 10 SPT test and 10 CPT tests are conducted which are shown in Figure 8. There are 15 piezocone dissipation tests were conducted. SPT test was conducted by 125mm diameter boring and soil sample are collected by soil sampler, 72mm diameter at the depth up to 50m. Test assessment and analysis was particularly concerned with the potential for the existing subsoil to support the proposed plant recommended foundation and to evaluate the groundwater conditions.

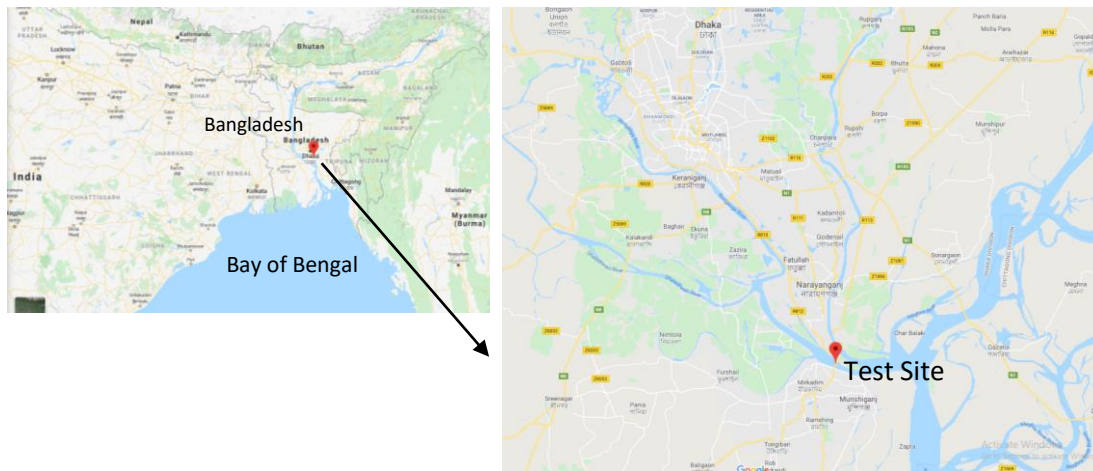


Figure 7: Location of the CPT test site in VRM Project, Munshiganj, Bangladesh

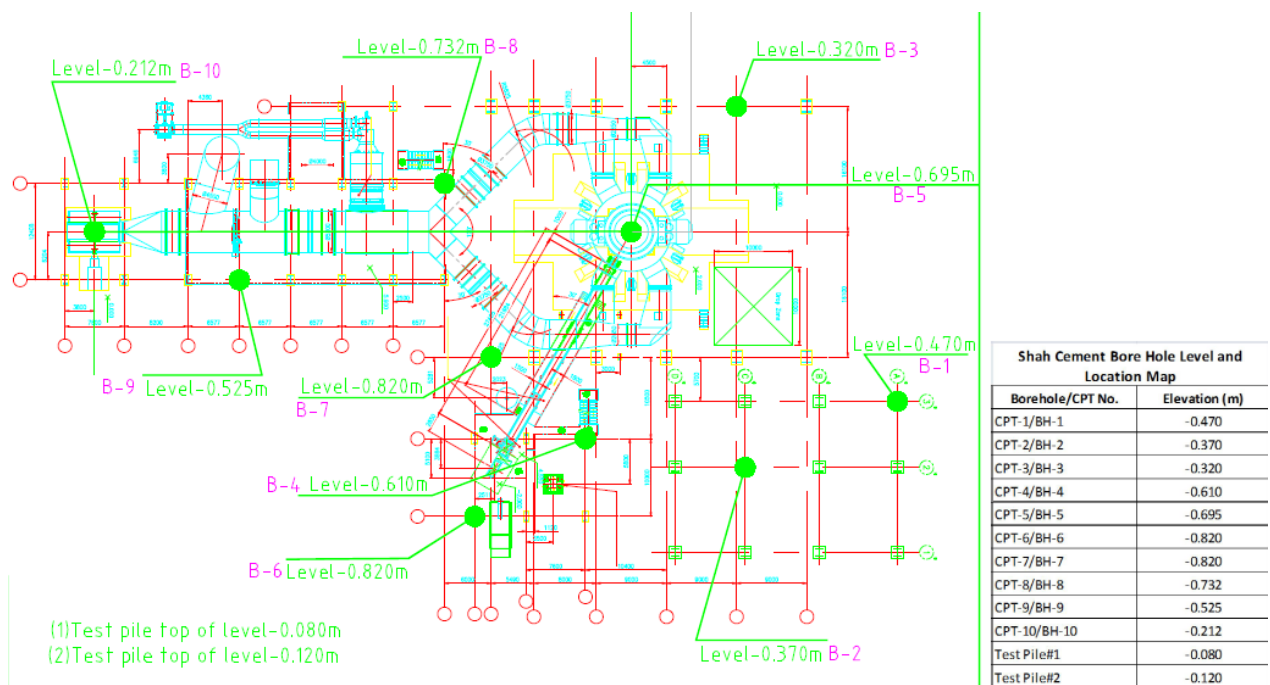
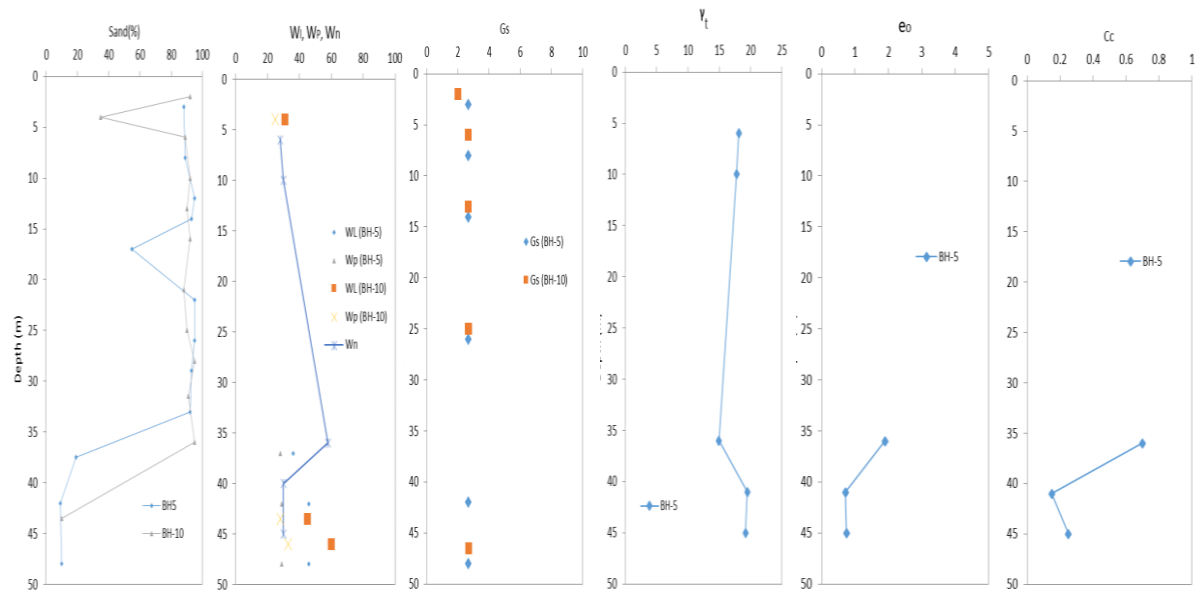


Figure 8: SPT and CPT Test locations in VRM project Site (DCL, 2016)

Figure 9 shows the summarize of some physical and mechanical properties of soil at the VRM project sites in Munshiganj. The test site is at the Pashur river embankment (DCL 2016). At this site, toplayer the thickness of sensitive, fine grained soil is about 0-.5 m. The top crust is about 0 to 2.0 m thick clayey silt to silty clay. Below it, the soil is fine sand normally to slightly over-consolidated at the depth of 2-3m. The condition of the soil 3 to 5m is clay silt to silty clay and 6m to 40m layer is sand mixed with silty clay. Clays clay to silty clay are present in 40m to 50m depth.



* w_n : Water content, w_l : Liquid limit, w_p : Plastic limit, G_s : Specific gravity, γ_t : Unit weight, e_0 : Initial void ratio and C_c : Compression Index

Figure 9: Some physical and mechanical properties of soil at Munshiganj Site, Bangladesh

Cone penetration was carried out using cones 60° apex angle and 225 cm² friction sleeve area advance using a 20 Ton hydraulic penetrometer. Throughout the test the cone was advanced by applying thrust on 1m long 36mm diameter rod at a rate of 2.0cm/sec. Tip resistance of the cone, sleeve friction and pore water pressure are measured from cone penetration test in Munshiganj VRM site which is shown in Figure 10 (DCL, 2016). 15 nos cone penetration dissipation tests are conducted in this site. From dissipation curves it is depicted that 13 nos curves are Standard dissipation curves and 2 nos are Non-standard dissipation curves.

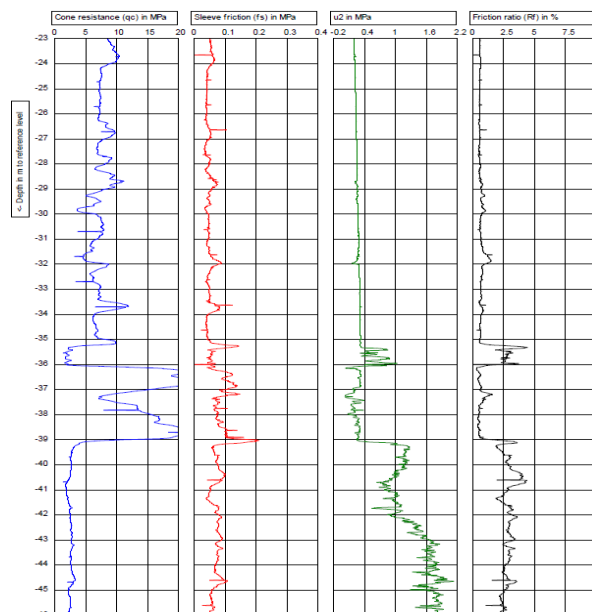


Figure 10: Cone Penetration Test (test-1) results in VRM project Site (DCL, 2016)

Figure 11 show the normalized non-standard dissipation curves at Munshiganj sites in Bangladesh. Table 2 presents a summary of the field CPTu dissipation test results and calculated c_{hp} values. In the calculation I_r of 100 has been assumed.

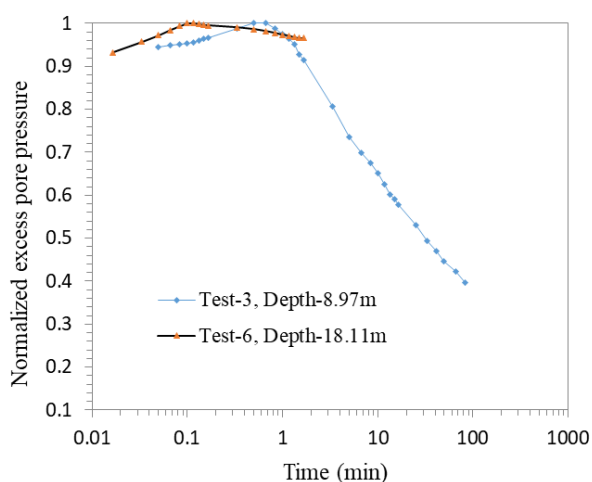


Figure 11: Non-standard dissipation curves at Munshiganj Sites, Bangladesh

Table 2: Field dissipation test results at Munshiganj Site in Bangladesh

Test point No.	Depth (m) CPTu	$t_{u\max}$ (min)	u_{\max} (kPa)	t_{50} (min)	t_{50m} (min)	c_{hp} (cm ² /min)	
						\sqrt{t} method	t_{50c} method
CT 3-1	8.97	0.67	83	32.66	15.46	0.112	0.356

3.3 Other Available Sites

The results of four (4) field cases, Canon’s Park; UK (Bond and Jardine 1991), St. Lawrence Seaway; N.Y. (Lutenegger and Kibir 1987); Taranto, Italy (Battaglio et al. 1986) and University of British Columbia test site (Sully et al. 1999) with “non-standard” dissipation curves are summarized in Table 3. The corresponding normalized dissipation curves are shown in Fig. 12.

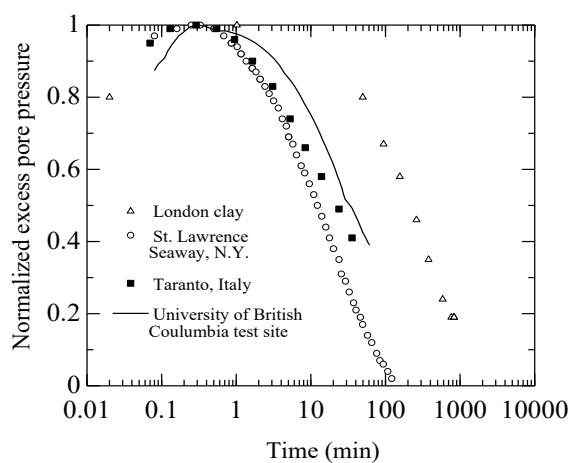


Figure 12: Non-standard dissipation curves at others test sites (Chai et al. 2012a)

Table 3: Field dissipation and laboratory consolidation test results at four sites

No	Site	Depth (m)	Diameter of cone (mm)	u_{max} (kPa)	I_r	OCR	c_{hp} (cm ² /min)		c_v (cm ² /min) Oed.	References
							\sqrt{t} method	t_{50c} method		
1	London clay at Canon's Park, UK	5.70	102.0	377.6	100	14	0.040	0.408	0.012-0.018	Test data from Bond and Jardine (1991); Burns and Mayne (1998)
2	Crust of soft clay at St. Lawrence Seaway, N.Y.	6.10	35.7	291.2	50	3.5	0.603	1.032	0.15-0.48	Lutenegger and Kibir (1987); Burns and Mayne (1998)
3	Cemented clay, Taranto, Italy	9.00	35.7	1693.8	200	26	0.658	1.032	0.06-0.15	Battaglio et al. (1986); Burns and Mayne (1998)
4	Strong pit clay, University of British Columbia test site	6.65	35.7	1261.1	200	4.0	0.441	0.630	OC:0.12-0.3 NC:0.042-0.06	Sully et al. (1999)

4. COMPARISON OF c_{hp} AND c_v VALUES

From the results in Tables 1, 2 and 3, it clearly shows that c_{hp} values estimated by t_{50c} method are higher than that from \sqrt{t} method. Since \sqrt{t} method does not consider the fundamental mechanism of causing non-standard dissipation curve, and we believe that the results from t_{50c} method are closer to "true" field values. Therefore, comparisons of the values of c_{hp} from t_{50c} method and laboratory c_v values are plotted in Figs. 10 for one site in Saga, Japan, and other four sites, respectively. c_v values are not got available from Munshiganj sites, so it is not possible to comparison of c_v and c_{hp} values. For almost all cases, $c_{hp} > c_v$. Although the data are scattered, for the data from the site in Saga, Japan $c_{hp} \sim 4c_v$. There are two reasons for $c_v < c_{hp}$. One is that the laboratory c_v is generally lower than the corresponding field value. Chai and Miura (1999) reported that for Ariake clay deposit in Saga, Japan, field c_v value is about 2 times of the corresponding laboratory value. Another reason is due to anisotropic consolidation behavior of clay deposit, and normally the coefficient of consolidation in the horizontal direction is higher than that in the vertical direction. For Ariake clay, Chai et al. (2012b) reported a c_h/c_v ratio of about 1.6 from laboratory constant rate of strain (CRS) consolidation test results. Combining these two factors, a c_{hp}/c_v ratio of about 3.2 can be obtained. Therefore, for the results from the site in Saga, Japan, $c_{hp} \sim 4c_v$ is quite reasonable. The data from Munshiganj, Bangladesh the values corresponding c_v are measured from c_{hp} values with an average c_{hp}/c_v ratio of about 4 (Fig. 13 (a)). For other four (4) sites investigated, c_{hp} is about 3 to 30 times of c_v .

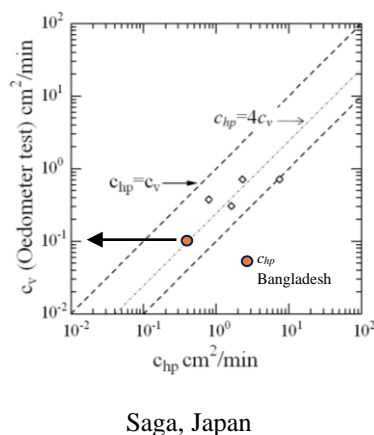


Figure 13: Comparisons of c_{hp} and c_v (Oedometer) values

5. CONCLUSIONS

Two methods, for estimating field coefficient of consolidation in the horizontal direction (c_{hp}) from non-standard piezocone dissipation curve (measured excess pore water pressure (u_2) initially increases and then decreases), namely, Sully et al. (1999)'s extrapolation of root time versus u_2 plot (\sqrt{t} method) and Chai et al. (2012a)'s correcting t_{50} method (t_{50c} method) are applied to field measurements from 11 sites in Japan, Bangladesh, USA, UK, Italy and Canada.

The estimated c_{hp} values from both the methods are compared each other as well as with the laboratory measured coefficient of consolidation in the vertical direction (c_v).

- (1) Generally t_{50c} method results in higher c_{hp} value than that of \sqrt{t} method. Using the available information about Ariake clay deposit in Saga, Japan, it has been shown that with c_{hp} value from t_{50c} method, the ratio of c_{hp}/c_v is closer to the "true" field value.
- (2) For most of the data from 11 sites, c_{hp}/c_v ratios varied from about 3 to about 10.
- (3) From the data of Munshiganj site c_v value is measured from the correlation of c_{hp}/c_v ratios which is reasonable.

REFERENCE

- Baligh, M.M. and Levadoux, J.N. (1986), "Consolidation after undrained piezocone penetration", II: interpretation, *Journal of Geotechnical Engineering*, ASCE, 112, 727-745.
- Battaglio, M., Bruzzi, D., Jamiolkowski, M. and Lancellotta, R. (1986), "Interpretation of CPTs and CPTU's: undrained penetration of saturated clays, In: *Proc. of the 4th inter geotechnical seminar, Field instrumentation and in-situ measurements*, Singapore, p. 129-56.
- Bond, A.J. and Jurdine, R.J. (1991), "Effects of installing displacement piles in a high OCR clay", *Geotechnique J.*, 41(3), 341-63.
- Burns, S.E. and Mayne, P.W. (1998), "Monotonic and dilatatory pore pressure decay during piezocone tests in clay" *Can. Geotech. J.*, 35, 1063-1073.
- Cai, G., Liu, S. and Puppala, A. J. (2012), "Predictions of coefficient of consolidation from CPTU dissipation tests in Quaternary clays", *Bull Eng Geol Environ*, 71, 337-350.
- Campanella, R.G. and Robertson, P.K. (1988), "Current status of the piezocone test", In: *Ruiter J, editor, penetration testing*, Balkema, Rotterdam, 93-116.
- Chai, J.-C. and Miura, N. (1999), "Investigation on some factors affecting vertical drain behavior", *J. of Geotechnical and Geoenvironmental Engineering*, 125(3), 216-226.

- Chai, J.-C., Carter, J.P., Miura, N, and Hino, T. (2004), “Coefficient of consolidation from piezocone dissipation test”, *Proc. of Int. Symposium on Lowland Technology, ISLT 2004*, Bangkok, Thailand, 1-6.
- Chai, J.-C., Miura, N, and Koga, H. (2005), “Lateral displacement of ground caused by soil-cement column installation” *Journal of Geotechnical and Geoenvironmental Engineering*, ASCE, 131(5), 623-632.
- Chai, J.-C., Agung, P.M.A., Hino, T., Igaya Y. and Carter J.P. (2011), “Estimating hydraulic conductivity from piezocone soundings”, *Geotechnique*, 61 (8), 699-708.
- Chai, J.-C., Sheng, D., Carter, J.P. and Zhu, H.-H. (2012a), “Coefficient of consolidation from non-standard piezocone dissipation curves”, *Computer and Geotechnics*, 41, 13-22.
- Chai, J.-C., Jia, R. and Hino, T. (2012b), “Anisotropic consolidation behavior of Ariake clay from three different CRS tests”, *Geotechnical Testing Journal*, ASTM, 35(6), 1–9, doi:10.1520/GTJ103848.
- Development Construction Ltd. (2016), *Geotechnical Investigation Report on VRM Project: Shah Cement Ltd.*
- Lunne, T., Robertson, P.K. and Powell, J.J.M. (1997), *Cone penetration testing in geotechnical practice*, London: E & FN Spon.
- Lutenegger, A.J. Kabir, M.G. (1987), *Pore pressure generated by two penetrometers in clays*, Department of Civil and Environmental Engineering, Clarkson University, Potsdam, NY, Report 87-2.
- Robertson, P.K. (2010), “Estimating in-situ soil permeability from CPT and CPTu”, *2nd International Symposium on Cone Penetration Testing*, Huntington Beach, CA, USA, 2-43.
- Sully, J.P., Robertson, P.K., Campanella, R.G., and Woeller, D.J. (1999), “An approach to evaluation of field CPTU dissipation data in overconsolidated fine-grained soils”, *Can. Geotech. J.*, 36, 369-381.
- Teh, C.I. and Houlsby, G.T. (1991), “An analytical study of the cone penetration test in clay”, *Geotechnique*, 41, 17-34.